Two Distinct Domains of MSP1 Recognize the Band 3-GPA Complex Mediating Malaria Invasion

A thesis

submitted by

Michael Baldwin

In partial fulfillment of the requirements
for the degree of

Doctor of Philosophy

in

Cell and Molecular Physiology

TUFTS UNIVERSITY

Sackler School of Graduate Biomedical Sciences

August, 2015

Adviser: Dr. Athar Chishti

Thesis Chair: Dr. Michael Forgac
Committee Member: Dr. Peter Juo
Committee Member: Dr. Mercio Perrin
Outside Examiner: Dr. Matthias Marti

Abstract

Each year there are approximately 200 million cases of human malaria and over 700,000 deaths. In order to prevent the spread of this lethal infectious disease we must design specific, effective therapies at its subcellular targets. This thesis investigates two essential malaria proteins and the roles they play in *Plasmodium falciparum* development and invasion in the hopes they may be used as components of a multi-drug therapy or multi-antigenic vaccine.

First, *Plasmodium falciparum* signal peptide peptidase (PfSPP) functions at the blood stage of malaria infection where it plays an essential role. Previous work demonstrated that SPP inhibitors are lethal to malaria parasite growth at the late-ring/early trophozoite stage of intra-erythrocytic development. Consistent with its role in development, we tested the hypothesis that PfSPP functions at the endoplasmic reticulum of *Plasmodium falciparum* where it cleaves membrane-bound signal peptides generated following the enzyme activity of signal peptidase. The localization of PfSPP to the endoplasmic reticulum was confirmed by immunofluorescence microscopy and immunogold electron microscopy. Biochemical analysis indicated the existence of monomer and dimer forms of PfSPP in the parasite lysate. A comprehensive bioinformatics screen identified several candidate PfSPP substrates in the parasite genome. Using an established transfection based *in vivo* luminescence assay, malaria heat shock protein 101 (HSP101) was identified as a substrate of PfSPP, and partial inhibition of PfSPP correlated with the emergence of gametocytes. This finding unveils the first known substrate of PfSPP, and provides a new target for the development of a multi-drug therapy at the erythrocyte stage of the parasite life cycle.

The second aspect of this study focused on the specific role of merozoite surface protein 1 (MSP1), a highly abundant ligand coating the merozoite surface in all species of malaria. MSP1 is essential for RBC invasion and considered a leading candidate for inclusion in a multi-subunit vaccine against malaria. Here, by employing phage display technology, we report a novel interaction between the N-terminus of MSP1 and RBC glycophorin A (GPA). Mapping of the binding domains established a direct interaction between malaria MSP1 and human GPA within a region of MSP1 previously shown to potently inhibit *P. falciparum* invasion of human RBCs. Additionally, a genetically modified mouse model lacking the band 3-GPA complex in RBCs is completely resistant to malaria infection *in vivo*. These findings suggest an essential role of the MSP1-GPA-band 3 complex during the initial adhesion phase of malaria parasite invasion of red blood cells. Furthermore, we developed specific antibodies against the 5C and 6A extracellular domains of band 3 to inhibit parasite invasion by targeting host receptors. We subsequently identified RhopH3 as a binding partner to MSP1 and band 3. The combination of these findings reveals the function of two essential protein complexes in intra-erythrocyte development and invasion of the malaria parasite.

Acknowledgements

The work discussed here would not be possible without the contributions of a large number of supportive people in my life. I am extremely fortunate to have Athar Chishti as my adviser. I arrived at Tufts in unique fashion, and Athar took a chance on me and allowed me to mature and develop as a scientist under his tutelage. Athar possesses an infectious level of excitement and enthusiasm about scientific research making the lab a great place to work. This drive has been an essential factor in the progress I have made in graduate school.

My thesis committee has provided invaluable guidance and direction in dealing with my laboratory projects. Thus I would like to thank Mike Forgac (chair), Peter Juo and Mercio Perrin. They were a key reason I was able to stay on track and ensure my research was headed in a specific direction. I also wanted to thank Matthias Marti for taking the time and effort to serve on my committee.

The Chishti lab was able to provide numerous contributions, both scientific and not, and I am grateful for the help that I have received. I have enjoyed working in a positive, friendly environment where a second opinion can be found just a few feet away. I specifically wanted to thank a number of current and past Chishti lab members: Donna-Marie Mironchuk, Toshihiko Hanada, Yunzhe Lu, James Schiemer, Jennifer Nwankwo, Adam Wieschhaus, Crystal Russo, Jiayi Wu, Gregory Mines, Sheila Amoako and Joshua Cole. I am going to miss working with such a fun group of people and I wish all of you the best of luck in the future. Outside of the Chishti lab I could always find a helping hand as being part of the physiology program offers a great sense of community. The

collaborative nature among students, faculty and staff has provided a highly supportive research environment.

I was very fortunate to find a strong support system made up of great family and friends. Mom, Dad, Ben and Mimi, I owe so much to the support you have provided me over the years. You have kept me humble, levelheaded and on the ball since day one. Sara, you have been unconditionally supportive of me during my tenure at Tufts. I know that you are always there to talk me through the harder times. Your charm, sense of humor and understanding were essential factors in keeping me centered these past few years. I cannot thank you enough.

Table of Contents

Abstract i

Acknowledgements iii

List of Tables vi

List of Figures vii

List of Abbreviations viii

Introduction 1

Malaria 1

Anopheles mosquito 4

Liver stage parasites 6

Blood stage 9

Parasite Proteases 30

Signal Peptide Peptidase 35

Merozoite Surface Protein 1 43

Glycophorin A 55

Band 3/Anion Exchanger 1 59

Chapter 2: Signal Peptide Peptidase 70

Rationale 71

Materials and Methods 73

Results 81

Chapter 3: Merozoite Surface Protein 1 98

Rationale 99

Materials and Methods 101

Results 113

Chapter 4: Discussion and Future Directions 148

***Plasmodium falciparum* signal peptide peptidase** 149

MSP1 binds to glycophorin A as part of malaria invasion 157

Band 3 as an antibody target for malaria invasion 164

Future Directions 170

References 176

List of Tables

Table 1. Erythrocyte receptors involved in *Plasmodium falciparum* invasion, their cognate ligands and enzyme sensitivity. 15
Table 2. Parasite SPP substrates predicted from the bioinformatics screen. 91
Table 3. Band 3 antibody equilibrium binding constants. 132
Table 4. IgY concentration-dependent inhibition of RBC invasion by the *P. falciparum* 3D7 strain. 134
Table 5. Inhibition of RBC invasion using 3D7, 7G8, FCR3, and Dd2 strains of *Plasmodium falciparum*. 140

List of Figures

Figure 1.1. The life cycle of *P. falciparum* infection occurs in three distinct stages including the mosquito, liver and blood stage. 3
Figure 1.2. Merozoite invasion of the erythrocyte occurs in several distinct steps. 11
Figure 1.3. A comprehensive view of the receptor-ligand interactions identified as occurring during *P. falciparum* erythrocyte invasion. 14
Figure 1.4. Tight junction formation and cytoskeletal propulsion allows for entry into the host cell. 25
Figure 1.5. The asexual stages of P. falciparum development account for the clinical manifestation of the disease. 28
Figure 1.6. Signal peptide peptidase (SPP) is a multi-transmembrane protein that cleaves signal peptides within the ER membrane. 33
Figure 1.7. SPP Inhibitors are lethal to parasite growth and development *in vitro*. 41
Figure 1.8. Merozoite surface protein 1 is processed into a multi-subunit polypeptide complex during merozoite invasion. 45
Figure 1.9. Glycophorin A topology model. 56
Figure 1.10. Band 3/Anion exchanger 1 is associated with several cellular functions. 61
Figure 2.1. Immunoblotting of PfSPP using the anti-C-terminal PfSPP antibody. 82
Figure 2.2. PfSPP co-localizes with Plasmepsin V to the endoplasmic reticulum. 88
Figure 2.3. PfSPP cleaves the signal peptide of HSP101 but not LSA-1. 92
Figure 2.4. Generation of chromosomal PfSPP-GFP chimera alters parasite morphology and PfSPP activity. 95
Figure 3.1. Domain organization of recombinant merozoite surface protein 1 (MSP1). 115
Figure 3.2. MSP1 binds to purified glycophorin A (GPA). 116
Figure 3.3. MSP1 binds to human erythrocytes and specifically binds to GPA in erythrocyte ghosts lysate. 119
Figure 3.4. MSP1 binds to a specific region of the GPA extracellular domain. 121
Figure 3.5. Resistance of band 3-GPA deficient mice to malaria infection. 124
Figure 3.6. Band 3 antibodies show specific activity against their epitopes by immunoblotting and immunofluorescence. 128
Figure 3.7. Binding of antibodies to intact RBCs by flow cytometry. 131
Figure 3.8. Band 3 antibodies inhibit *Plasmodium falciparum* invasion *in vitro*. 135
Figure 3.9. Antibodies against a specific region of band 3 specifically inhibit the SAID pathway of *P. falciparum* invasion *in vitro*. 139
Figure 3.10. RhopH3 binds to the 5ABC domain of band 3 on human erythrocytes. 142
Figure 3.11. Biochemical interactions between RhopH3, band 3, and MSP1. 144
Figure 3.12. MSP1 and RhopH3 compete for occupation of the 5ABC binding site of band 3. 146
Figure 4.1. Schematic depiction of HSP101 protein processing in the parasite endoplasmic reticulum. 152
Figure 4.2. PfSPP functions as a key part of the ERAD machinery in *P. falciparum*. 154
Figure 4.3. A putative model of the malaria MSP1-RBC receptor complex. 161
Figure 4.4. Merozoites are proposed to interact with band 3 via multiple ligands. 166

List of Abbreviations

ABRA	Acidic basic repeat antigen
AE1	Anion exchanger 1
AMA1	Apical membrane antigen 1
AP2	Activating protein 2
ATF6	Activating transcription factor 6
CR1	Complement receptor 1
CRMPs	Cysteine repeat modular proteins
CSP	Circumsporozoite protein
DBL	Duffy binding-like
EBL	Erythrocyte binding ligand
EL4	Extracellular loop 4
ERAD	Endoplasmic reticulum associated degradation
GPA	Glycophorin A
GPB	Glycophorin B
GPC	Glycophorin C
HGF	Hepatocyte growth factor
HSP101	Heat shock protein 101
HSPGs	Heparan sulfate proteoglycans
i-CLIPs	Intramembrane cleaving proteases
IMC	Innermembrane complex
LMW	Low molecular weight
MESH	Merozoite surface sheddase
MHC	Major histocompatibility complex
MJ	Moving junction
MSP	Merozoite surface protein
MSPDBL	Merozoite surface protein duffy binding-like
Nm	Neuraminidase
PEXEL	Plasmodium export element
PMV	Plasmepsin V

PNEP	PEXEL-negative exported proteins
PTEX	Plasmodium translocon of exported proteins complex
PV	Parasitophorous vacuole
PVM	Parasitophorous vacuole membrane
Rh	Reticulocyte binding homologue
RON2	Rhoptry neck protein 2
SAD	Sialic acid-dependent
SAID	Sialic acid-independent
SAO	Southeast Asian ovalocytosis
SP_{ase}	Signal peptidase
SPP	Signal peptide peptidase
SUB1	Subtilisin 1
SUB2	Subtilisin 2
TRAP	Thrombospondin-related anonymous protein
TRX	Thioredoxin
UOS3	Upregulated in oocyst sporozoites 3
UPR	Unfolded protein response

Introduction

Malaria

Malaria currently kills approximately 2000 patients each day (White et al., 2014). The majority of these cases are children in endemic regions like Sub-Saharan Africa and Southeast Asia. Infecting over 200 million people, malaria represents one of the most lethal infectious diseases in the world (Nunes et al., 2013). Due to the rapid rise of drug and insecticide resistance as well as socio-economic issues within endemic regions, efforts to control malaria are struggling to maintain efficacy (Bannister and Mitchell, 2003). Current therapies include drugs from a number of different classes. Chloroquine, quinine and mefloquine comprise the main members of the quinoline drug family, the most commonly used malaria treatment. During invasion the parasite acquires amino acids from the host cell via erythrocyte protein degradation, mostly from host hemoglobin. However, degradation produces the toxic by-product heme, which is converted by biocrystallization to non-toxic hemozoin. Quinolines are thought to inhibit this process, causing parasite lethality due to heme buildup (Hempelmann, 2007). Closely related to quinolines are the drugs halofantrine and lumefantrine. Their mechanism is unknown but thought to occur through inhibition of a hemozoin precursor (de Villiers et al., 2008). Artemisinin based therapies comprise another major class of malarial drugs. Activation of artemisinin occurs primarily via a reaction with the heme moiety found in the developing parasite as a result of hemoglobin breakdown. This activation of artemisinin produces oxygen radicals, thought to cause parasite lethality through as-yet unidentified mechanisms. Antifolates, like pyrimethamine, cause lethality by inhibiting tetrahydrofolic acid synthesis, a necessary precursor for DNA and RNA synthesis. Despite the availability of a variety of drugs, malaria parasites have demonstrated some

level of resistance to essentially all existing antimalarial drugs. The gradual failure of these drug treatments mainly due to resistance has led to an enormous increase in mortality and morbidity, requiring the innovation and discovery of novel therapies to combat this deadly disease (White et al., 1999).

Malaria life cycle and pathogenesis

Of the four malaria parasites, *Plasmodium falciparum* is the most lethal and will be the focus of this thesis. Its life cycle is characterized by several distinct stages (Figure 1.1). Transmitted by the bite of a mosquito, parasitic sporozoites are released into the host's circulation and invade the liver where it matures for 7-10 days in the dormant stage of human infection. Following this incubation, thousands of merozoites are released into the bloodstream. A single sporozoite in the liver can produce anywhere from 10,000 to more than 30,000 merozoites in the liver (Miller et al., 2013). Subsequently, merozoites infect erythrocytes and undergo asexual replication (Winzeler, 2008). A select number of asexual parasites in the blood stage convert to the sexual development pathway, at which point they can be transmitted via uptake during the blood meal of a female Anopheline mosquito (Aly et al., 2009). While there are currently a number of known triggers of gametocyte induction, the specific mechanism has not been completely elucidated. More specifically, alteration of culture conditions can increase gametocytogenesis including temperature changes, as well as the addition of red cell lysate, human serum, reticulocytes, and mammalian hormones (Baker, 2010; Carter and Miller, 1979; Dyer and Day, 2000; Lingnau et al., 1993; Maswoswe et al., 1985; Smalley and Brown, 1981; Talman et al., 2004; Trager and Gill, 1992).

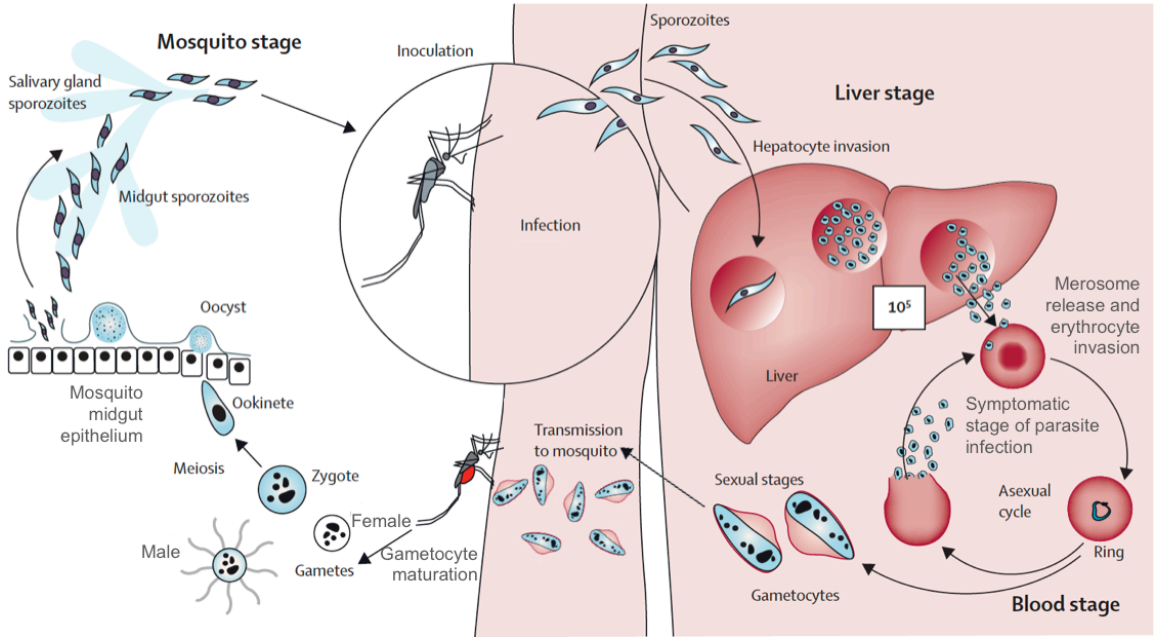

Figure 1.1. The life cycle of *P. falciparum* infection occurs in three distinct stages including the mosquito, liver and blood stage.
Transmitted by the bite of a mosquito, sporozoite stage parasites travel to the liver where they invade hepatocytes and multiply for approximately 7-10 days. Following this incubation period a liver schizont or "merosome" bursts, releasing thousands of invasive parasites or merozoites into the circulation to begin the blood stage of parasite infection. Rapid multiplication occurs in 48 hour cycles, and a very small fraction develops into the sexual stage, or gametocyte stage, of parasite infection where they can be transmitted via the bite of a mosquito. The feeding female anopheline vector allows sexual reproduction where the ookinete is formed as a result of maturation by the fertilized zygote. It then migrates through the mosquito midgut epithelium where it forms a sessile oocyst, which grows to an enormous size resulting in the release of sporozoites capable of invading the mosquito salivary glands allowing for subsequent transmission during the next blood meal. (Adapted from White et al., 2014)

More recent studies have determined one specific mechanism by which ER stress can trigger gametocytogenesis in culture (Chaubey et al., 2014). Two other studies independently determined transcriptional switches underlying sexual development. The specific proteins essential for this process were identified as apicomplexan AP2 DNA-binding proteins (ApiAP2) (Sinha et al., 2014). The PfAP2-G protein is essential for parasite sexual reproduction. It is believed that this gene is silenced via epigenetic mechanisms, and random activation is likely to be a cause of gametocyte induction (Kafsack et al., 2014). Some downstream targets are predicted; however the triggers and subsequent expression changes are not yet known. Further investigations will provide a mechanism for the regulation of this switch to the sexual stage of parasite reproduction.

Anopheles mosquito

During a blood meal the mosquito will ingest both female and male gametocytes (Figure 1.1). These gametocytes mature into female macrogametes and male microgametes, respectively (Aly et al., 2009). Fertilization of these two gametes results in the formation of a zygote. A zygote grows into an ookinete while in the midgut lumen of a mosquito following a blood meal. Maturation enables the ookinete to develop secretory organelles used to give it motility, allowing for it to move through tissue and exit the midgut. Ookinete exit from the midgut allows movement into the epithelium, where it migrates through the peritrophic matrix, activates sessile mode and induces oocyst formation. The oocyst matures over the course of about 10-12 days in what is the only extracellular environment where parasite growth and development is possible. It grows to an enormous size approximately fifty times the diameter of a merozoite. A number of

subcellular steps occur at this stage including meiosis and the expression of sporozoite-specific proteins. These proteins include circumsporozoite protein (CSP), which begins expression and accumulation on the oocysts plasma membrane during maturation (Thathy et al., 2002). The bursting of the oocyst releases thousands of motile sporozoites. A major conclusion from these studies was that protein expression dictates the transition and morphology of the sporozoite stage. However, the triggers for the regulation and expression of these proteins have not been identified. The transition is further marked by the presence of CSP on the membrane, and daughter nuclei assembly at the periphery. A protein on the inner membrane complex (IMC) termed IMC1 causes the shape determination of sporozoites and is required for their motility (Khater et al., 2004).

Sporozoite release from the oocyst allows the parasites to enter the natural circulation where they are carried to the salivary glands. The specific molecular details of salivary gland entry are unknown, however it is likely to include specific protein-protein interactions governing its interaction and invasion (Aly et al., 2009). Details have been gleaned indicating that sporozoites attach, transverse the basal lamina, and invade secretory acinar cells of the saliva glands (Pimenta et al., 1994). Invasion results in the formation of a vacuolar membrane, a process that differs considerably from parasite invasion at the liver and blood stages of the parasite life cycle. And while a detailed mechanism is not known, several essential ligands are recognized including CSP, thrombospondin-related anonymous protein (TRAP), cysteine repeat modular proteins (CRMPs) upregulated in oocyst sporozoites 3 (UOS3), and MAEBL, a protein found in the micronemes of the erythrocyte stage (Aly et al., 2009). Despite the recognition of several essential genes, the invasion and development stages within the sporozoite stage

remain largely a mystery. Nonetheless, the salivary glands of the mosquito allow for invasion and development of sporozoites until they are transmitted to the mammalian host during the next blood meal (Dyer and Day, 2000). The mosquito blood meal requires an initial bite, at which point sporozoites contained within the mosquito saliva invade the human host (Aly et al., 2009). During the bite of a mosquito, the *Anopheles* proboscis searches the skin for a blood vessel and simultaneously ejects saliva. This saliva contains a number of factors including anti-coagulants as well as enzymes facilitating blood ingestion. These secreted factors allow for proper breakdown of the components within the blood that are required by the female *Anopheline* mosquito for the development of eggs. It is during this stage that sporozoites contained within the mosquito saliva can transverse into the dermis of the human host to begin infection (Baldacci and Menard, 2004; Das et al., 2010).

Liver stage parasites

The sporozoites located in the salivary glands are released into the skin, in a range that can vary widely between 15-120 sporozoites (Prudencio et al., 2006). Some debate has lingered whether the sporozoites are deposited onto the skin or directly into circulation. This phenomenon is discussed thoroughly in a review by Prudencio *et al.* (2006), and therefore will not be the focus in this thesis. The motile parasites have the ability to enter the circulatory system, which allows for movement through the bloodstream and eventually to the liver. Sporozoites have been proposed to enter the body via the: (a) circulatory system (Mota and Rodriguez, 2002), (b) lymphatic system (Krettli and Dantas, 2000), or (c) both (Amino et al., 2006a; Amino et al., 2006b).

However, the research demonstrating infection of both the circulatory and lymphatic systems by sporozoites indicates the majority of lymphatic sporozoites are phagocytosed by dendritic cells and do not result in liver stage infection. Yet a number of studies have shown the invasive capability of sporozoites into macrophages, which supports this alternative "taxicab hypothesis". A mechanism is supported by which sporozoite invasion of macrophages carries the parasite through the lymph nodes to avoid immune surveillance and thus permitting liver infection (Krettli and Dantas, 2000).

Considerable evidence exists demonstrating that a significant portion of sporozoites released during the mosquito bite enter the bloodstream and migrate to the liver for hepatocyte invasion. This highly selective process of hepatocyte infection is thought to incorporate a number of receptor-ligand interactions analogous to the erythrocyte stage (Prudencio et al., 2006). A key molecule in this process is CSP, which interacts with heparan sulfate proteoglycans (HSPGs) in the liver. These HSPGs are proposed to extend all the way through the endothelial fenestrations where they can interact directly with sporozoites via the surface expressed CSP (Sinnis et al., 1996; Ying et al., 1997). Interestingly, a number of tissues possess HSPGs, thus the sulfation pattern of liver cell HSPGs is likely a key determinant of its affinity for CSP. It is thought that the high degree of sulfation observed on the heparin sulfate proteoglycans found on the liver confers organ specificity (Lyon et al., 1994). Additional studies have demonstrated that these sulfate moieties are required for sporozoite binding to liver cells, and can be partly inhibited through the use of heparin (Pinzon-Ortiz et al., 2001). Thus this is likely to be a key determinant in the sporozoite attachment step to hepatocytes.

Liver defense cells including Kupffer and stellate cells are unable to prevent

invasion of the liver. Given their role in cellular defense, parasite evasion of the host immune system at the liver stage is an intriguing phenomenon whose mechanism is not yet known. However, mounting evidence is growing that sporozoites must traverse through Kupffer cells, the resident liver macrophages, on their way to entering host hepatocytes (Frevert et al., 2005; Pradel and Frevert, 2001). Sporozoites can traverse through a number of hepatocytes before invading specific cells to form the parasitophorous vacuole (PV). This stage of development is also known as the exoerythrocytic form. And while it does not present with any symptoms, it is still a viable stage for targeting with antimalarial therapeutics (Vaughan et al., 2012). Liver injury is present at the micro level during infection, and this causes secretion of a number of different factors including hepatocyte growth factor (Carrolo et al., 2003). Secretion of hepatocyte growth factor (HGF) activates MET and allows for hepatocytic cytoskeletal rearrangements compatible with parasite invasion and development. The infection of hepatocytes and subsequent HGF secretion increases the likelihood of sporozoite invasion in neighboring hepatocytes where parasite multiplication can occur. Despite liver injury and infection, this stage of parasite development does not present with any clinical dysfunction.

During multiplication, a liver stage schizont develops into thousands of merozoites (Figure 1.1). Parasite release from the liver stage is one of the most poorly understood processes in the malaria life cycle. It remains controversial whether hepatocyte rupture or other mechanisms are responsible for merozoite release. However, it is known that vesicles containing merozoites, known as merosomes, contain plasma membrane from the host cell and are therefore not recognized by the Kupffer defense

cells (Sturm et al., 2006; Wickham et al., 2003). Thus, the merosome is not phagocytosed but thought to bud off from the liver into the bloodstream where merozoites are released into the blood stream to begin the symptomatic blood stage of malaria infection (Prudencio et al., 2006).

Blood stage

Upon release into the bloodstream, merozoites have approximately 60-90 seconds to adhere and invade their next host cell. This limitation is imposed because the merozoites are highly prone to immune attack and therefore must rapidly undergo successive rounds of invasion (Cowman and Crabb, 2006). An invading merozoite is one of the smaller known eukaryotic cells, measuring 1-2 μm in diameter. It contains subcellular organelles including micronemes, rhoptries, dense granules, exonemes, a plastid structure, as well as mitochondria and a nucleus (Bannister et al., 2000). Broadly, invasion can occur through two distinct pathways including the sialic acid-dependent (SAD) and sialic acid-independent (SAID) mechanisms of invasion (Oh and Chishti, 2005). As the name implies, the SAD mechanism largely relies on sugar moieties, specifically sialic acids, on the surface of the erythrocyte. Sialic acids are present in a number of organisms where they occur as a component of a specific oligosaccharide chain, commonly in glycoproteins. Frequently these occupy the terminal position (Wang and Brand-Miller, 2003). Within the erythrocyte plasma membrane, the majority of sialic acids are found on the glycophorins, with glycophorin A being the most abundant. The dependence of *P. falciparum* invasion on sialic acids and specific receptor-ligand interactions has shown to be heavily strain-specific (Oh and Chishti, 2005). A study

outlined a number of these steps via microscopy and video analysis; however the specific molecular mechanism of this process remains to be fully elucidated (Weiss et al., 2015) (Figure 1.2). Generally it is thought to occur in four steps: (1). Adhesion or initial attachment, (2). Reorientation towards the apical tip, (3). Tight junction formation, and (4). Propulsion and re-sealing (Figure 1.2).

Adhesion

The merozoite surface is coated with a number of different proteins and a majority of them are glycosylphosphatidylinositol (GPI) anchored to the membrane surface (Gilson et al., 2006). Among these proteins, Merozoite surface protein 1 (MSP1) is the most abundant and well-studied protein on the merozoite surface and will be the primary focus of this thesis (Holder, 1988). A number of other proteins are also bound to the merozoite surface via their GPI anchor or as associated proteins. These include Pf12, Pf38, Pf41 MSPDBL-1 and MSPDBL-2 in addition to several others (Cowman et al., 2012). The MSPDBL proteins were identified as part of the larger MSP1 complex, and they bind to human erythrocytes with high specificity and affinity (Lin et al., 2014). However, their cognate receptor(s) remains unknown. Other parasite proteins associated with MSP1, such as MSP9, have been investigated in the context of their role on the merozoite surface. MSP9 does not carry a GPI anchor or any obvious transmembrane domain, but it forms a complex with MSP1 and binds to band 3 (Kariuki et al., 2005; Li et al., 2004). While the receptor-ligand interactions that occur in the reorientation stage have been characterized in detail, the interactions governing the initial adhesion stage are largely unknown.

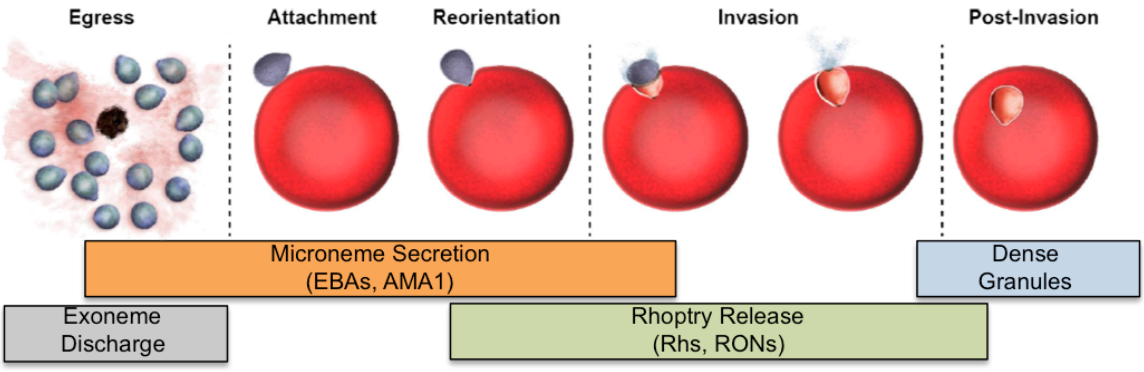

Figure 1.2. Merozoite invasion of the erythrocyte occurs in several distinct steps. Merozoite invasion can be subdivided into key steps including the attachment, reorientation, and invasion. Distinct subcellular organelles are released at specific stages during the invasion process. Exoneme secretion occurs during merozoite egress and release from the host, while microneme secretion is thought to occur as a result of environmental triggers in the host circulation. Release of the rhoptry results in the formation of the parasitophorous vacuole, and the "sealing" of the membrane following the completion of the invasion process. The precise mechanisms of this process have not been identified. (Adapted from Cowman et al., 2012)

Given the propensity of merozoites to bind to erythrocytes regardless of orientation, this feature implies that the interactions necessary for this adhesion are distributed across the surface of the merozoite and do not require ligands secreted from the apical tip including the micronemal and rhoptry contents. Inhibition of some micronemal ligands is known to have no effect on the initial adhesion (Mitchell et al., 2004). We hypothesize that a large number of low-affinity interactions are responsible for the initial adhesion, in agreement with others (Cowman et al., 2012). Although not confirmed, this step is thought to occur via random collisions between the merozoite and host cell that allows for transient low affinity interactions.

In this thesis I will focus on the role of MSP1, which we hypothesize to be involved in the initial adhesion step to host erythrocytes. This view has been proposed previously; however it has not been experimentally tested in terms of ligand-receptor interactions (Cowman and Crabb, 2006). MSP1 is known to bind to band 3 during the invasion process via its C-terminal 19 kDa domain, $MSP1_{19}$ (Goel et al., 2003). Furthermore, antibodies against MSP1 inhibit parasite invasion, as do small molecule inhibitors targeted at the C-terminal domain (Chandramohanadas et al., 2014; Woehlbier et al., 2006). Given its abundance and putative role in invasion, it is likely to be a key protein involved in merozoite adhesion. Further discussion of MSP1 properties and function is included in the section below titled “Merozoite Surface Protein 1”.

Reorientation

Merozoite adhesion occurs irrespective of its apical orientation, and thus the key ligands responsible for adhesion are likely to be distributed across its surface (Figure

1.3). This step is followed by the merozoite undergoing reorientation via a "rolling" action. The molecular process involved in this step is largely theoretical, however one specific mechanism has been proposed. The authors hypothesized that secretion of erythrocyte binding ligands onto the apical tip of the merozoite creates a gradient where high affinity ligands are most abundant at the apical tip and lowest at the basal pole (Dutta et al., 2005; Mitchell et al., 2004). This gradient would theoretically drive the reorientation process towards the apical tip, the membrane region containing the highest concentration of parasite ligands. These ligands will be discussed below under two groups including the microneme and rhoptry proteins.

Merozoite release from infected erythrocytes exposes the parasite to extracellular conditions found in the bloodstream. Relative to the intra-erythrocyte milieu, this environment contains low levels of potassium and triggers a signaling cascade releasing calcium from its subcellular compartments. The calcium flux leads to secretion of various parasite ligands in the micronemes, rhoptries, exonemes, and dense granules (Singh et al., 2010; Singh and Chitnis, 2012; Treeck et al., 2009). These proteins can be sub-divided among a number of different classes but generally fall into two main protein families including the erythrocyte binding ligands (EBLs) found in the microneme and reticulocyte binding homologues (Rhs) located largely in the rhoptry. These include EBA-175, EBL-1, EBA-140, EBA-181, Rh1, Rh2a, Rh2b, Rh4, and Rh5 (Figure 1.3), reviewed comprehensively elsewhere (Tham et al., 2012). A comprehensive list of known receptor-ligand interactions, enzyme sensitivities, and antibody inhibition can be seen in Table 1 (Collins et al., 2007; Douglas et al., 2014; Gao et al., 2008; Jiang et al., 2011; Tham et al., 2010; Triglia et al., 2011; Woehlbier et al., 2006).

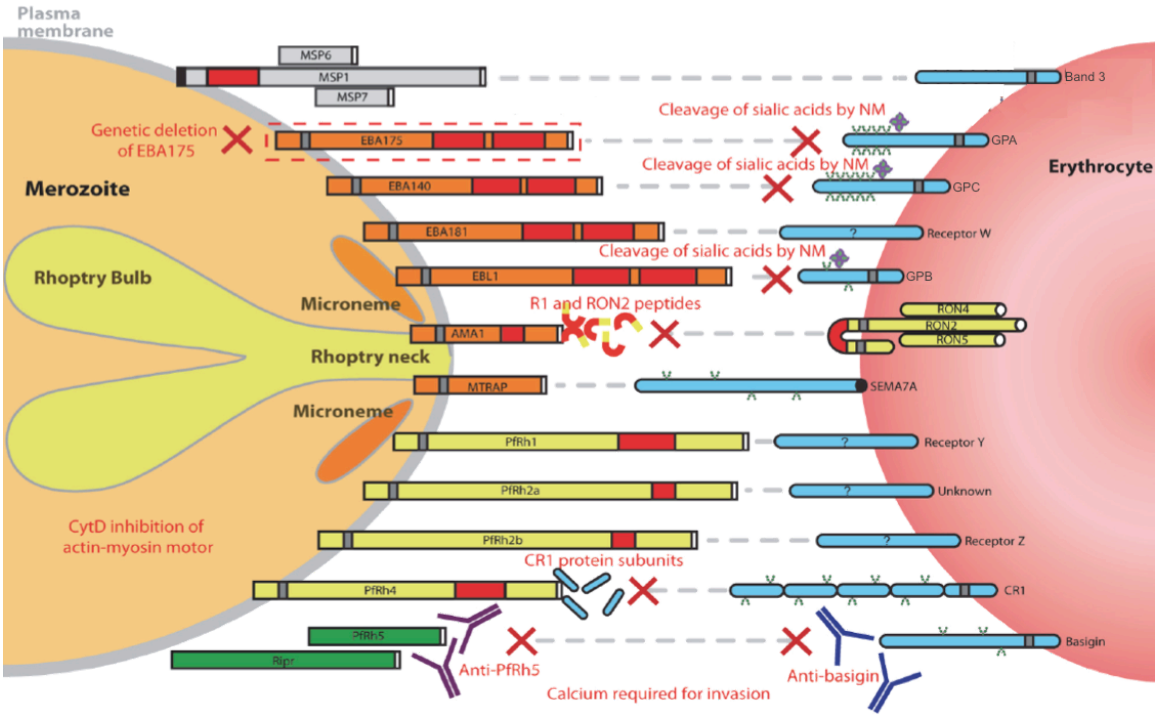

Figure 1.3. A comprehensive view of the receptor-ligand interactions identified as occurring during *P. falciparum* erythrocyte invasion.
Merozoites possess a diverse set of surface ligands involved in host invasion. Surface ligands (grey), micronemal proteins (orange), and rhoptry ligands (yellow) are likely to play sequential roles in attachment, reorientation, and invasion. Receptors are designated in blue, and several host proteins binding to merozoite ligands have not been identified or are characterized only by their sensitivity to specific proteases. MSP, merozoite surface protein; EBA, erythrocyte binding antigen; EBL, erythrocyte binding ligand; AMA1, apical membrane antigen 1; Rh, reticulocyte-binding homologue; Ripr, Rh5 interacting protein; MTRAP, merozoite thrombospondin-related anonymous protein; GPA, glycophorin A; GPB, glycophorin B; GPC, glycophorin C; RON, rhoptry neck protein; CR1, complement receptor 1. (Adapted from Weiss et al., 2015)

Table 1. Erythrocyte receptors involved in *Plasmodium falciparum* invasion, their cognate ligands and enzyme sensitivity.

Receptor	Ligand	Neuraminidase	Trypsin	Chymotrypsin	Antibody inhibition *in vitro*?
Band 3	MSP1	R	R	S	Y
Band 3	MSP9/ABRA	R	R	S	
Glycophorin A	EBA-175	S	S	R	Y
Glycophorin B	EBL-1	S	R	S	
Glycophorin C	EBA-140	S	S	R	
Receptor W	EBA-181	S	R	S	
Receptor Y	Rh1	S	R	S	Y
Receptor Z	Rh2a/Rh2b	S*	R	S	Y
CR1	Rh4	R	S	S	Y
Basigin	Rh5	R	R	R	Y
RON2	AMA-1	R	R	R	Y
CD55	Unknown	N/A	N/A	N/A	

*The neuraminidase sensitivity of this receptor-ligand interaction remains controversial
R= resistant, S = sensitive, Y = Antibodies demonstrate inhibition of invasion *in vitro*

These protein ligands and their nomenclature have changed significantly over the course of their discovery and characterization; however the nomenclature indicated above will be used throughout this thesis. Several receptors of these ligands are known. For example, EBA-175 binding to glycophorin A (GPA), EBL-1 binding to glycophorin B (GPB), and EBA-140 binding to glycophorin C (GPC) are well characterized (Duraisingh et al., 2003a; Gilberger et al., 2003; Li et al., 2012; Lobo et al., 2003; Mayer et al., 2009). Similarly, Rh4 binds to complement receptor 1 (CR1), and Rh5 binds to CD147 also known as Basigin while the receptors for EBA-181, Rh1, Rh2a, and Rh2b are currently unknown (Figure 1.3) (Crosnier et al., 2011; Duraisingh et al., 2003b; Maier et al., 2009a; Triglia et al., 2005). Interestingly, the majority of these interactions demonstrate some level of redundancy. However, Rh5 binding to Basigin has proven to be indispensable for parasite invasion (Crosnier et al., 2011; Reddy et al., 2014). The specific step-by-step mechanism by which these microneme and rhoptry ligands bind to their cognate receptors is not known, and requires an in-depth analysis using microscopic and molecular tools. Therefore, several specific pairs of ligand-receptor interactions have been independently identified along with their functional role in invasion (Figure 1.3). A recent study determined that these interactions are key events in the subsequent strong deformation of the host erythrocyte following initial adhesion (Weiss et al., 2015). Given the large number and variety of these interactions exhibiting high redundancy, they will be discussed in the next two sections below.

Micronemal Invasion Ligands

EBA-175 is one of the most well investigated parasite ligands. Initial studies

elucidated its invasion-specific function (Orlandi et al., 1992; Sim et al., 1990) as binding to erythrocytes in a sialic acid-dependent fashion (Sim et al., 1994b). Interestingly, antibodies against EBA-175 inhibit parasite invasion, but genetic disruption of EBA-175 revealed no effect on parasite invasion (Kaneko et al., 2000; Narum et al., 2000). A number of studies have confirmed the binding of EBA-175 to the sialic acid domain of GPA (Duraisingh et al., 2003a; Ockenhouse et al., 2001). Some evidence for the interaction of EBA-175 to the GPA peptide backbone also exists (Sim et al., 1994b). Interestingly, one study used sialic acid analogues comparable to those found on GPA, and demonstrated inhibition of parasite invasion (Bharara et al., 2004). Detailed characterization of the interaction between EBA-175 and GPA has designated a signaling role for this interaction. Upon merozoite release into the extracellular environment, the release of intracellular stores of calcium is thought to signal for the secretion of micronemal proteins like EBA-175 to the apical surface of the invading merozoite. Furthermore, one study found that the binding of EBA-175 to GPA returns merozoite cytosolic calcium levels to basal levels and subsequently triggers the release of rhoptry proteins (Singh et al., 2010). However, conflicting reports exist indicating the opposite phenomenon, stating that rhoptry ligand binding signals the release of micronemal contents, thus further studies are required to clarify this phenomenon conclusively (Gao et al., 2013). A key finding determined that parasites lacking EBA-175 due to genetic disruption, switch to a sialic acid-independent mechanism of invasion (Duraisingh et al., 2003a). The conclusion drawn from this study is that EBA-175 represents the major chymotrypsin-resistant invasion pathway. However, subsequent studies have confirmed the presence of a number of other ligands that are also resistant to chymotrypsin

treatment (Lobo et al., 2003). Furthermore, the disruption of EBA-175 results in increased transcription of Rh4, which can be selected for via growth on neuraminidase (Nm)-treated erythrocytes (Lopaticki et al., 2011; Stubbs et al., 2005). One of the key interpretations of this body of work is the concept that *P. falciparum* depends on a number of receptor-ligand interactions for invasion which exhibit significant redundancy and compensatory mechanisms.

Each subsequent discovery has added weight to this theory, including the identification of a binding interaction between EBL-1 and GPB. The discovery of EBL-1 led to its recognition as a close relative of the EBA-175 protein, falling into the larger class of erythrocyte-binding antigens (Peterson and Wellems, 2000). It took nearly nine years for a group to identify GPB as its cognate receptor (Mayer et al., 2009). This interaction was characterized further in subsequent studies as being neuraminidase and chymotrypsin sensitive, but trypsin resistant (Li et al., 2012). Additionally, peptides contained within the erythrocyte-binding region of EBL-1 inhibited parasite invasion *in vitro* (Li et al., 2012).

Two other erythrocyte-binding antigens have been identified and studied, including EBA-140 and EBA-181. EBA-140 is recognized as the parasite ligand that binds to GPC in a sialic acid-dependent fashion, and is sensitive to trypsin treatment (Lobo et al., 2003; Malpede et al., 2013). The host receptor for EBA-181 has not been identified, however it binds to erythrocytes in a neuraminidase and chymotrypsin sensitive manner (Maier et al., 2009a). One study demonstrated its binding to protein 4.1 in the erythrocyte, although this interaction is unlikely to be directly involved in the initial steps of invasion given its location on the cytosolic side of the erythrocyte

membrane (Lanzillotti and Coetzer, 2006). While its localization has been conclusively demonstrated, the receptor sensitivity and specificity of EBA-181 remains controversial (Maier et al., 2009a; Mayer et al., 2004). Although genetic disruption of EBA-175 significantly increases the mRNA expression of Rh4, this phenomenon is not observed following the disruption of EBA-181 or EBA-140, respectively (Lopaticki et al., 2011). AMA1 is another micronemal protein required for parasite invasion; however given its function in formation of the tight junction, it will be discussed in a separate section (Cao et al., 2009).

Rhoptry Invasion Ligands

Apicomplexan protozoan parasites contain a club-shaped secretory organelle localized to the apical end of the merozoite termed the rhoptry. Generally, rhoptry contents are important for host-parasite interactions (Bradley et al., 2005). Several of the aforementioned rhoptry proteins have been studied in the context of invasion. Reticulocyte binding homologue 4 (Rh4) has been studied extensively, specifically given that its transcriptional expression is altered by the expression of EBA-175 (Lopaticki et al., 2011). This altered expression is linked to a change in the SAID mechanism of invasion (Gaur et al., 2006). Its cognate receptor has been identified as complement receptor 1 (CR1). CR1 was identified as an erythrocyte receptor as part of the SAID pathway and subsequently, Rh4 was identified as its binding ligand (Spadafora et al., 2010; Tham et al., 2010). Soluble CR1 inhibits invasion in strains where EBA-175 was disrupted, or erythrocytes had been treated with neuraminidase. This indicates that its specific function is likely in the SAID mechanism of invasion (Tham et al., 2010). While

Rh1, Rh2a, Rh2b and Rh5 show clear rhoptry localization, Rh4 has a distinct localization pattern that overlaps with both the rhoptry and micronemal organelles (Rodriguez et al., 2008). This unique localization requires further investigation (Gaur et al., 2007).

Rh1, Rh2a, and Rh2b have all been studied in the context of parasite ligands that bind to human erythrocytes. Each is neuraminidase sensitive and trypsin resistant. However, Rh2b binding demonstrates chymotrypsin resistance while binding of Rh1 and Rh2a are sensitive to chymotrypsin pre-treatment of erythrocytes (Duraisingh et al., 2003b; Triglia et al., 2005). Some functional studies have been performed on these ligands, including the discovery that Rh1 is important for the SAD mechanism of invasion (Triglia et al., 2005). Some elucidation of the importance of protease processing of Rh1 has been discussed in the literature, however this has not been conclusively demonstrated (Triglia et al., 2005). Rh2a and Rh2b show a high level of sequence identity across parasite strains, but varying levels of expression (Duraisingh et al., 2003b). Thus it is unlikely that these ligands are essential for parasite invasion. Rh1 is expressed consistently across all parasite strains, and may be a key determinant of SAD invasion. Rh1 disruption results in the utilization of interactions that are resistant to neuraminidase treatment (Triglia et al., 2005). As indicated above, one study showed that binding of Rh1 to the erythrocyte surface signals for microneme release, and not the EBA-175-GPA interaction as previously thought. This study proposed that Rh1 binding triggers the intracellular calcium flux and subsequent release of micronemal proteins (i.e., EBLs) (Gao et al., 2013). This finding is in direct conflict with the evidence that the EBA-175/GPA interaction triggers rhoptry release and thus remains controversial (Singh et al., 2010). Finally, antibodies against Rh1 also demonstrate significant inhibition of

parasite invasion *in vitro* (Gao et al., 2008).

One of the highest impact findings of the malaria field in recent years was the discovery and characterization of the reticulocyte binding homologue 5 (Rh5). Identified as an erythrocyte binding parasite ligand, Rh5 was shown to bind to the erythrocyte surface protein, CD147, or Basigin (Figure 1.3) (Crosnier et al., 2011; Hayton et al., 2008; Rodriguez et al., 2008). This discovery was perplexing as Rh5 lacks a transmembrane domain and thus was hypothesized to associate with a separate merozoite surface protein for membrane anchoring. Using immunoprecipitation and mass spectrometry, a membrane protein *P. falciparum* Rh5 interacting protein (PfRipr) was identified as an associated polypeptide. However, PfRipr also does not contain a specific GPI-anchor or transmembrane domain (Chen et al., 2011). It was only recently that an associated GPI-anchored protein was identified as being putatively responsible for anchoring Rh5 to the merozoite surface (Reddy et al., 2015). The successful discovery and analysis of this interaction has led to an increased optimism of using Rh5 as a blood stage malaria vaccine candidate. Erythrocytes lacking Basigin show a drastically reduced level of parasite invasion, while soluble Basigin and antibodies also potently block parasite invasion (Crosnier et al., 2011). Antibodies inhibiting this interaction block invasion by preventing tight junction formation (Douglas et al., 2014). Furthermore, this study elucidated the specific amino acid motif where the inhibitory antibodies bind. More importantly, the essentiality of Rh5 has been illustrated across a number of strains (Crosnier et al., 2011). Therefore, Rh5 represents a highly attractive target as part of an antimalarial vaccine. Currently there are three parasite ligands that are necessary for invasion across all strains of *P. falciparum* and these include MSP1, AMA1 and Rh5.

MSP1 and AMA1 demonstrate considerable variation in their sequences, however Rh5 is highly conserved and antibodies against this protein inhibit invasion in a strain-transcendent manner (Douglas et al., 2014). Thus Rh5 is currently the most promising merozoite antigen towards the development of a malaria vaccine.

While other micronemal and rhoptry ligands are responsible for strong erythrocyte deformation, Rh5 is not required for this step. However, it is essential for tight junction formation, and is thought to occur prior to the apical membrane antigen 1-rhoptry neck protein 2 (AMA1-RON2) interaction, as discussed in the next section (Weiss et al., 2015). It has been proposed that the Rh5-Basigin interaction results in the pore formation between the host and parasite cell by which small molecules can travel. These findings are at a preliminary stage, and authors suggest that invasion components may flow through this pore, however this model has not been conclusively proven.

Other rhoptry protein classes have also been linked to a role in invasion. Generally, the rhoptry contains proteins in three distinct classes. These include the reticulocyte binding homologues, the rhoptry high molecular weight (RhopH) protein complexes, and low molecular weight complexes (LMW) (Kats et al., 2006). Rhoptry proteins located in the "bulb" of the organelle have been studied in the context of invasion. However, their release is timed to occur later than the reticulocyte binding homologues (Proellocks et al., 2010). The high molecular weight (HMW) complex consists of RhopH1, RhopH2, and RhopH3. The function of these proteins is largely unknown, however some evidence exists implying the HMW complex as an "adhesin" or erythrocyte binding protein during invasion (Siddiqui et al., 1987). Subsequent work has further linked RhopH3 with a role as part of an invasion protein complex (Ranjan et al.,

2011). Some evidence exists implicating Rhoptry associated protein 2 (RAP2) of the LMW and RAM in erythrocyte binding and invasion (Kats et al., 2006; Topolska et al., 2004). However, systematically identifying proteins specifically located in the rhoptry is problematic due to the high degree of technical difficulty associated with purifying the rhoptry organelles. Currently there is no explanation available for the sub-compartmentalization of the rhoptry organelle. One study suggests trafficking from the Golgi to the rhoptry bulb, however this has not been definitively proven (Kats et al., 2006).

Additional rhoptry proteins have been investigated in the context of erythrocyte binding and their role in invasion, however they are still at the preliminary stage and have not been conclusively studied (Arevalo-Pinzon et al., 2010; Zhao et al., 2014). The rising number of interactions occurring during invasion is encouraging, but also demonstrates the difficulty in designing a potent inhibitory vaccine. Thus the field is lacking a cohesive step-by-step mechanism over the course of merozoite binding and re-orientation. Once successful re-orientation occurs and the tight junction forms, the parasite can successfully invaginate the host cell, as outlined in the next section.

Tight junction formation and Propulsion

AMA1, a micronemal protein, will be discussed in this section due to its significant role in the formation of the tight junction and its binding to a parasite secreted protein and not an erythrocyte receptor. The invasion protein AMA1 binds to another parasite protein termed RON2, which is secreted onto the erythrocyte membrane during the re-orientation process and tight junction formation (Figure 1.3) (Lamarque et al.,

2011; Mitchell et al., 2004; Richard et al., 2010; Srinivasan et al., 2013). This interaction is essential for parasite invasion as inhibitors interfering with this interaction prevent parasite invasion *in vitro*. This interaction is required for the formation of the tight junction allowing movement of the merozoite into the host cell, also known as the moving junction (MJ) (Figure 1.4) (Gaur and Chitnis, 2011). The MJ, a highly conserved process across apicomplexans, remains in place via its anchor to the host membrane, and is driven by parasite propulsion. The underlying cytoskeleton within the merozoite propels the parasite via its acto-myosin motor involving components of the cytoskeletal network originating from the parasite membrane and its IMC. Furthermore, the host cell cytoskeleton is bound to the parasite RON protein complex required for anchoring of this propulsion mechanism. This process is laid out in detail in Figure 1.4. This acto-myosin motor, known as the glideosome, uses adhesins like AMA1 to leverage the propulsion force towards the posterior end of the parasite so it is engulfed by the host (Figure 1.4) (Besteiro et al., 2011). While the majority of this work was characterized in alternative apicomplexans, the gliding process is highly conserved across multiple species. Mechanistically, aldolase links actin and TRAP in *P. falciparum* to couple the recognition with the motor system. It is termed "treadmilling" of the adhesins. In this case, treadmilling involves AMA1 binding to RON2 held in place by a number of other RON proteins including RON4 and RON5 (Besteiro et al., 2011; Gaur and Chitnis, 2011). Studies have demonstrated that the driving force of invasion comes as a result of myosin, GAP45, the IMC, and the plasma membrane.

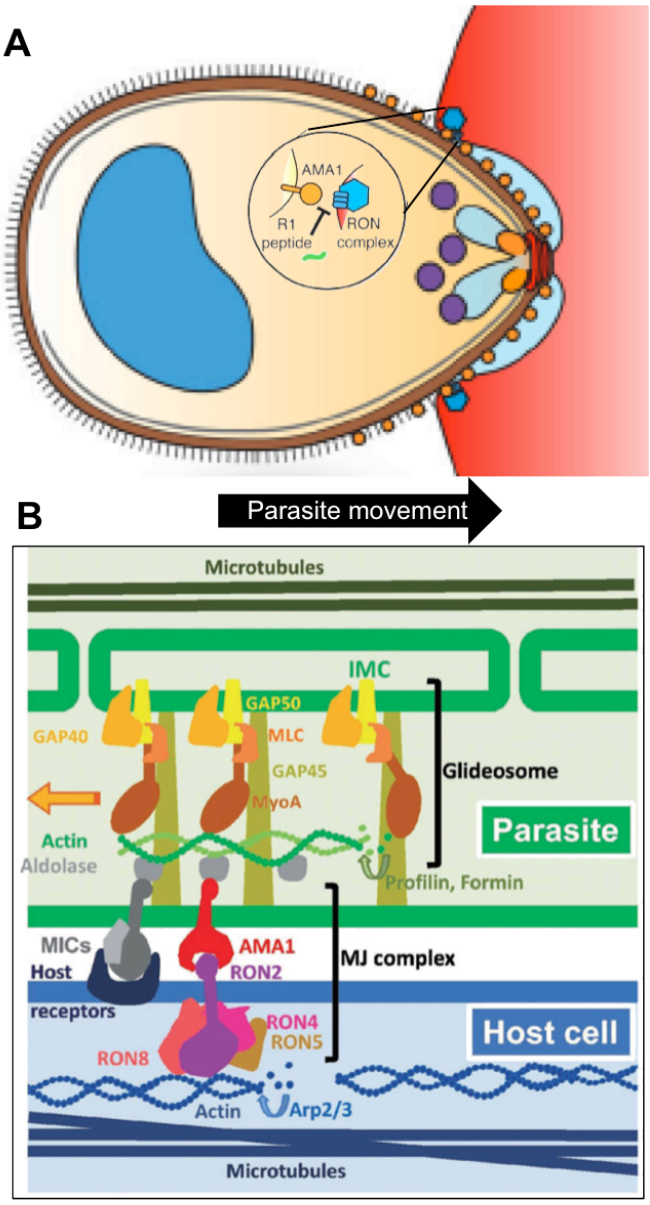

Figure 1.4. Tight junction formation and cytoskeletal propulsion allows for entry into the host cell.
(A) Tight junction formation between the merozoite and host erythrocyte. Binding of AMA1 to the RON complex is a key step in this process enabling both the release of the rhoptry bulb as well as providing traction for the action of the acto-myosin motor (Adapted from Richard et al., 2010). (B) The moving junction (MJ) requires the attachment of the MJ complex to the respective host and parasite cytoskeletal components enabling parasite motility. This action allows propulsion of the invading merozoite to completely invaginate within the host cell. (Adapted from Besteiro et al., 2011)

The concentration of actin filaments forms a ring-like distribution, thus enabling the head of the myosin to generate propulsion until the merozoite is drawn into the erythrocyte and the red cell membrane has re-sealed (Dasgupta et al., 2014). The posterior end of the invading merozoite reaches the tight junction and the membrane is resealed by an as yet unidentified mechanism. However, this is proposed to occur via the fusion of the erythrocyte and parasitophorous vacuole membranes (Riglar et al., 2011). Following a brief period of echinocytosis in the minutes following invasion, the erythrocyte membrane returns to its normal shape and subsequent development-related morphological alterations occur (Gilson and Crabb, 2009).

Parasite Development and Egress

The parasite life cycle is characterized by the ring, trophozoite, and schizont stages before undergoing subsequent rounds of invasion (Figure 1.5). Immediately following invasion, the ring stage takes place when a biconcave disc of the intracellular parasite forms resembling a ring shape. During the first 24 hours post-invasion, parasite export begins thus setting the stage for evasion from spleen filtration and immune detection by promoting adhesion to other RBCs and/or endothelial cells (Bannister and Mitchell, 2003). Beginning at the late ring-stage, parasites are able to evade the host immune and filtration systems via cytoadherence to the host microvasculature (Pouvelle et al., 2000).

Maturation into the trophozoite stage results in the observation of hemozoin crystals as a result of hemoglobin breakdown. The trophozoite stage occurs between 24-36 hours post-invasion. Detectable knobs, containing parasite proteins like *P. falciparum*

erythrocyte membrane protein 1 (PfEMP1), bind to receptors on the host endothelium promoting stronger adhesion. Additional parasite proteins expressed at the erythrocyte surface include ion channels and cytoadherence-linked asexual genes that increase erythrocyte membrane permeability (Desai, 2014; Gupta et al., 2015). This stage is characterized by a highly active state of growth and erythrocyte alterations. More specifically, Maurer's clefts are observed at this stage (Aikawa et al., 1986). Maurer's clefts are membrane structures of parasite origin found in the erythrocyte cytosol and thought to be involved in protein trafficking to the erythrocyte membrane (Mundwiler-Pachlatko and Beck, 2013). Often the transition from the trophozoite to schizont stage is unclear. However, the timing of the schizont stage takes place between 36-48 hours post invasion and can be identified by the presence of as many as 16 separate nuclei and the generation of molecules key to merozoite invasion (Bannister and Mitchell, 2003). Thus the schizont stage is often recognized as preceding merozoite exit from the host erythrocyte. This process can be inhibited and investigated at the molecular level via the use of specific protease inhibitors. While initial reports hypothesized that the host erythrocyte ruptures first, followed by escape from the PVM, other studies have demonstrated conflicting results. This includes PVM rupture prior to lysis as well as concurrent lysis (Glushakova et al., 2005; Salmon et al., 2001; Soni et al., 2005; Wickham et al., 2003). Given their occurrence in rapid succession, it is quite difficult to conclusively determine their specific sequence.

Upon successful invasion, the parasite immediately begins host remodeling, in which a large number of proteins are exported into the erythrocyte cytosol via a highly complex trafficking network (Boddey and Cowman, 2013).

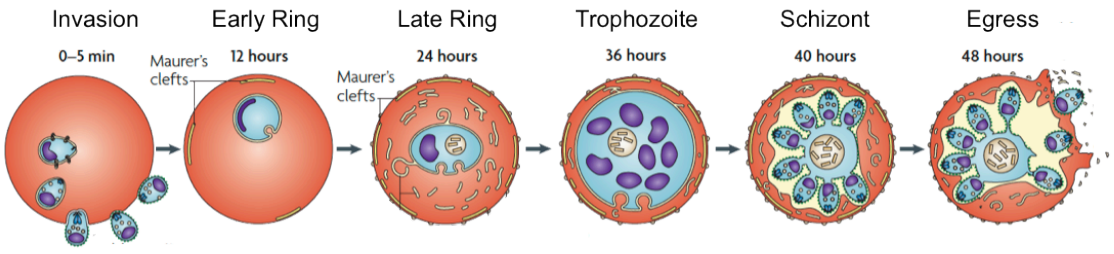

Figure 1.5. The asexual stages of P. falciparum development account for the clinical manifestation of the disease.
The erythrocyte stage of parasite infection can be characterized by a 48-hour cycle divided into several stages including the ring (0-24h) trophozoite (24h-36h) and schizont (36h-48h) stages. Generally the bursting schizont is estimated to release anywhere from 12-30 daughter cells/merozoites, for subsequent rounds of invasion. Merozoite invasion is known to occur in 1-2 minutes following the release from a mature schizont. Maurer's clefts are first observed at the early ring stage and allow for trafficking of proteins into the host erythrocyte. Deformation of the host erythrocyte as a result of knob formation begins in the later ring stages. (Adapted from Maier et al., 2009)

Imaging studies have examined the structural changes induced during parasite maturation at very high resolution (Gruring et al., 2011). The parasitophorous vacuole envelops the parasite within the host cell and almost immediately, the parasite initiates a complex trafficking pathway by which multiple proteins can be secreted into the erythrocyte cytoplasm. A number of studies have investigated this phenomenon and one key investigation resulted in the identification of a complex at the parasitophorous vacuole required for parasite protein export into the host cell (de Koning-Ward et al., 2009). Proteins are translated containing a signal element designating it for export, termed the *Plasmodium* export element (PEXEL). However, there are several proteins trafficked to the erythrocyte cytosol lacking a PEXEL. These are termed PEXEL-negative exported proteins (PNEP) and are exported through the same process but do not contain this specific domain (Deponte et al., 2012; Spielmann and Gilberger, 2010). During the mature stage, the parasite also consumes a large amount of erythrocyte hemoglobin.

It is estimated that 70% of the host's hemoglobin is digested by the parasite, releasing amino acids that are required for the parasite protein translation machinery (Mohandas and An, 2012). A detailed characterization of hemoglobin uptake has been performed that includes four specific processes by which the parasite acquires hemoglobin over the 48-hour life cycle (Elliott et al., 2008). The heme moiety at the center of the hemoglobin is detoxified via a biocrystallization process resulting in the formation of hemozoin crystals within the food vacuole of maturing parasites. This process is the site of chloroquine antimalarial activity (Sullivan et al., 1996).

Significant structural changes in the host can be observed, with thousands of

"knobs" appearing on the infected erythrocyte surface (Mohandas and An, 2012). The function of these structures is to increase the adherence of an infected cell in order to evade immune surveillance and clearance by the spleen. It is composed of a number of proteins including knob-associated histidine rich protein (KAHRP) and PfEMP1. A large number of other proteins are also known to play a role in host remodeling that allow for immune evasion and spleen clearance including *P. falciparum* erythrocyte membrane protein 3 (PfEMP3), ring-infected erythrocyte surface antigen (RESA), mature parasite-infected erythrocyte surface antigen (MESA), membrane-associated histidine-rich protein 1 (MAHRP1), ring-exported protein 1 (REX1), and *P. falciparum* skeleton binding protein 1 (PfSBP1). These subunits make up a large multi-component protein complex required for proper architecture and formation of specific adhesion-related organelles, and are tethered to the erythrocyte membrane (Maier et al., 2009b; Voigt et al., 2000).

Parasite exit from the host cell involves disruption of both the host membrane and the parasitophorous vacuole (Yeoh et al., 2007). This egress is the result of both increased pressure and cytoskeletal degradation, although the precise molecular details are not completely understood. However, escape from the parasitophorous vacuole membrane (PVM) is inhibited by a class of cysteine-protease inhibitors and therefore requires protease activity (Salmon et al., 2001).

Parasite Proteases

The intraerythrocytic stage of parasite infection accounts for the clinical manifestation of the disease. Key to the development of this stage is the activity of several intracellular proteases. While parasites express a variety of metallo-, serine, and

cysteine proteases, the focus of the work done in this thesis revolves around aspartic acid proteases, specifically signal peptide peptidase (SPP). Parasite aspartic acid proteases have long been considered viable drug targets. In 2008, SPP was confirmed as a viable drug target in *P. falciparum* and its role within the parasite will be discussed further (Li et al., 2009). Here we will broadly discuss the class of SPP proteases across a number of organisms in order to summarize their putative function.

I-CLIPs

SPP falls into a class of proteases termed intramembrane-cleaving proteases, or i-CLIPs. This group was defined by Golde *et al.* (2009) as polytopic membrane proteases that carry out peptide bond hydrolysis in the hydrophobic plane of the membrane. This family of proteases also include presenilins (Golde et al., 2009). Presenilins represent a homologous class of proteins to SPP. Presenilins and SPP exhibit opposite membrane topology as their active site aspartic acid residues show inverted membrane topology. Presenilins cleave Type I transmembrane proteins whereas SPP cleaves Type II transmembrane proteins (Figure 1.6) (Friedmann et al., 2004; Wolfe, 2010). Furthermore, presenilins require the presence of additional cofactors including nicastrin, Aph-1 and Pen-2 to form the γ-secretase complex for protease activity (Martoglio and Golde, 2003; Wolfe and Kopan, 2004). Their activities have been investigated extensively with regards to their role in amyloid-β production and its link to Alzheimer's disease (Citron et al., 1997; Scheuner et al., 1996). SPP functions as an independent protease without the requirement for additional cofactors (Xia and Wolfe, 2003). Furthermore, it has proven to be an essential protease for a number of different organisms including *C. elegans*, *D.*

rerio, and *D. melanogaster* (Casso et al., 2005; Grigorenko et al., 2004; Krawitz et al., 2005).

Other homologues of SPP like SPPL2A, SPPL2B, SPPL2C, SPPL3 have also been identified in the human genome and compared in the context of intramembrane cleavage (Fluhrer et al., 2006; Friedmann et al., 2006; Martin et al., 2009; Schneppenheim et al., 2014b). Additional homologues have been investigated in other species including SPPL4 in *Arabidopsis thaliana* (Tamura et al., 2008). These proteases share similar protease activity, topology, with a conserved aspartic acid motif at its catalytic center within the membrane. Despite the hydrophobic nature of their catalytic residues, their mechanism of action is similar to that of all members of the aspartic acid family of proteases, and they are able to carry out peptide bond hydrolysis within the membrane. Some structural studies have hinted at a pore within the membrane of i-CLIPs that would allow water to access the active site, and facilitate aspartic acid protease catalysis (Lazarov et al., 2006). Generally, ectodomain shedding is required prior to the activity of the i-CLIPs, and this step is performed by a number of different proteases including SP_{ase} for SPP, A Disintegrin and Metalloprotease (ADAMs) for SPPL2A and SPPL2B, and β-secretase for presenilins in the γ-secretase complex (Fluhrer et al., 2003; Kirkin et al., 2007; Martin et al., 2008).

Members of the i-CLIP family vary in their subcellular localization. Generally, SPP and SPPL's can be detected across the cell at nearly all vesicular membranes. This distribution may provide some measure of redundancy; however substrate specificity can vary significantly between the family members. SPP is localized at the ER along with SPPL2C (Friedmann et al., 2006; Krawitz et al., 2005).

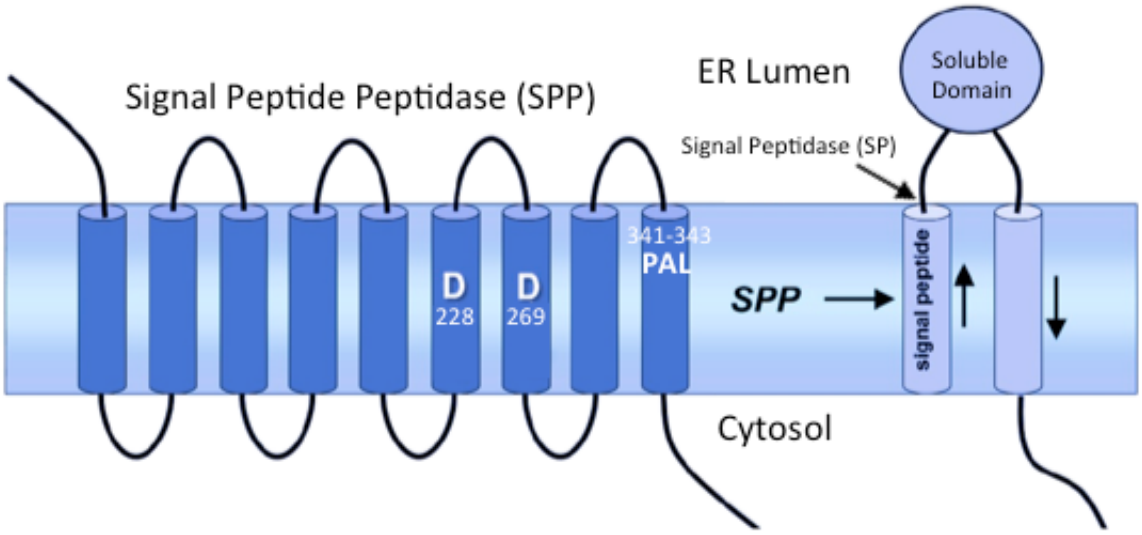

Figure 1.6. Signal peptide peptidase (SPP) is a multi-transmembrane protein that cleaves signal peptides within the ER membrane.
Signal peptides are processed in the ER following the action of a signal peptidase (SP). SPP is predicted to have 9 transmembrane helices with the key catalytic aspartic acid residues being present in TM domains 6 and 7. A PAL domain, required for SPP activity, is found in the C-terminal transmembrane. The specific residues in *P. falciparum* are labeled by their amino acid number within the polypeptide sequence. (Adapted from Wolfe et al., 2010)

SPPL3 demonstrates limited expression at the ER, however more recent evidence indicates the presence of this protease at the Golgi (Krawitz et al., 2005; Kuhn et al., 2015). Other members of the family are found in the secretory pathway including the SPPL2A and SPPL2B homologues are seen in the endosomes, lysosomes, and even at the plasma membrane (Krawitz et al., 2005). While initial studies indicated a broad expression profile of SPPL2A and SPPL2B across a number of organelles, it appears that this may be due to a cellular model in which these were overexpressed. Experiments investigating these proteases under endogenous conditions localize SPPL2A expression specifically to lysosomes and late endosomes, and SPPL2B to the plasma membrane, with relatively little overlap between the closely related genes (Schneppenheim et al., 2014b). Some physiological substrates have been identified for these proteases. A recent study demonstrated catalytic activity of SPPL3 against specific glycosylating enzymes found in the Golgi as well as a foamy virus envelope protein (Kuhn et al., 2015; Voss et al., 2012; Voss et al., 2014). Interestingly, the cleavage activity of SPPL3 did not appear to require ectodomain shedding, as it was able to perform this ectodomain shedding function. Both SPPL2A and SPPL2B demonstrate cleavage activity against TNFα and Bri2 (Fluhrer et al., 2006; Friedmann et al., 2006; Martin et al., 2008). The released intracellular domain of TNFα plays a functional role by increasing the expression of IL-12 through an unknown mechanism (Friedmann et al., 2006). The Fas ligand (FasL) and CD74 serve as cellular substrates of SPPL2A, but not of SPPL2B (Kirkin et al., 2007; Schneppenheim et al., 2014a). While SPPL2A and SPPL2B often demonstrate overlapping cleavage activity of specific substrates *in vitro*, it is thought that the distinct subcellular localizations under endogenous conditions promote substrate specificity of

the respective enzymes (Schneppenheim et al., 2014b). SPPL2A plays a key role in splenic B cell maturation via the cleavage of CD74, and genetic knockout of SPPL2A in mice leads to a deficiency of B cells (Schneppenheim et al., 2014a). Interestingly, SPPL2A-deficient mice also demonstrate a deformation in tooth enamel formation through an undefined mechanism (Bronckers et al., 2013). SPPL2C currently has no putative physiological function, and some groups believe this homologue evolved as a pseudogene since it does cleave any known substrates of SPPL2A/B (Golde et al., 2009).

Signal Peptide Peptidase

Signal peptide peptidase was discovered in mammals about 15 years ago when analyzing the degradation of signal peptides (Weihofen et al., 2002; Weihofen et al., 2000). SPP functions by cleaving membrane-bound signal peptides with type II transmembrane orientation following the activity of a signal peptidase (SP_{ase}) (Figure 1.6) (Lemberg and Martoglio, 2002). Initially it was assumed that its role was to release the remaining signal peptides from the ER membrane; however a number of studies later elaborated on this function by identifying other intracellular roles. The peptidase activity has been characterized further as occurring within the hydrophobic transmembrane region, with the remaining signal peptide being subsequently released to undergo subsequent processing by aminopeptidases in the cytosol (Weihofen et al., 2000). Additional work examining the cleavage region at the amino acid level concluded that "flexibility" within the lipid bilayer is required in order for SPP to access the peptide for cleavage (Lemberg and Martoglio, 2002). The key aspartic acid catalytic residues of SPP are conserved across all isoforms and homologues. Thus they are sometimes known as

members of a GXGD protease family (Martin et al., 2009; Ponting et al., 2002). This signature includes the GXGD domain coupled to a second aspartic acid domain YD and a conserved C-terminal PAL sequence essential for proper function of the protease (Figure 1.6). Biochemical evidence indicates that SPP is present as a stable homodimer (Nyborg et al., 2004b). Additional structural evidence implies a homo-tetramer responsible for its cleavage activity (Miyashita et al., 2011). Similarly, other studies have shown the presence of both dimer and higher order oligomeric species of SPP (Schrul et al., 2010). It is likely that the multimeric form of SPP is dependent on the conditions of enzyme isolation as well as the presence of specific associated proteins and substrates within the hydrophobic environment.

Substrate Cleavage and Function

The putative function of SPP is to clear the ER-bound signal peptides, and this aspect of SPP will be the focus of this thesis, specifically as it relates to malaria growth and development. Several SPP substrates in mammals have been identified and their functions have been elucidated. During hepatitis C virus (HCV) infection, production of a viral polyprotein occurs which is processed by the mammalian host cell machinery. In the case of HCV, there is an internal signal sequence included in the full-length polyprotein and this highly hydrophobic region functions as a signal sequence by targeting the protein to the ER. It undergoes cleavage by SP_{ase} and SPP and the core protein can be released into the cytosol as a mature protein (McLauchlan et al., 2002). This step is critical for HCV maturation and virus production (Targett-Adams et al., 2008; Targett-Adams et al., 2006). More specifically, the virus capsid requires core protein release following SP_{ase}

and SPP cleavage. This SPP cleavage step is essential as it enables the core protein to transition from the ER membrane to lipid droplets (McLauchlan et al., 2002; Targett-Adams et al., 2006). The same process is required for GB virus-B and classical swine fever virus (Targett-Adams et al., 2008). Thus, SPP function is relevant to proper ER function in a number of species and may be targeted for future anti-viral therapies.

Cleavage of signal peptides represents the main function of SPP within the cell. This cleavage generally occurs at the ER or within membranes in the vesicular trafficking pathway. This function may be required for proper ER function, clearance from vesicular membranes, or the released signal peptide fragments may play post-targeting functions within the cell. Proteins containing a signal peptide are recognized at the ER where they are targeted to the secretory pathway. Generally the signal peptide is clipped from the soluble domain following the action of a signal peptidase. Subsequently the cleaved soluble domain is targeted to its relevant compartment within the cell, while the remaining signal peptide can be processed by SPP, or released from the ER membrane (Dultz et al., 2008). The substrates of SPP have been investigated extensively regarding their subsequent signaling roles within the cell (Fluhrer et al., 2006; Friedmann et al., 2006). Cleavage of its most frequently studied substrate, preprolactin (p-Prl) is known to bind to calmodulin and may alter Ca^{2+} signaling (Martoglio et al., 1997). In mammals, the SPP pathway aids in immune surveillance where cleaved signal peptides are presented on the surface of natural killer cells to indicate that the synthesis of the major histocompatibility complex is processing correctly (Lemberg et al., 2001). In this regard, SPP has been linked to the process of viral immunoevasion. Unique short glycoprotein 2 (US2), a viral immunoevasion protein was recently demonstrated to associate with SPP

(Loureiro et al., 2006; Stagg et al., 2009). These proteins cause ER-dislocation of MHC complexes required for proper antigen presentation at the cell surface and target them for degradation by the proteasome. In this way, virally infected proteins can evade immune surveillance. More specifically, US2-dependent dislocation of major histocompatibility complex (MHC) class I heavy chains from the ER during human cytomegalovirus infection requires SPP. US2 was found to bind directly to SPP where it is thought to exert its role as an immunoevasin via MHC dislocation (Loureiro et al., 2006; Stagg et al., 2009). Thus, SPP is associated with a function in immune processing.

A number of other roles have also been tied to the intramembrane protease activity of SPP. Additional evidence indicates that SPP is involved in ER-associated degradation (ERAD) and targeting of misfolded proteins within the ER (Avci et al., 2014; Harbut et al., 2012; Lee et al., 2010; Schrul et al., 2010). SPP directly associates with a number of proteins involved in the unfolded protein response within a protein complex (Chen et al., 2014). More specifically, Derlin1, a member of the ERAD machinery was found to form a complex with SPP in addition to the E3 ubiquitin ligase TRC8 in a 500 kDa ERAD complex. This complex degrades X-box binding protein 1 (XBP1u), a negative regulator of the unfolded protein response (UPR). In this model, Derlin1 recognizes XBP1u, which is then cleaved by SPP and released from the membrane (Chen et al., 2014). Membrane release of XBP1u results in its degradation by the proteasome. Thus, the cleavage activity of SPP alters the abundance of a key regulator of the cellular ERAD response.

Related to a role in ERAD, one of the initial studies of SPP revealed that misfolded transmembrane proteins associate with SPP (Crawshaw et al., 2004). Other

studies have also demonstrated similar results (Schrul et al., 2010). SPP interacts with a diverse class of newly synthesized membrane proteins, and it is often found in multimeric complexes of 200, 400, and 600 kDa species. These findings suggest that SPP "collects" preproteins, as well as misfolded membrane proteins being destined for degradation (Schrul et al., 2010). Evidence from several studies has proposed that the species of SPP observed at approximately 200 kDa is specific for its signal peptide cleavage function and the higher order species (>400 kDa) are responsible for alternative functions (Chen et al., 2014; Lu et al., 2012; Schrul et al., 2010). While the purported molecular weight of the higher order species varies by study, the identification of a 200 kDa species responsible for signal peptide cleavage is consistent across several studies (Chen et al., 2014; Schrul et al., 2010).

It is appealing to hypothesize that SPP cleaves all signal peptides possessing type II transmembrane orientation. However, the dearth of bona fide substrates coupled to subsequent studies has raised concerns about this model. First, not all type II signal peptides are sensitive to SPP cleavage (Lemberg and Martoglio, 2002). Second, signal peptides can undergo membrane release independent of SPP activity (Dultz et al., 2008). Therefore while SPP is likely to cleave a variety of signal peptides, alternative means of degradation and/or release from the ER membrane are present. Finally, the presence of additional membrane proteases at the ER raises the notion that these enzymes may play a role in intramembrane cleavage. This family includes a class of rhomboid proteases. One specific rhomboid protease was identified as cleaving ubiquitinated ERAD substrates (Fleig et al., 2012). This protease cleaved both single spanning and polytopic membrane proteins, and its dislocated products are degraded by the proteasome, analogous to several

SPP substrates. Similar mechanisms raised the possibility that alternative proteases like rhomboids may be cleaving signal peptides at the ER. However, this model has not been tested experimentally.

Plasmodium falciparum SPP

Given the variety of functions and its essentiality, SPP represents a highly intriguing protease for future studies. The malaria parasite homologue of SPP was identified in the *P. falciparum* genome database, and tested for its cleavage activity against a model substrate (Nyborg et al., 2006b). Further evidence indicated that this represented a highly promising antimalarial drug target. Inhibitors originally designed to target the presenilin class of proteases could be used to inhibit SPP, and such treatment was lethal to parasite growth and development (Figure 1.7) (Li et al., 2009). These inhibitors represent attractive drug leads and offer new strategies towards an antimalarial therapeutic intervention. While humans possess a variety of different SPP and SPPL enzymes, the malaria genome shows a single PfSPP gene. Protozoan parasites responsible for toxoplasmosis and trypanosomiasis contain a minimal ERAD system and a single SPP orthologue (Harbut et al., 2012). Thus this is an attractive target not only in malaria but also in a number of different protozoan-based diseases. The mechanism by which inhibition of PfSPP causes cell death in malaria is not currently known. However, given its link to the ERAD pathway it is hypothesized to be a consequence of ER stress caused by the build-up of signal peptides within the ER membrane.

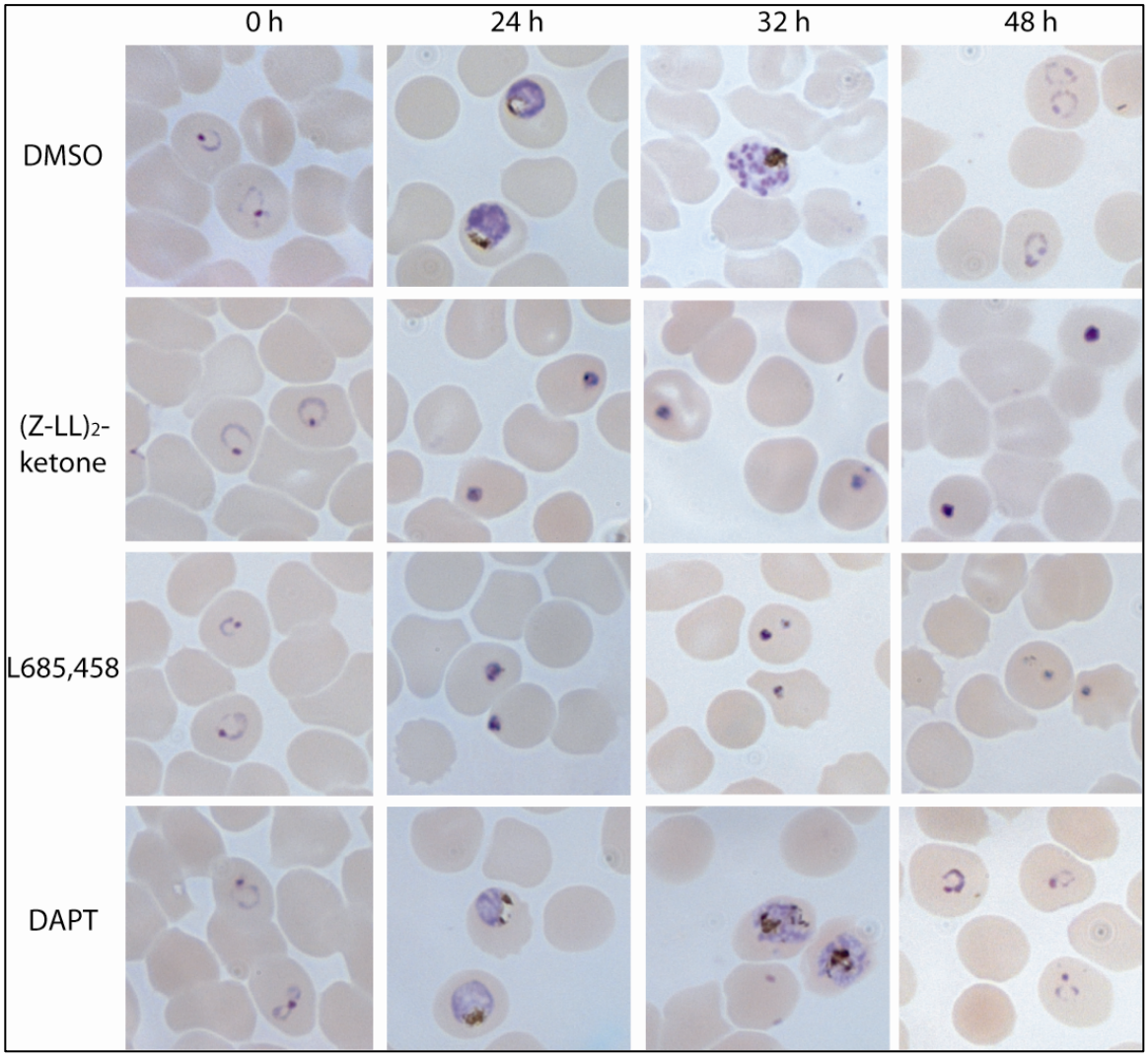

Figure 1.7. SPP Inhibitors are lethal to parasite growth and development *in vitro*. Synchronized parasites were grown in the presence of SPP inhibitors (L-685,458 and (Z-LL)$_2$-ketone), a presenilin specific inhibitor (DAPT) and DMSO as a vehicle control. Growth was inhibited in the presence of the SPP inhibitors. (Adapted from Li et al., 2009)

Interestingly, the SPP inhibitors are also lethal to the liver stage of *P. falciparum* infection, thus PfSPP represents a highly intriguing target for multi-stage antimalarial drug development (Parvanova et al., 2009). Using a mouse model of malaria, this study demonstrated a decreased parasite load in the liver *in vivo*. Furthermore, resistance to cerebral malaria was improved by over 50% (Harbut et al., 2012; Parvanova et al., 2009). *In vitro* experiments performed with hepatoma cell lines showed an IC_{50} of 80 nM using the SPP inhibitor, LY411,575. This inhibitory effect was specific, as inhibitors targeting the presenilin homologues did not demonstrate malaria toxicity (Parvanova et al., 2009). The *P. berghei* and *P. falciparum* homologues of SPP share approximately 78% identity, and thus it is likely that these inhibitors would be effective against several other *Plasmodium* species, as well as other protozoan parasites (Li et al., 2008b). As expected, these inhibitors also show activity against human SPP (Nyborg et al., 2004a; Nyborg et al., 2006b). Therefore, a highly selective protease inhibitor would need to be developed to specifically target the parasite protease and avoid the host enzyme.

Some progress has been made on this front, including the demonstration that inhibitors targeting SPP increased sensitivity of malaria parasites relative to host cells. This increase is greater than ten-fold selectivity for parasites relative to a human liver cell line (Harbut et al., 2012). Using low doses of SPP inhibitors, specific amino acid mutations in PfSPP were identified that correlated with resistance. One substitution, L333F, was associated with a twofold increase in resistance to a specific SPP inhibitor. This residue is found in the eighth predicted transmembrane domain just adjacent to the key aspartic catalytic residues contained in the sixth and seventh domains, and also close to the essential PAL motif in the ninth transmembrane domain. The lack of a detailed

crystal structure of this peptidase precludes the possibility of identifying the specific mechanism by which this L333F mutation can increase inhibitor resistance. Thus, selective inhibitors of PfSPP must be used in combination with other therapies to avoid potential drug resistance (Harbut et al., 2012).

A key experimental advance to study SPP was the development of a functional assay. This assay requires expression of SPP in heterologous HEK293T cells in combination with a putative signal peptide substrate, which is linked to an N-terminal ATF6 tag. Upon cleavage, released ATF6 translocates to the nucleus and increases the expression of a luciferase reporter gene (Nyborg et al., 2004a). This approach was adapted to measure the function of SPP and its homologues SPPL2B and SPPL3 (Nyborg et al., 2006b). Not only did this assay allow for the study of these intramembrane proteases, but enabled the rapid detection of potential SPP substrates in a model system. As indicated earlier, the ERAD system in protozoan pathogens is highly limited. The parasite ER stress response is also likely to be limited to overcome ER stress. Thus, *P. falciparum* ERAD regulatory proteins may serve as attractive therapeutic targets. Malaria SPP involvement with this phenomenon renders it a highly appealing drug target given its essentiality and link to a role in proper ERAD function.

Merozoite Surface Protein 1

Merozoite surface protein 1 (MSP1) is one of the most well studied parasite proteins due to its abundance on the merozoite surface. It was discovered nearly 35 years ago when antibodies generated against merozoite antigens identified a protein with a molecular weight of 195 kDa, which represents the full-length MSP1 polypeptide (Perrin

et al., 1980). MSP1 was confirmed as an established merozoite surface protein (Freeman and Holder, 1983). It is initially expressed as a precursor that gets cleaved into four subunits of 83 kDa, 30 kDa, 38 kDa, and 42 kDa in order from N to C-terminus (Figure 1.8) (Holder and Freeman, 1982; Kadekoppala and Holder, 2010). This primary processing step is performed by a serine protease termed subtilisin 1 (SUB1) that is released into the parasitophorous vacuole in the steps just prior to merozoite egress (Figure 1.8B) (Koussis et al., 2009). Two pairs of tight association characterize the high-affinity interactions among the four subunits. The N-terminal $MSP1_{83}$ domain interacts strongly with $MSP1_{30}$, whereas $MSP1_{38}$ binds tightly to $MSP1_{42}$ (Kadekoppala and Holder, 2010; Kauth et al., 2003). $MSP1_{30}$ also binds to $MSP1_{38}$ and $MSP1_{42}$ and is the only subunit known to interact with all three other domains allowing for the formation of a multi-protein 195 kDa complex. Notably, the interaction between $MSP1_{30}$ and $MSP1_{42}$ is significantly weaker than the binding among other subunits. Interestingly, the only subunit that binds $MSP1_{83}$ is the $MSP1_{30}$ domain (Kadekoppala and Holder, 2010; Kauth et al., 2003).

The 42 kDa C-terminal subunit is processed by subtilisin 2 (SUB2) into two smaller proteins termed $MSP1_{33}$ and $MSP1_{19}$ (Figure 1.8) (Harris et al., 2005). This secondary processing step releases the majority of the MSP1 complex from the merozoite surface, leaving just the C-terminal GPI-anchored $MSP1_{19}$ domain. Following invasion, this subunit is internalized into the host erythrocyte. The $MSP1_{19}$ subunit is found at the food vacuole membrane and is thought to play a key role within this compartment (Dluzewski et al., 2008). Its cysteine-rich structure is predicted to form three disulfide bonds in each of its two epidermal growth factor-like (EGF) motifs.

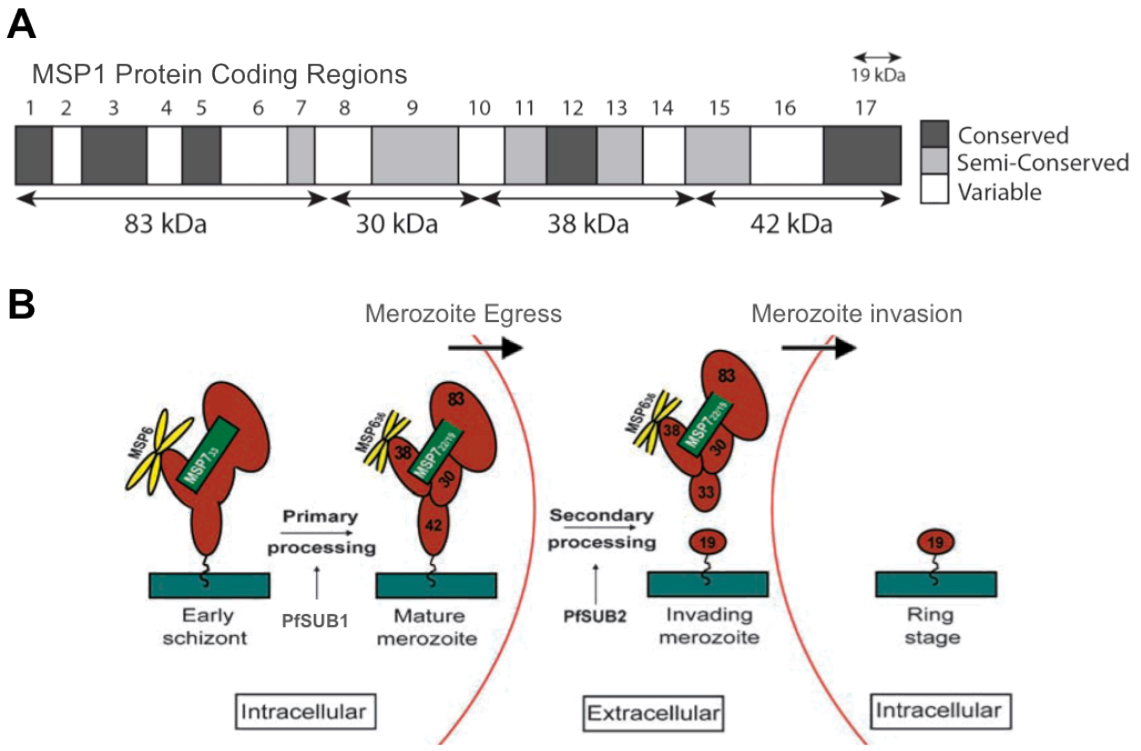

Figure 1.8. Merozoite surface protein 1 is processed into a multi-subunit polypeptide complex during merozoite invasion.
(A) The full-length 195 kDa MSP1 protein is made up of 17 regions with varying degrees of conservation. Areas shaded in white are variable, those in light grey are semi-conserved, and in dark grey are highly conserved regions. The four subunits of MSP1 are labeled by size under the polypeptide block diagram. (B) Flow diagram of MSP1 processing divided by the stage of parasite invasion. During the primary processing, MSP1 is cleaved into four subunits of 83, 30, 38, and 42 kDa. Following merozoite egress and invasion, subsequent processing releases the majority of the complex from the surface retaining only the 19 kDa C-terminal domain of MSP1 linked by a GPI anchor to the membrane surface. The 19 kDa domain of MSP1 is then internalized and localized at the food vacuole during the ring stage of parasite development. (Adapted from Koussis et al., 2009)

Antibodies against this subunit can only recognize the non-reduced form of the protein (Burghaus and Holder, 1994). A key difference between the EGF-like domain in MSP1 and other EGF domains is the lack of a conserved Ca^{2+} binding sequence. Therefore, the presence of calcium does not have any effect on the structure of this domain. Hydrophobic phenylalanine, leucine, and isoleucine residues mediate binding between these two EGF-like domains (Morgan et al., 1999). The MSP1 complex is characterized by an intricate set of interactions among several subunits that are processed by two distinct serine proteases. Furthermore, it represents one of the most fundamentally intriguing biological protein complexes in the field of parasite biology given its abundance on the merozoite and potential as a malaria vaccine target.

Genetic Analysis/Isotypes

MSP1 consists of 1,640 amino acids including a signal peptide at the N-terminus, and a cysteine-rich region at the C-terminus containing the EGF-like motifs (Holder et al., 1985). The gene is characterized by 17 individual regions or "blocks". Genetic analysis has categorized these into three different groups including highly conserved, semi-conserved, or variable blocks (Tanabe et al., 1987). Conserved blocks include 1, 3, 5, 12 and 17, semi-conserved blocks include 7, 9, 11, 13 and 15 while the variable regions include 2, 4, 6, 8, 10, 14 and 16 (Figure 1.8). The genetic structure of MSP1 is generally classified as dimorphic and falling into two sub-types including the K1-type or the MAD20 type. The MAD20 form is slightly larger due to multiple insertions (Tanabe et al., 1987). Interestingly, these two dimorphisms can be detected within the same malaria-infected patient. Subsequent allelic types have been defined including RO33 and

MR; however they show specific combinations of the K1 and MAD20 sequences (Sakihama et al., 2001; Takala et al., 2002; Takala et al., 2006).

Serine Protease Processing

Two serine proteases, SUB1 and SUB2, are thought to "prime" the merozoite for invasion (Koussis et al., 2009) (Fleck et al., 2003; Howell et al., 2003). Genetic disruption of these genes is lethal, and initial characterization led to an improved understanding of the steps preceding merozoite invasion and their function with regards to MSP1 processing (Harris et al., 2005; Yeoh et al., 2007).

SUB1 and its discovery led to the identification of a novel organelle termed the exoneme (Janse and Waters, 2007). Given the function of SUB1, the exoneme is putatively thought to be essential for merozoite egress from the infected erythrocyte. Furthermore, the expression pattern of SUB1 is consistent with that of parasite egress since its highest expression is detected during the schizont stage. Inhibitors against SUB1 prevent schizont rupture, and its activity is essential for erythrocyte reinvasion (Yeoh et al., 2007). This essential function likely originates from the "priming" of the merozoite during invasion via its MSP1 cleavage activity (Koussis et al., 2009). A key study by Koussis *et al.* (2009) confirmed that SUB1 processes MSP1, MSP6, and MSP7 at specific homologous cleavage sequences. As a result, the 195 kDa MSP1 precursor is processed into the 83 kDa, 30 kDa, 38 kDa, and 42 kDa subunits, respectively (Figure 1.8). Inhibiting SUB1 activity results in the failure to generate the four subdomains of MSP1 observed on the merozoite surface. Studies focusing on the liver stage of the parasite have indicated an essential role of SUB1 in parasite pathogenesis (Suarez et al., 2013).

Thus, SUB1 function is required for multiple phases of the parasite life cycle and may offer a promising target for an antimalarial therapy targeting multiple stages of malaria pathogenesis.

SUB2 is responsible for the secondary processing of MSP1 in which the 42 kDa subunit is processed into $MSP1_{33}$ and the well characterized $MSP1_{19}$ C-terminal domain (Child et al., 2010; Harris et al., 2005). The $MSP1_{19}$ domain remains anchored on the merozoite surface, whereas the $MSP1_{33}$ domain along with the remaining N-terminal subunits ($MSP1_{83}$, $MSP1_{30}$ and $MSP1_{38}$), are released. SUB2 is a micronemal protein that is secreted onto the parasite surface immediately prior to invasion and thus designated as merozoite surface sheddase (MESH) (Alam, 2014; Harris et al., 2005). Both SUB1 and SUB2 are known to cleave other substrates in addition to MSP1. These MSP1 independent substrates of SUB1 and SUB2 have been thoroughly reviewed recently and will not be discussed here (Alam, 2014).

Putative function

MSP1 is hypothesized to play a key role in invasion. Although its precise mechanism is not completely understood, evidence shows that antibodies against MSP1 inhibit parasite invasion (Woehlbier et al., 2010). A large focus of these studies has been on the C-terminal $MSP1_{19}$ domain, and antibodies against this region have repeatedly shown reduced parasite invasion (Holder, 2009; O'Donnell et al., 2000). A more recent study designed a specific inhibitor against the $MSP1_{19}$ subunit that significantly reduced parasite invasion (Chandramohanadas et al., 2014). This inhibitory effect was specific to the invasion stage, and consistent across multiple *Plasmodium* species indicating its

conserved function. Several strains of *P. falciparum* were tested and demonstrated a similar sensitivity to this novel inhibitor termed "NIC". Its functional activity is specifically targeted at the EGF-like domain of $MSP1_{19}$, which is highly conserved across strains and species of malaria. Therefore, small molecules targeting the C-terminal domain of MSP1 represent a highly intriguing avenue for targeting antimalarial therapeutics.

The inhibitory activity of antibodies and compounds against the C-terminal domain of MSP1 is likely due to its band 3 binding activity. It was discovered that this domain interacts with the 5ABC (amino acids 720-761) region of band 3 as part of the parasite invasion mechanism (Goel et al., 2003). Other studies have identified a similar function albeit with various subunits of MSP1. One study demonstrated inhibition of merozoite invasion as a result of heparin binding to the MSP_{33} domain, which was able to inhibit proteolytic processing (Boyle et al., 2010). The initial hypothesis that MSP1 is an invasion ligand relied on the finding that full-length MSP1 binds to erythrocytes in a SAD fashion (Perkins and Rocco, 1988). One study divided MSP1 into 90 short peptide regions to determine their affinity for erythrocyte binding, and potential for invasion inhibition (Urquiza et al., 1996). Selected peptides derived from the 83 kDa, 38 kDa and 42 kDa subunits bound to erythrocytes with high affinity, and six of these peptides significantly inhibited parasite invasion. Thus, there is a comprehensive body of evidence supporting a functional role of MSP1 in parasite invasion. One proposed function for MSP1 is its ability to act as a scaffold for the merozoite surface protein Duffy binding-like (MSPDBL) proteins. This recent finding is supported by evidence indicating their association on the merozoite surface, specifically binding the $MSP1_{83}$, $MSP1_{38}$, and

$MSP1_{42}$ subunits but not the $MSP1_{30}$ domain (Lin et al., 2014).

A secondary function of MSP1, specifically the $MSP1_{19}$ domain, is highlighted by its internalization during parasite invasion in erythrocytes, while the remainder of the 195 kDa protein is released by the SUB1 and SUB2 proteases (O'Donnell et al., 2000). The developing parasite contains the internalized protein as part of its food vacuole membrane. The food vacuole is formed by endocytic vesicles during the ring stage of parasite maturation, and it is within these vesicles that hemoglobin is broken down to provide amino acid building blocks for the developing parasite (Dluzewski et al., 2008). It has been proposed that $MSP1_{19}$ plays an essential role during the biogenesis and function of the food vacuole. The authors propose three possible functions for $MSP1_{19}$: (1). Membrane protection against proteases within the vacuole due to its protease-resistant structure, (2). Accelerating hemozoin crystallization linked to lipid droplets in the food vacuole, and (3). Physical stabilization of the food vacuole membrane via its association with the cholesterol-rich lipid microdomains (Dluzewski et al., 2008).

MSP1 as a therapeutic target

A number of studies have designed antibodies against MSP1 to inhibit parasite invasion since MSP1 is the most abundant protein on the surface of the merozoite. Antibodies against MSP1 can inhibit the life cycle at multiple points including invasion, intraerythrocytic development, MSP1 processing, and agglutination of free merozoites (Blackman et al., 1994; Woehlbier et al., 2006). One of the drawbacks in the development of an MSP1-based vaccine is that three different types of antibodies can compete for epitope recognition. First, there are the inhibitory antibodies directly

impeding MSP1 function, second are antibodies that actually interfere with inhibitory antibodies and are termed "blocking" antibodies, and the third type are antibodies with currently no defined effect on protein function (Cheng et al., 2007; Nwuba et al., 2002). Given its putative function and high level of conservation, most antibodies have been raised against the $MSP1_{19}$ domain. However, inclusion of the $MSP1_{33}$ domain has provided a much higher level of antigenicity encouraging its inclusion in the $MSP1_{19}$ based vaccine (Egan et al., 1997).

Outside of the C-terminal domain, vaccines have used block 2 from the $MSP1_{83}$ subunit as an antigen. This domain also serves as a target of the host immune response. While these antibodies could distinguish between various MSP1 isotypes, they demonstrate an extremely short half-life (Cavanagh et al., 2001; Cavanagh et al., 2004; Cavanagh and McBride, 1997; Sowa et al., 2001). Given the brief duration of these antibodies, continuous stimulation is required and thus vaccine development has been quite difficult against this domain (Cavanagh et al., 2001). Follow-up studies concluded that antibodies against block 2 from the $MSP1_{83}$ region do not protect at the desired level, and some researchers believe that the presence of these antibodies is a sign of infection and not necessarily protection (Ekala et al., 2002; Scopel et al., 2005). A polyvalent hybrid protein containing this region has shown promise, and therefore this may warrant further investigation (Tetteh and Conway, 2011). The $MSP1_{38}$ subunit has also been targeted as a viable vaccine candidate. Using the 115 amino acids termed "p115MSP1", this region elicited an antibody response that led to reduced parasite invasion. While it did not offer complete protection, partially reduced parasitemia is a promising avenue for future studies (Nikodem and Davidson, 2000). The transition from promising antibody

responses and protection to an effective antimalarial vaccine has proved to be extremely difficult. One of the biggest challenges is the extremely short half-life of antimalarial antibodies in the serum. Furthermore, the aforementioned "blocking" antibodies add an enormous level of complexity when evaluating an immune response.

Several attempts have been made to generate a multi-target malaria vaccine by including sub-domains of MSP1. One of the initial developments was a malaria peptide vaccine called SPf66 containing antigens from the sporozoite and blood stage, including circumsporozoite antigen and MSP1, respectively (Lopez et al., 1994). While some initial promise was observed, overall the SPf66 vaccine did not provide uniform protection and failed to reduce hospital admissions as a result of severe malaria (Masinde et al., 1998). Other failures include limited immunogenicity, and repeated attempts have failed to reach an effective threshold protection without subsequent boosters (Egan et al., 2000; Keitel et al., 1999). More attempts against various subdomains and synthetic combinatorial proteins have been attempted without attaining the required level of efficacy for widespread implementation (Huaman et al., 2008; Malkin et al., 2007). Thus, it appears that current strategies being undertaken to develop vaccines against MSP1 will not yield the intended effect without a complete understanding of MSP1 function. Ultimately, an ideal group of antigens will be combined to offer protection against a number of strains while still generating high affinity antibodies.

Associated Proteins

Additional proteins have been found to both co-localize with and bind to MSP1. Extensive characterization has elucidated details of a complex containing several MSPs.

Proteins found in complex with MSP1 include MSP6, MSP7, MSP9, MSPDBL1 and MSPDBL2 (Kadekoppala and Holder, 2010; Kariuki et al., 2005; Kauth et al., 2006; Li et al., 2004; Pachebat et al., 2001; Trucco et al., 2001). MSP6 was identified as a 36 kDa protein released into the culture supernatant during parasite invasion, and similar to MSP1, MSP6 also demonstrates dimorphism (Kadekoppala and Holder, 2010; Pearce et al., 2004; Trucco et al., 2001). Its interaction with MSP1 occurs through the $MSP1_{38}$ domain but not with the other three subunits (Figure 1.8) (Kauth et al., 2003; Kauth et al., 2006). The proposed timing of this event is thought to occur just prior to merozoite release with the processed 36 kDa form of MSP6.

MSP7 is highly conserved and interacts with three subunits including $MSP1_{83}$, $MSP1_{30}$, and $MSP1_{38}$ but not with the $MSP1_{42}$ subunit (Figure 1.8) (Kauth et al., 2003; Kauth et al., 2006). It's proposed that this interaction occurs in the ER, and this associated complex is translocated to the merozoite surface. MSP7 is initially translated as a 33 kDa fragment, which is subsequently processed into a 22 kDa protein, at the same stage when primary MSP1 processing occurs (Pachebat et al., 2007). Thus, on the surface of the merozoite, MSP7 is found as a 22 kDa protein as part of the shed complex. The significance of MSP7 binding to MSP1 is currently unknown. Similar to MSP6, antibodies against MSP7 have demonstrated a marginal level of invasion inhibition (Kauth et al., 2006).

MSP9, also known as acidic basic repeat antigen (ABRA), was identified as an MSP1 associated protein (Kariuki et al., 2005; Li et al., 2004). It was further confirmed that this protein also plays a role to some extent as a parasite ligand via its band 3 binding to the 5ABC region (Kushwaha et al., 2002; Li et al., 2004). It was proposed that these

two proteins, MSP1 and MSP9, bind to form a co-ligand complex that is involved in invasion. The MSP9 protein binds to MSP1 and band 3 via the same two distinct domains of amino acids 77-183 and 364-528 suggesting the existence of a ternary complex. It is possible that this complex provides some measure of redundancy for the invasion pathway and the interaction between the merozoite and band 3. There is some evidence that recombinant MSP9 can partially inhibit merozoite invasion *in vitro* (Li et al., 2004). However, its precise mechanism is unknown and may be a result of steric hindrance, blocking 5ABC binding to other parasite ligands.

More recently, the MSPDBL proteins were identified as being associated with the MSP1 complex (Lin et al., 2014; Wickramarachchi et al., 2009). These proteins bind to erythrocytes in a protease-resistant fashion; however their host receptor is currently unknown. Antibodies against these proteins reduced parasite propagation over multiple rounds of growth and invasion *in vitro*, however the specific step of inhibition is unclear (Chiu et al., 2015). Clearly, the function of MSP1 in relationship to the MSPDBL proteins requires a detailed investigation to determine the possible relationship between the two putative parasite ligands.

MSP1 is a key ligand in the invasion process, as well as a number of other cellular processes. We will now discuss two essential erythrocyte receptors with abundant expression on the red blood cell surface. These receptors called glycophorin A (GPA) and band 3 are known to be involved in the merozoite invasion process. We will discuss their functions and properties, as well as role as it relates to malaria invasion.

Glycophorin A

Glycophorins were initially isolated from human red cells over forty years ago resulting in the definitive identification of a major glycoprotein in the erythrocyte membrane (Marchesi and Andrews, 1971). One of the glycophorins, termed glycophorin A became the first transmembrane protein to be sequenced (Furthmayr et al., 1978; Tomita et al., 1978; Tomita and Marchesi, 1975). Eventually, the glycophorins were shown to include a family of proteins termed glycophorin A, B, C, and D, respectively (Chasis and Mohandas, 1992). While estimates of their content vary, the glycophorins are one of the most abundant membrane proteins in the erythrocyte, with GPA being present at approximately one million copies per cell. More importantly, their high sialic acid content accounts for the majority of the erythrocyte surface charge (Figure 1.9).

GPA is found on chromosome 4 and contains 7 exons encoding 131 amino acids. GPA is a type I transmembrane protein with a single membrane-spanning domain (Figure 1.9). Genetic analysis of the 5' region and 3' UTR of GPA and GPB indicates these genes share more than 95% sequence identity (Kudo and Fukuda, 1989). It is hypothesized that GPA and GPB arose from a common gene involving recombination of specific sequences (Lemmon et al., 1992). Two regions unique to GPA include its cytoplasmic domain and a segment defined by amino acids 26-58 within its extracellular domain (Chasis and Mohandas, 1992). Various mutant phenotypes associated with a lack of or mutated GPA include the Miltenberger V, En(a-), and M^kM^k individuals. The Miltenberger V gene is a result of unequal crossing over between the GPA and GPB genes. As a result, it is a chimeric protein containing GPA exons 1-3 and GPB exons 3-5.

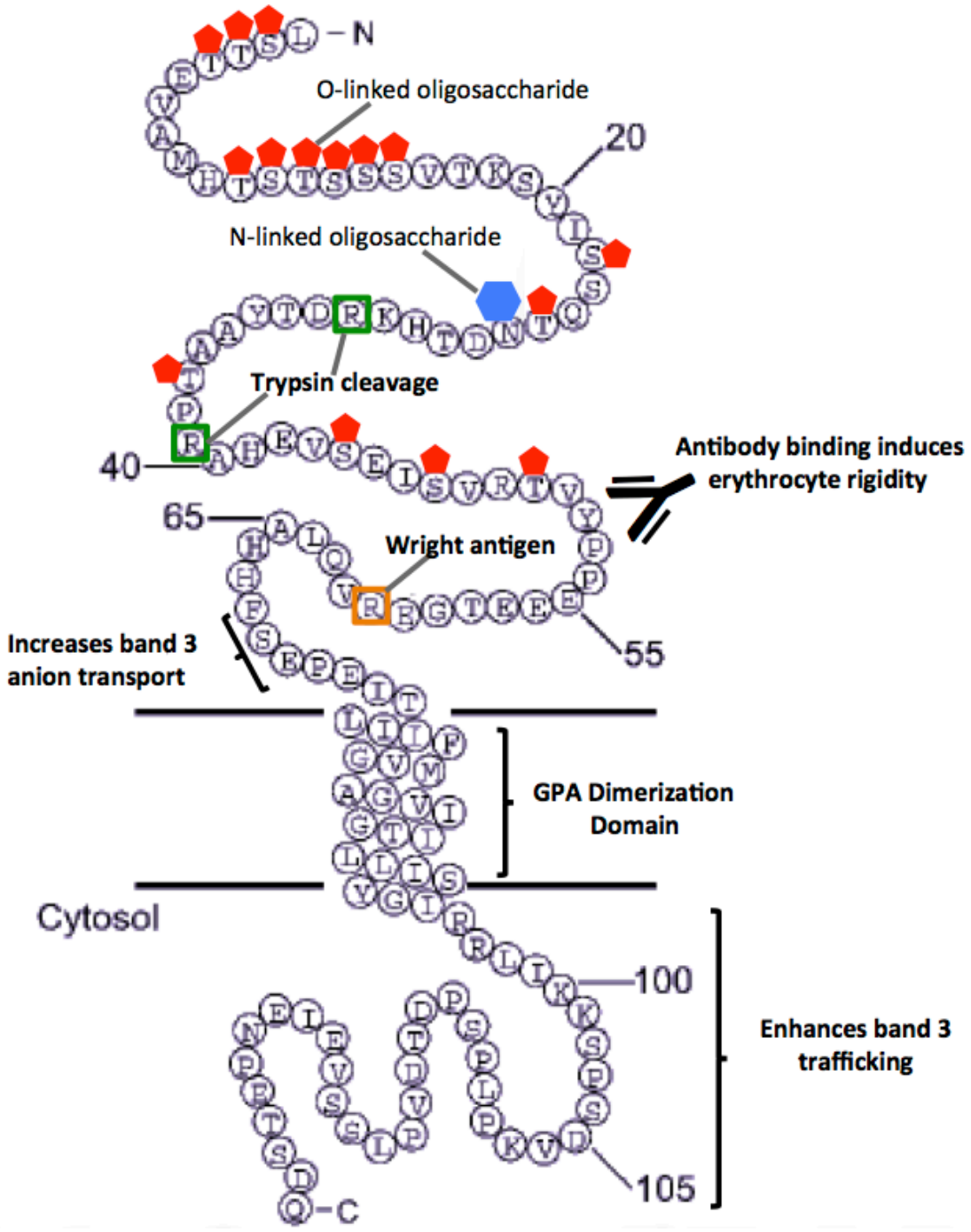

Figure 1.9. Glycophorin A topology model.
Glycophorin A is a highly abundant transmembrane protein on the erythrocyte surface. It is O-glycosylated on 15 specific residues (pentagons in red), and N-glycosylated on one residue (hexagon in blue). Trypsin cleavage is known to occur at two specific arginine residues squared in green. It is predicted that amino acids 1-72 are present on the extracellular domain. (Adapted from Young et al., 2003)

This variant is only detectable by serological means. En(a-) patients lack only GPA but this phenomenon is extremely rare. M^kM^k individuals are deficient in both GPA and GPB (Tanner et al., 1976). Using ektacytometry, En(a-) erythrocytes did not show any alterations in mechanical stability or deformability. Thus, erythrocytes lacking GPA either exhibit a compensatory mechanism to retain proper membrane stability or GPA is not required for normal membrane structural stability (Reid et al., 1987).

The majority of GPA in the erythrocyte membrane is present as a homodimer. However, GPA is also observed as a monomer and forms a heterodimer with GPB (Lemmon et al., 1992). The region responsible for its dimerization is located within an alpha-helical region of the transmembrane domain. The extracellular domain contains the sialic acid content of GPA. There are 15 residues containing an O-linked oligosaccharide side chain, and a single N-linked oligosaccharide side chain (Chasis and Mohandas, 1992). As a result, it accounts for the majority of the negative charge on the surface of the erythrocyte. Later it was discovered that the Wright antigen (Wr^b) is dependent on the presence of Arg_{61} of GPA in addition to specific residues within band 3 (Bruce et al., 1995). Similarly, the association of GPA with band 3 in the erythrocyte membrane has been investigated extensively. Band 3 can traffic to the cell membrane in the absence of GPA; however GPA speeds up this process, supporting the idea that they may be trafficked as part of the same complex (Groves and Tanner, 1994). Subsequently, in mouse erythrocytes it was determined that a loss of band 3 resulted in nearly complete deficiency of GPA protein. However, GPA mRNA was still present, indicating that band 3 is likely to be essential for proper protein expression and trafficking of GPA to the erythrocyte surface (Hassoun et al., 1998). Further evidence supporting the existence of a

co-trafficking complex comes from the observation that a relatively higher content of band 3 is observed at the membrane surface in *Xenopus* oocytes in the presence of GPA (Young et al., 2000). Similarly, a detailed analysis of GPA subdomains identified several specific residues that increased the functional transport activity of band 3 (Figure 1.9) (Young and Tanner, 2003). The cytoplasmic tail of GPA was identified to aid in band 3 trafficking, while its membrane-adjacent extracellular domain plays a role in band 3 transport activity (Young and Tanner, 2003).

The role of GPA has been investigated in regards to erythrocyte hematology, cell-cell aggregation, band 3 function, erythrocyte rigidity, and parasite invasion. Initial experiments determined that GPA is not essential for proper erythrocyte function as its knockout shows a relatively mild hematological phenotype in humans and no phenotype in mice (Arimitsu et al., 2003). A major conclusion from this study regarding the hematological effect of GPA knockout was that erythrocytes became more sensitive to hypo-osmotic stress. However, GPA null erythrocytes showed no aggregation phenotype due to a loss of sialic acid content and thus reduced surface negative charge. This finding may be explained by the compensatory response in GPA knockout where an increase in sialic acid content has been observed on band 3 (Chasis and Mohandas, 1992). It is believed that the negative charge of the sialic acids from GPA contributes to decreased cell-cell interactions *in vivo*.

Interestingly, increased erythrocyte rigidity was observed following antibody binding to the extracellular domain of GPA (Chasis et al., 1985). The degree of increase in cellular rigidity is dependent on the region of GPA binding. More specifically, binding to more distal residues of the extracellular domain showed limited increases in membrane

rigidity. Binding to amino acid regions in closer proximity to the erythrocyte membrane demonstrate a significantly higher increase in membrane rigidity (Chasis et al., 1985; Chasis et al., 1988). This phenomenon is not observed with binding to band 3, and is therefore likely to be specific to GPA. Thus, in the context of erythrocyte hematology and deformability, multiple functions associated with GPA include ligand-induced rigidity changes, stability in hypo-osmotic conditions, and a role in preventing cell-cell aggregation due to its high negative charge.

GPA has been studied extensively in the context of malaria. GPA is known to play a functional role as a receptor for the parasite ligand EBA-175 (Duraisingh et al., 2003a). Its role in malaria invasion was discovered in 1982 when it was shown that erythrocytes lacking glycophorin A, En(a-) cells, showed increased resistance to malaria invasion *in vitro* (Pasvol et al., 1982). A subsequent study also demonstrated that purified GPA reconstituted in liposomes could significantly inhibit parasite invasion (Okoye and Bennett, 1985). These initial findings led to the discovery of EBA-175 as the cognate ligand of GPA. Subsequent studies further characterized this interaction as a key step for intracellular merozoite calcium signaling during parasite invasion (Singh et al., 2010). However, GPA-null mice that retain band 3 do not show any resistance to *P. yoelii* infection (Hamamoto et al., 2008). Thus, the functional importance of GPA is highly dependent on the species of malaria being investigated.

Band 3/Anion Exchanger 1

Human anion exchanger 1 (AE1), also known as band 3, is the most abundant protein on the erythrocyte surface with approximately one million copies per cell (Poole,

2000; Steck, 1978). Band 3 is encoded by the *SLC4A1* gene and has been investigated for nearly fifty years with regards to its function within the red cell. Initial studies identified a band of about 100,000 kDa within erythrocyte membranes (ghosts) (Steck, 1978). Current structural models predict a protein containing 14 transmembrane domains assembled by 911 amino acids (Figure 1.10) (Hirai et al., 2011; Yamaguchi et al., 2010a). This topology accounts for a protein of 95 kDa, which is most often observed as a dimer (Nigg and Cherry, 1979). Two conformations of band 3 have been recognized. One form faces inward and binds an anion from the cytoplasmic side, while the outward facing form binds to an anion on the extracellular surface (Passow, 1986; Ruffing et al., 1996). Generally, band 3 function is associated with three subdomains: the N-terminal cytoplasmic domain, the membrane-spanning domain that accounts for its transport activity, and a relatively small C-terminal cytoplasmic domain.

N-terminal associated proteins

The N-terminal domain of band 3 is a 40 kDa water soluble polypeptide that functions as a binding site for a number of erythrocyte proteins (Hamasaki, 1999). Specific interactions with protein 4.1, protein 4.2, and ankyrin (An et al., 1996; Bennett and Stenbuck, 1980; Cohen et al., 1993) indicate that this is the major attachment point between the red cell membrane and its interior cytoskeleton (Bruce et al., 2003; Grey et al., 2012). Another study demonstrated the biochemical interaction between the erythrocyte Rh complex and band 3 in erythrocytes using a number of immunoprecipitation experiments.

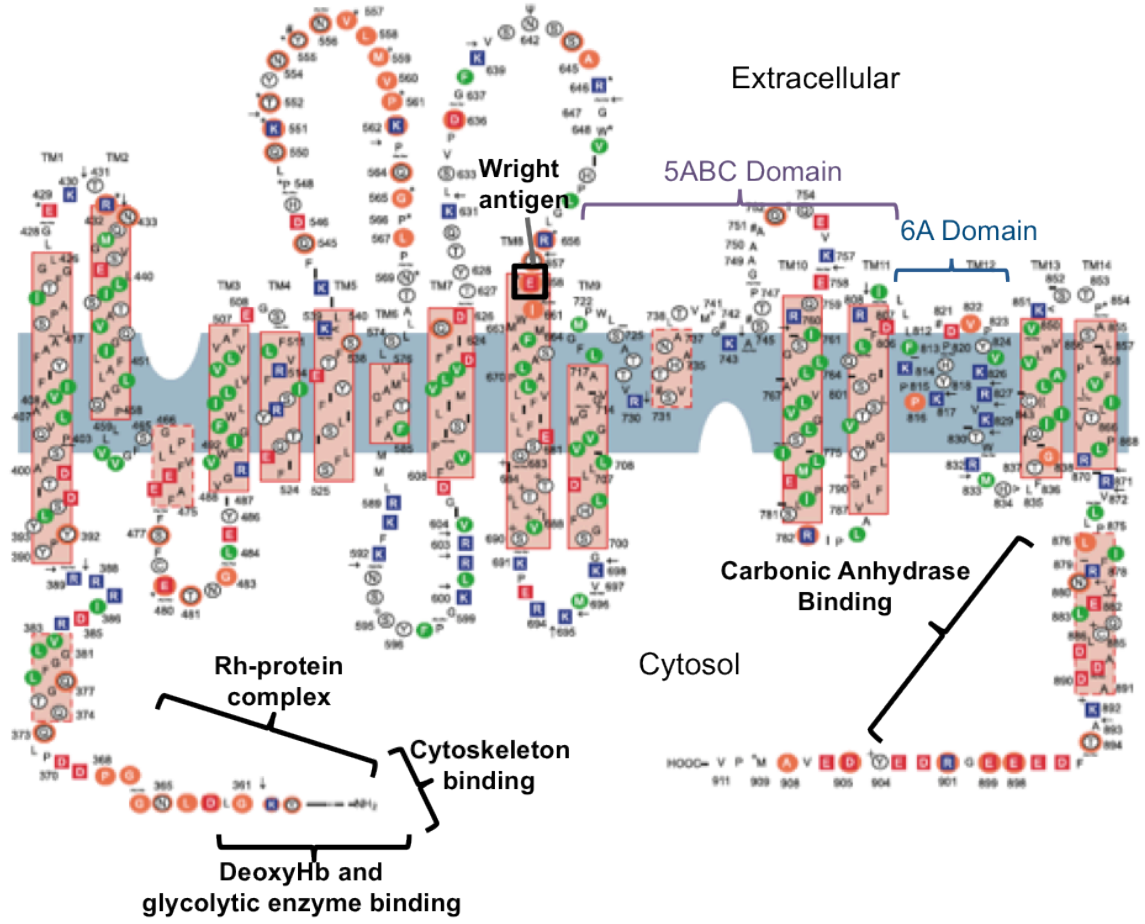

Figure 1.10. Band 3/Anion exchanger 1 is associated with several cellular functions. Band 3 possesses 14 transmembrane segments on the erythrocyte surface membrane. The N-terminal domain associates with a number of erythrocyte cytoskeletal proteins within the cytoplasm, in addition to glycolytic enzymes and deoxyhemoglobin. The membrane-spanning domain accounts for the anion transport activity, and contains the 5ABC region (in purple), a putative receptor for the malaria protein $MSP1_{19}$. The short cytosolic C-terminal domain binds to carbonic anhydrase, which increases its activity significantly. (Adapted from Hirai et al., 2011)

The band 3 complex contains Rh associated glycoprotein, Rh polypeptides, glycophorin B, CD47, and LW (Bruce et al., 2003). The function of the Rh proteins is not fully elucidated, but its genetic disruption results in morphological abnormalities of the erythrocyte, indicating a role in mechanical stability of the erythrocyte cytoskeleton and membrane (Van Kim et al., 2006). Additional evidence suggests they function via a putative role in gaseous transport as nonspecific channels allowing the passage of carbon dioxide and oxygen (De Rosa et al., 2008).

Hemoglobin Binding

The N-terminal cytoplasmic domain of band 3 also interacts with hemoglobin. This interaction allows hemoglobin to preferentially bind oxygen on the inner surface of the red cell membrane. Interaction of band 3 with hemoglobin is thought to function as an allosteric regulator of hemoglobin activity by decreasing its affinity for oxygen (Figure 1.10) (Zhang et al., 2003). It is believed that deoxyHb could displace glycolytic enzymes from the membrane by disrupting their association with band 3 (Sega et al., 2012). The functional significance of this interaction is discussed in the next section.

Glycolytic Enzymes

Glycolysis can be significantly modulated by band 3. Several glycolytic enzymes bind specifically to the N-terminal cytoplasmic domain of band 3 (Figure 1.10). This binding alters the presence of glycolytic intermediates by inhibiting glycolysis. Thus, band 3 binding to glycolytic enzymes is a key mechanism of metabolic regulation in erythrocytes (Low et al., 1993). The enzymes involved in this regulation and interaction

include glyceraldehyde-3-phosphate dehydrogenase (GAPDH), aldolase, phosphofructokinase, pyruvate kinase, and lactate dehydrogenase (Campanella et al., 2005; von Ruckmann and Schubert, 2002). GAPDH binds to an acidic sequence within the N-terminal domain with high affinity that is dependent on the buffer conditions (Kliman and Steck, 1980; Rogalski et al., 1989; von Ruckmann and Schubert, 2002). Some studies have implied that deoxyHb competes with glycolytic enzymes for the N-terminal domain of band 3 (De Rosa et al., 2008). In a reduced oxygen state, the higher abundance of deoxyHb would release glycolytic enzymes from band 3 and increase glycolysis. Thus, the oxygen state can dictate the metabolic state within the erythrocyte via its regulation by band 3.

Glycolytic activity is relevant to the state of the red cell for several reasons. Mature erythrocytes do not contain mitochondria but rely on glycolysis as their primary source for energy production in the form of NADH and ATP. ATP is required for ion transport, energy dependent enzyme reactions and maintenance of red cell membrane organization. Erythrocytes possess a unique glycolytic bypass known as the Rapoport-Luebering Shunt. This bypass allows for production of 2,3-DPG, which promotes oxygen release from hemoglobin. Band 3 binding and inhibition of glycolytic enzymes results in the accumulation of glycolytic products and an increase of 2,3-DPG (van Wijk and van Solinge, 2005). Therefore, interaction of glycolytic enzymes with band 3 can play a key role in regulating oxygen binding to and release from hemoglobin.

NADPH is critical for maintaining redox potential in erythrocytes due to its role in the production of reduced glutathione (GSH) (Siems et al., 2000). The majority of NADPH in red cells is produced in the pentose-phosphate pathway. Under high oxygen

conditions, glycolytic enzymes bind to the N-terminus of band 3, and this interaction inhibits their enzyme activity. This inhibition allows the build-up of glycolytic intermediates to enter the pentose-phosphate pathway thus producing sufficient NADPH. High NADPH provides partial protection for the erythrocyte under high oxidative stress conditions (Filosa et al., 2003).

Finally, erythrocytes also require ATP for membrane fluctuations. It is proposed that this is regulated through continuous phosphorylation and dephosphorylation of the membrane proteins including protein 4.1R, which alters the spectrin network (Betz et al., 2009). ATP produced by glycolysis within the erythrocyte cytoplasm is thought to provide energy required for regulating this process (Gov and Safran, 2005). Thus, the cytoplasmic domain of band 3 serves a key role in regulating membrane fluctuations.

Role of phosphorylation

Protein phosphorylation plays a significant role in the regulation of a number of erythrocyte membrane properties, specifically involving band 3 (Harrison et al., 1994). Band 3 contains two primary phosphorylation sites at tyrosine 8, tyrosine 21 (Y8 and Y21), and two secondary sites at Y359 and Y904 (Brunati et al., 2000). Two proposed kinases are spleen tyrosine kinase Syk and Lyn as part of a sequential process where $p72^{syk}$ has been conclusively demonstrated to phosphorylate band 3 (Brunati et al., 1996). This phosphorylation step regulates the specific function of band 3 by blocking the interaction of glycolytic enzymes with the N-terminal domain of band 3 (Low et al., 1987). Phosphorylation of band 3 also modulates the overall cytoskeletal organization within the red cell by a decreased affinity of band 3 for ankyrin and therefore reduced

association with the spectrin-actin cytoskeleton (Ferru et al., 2011). Finally, phosphorylation is associated with increased glycolytic rates (Harrison et al., 1991). This finding is consistent with the previous observation that band 3 inhibits the activity of these enzymes, and phosphorylation of band 3 blocks this inhibitory interaction. A later study confirmed the fact that phosphorylation of band 3 results in the release of multiple glycolytic enzymes from band 3 (Campanella et al., 2005). One specific region required for phosphorylation (Y8) was later identified as being located within the N-terminal domain of 11 amino acids (Perrotta et al., 2005). Thus, phosphorylation plays a key role in modulating the activity of band 3 in the red cell membrane.

Transport Activity

The membrane-spanning 55 kDa hydrophobic domain includes the 14 transmembrane segments of the protein (Figure 1.10). As mentioned earlier, this domain is responsible for the anion exchange activity of band 3 (Hamasaki, 1999). More specifically, this domain exports the bicarbonate ion outside of the red cell, and subsequently allows chloride import into the erythrocyte cytoplasm. Generally, bicarbonate is produced as a result of carbon dioxide uptake and carbonic anhydrase activity (Hamasaki, 1999). Erythrocytes carry oxygen in the blood using the high abundance of hemoglobin within the cytoplasm. Diffusion of CO_2 in erythrocytes leads to its conversion to H_2CO_3 by carbonic anhydrase, which will be discussed in the next section. Subsequent dissociation of H_2CO_3 into HCO_3^- and H^+ allows for band 3 to export the HCO_3^- in exchange for Cl^- import. The subsequent acidification of the erythrocyte facilitates the release of oxygen from the abundant oxyhemoglobin located in the

erythrocyte cytoplasm (Hamasaki, 1999). The resulting deoxyHb then competes with glycolytic enzymes for the N-terminus of band 3 (De Rosa et al., 2008).

Carbonic Anhydrase Association

The C-terminal cytoplasmic domain of band 3 contains approximately 40 amino acids, which represents a relatively small portion of the 911 amino acid polypeptide (Hirai et al., 2011). Yet, this region contains a key binding site for carbonic anhydrase II (Figure 1.10), and this interaction is involved in the transport activity of band 3 (Sterling et al., 2001b). More specifically, inhibiting carbonic anhydrase reduces the transport activity of band 3 by approximately 50%. Carbonic anhydrase catalyzes the reaction of carbon dioxide and water to carbonic acid, which dissociates to produce bicarbonate, the aforementioned substrate for band 3 export. Thus the association of carbonic anhydrase with the C-terminus of band 3 places the enzyme in close proximity to the transporter responsible for bicarbonate efflux from the erythrocyte (Sterling et al., 2001a). These two linked proteins are playing a key role in driving transport of bicarbonate across the erythrocyte membrane. As a result, the carbonic anhydrase-band 3 interaction is often designated as a "transport metabolon" because it involves a membrane protein complex regulating both transport and metabolism of bicarbonate in the membrane (Reithmeier, 2001; Sterling et al., 2001b).

Other roles of Band 3

As discussed previously, band 3 is required for the Wright blood group antigen (Wr^b) (Bruce et al., 1995). More specifically, the residue at position 658 of band 3

provides the determination of Wr^a and Wr^b or antigenicity. The Wr^a polymorphism is associated with Lys_{658} whereas the Wr^b polymorphism contains Glu_{658} of band 3. This Lys658Glu substitution accounts for the antigen, and the Wr^b polymorphism containing Glu_{658} demonstrates interaction with Arg_{61} of GPA to form this antigen.

Southeast Asian Ovalocytosis (SAO) is directly related to the status of band 3, specifically a deletion within the N-terminal cytoplasmic domain has been linked to the etiology of this disease (Liu et al., 1995). As a result, SAO erythrocytes show some resistance to malaria parasite infection and invasion (Hadley et al., 1983; Jarolim et al., 1991). The mechanism of this strain-specific phenomenon is not fully understood, but may be linked to alterations in the adhesion of infected SAO erythrocytes (Williams, 2006). Band 3 contains some sialic acids, but GPA provides the majority of the negative charge on the erythrocyte surface from its sialic acid residues. However, in the context of GPA knockout, band 3 has demonstrated a significant increase in its sialic acid content (Chasis and Mohandas, 1992). Thus, band 3 sialylation may function as a compensatory mechanism to increase the negative surface charge on red cell surface as a result of the loss of GPA.

Role of band 3 as a malaria receptor

Band 3 has been implicated as a receptor in malaria invasion for many years. The first definitive evidence came from a study by Okoye *et al.* (1985) where purified band 3 from erythrocyte. The first mechanistic evidence of band 3 as a malaria receptor came when it was demonstrated that it serves as the receptor for the C-terminal domain of MSP1, termed $MSP1_{19}$ (Goel et al., 2003). Subsequent studies demonstrated the binding

of other malaria proteins associated with MSP1 such as MSP9 to band 3 (Kariuki et al., 2005; Li et al., 2004). The region within band 3 where this interaction occurs was termed the 5ABC domain defined by amino acids 720-761 (Figure 1.10). The specific mechanism of this interaction within the merozoite invasion has not been delineated; however it is thought to be involved during the initial adhesion steps given its abundance and distribution of MSP1 across the merozoite surface.

Summary of work

The bulk of my thesis work revolves around two specific, independent, and interconnected projects directed towards increasing the knowledge of developing therapeutic strategies against the malaria parasite. In Chapter 2, I will discuss the function and properties of an essential aspartic acid protease in parasite development. This protease, termed *P. falciparum* signal peptide peptidase (PfSPP), was verified as a viable drug target both at the blood and liver stage of malaria infection. Furthermore, we performed a bioinformatics screen to determine its putative physiological substrates. Its localization as an ER-resident protease was verified, and additional functions of this protease were investigated. Finally, using an established cell-based cleavage assay, we determined the first bona fide substrate of PfSPP in *P. falciparum*. The outcome of these studies is anticipated to provide multiple targets for a PfSPP-based antimalarial therapeutic approach *in vivo*.

Chapter 3 will outline an in-depth account of the role of MSP1 in parasite invasion. While the C-terminal domain of MSP1 is known to bind band 3, we will discuss a functional role of the N-terminal domain as an invasion ligand. More specifically, a

region of this N-terminal 83 kDa domain was identified in two independent phage display screens binding to intact human erythrocytes as well as purified glycophorins. Subsequent binding assays demonstrated it specifically binds to human glycophorin A (GPA) on the erythrocyte surface. This interaction is resistant to trypsin, chymotrypsin, and neuraminidase. The binding domain was identified in the trypsin-resistant region (amino acids 31-72) within the extracellular domain of GPA. Finally, in mice lacking the band 3-GPA complex in erythrocytes, parasite infection did not occur. While genetic knockout of erythrocyte GPA alone had little effect on parasite invasion, elimination of the band 3-GPA complex results in the eradication of malaria infection *in vivo*. Thus, the band 3-GPA complex and its putative role as a receptor for multiple domains of MSP1 defines an essential interaction for parasite invasion and development.

Chapter 2: Signal Peptide Peptidase

A malaria peptidase essential for parasite development cleaves type II signal peptides at the endoplasmic reticulum

Rationale

Plasmodium falciparum represents the most lethal parasite causing human malaria. Millions of infections occur each year, causing approximately 700,000 deaths, the majority of which occur in young children (Winzeler, 2008). The clinical manifestation of malaria is due to the blood stage of the parasite life cycle. Increasing drug resistance coupled to the lack of an effective vaccine, stresses the urgent need to identify new drug targets. Furthermore, aspartic acid proteases have long been considered viable drug targets.

A significant advance toward the development of antimalarial drugs was the identification of PfSPP as an essential gene, and viable drug target (Li et al., 2009; Li et al., 2008b; Nyborg et al., 2006b; Parvanova et al., 2009). Studies into this field are able to leverage classes of inhibitors being investigated for use against presenilin proteases. Presenilin, a close homologue of SPPs, contains the same specific catalytic motif albeit with an inverted membrane topology. The presenilins are predicted to play a key role in the onset of Alzheimer's Disease. Thus, a variety of tools are available designed against a highly relevant protease that could be re-purposed for targeting PfSPP. Coupling these relevant tools to the importance of identifying new drug targets for the most lethal form of human malaria motivated us to pursue this area of study.

The malaria homologue of SPP is not well understood. Coupling this limited knowledge to the highly complex trafficking and endomembrane pathway of malaria requires a deeper understanding into the properties of this potential drug target. Therefore, the goal of our study was to characterize this specific protease via the identification of its localization, mechanism, and endogenous substrates. Combined with

immunolocalization, bioinformatics screening, and luminescence assays, we localized PfSPP within the intracellular parasite and discovered its first known substrate. It is our hope that SPP and its associated proteins can be used as part of a multi-targeted therapeutic approach to eradicate *P. falciparum* mediated pathology.

Materials and Methods

Parasite Culture

P. falciparum was maintained in continuous culture in a 5% suspension of fresh human erythrocytes in RPMI 1640 with 0.5% AlbuMAX II (Invitrogen) at 37°C under 5% CO_2, 5% O_2, and 90% N_2 as previously described (Li et al., 2008b; Trager and Jenson, 1978). Ring-stage parasites were synchronized by using 5% sorbitol treatment, and late-stage parasites were enriched to >95% by centrifugation using 63% (v/v) Percoll as described (Goel et al., 2003).

Monospecific PfSPP-CT Antibody

A peptide matching the C-terminal amino acids 393-412 (EIPKIQETPVSNAKKRITNK) of PfSPP was synthesized. This region was then conjugated via the N-terminus to Keyhole Limpet Hemocyanin (KLH). Using this peptide, Alpha Diagnostic International (ADI, San Antonio) generated an antibody which we titled PfSPP C-terminus (PfSPP-CT). The polyclonal antibody was affinity-purified using the synthetic C-terminal PfSPP peptide conjugated to beads. Biotinylated antibody was generated by labeling the affinity-purified antibody with the EZ-Link Sulfo-NHS-LC-Biotin kit (Thermo). The affinity-purified antibody was stored at -20°C in 50% glycerol.

Western Blotting

Parasite protein extract was prepared by solubilizing an enriched fraction of mature parasites with an extraction buffer (50 mM Tris-HCl, pH 8.0, 150 mM NaCl, 5 mM EDTA, 5 mM EGTA, 0.5% Triton X-100) supplemented with 2 μg/ml Aprotinin, 1.0

μg/ml of Leupeptin, Pepstatin A, Bestatin, 1 mM phenylmethylsulfonyl fluoride (PMSF), and a cocktail of protease inhibitors (Roche). For lysis of HEK293T cells radioimmunoprecipitation (RIPA) buffer was used to harvest cells and for visualization by western blotting. Boiling of samples significantly altered migration patterns of PfSPP. Transfected HEK293T samples were treated at 37°C for 10 minutes or sonicated in order to ease loading onto a 10% sodium dodecyl sulfate (SDS)-PAGE gel for analysis. Nitrocellulose membranes were blocked in 5% milk in Tris buffered saline-Tween (TBS-T) solution and incubated with the primary biotin-conjugated antibody in the blocking solution overnight at 4°C. After washing the membrane, the secondary HRP-Streptavidin antibody was used to detect the PfSPP signal on the membrane using the standard ECL detection kit. In addition, we used unlabeled purified PfSPP antibody for Western Blotting with similar results.

Co-Immunoprecipitation

The lysis buffer used to prepare parasite lysate contained 50 mM Tris-HCl, pH 8.0, 150 mM NaCl, 1% NP-40, 0.5% Sodium deoxycholate, 0.1% SDS, 5 mM EDTA, 5mM EGTA. Protein A beads were used to pre-clear the lysate, upon which 300 μL of supernatant was incubated with the PfSPP-CT antibody overnight at 4°C. The pre-immune rabbit IgG was used as a control. Protein A beads were added to the mixture and incubated at 4°C for 3 hours. Beads were then washed with RIPA buffer, and rinsed once in PBS prior to the elution of immune-complex.

Immunofluorescence Microscopy

Plasmodium falciparum infected erythrocytes were smeared and air-dried on glass slides, and fixed with methanol for 30 minutes at -20°C. Slides were incubated for two hours with the affinity purified anti-PfSPP-CT antibody and anti-PMV antibody at room temperature. Slides were washed 3 times in PBS, 0.05% Tween 20 (PBS-T) and incubated for one hour with respective secondary antibodies, anti-rabbit Alexa 488 (green) and anti-mouse Alexa 594 (red). Immunofluorescence images at 100X magnification were captured using the Zeiss LSM510 confocal microscope (Germany).

Immunogold Electron Microscopy

P. falciparum infected erythrocytes were washed in RPMI 1640 and fixed for 1 h at 4°C in a solution containing 4% paraformaldehyde, 0.1% glutaraldehyde in 0.1M sodium phosphate buffer (pH 7.2), and embedded in white London resin. Ultra-thin sections were blocked in 1% bovine serum albumin (BSA) in PBS before incubating with anti-PfSPP-CT antibody diluted in blocking solution. Samples were washed and incubated with secondary antibody conjugated to gold particles (15 nm diameter) at a 1:10 dilution for 1 hour. Upon successful labeling sections were stained with both uranyl acetate and lead citrate for visualization. The instrument used to visualize these slides was a Philips FEI Tecnai F30 transmission electron microscope at 300 kV at the University of Chicago EM facility.

Bioinformatics Screen

We performed a bioinformatics search for PfSPP substrate candidates by selecting for genes in PlasmoDB that only match the selected criteria. These criteria included seven

steps, several of which were performed by searching through the properties of the remaining genes at each step. Using this bioinformatics search strategy, we selected for genes in *Plasmodium falciparum*, which are protein coding, exist as a single copy gene, and contain a signal peptide. These genes were further narrowed down by restricting this signal peptide to only account for type II transmembrane domains, specifically containing a protein motif pattern 6666996666 (where 6 represents a hydrophobic AA residue, and 9 represents a small AA residue). The final list only accounted for genes in which the signal peptide and type II transmembrane domain overlap, ensuring a type II orientation of the SP region. By applying each of these criteria as a "step" in a PlasmoDB search strategy, we identified a core group of potential PfSPP substrates.

PfSPP Luminescence Assay

The signal peptide sequence was cloned into the pCGN-HA-ATF6 vector containing the following sequence of tags: N—HA-ATF6-Strep-MKC-SP-Myc—C. The affinity tags are HA, Strep, and Myc, and the amino acid sequence MKC (methionine, lysine, cysteine) functions as a leader sequence adjacent to the signal peptide. This MKC sequence corresponds to the N-region of the vesicular stomatitis virus G-protein (VSV-G) signal peptide. SP indicates the amino acid sequence of the signal peptide of interest. The HSP101 signal peptide sequence used is: YLKYYIFVTLLFFVQVINNVLCA. The pCGN-HA-ATF6 plasmid was acquired and required the synthesis of the various aforementioned tags and signal peptide of the substrate of interest. These were synthesized in a number of PCR steps beginning with oligo extension of the HSP101 SP region. In a 20 µL PCR reaction containing 0.5 µL of EconoTaq polymerase, 2 µL of 10X

Econotaq buffer and 1 mM dNTPs 2 overlapping oligos were used at 2.5 μM including HSP101F, 5'-ATGGCCTGGCGGCACCCCCAGTTCGGCGGCATGAAGTGCTATT TGAAGTATTATATTTTTGTGACCTTGTTGTTTTTTGTGCAGGTGATTAAT-3' and HSP101R, 5'-GAGGTCCTCCTCGCTGATGAGTTTCTGCTCAGCGCACAACA CATTATTAATCACCTGCACAAAAAA-3'. A subsequent PCR reaction was performed using this PCR product as a template and new primers containing the Strep, MKC and Myc tags required for this experiment. Thus in a typical PCR reaction the following primers were used StrepF 5'-CGGGGATCCATGGCCTGGCGGCACCCC-3' (BamHI underlined) and MycR 5'-CGGGGATCCGAGGTCCTCCTCGCTGATGAG-3' (BamHI underlined) and products were gel purified using the QIAGEN Gel purification kit. Purified products were digested with BamHI, ligated into the aforementioned pCGN-HA-ATF6 plasmid, and transformed into DH5α *E. coli* cells.

To construct a mutant version of PfSPP, we used the QuikChange mutagenesis kit (Agilent Technologies). Using the following primers, generated by the QuikChange Primer Design program, 5′-AGGGCTCTTTGTGTACGCCATCTTTTGGGTCTTTG-3′ (sense) and 5′- CAAAGACCCAAAAGATGGCGTACACAAAGAGCCCT-3′ (anti-sense), and 5′-GCTGGGACTGGGCGCTATCATCATCCCAG-3′ (sense) and 5′-CTGGGATGATGATAGCGCCCAGTCCCAGC-3′ (anti-sense), residues D228A and D269A were mutated, respectively. This targeted the catalytic motif containing two highly conserved residues required for activity. This catalytically inactive mutant was used in the luminescence assay as described above. A pCDNA6-PfSPP-GFP construct was generated by cloning GFP out of the pEGFP-C1 plasmid using the following primers 5′-GCTCTAGAATGGTGAGCAAGGGCG-3′ (Forward, XbaI) and

5′-GCTCTAGACTACTTGTACAGCTCGTCCATGC-3′ (Reverse, XbaI). The modified GFP fragment with XbaI sites was then cloned onto the C-terminus of PfSPP in the pCDNA6 plasmid. The pCDNA6-PfSPP-GFP construct was used in transfections as described above to test for its activity and the effect of a C-terminal GFP tag on PfSPP activity. The luciferase reporter constructs pRL-SV40 and p5XATF6-GL were acquired and used as previously. HEK293T cells were grown in DMEM and 10% fetal bovine serum.

Twenty-four hours prior to transfection, HEK293T cells were plated at 60-70% confluency according to the FuGENE HD transfection protocol (Promega). Three hours prior to transfection, fresh media was added to each well. Cells were then transiently transfected with 50 µl of serum-free Opti-MEM, 6 µl FUGENE, and the following plasmids: 0.02 µg of pRL-SV40 *Renilla* to normalize transfections, 0.25 µg of p5XATF6-GL for a Firefly luciferase reporter, 0.25 µg of pCGN-HA-ATF6 (1-373)-HSP101 substrate plasmid, and 1.5 µg of pCDNA6-PfSPP coding for full-length *Plasmodium falciparum* signal peptide peptidase, which has been codon optimized for expression in a mammalian expression system. A pCGN-HA-ATF6 (1-373)-LSA1 substrate plasmid was also constructed and used as mentioned above (MKHILYISFYFILVNLLIFHINGKIIK). Cells were incubated for 20-24 hours with the plasmids and transfection reagent and lysed and assayed for luciferase activity using the Dual Luciferase Reporter Assay System (Promega). Cells were lysed in passive lysis buffer, cleared by centrifugation for 1.0 minute at 14,000 x g, and then 20 µL of supernatant lysate was used to measure the luminescence signal using the Tecan SpectraFluor Plus. Firefly reporter signal was normalized using the activity of the *Renilla* luciferase. For assays involving SPP

inhibitors $(Z\text{-}LL)_2$ ketone (10 μM) and L-685,458 (25 μM), 3-4 hours after incubating with the transfection mixture, media was replaced with fresh media containing the two inhibitors mentioned above. For dose-dependent studies, varying concentrations (2, 10 and 25 μM) of $(Z\text{-}LL)_2$ ketone were used as described above. DMSO was used as a vehicle control, and the presenilin specific inhibitor DAPT (15 μM) was used as a negative control. The concentration of $(Z\text{-}LL)_2$ ketone inhibitor used in this assay corresponds to the established SPP cleavage assay for human SPP, while we used a slightly higher concentration of DAPT to ensure that it was not a result of nonspecific inhibition (Nyborg et al., 2004a). Furthermore, a previous study has used a relatively specific γ-secretase inhibitor, L-685,458, at concentrations of 25 and 50 μM in 293T cells under similar conditions (Okamoto et al., 2008). Both studies showed significant SPP inhibition. We used the lower concentration of L-685,458 in our study.

Transfection of malaria parasite by PfSPP-GFP construct

Using the following primers 5′-CCGCTCGAGGCCATATCTTTGGTAATTCTT-3′ (Forward, XhoI) and 5′-GCACGCCTAGGTTTATTGGTAATTCTTTTTTT-3′ (Reverse, AvrII), an 883 bp fragment from the C-terminal region of the PfSPP genomic DNA sequence was synthesized via PCR. This region was then inserted into the pPM2GT vector in frame to the C-terminal GFP tag followed by a hDHFR cassette expressing resistance to the antifolate drug WR99210 as described previously (Klemba et al., 2004). We termed this vector, pSPPGT. Transfections were performed using the plasmid DNA-loaded human erythrocytes suitable for parasite invasion (Deitsch et al., 2001). Human erythrocytes (350 μL) were washed 3X in Incomplete Cytomix and 50 μL of 1.0 μg/μL

pSPPGT was added for a final volume of 400 µL (Wu et al., 1995). Cells were then electroporated using the following conditions: 0.31 kV, and 960 µFD with a time constant of about 10 ms using the Bio-Rad GenePulser. Cuvettes were washed and inoculated with a synchronized trophozoite-schizont stage *P. falciparum* 3D7 culture. On day 2 following transfection, parasites were selected in the presence of 5 nM WR99210, with media changes on every other day, and fresh erythrocytes were added as needed. Transfections were also performed on *P. falciparum* residing within human red blood cells (Crabb et al., 1997). Synchronized ring-stage parasite culture at high parasitemia was combined with the aforementioned construct in Cytomix buffer and electroporated at 0.31 kV, 960 µFD with a time constant of about 10 ms. Cells were then immediately placed on ice, washed with culture medium, and returned to culture. Selection with WR99210 started on day 3 post-transfection.

Results

Biochemical Characterization of Plasmodium falciparum Signal Peptide Peptidase

Homologous signal peptide peptidase proteins across several organisms are known to localize to the endoplasmic reticulum (ER), and play essential roles in development (Dev et al., 2006; Friedmann et al., 2006; Urny et al., 2003). Consistent with this subcellular localization and role in development, our previous studies have shown that *P. falciparum* failed to mature beyond the late-ring and/or early trophozoite stage of intra-erythrocytic development in the presence of pharmacological inhibitors of SPPs (Li et al., 2009). In our previous studies, we utilized an antibody raised against the exofacial loop 4 (EL4) of PfSPP (Figure 2.1A, red line) (Li et al., 2009). Based on predicted topology of SPPs, EL4 is expected to face the lumen of the ER, and may not be an accessible epitope for the detection of PfSPP under certain experimental conditions. Although the affinity-purified polyclonal antibody against EL4 epitope detected PfSPP in the parasite lysate by immunoblotting, it was not effective for immunoprecipitation of PfSPP. Similarly, this antibody produced a relatively weak signal for immunolocalization studies of PfSPP. To overcome these limitations, we generated a new polyclonal antibody against the C-terminal 20 amino acids of PfSPP (EIPKIQETPVSNAKKRITNK) to investigate the role of PfSPP at the early stages of parasite development (Figure 2.1A, green line). The C-terminal peptide EIPKIQETPVSNAKKRITNK of PfSPP did not show any significant homology with the corresponding sequence LDCATNEENPVISGEQIVQQ of human signal peptide peptidase (SPPL2A). Therefore, it is unlikely that the polyclonal anti-PfSPP-CT antibody would recognize orthologous SPPs in mammalian cells.

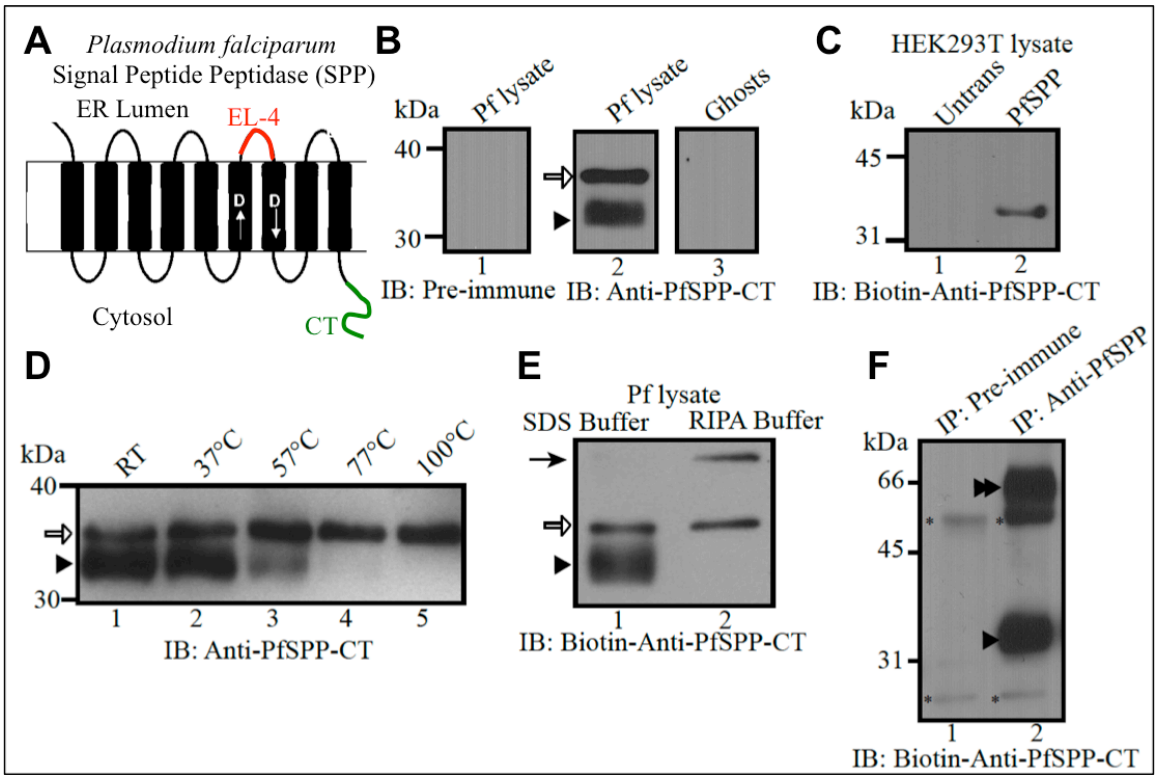

Figure 2.1. Immunoblotting of PfSPP using the anti-C-terminal PfSPP antibody. (A) Predicted membrane topology of SPP according to Wolfe *et al*. (2010). Highlighted area in red is the exofacial loop 4 of PfSPP, where the antibody used in our previous study was generated. Highlighted area in green corresponds to the C-terminal domain of PfSPP, where the antibody used in this study was raised. (B) Immunoblotting detected two bands of PfSPP as indicated by arrows (white arrow for 35 kDa, and black arrowhead for 32 kDa, lane 2). (C) Transient transfection of a synthetic PfSPP construct (pCDNA6-PfSPP) resulted in PfSPP expression in HEK293T cells. Cell lysate was then analyzed by immunoblotting using the biotinylated anti-PfSPP antibody. (D) Sample incubation at different temperature alters the mobility of PfSPP with the disappearance of the 32 kDa band at higher temperatures (arrowhead). (E) Lysis conditions significantly alter the mobility of PfSPP. Lysing directly in sample buffer results in the detection of the 35 kDa and 32 kDa bands (white arrow and black arrowhead, respectively). The use of RIPA buffer results in the elimination of the 32 kDa band, but the presence of a larger band at approximately 47 kDa (black arrow). (F) Immunoprecipitation of PfSPP from parasite-infected erythrocyte lysate. Two bands of PfSPP were pulled down using the anti-PfSPP-CT antibody. The single arrowhead indicates the 35 kDa band and a double arrowhead indicates the 65 kDa band of PfSPP. Asterisks correspond to heavy and light chain bands in the pre-immune IgG negative control (Lane 1).

The anti-PfSPP-CT antibody detected two specific bands of PfSPP corresponding to sizes of 35 kDa and 32 kDa in the *P. falciparum* lysate by immunoblotting as indicated by the white arrow, and black arrowhead, respectively (Figure 2.1B, D, E). A similar pattern of PfSPP bands was observed using both unconjugated and biotin-conjugated anti-PfSPP-CT antibody (Figure 2.1B, C, E). The predicted MW of PfSPP is 47 kDa from the primary structure deposited in the PlasmoDB, however a previous study expressed a codon-optimized version of PfSPP in mammalian cells and observed a 35 kDa band by immunoblotting using an anti-tag antibody (Nyborg et al., 2006b). The synthetic PfSPP gene sequence used in the previous study lacked a six amino acid peptide VFTTIL, which we later identified in our full length PfSPP sequence (Li et al., 2009; Nyborg et al., 2006b). It is unlikely that the presence of this hydrophobic VFTTIL insert would alter the mobility of full length PfSPP by SDS-PAGE. However, we noticed that the gel mobility of PfSPP bands was markedly affected by the parasite lysis and sample preparation conditions. For example, detection of 32 kDa band was dependent upon the temperature of sample preparation. Parasite lysate prepared at 77°C and 100°C resulted in the complete loss of 32 kDa band, possibly as a result of degradation or aggregation (Figure 2.1D). Furthermore, parasites lysed directly in SDS sample buffer showed the presence of the two aforementioned 35 and 32 kDa bands, whereas lysate prepared in RIPA buffer prior to SDS-PAGE showed the presence of a 47 kDa band, and complete elimination of the 32 kDa band (Figure 2.1E). Thus, the migration size of PfSPP is highly dependent on lysis and temperature conditions. Lysis directly in SDS sample buffer was used as it precluded the need for an additional lysis step including RIPA buffer. The anti-PfSPP-CT

antibody did not detect any band in the plasma membrane proteins (ghosts) from uninfected human erythrocytes (Figure 2.1B).

To resolve the observation of multiple bands in the parasite lysate, we expressed recombinant PfSPP in heterologous HEK293T cells and detected a single 35 kDa band using the biotinylated anti-PfSPP-CT antibody (Figure 2.1C). This band could not be seen in samples that had been boiled, likely due to aggregation of transmembrane proteins. Similarly, lysis of parasite-infected erythrocytes in RIPA buffer resulted in the presence of a 47 kDa band of PfSPP (Figure 2.1E). These observations are consistent with the previous observations that differential mobility of several transmembrane proteins is influenced by conditions of sample preparation prior to SDS-PAGE (Rath et al., 2009). Similarly, the mobility of eukaryotic SPPs has been shown to vary depending upon the presence of associated proteins (Lu et al., 2012; Schrul et al., 2010). Based on our cross-blotting experiments using anti-PfSPP-CT and anti-PfSPP-EL4 antibodies, and immunoblotting and immunoprecipitation of PfSPP under multiple lysis and incubation conditions, we suggest that the 35 kDa and 32 kDa bands are likely to represent either the same PfSPP species or a consequence of some unknown post-translational modification during sample preparation. The 35 kDa form of PfSPP is consistent with the recent demonstration of 35 kDa species of PfSPP under similar conditions (Marapana et al., 2012). The molecular nature of 47 kDa band, detected by our anti-PfSPP-CT biotinylated antibody in parasite lysate, remains unknown at this stage. Moreover, we did not detect any dimer form of PfSPP under direct lysis conditions of immunoblotting (Figure 2.1 B, D, E). It is noteworthy that human SPP is known to form a stable dimer species under similar conditions of immunoblotting (Nyborg et al., 2004b; Nyborg et al., 2006b).

Plasmodium falciparum SPP: evidence for dimer formation

PfSPP was immunoprecipitated from parasite-infected erythrocyte lysate using the unconjugated affinity-purified anti-PfSPP-CT antibody. Immunoprecipitated material was then detected by immunoblotting using the same biotinylated anti-PfSPP-CT antibody to avoid the potential complications of spurious reactivity often encountered from the secondary antibody (Figure 2.1F). A band of 35 kDa was detected (Figure 2.1F, arrowhead) consistent with a similar band of PfSPP detected under direct immunoblotting conditions (Figure 2.1B-E). Interestingly, we also detected a higher molecular weight band at approximately 65 kDa (Figure 2.1F, double arrowheads). This 65 kDa band corresponds to the approximate position of a putative PfSPP dimer. While we did not detect any dimer band of PfSPP in the direct immunoblotting experiments (Figure 2.1B-E), immunoprecipitation of PfSPP from parasite lysate solubilized under mild detergent conditions likely preserved the dimer species, which persisted under conditions of SDS-PAGE. This observation is consistent with prior evidence showing that homologous signal peptide peptidases form dimers, and may function as dimers *in vivo* (Nyborg et al., 2006a; Nyborg et al., 2004a). Evidence for the existence of PfSPP as a dimer in the parasite-infected erythrocyte lysate is consistent with published evidence demonstrating the migration of recombinant PfSPP as 35 and 70 kDa bands when expressed in the HEK293T cells (Dev et al., 2006; Nyborg et al., 2006b). These observations suggest that native PfSPP exists as a dimer in infected erythrocytes and perhaps in hepatocytes. This finding is in agreement with evidence suggesting that human SPP primarily exists as a

homodimer *in vivo* (Nyborg et al., 2004b). However, biochemical characterization of PfSPP in the hepatocyte stage of parasite infection requires further characterization.

Localization of PfSPP to the parasite endoplasmic reticulum

We have shown that pharmacological inhibition of PfSPP prevents parasite maturation in erythrocytes indicating a functional role in development (Li et al., 2009). Previous studies have also documented immunolocalization of eukaryotic SPPs to the ER (Dev et al., 2006; Friedmann et al., 2006; Urny et al., 2003). Homologous proteases also share similar localizations within the endomembrane system. While PfSPP does not share the C-terminal KKXX retrieval signal at the -3 and -4 positions known to signal for ER retention, it does contain a dilysine motif at the -6 and -7 positions. We hypothesize this dilysine motif performs the ER localization function of PfSPP. The essential role of PfSPP in early parasite development, coupled with the ER localization of closely related SPPs, suggested that PfSPP might be localized to the parasite ER. We examined the localization of PfSPP in infected erythrocytes using our affinity-purified anti-PfSPP-CT antibody. The subcellular localization of PfSPP was examined in trophozoite-infected human erythrocytes via indirect immunofluorescence microscopy. PfSPP specifically co-localized with Plasmepsin V (PMV), a known ER-marker (Figure 2.2A-F). The mesh-like network of PfSPP is consistent with the perinuclear endomembrane system observed at the late stages of intra-erythrocytic parasite development (Lee et al., 2008; van Dooren et al., 2005). Further analysis by immunofluorescence microscopy using an antibody against parasite-derived BiP, another ER marker, found a similar co-localization pattern with PfSPP thus verifying the ER localization of PfSPP in infected erythrocytes.

To further confirm the ER localization of PfSPP, immunogold electron microscopy was performed. PfSPP was visualized using the affinity-purified anti-PfSPP-CT antibody followed by a secondary antibody conjugated to 15 nm gold particles (Figure 2.2G, H). Gold particles, shown as black dots, were visualized in a diffuse pattern across the parasite cytoplasm at all stages of parasite development, including the trophozoite and schizont stages (Figure 2.2G, H), as well as the late ring stage. PfSPP was not detected in the food vacuole or endosomal compartments of infected erythrocytes (Figure 2.2G, H). The diffuse pattern of PfSPP throughout the parasite cytoplasm is consistent with the mesh-like network/or perinuclear endomembrane system shown in previous studies (Lee et al., 2008; van Dooren et al., 2005). These results further confirm the localization of PfSPP to the parasite endoplasmic reticulum, and are consistent with the localization of PfSPP in the ER-like structures in infected erythrocytes (Marapana et al., 2012).

Bioinformatics analysis of potential PfSPP substrates

Subcellular localization of PfSPP to the ER is consistent with the localization of SPPs from several other species (Dev et al., 2006; Friedmann et al., 2006; Urny et al., 2003). Furthermore, this confirmed that potential substrates accessible to PfSPP might include proteins containing a signal peptide processed within the ER. While homologous forms of SPPs cleave multiple substrates in various organisms, several known characteristics and motifs of these substrates appear to be conserved across a number of species. To identify putative substrates of PfSPP, we performed a hypothetical substrate search screen using a specific set of parameters.

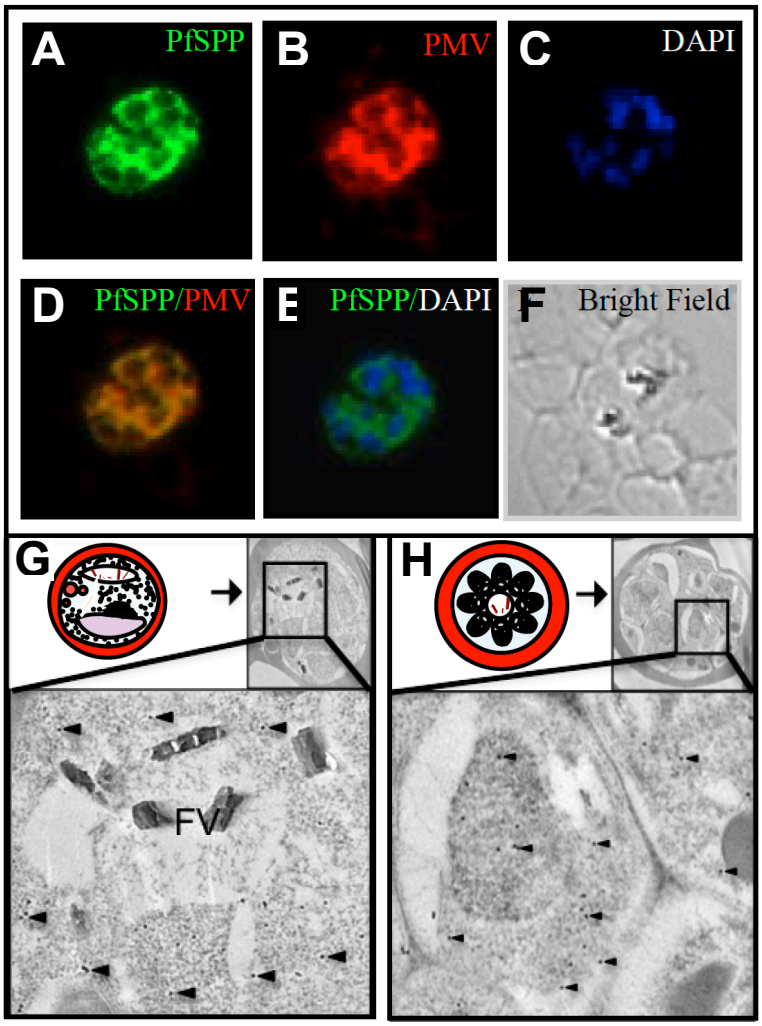

Figure 2.2. PfSPP co-localizes with Plasmepsin V to the endoplasmic reticulum. Indirect immunofluorescence microscopy using specific antibodies demonstrates PfSPP (green) co-localizes with a known parasite ER marker Plasmepsin V (red) in the *Plasmodium falciparum* (3D7) trophozoite. (A) Staining of PfSPP. (B) Staining of known ER marker, Plasmepsin V. (C) DAPI stain shows parasite DNA. (D) PfSPP and PMV overlay shows co-localization at the ER. (E) Overlay of PfSPP and DAPI stain did not show any significant co-localization. (F) Bright field microscopy shows mature trophozoite stage infected erythrocytes. (G, H) Immunogold electron microscopy of PfSPP in the parasite infected erythrocytes. PfSPP is indicated by black dots and several spots are identified by black arrowheads. (G) Schematic illustration of a mature trophozoite stage parasite in the infected erythrocyte (Adapted from Bannister et al., 2000). PfSPP staining in the trophozoite shows a diffuse staining pattern throughout the perinuclear endomembrane system/ER. (H) Illustration of a late schizont-stage parasite in an infected erythrocyte (Adapted from Bannister et al., 2000). PfSPP staining in the late-schizont stage of parasite development shows staining throughout the perinuclear endomembrane system/ER.

Because eukaryotic SPPs are known to cleave type II transmembrane proteins, we limited our search criterion to single copy genes of known function. They must contain a single transmembrane domain coded for by the SP region, and it has to be of type II transmembrane orientation. Finally, it must contain a protein motif pattern commonly observed in human SPP substrates. Model SPP substrates generally contain 8-14 aliphatic hydrophobic residues flanking two small residues at the center of the hydrophobic transmembrane domain (Dev et al., 2006; Nyborg et al., 2004a). We applied this stringent search criterion to narrow down a list of 6 potential substrates (Table 2). Of these potential substrates, the most intriguing was *Plasmodium falciparum* heat shock protein 101 (HSP101). Previous evidence indicates that HSP101 encodes an N-terminal ER signal (de Koning-Ward et al., 2009; Dev et al., 2006), consistent with the ER localization of PfSPP. While HSP101 is essential for parasite protein export and translocation, a functional role of its signal peptide is not known. Based on the known characteristics of HSP101, and its critical role in parasite development, we hypothesized that parasite HSP101 serves as a natural substrate of PfSPP in *Plasmodium falciparum* infected human erythrocytes. The *P. falciparum* genome contains over 5,000 genes, approximately 1,000 of those are predicted to contain a signal peptide. When selected for the putative SPP cleavage motif to identify highly promising substrates, the resulting list is narrowed down to 260 proteins. Differentiating between type I and type II signal peptides is extremely difficult in the intracellular organelles. But given the extensive list of potential substrates, it is likely that PfSPP cleaves signal peptides outside of the short list outlined in Table 2. However, Table 2 includes a list of the most promising hits using a strict criterion towards identification of the first known substrate of PfSPP. One

possible method for future discovery of PfSPP substrates is to identify type II signal peptides from an expanded list with less stringent criteria.

Identification of HSP101 as a substrate of PfSPP by luminescence cleavage assay

To investigate if any of the putative type II transmembrane proteins identified in our bioinformatics screen (Table 2) can serve as a substrate of PfSPP, we utilized a transient transfection assay approach optimized for human embryonic kidney 293T cells. This assay has been previously used to demonstrate the enzyme activity of synthetic PfSPP against a model substrate (Dev et al., 2006; Nyborg et al., 2006b). A schematic diagram of the transient assay, adapted from Nyborg *et al*., is shown in Figure 2.3A (Dev et al., 2006; Nyborg et al., 2004a). This assay utilizes a model substrate linked to activating transcription factor-6 (ATF-6), which is released from the membrane upon cleavage by PfSPP. ATF-6 binds to the promoter region of a plasmid containing a Firefly Luciferase reporter gene. Thus, expression and activity of Firefly Luciferase provides a metric for measuring PfSPP activity. We adapted this assay to validate putative substrates in our bioinformatics screen (Table 2). The cell-based cleavage assay demonstrated significant cleavage of parasite HSP101 signal peptide by PfSPP compared to endogenous luciferase activity (Figure 2.3B). PfSPP activity against HSP101 was markedly inhibited by the pharmacological inhibitors of SPP termed $(Z\text{-}LL)_2$ ketone and L-685,458 (Figure 2.3B). In contrast, DAPT, a presenilin-specific inhibitor, showed no inhibitory effect on the cleavage activity of PfSPP against HSP101 (Figure 2.3B). These findings indicate that malaria parasite HSP101 serves as a substrate of PfSPP under these conditions.

Table 2. Parasite SPP substrates predicted from the bioinformatics screen.

Gene Identified	Gene ID	Predicted Function
Heat Shock Protein 101 (HSP101)	PF11_0175	Component of protein export machinery
Erythrocyte Membrane Protein 3 (PfEMP3)	PFB0095c	Destabilization of erythrocyte membrane skeleton
Aspartate Carbamoyltransferase	MAL13P1.221	Role in pyrimidine biosynthesis
Liver Stage Antigen 1 (LSA1)	PF10_0356	Putative role in liver schizogony and merozoite release
Malonyl CoA-acyl Carrier Protein Transacylase Precursor	PF13_0066	Involved in fatty acid biosynthesis
Apicoplast Ribosomal Protein L21 Precursor, putative	PF08_0014	Member of large ribosomal subunit; role in protein synthesis

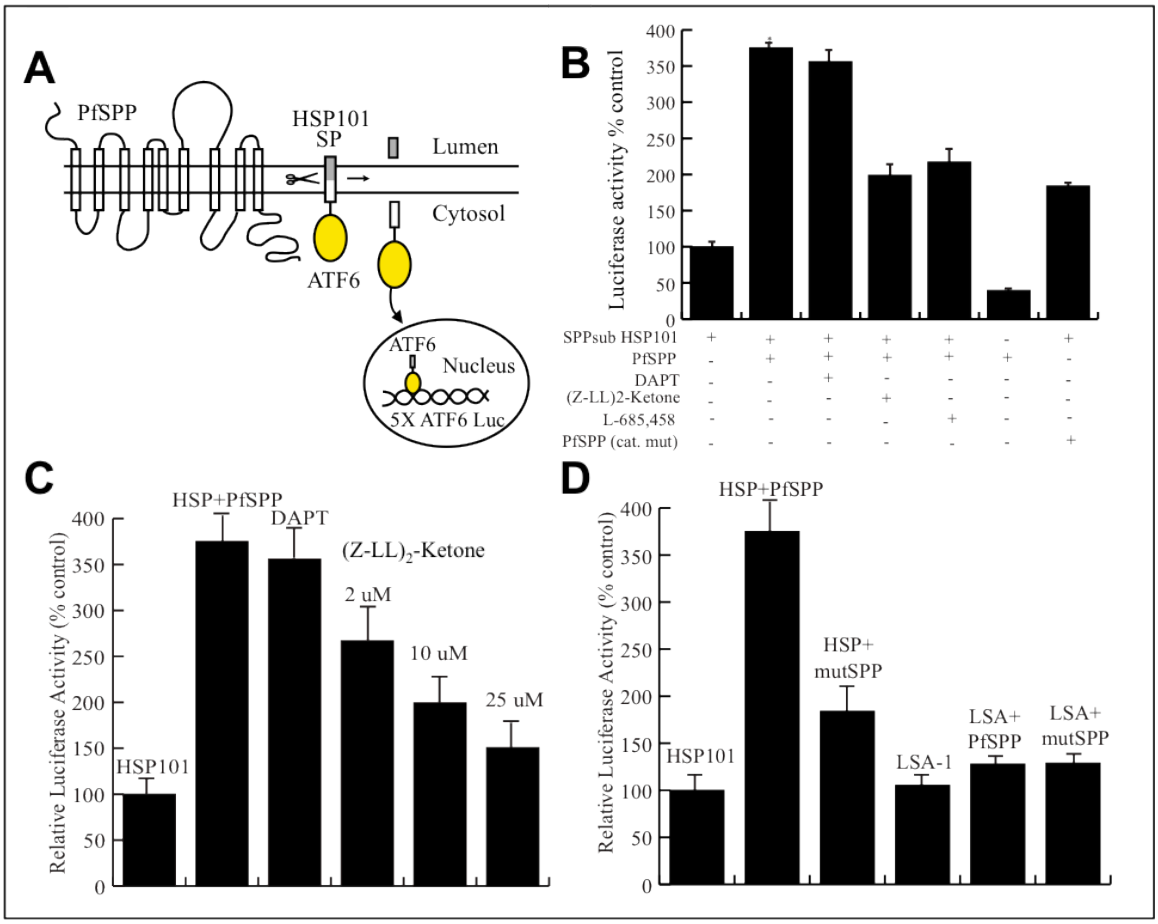

Figure 2.3. PfSPP cleaves the signal peptide of HSP101 but not LSA-1.
HEK293T cells were transiently transfected with a combination of plasmids expressing PfSPP, HSP101/LSA-1 SP, *Renilla* luciferase, and Firefly Luciferase. (A) Schematic diagram of ATF6-linked substrate cleavage by PfSPP resulting in increased Luciferase expression (Adapted from Nyborg et al., 2004). (B) Overexpression of PfSPP significantly increased peptidase activity relative to endogenous activity (*P<0.01). This cleavage activity was inhibited by the SPP inhibitors $(Z\text{-}LL)_2$ ketone (10 µM) and L-685,458 (25 µM), whereas the presenilin-specific inhibitor DAPT (15 µM) did not show inhibition of PfSPP activity. Furthermore, the use of a mutant PfSPP with its catalytic residues modified, (D228A and D269A) significantly reduced HSP101 cleavage activity to near baseline levels. (C) A dose-dependent analysis was performed using the $(Z\text{-}LL)_2$ ketone SPP-specific inhibitor. PfSPP protease activity against HSP101 was measured in the presence of three different concentrations (2, 10 and 25 µM) of inhibitor. (D) LSA-1 was tested as a substrate of PfSPP. Luminescence activity of LSA-1 was measured alone, in the presence of the wild type PfSPP, and a catalytically inactive mutant of PfSPP. LSA-1 expression in the presence of PfSPP showed no measurable change of luciferase activity relative to baseline, or in the presence of the catalytically inactive mutant of PfSPP.

While the SPP inhibitors did not completely eliminate the luminescence signal, this is likely due to the fact that the SPP inhibitors were added to the media 3-4 hours after incubation with the transfection reagent and plasmids, thus allowing partial cleavage of HSP101 to occur. Concerns of cross-reactivity and toxicity between the transfection reagent, vehicle, and inhibitors precluded the addition of protease inhibitors at the time of transfection.

Moreover, we generated a catalytically inactive mutant of PfSPP where the two active site aspartic acid residues (D228 and D269) were mutated to alanine, as described in the Methods section.

As expected, the cleavage of HSP101 by PfSPP mutant was markedly reduced to a level that is similar to that observed in the presence of SPP inhibitors (Figure 2.3B). Together, these data are consistent with previous studies demonstrating reduced enzyme activity of aspartic acid mutants of SPP (Dev et al., 2006; Matsumi et al., 2006; Nyborg et al., 2004a). To further verify the susceptibility of HSP101 as a substrate of PfSPP, we investigated whether the catalytic activity of PfSPP was inhibited in a dose-dependent manner by the SPP inhibitor $(Z\text{-}LL)_2$ ketone. The cleavage of HSP101 by PfSPP was inhibited in a dose-dependent manner at three concentrations of $(Z\text{-}LL)_2$ ketone (2, 10, and 25 μM)(Figure 2.3C). A cell-free cleavage assay system has been used previously to measure the protease activity of newly identified substrates of SPP by utilizing their synthetic signal peptide sequences (Dev et al., 2006; Lemberg and Martoglio, 2002). However, this approach was not feasible because the putative signal peptide sequence of parasite HSP101 (YLKYYIFVTLLFFVQVINNVLCA) is extremely hydrophobic, and our multiple attempts to synthesize this peptide sequence failed. Genetic tractability of

the malaria parasite posed unique technical barriers for biochemical analysis of PfSPP substrates under endogenous conditions. For example, both genetic and pharmacological inhibition of PfSPP are lethal (Dev et al., 2006; Li et al., 2009). The putative endogenous cleavage of signal peptides is likely to occur rapidly, thus precluding the possibility of detecting PfSPP-associated substrates by conventional pull-down assays. Therefore, a cell-based assay, as described above, offers the most practical approach to measure the protease activity of PfSPP, and for identification of endogenous substrates. Finally, to further confirm the specificity of our cell-based cleavage assay, we measured the cleavage susceptibility of liver stage antigen-1 (LSA-1) (MKHILYISFYFILVNLLIFHINGKIIK) identified as a potential substrate of PfSPP in our bioinformatics screen (Table 2). PfSPP did not cleave LSA-1 under the same experimental conditions (Figure 2.3D). Both wild type and catalytically inactive mutants of PfSPP showed the same basal level of protease activity against LSA-1, further confirming the specificity of HSP101 cleavage by PfSPP (Figure 2.3D).

Reduced PfSPP activity correlates with gametocytogenesis

Subcellular localization of PfSPP in the micronemes (Dev et al., 2006; Li et al., 2008b) and ER (Figure 2.2) suggested that a defined trafficking pathway might regulate the delivery and localization of PfSPP to specific organelles. To address this issue further, we generated a PfSPP-GFP (pSPPGT) chimeric construct to monitor the trafficking of PfSPP in live parasites in infected human erythrocytes (Figure 2.4A). Two separate methods of parasite transfection were used, and both methods gave rise to similar results.

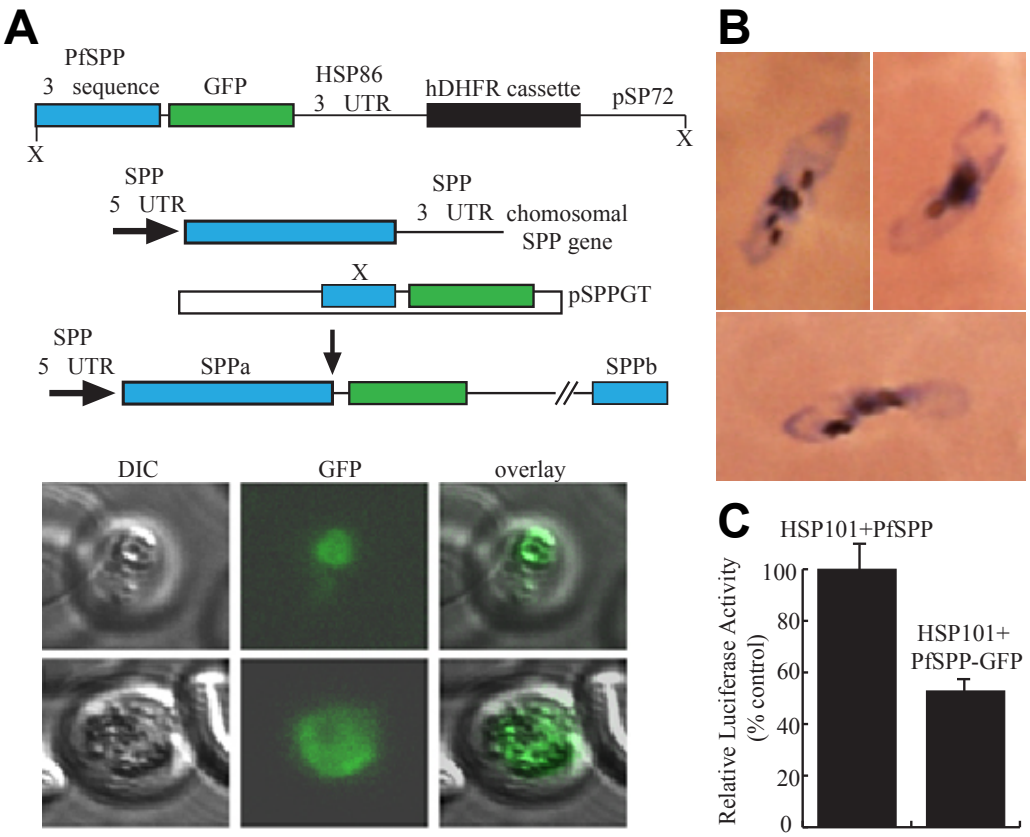

Figure 2.4. Generation of chromosomal PfSPP-GFP chimera alters parasite morphology and PfSPP activity.
(A) Schematic outline of PfSPP vector with GFP inserted at the C-terminus. Single-site homologous recombination between the episomal pSPPGT target sequence and the chromosomal PfSPP locus generated the SPP-GFP chimera. The integration event produced a full-length PfSPP open reading frame fused to GFP and a downstream promoter-less copy of the SPP target sequence. The bottom panel shows both young and mature parasites displaying GFP fluorescence along with the DIC images of live parasites. (B) A montage of gametocyte-like parasites recovered after transfection and selection in the presence of WR99210. (C) Quantification of HSP101 cleavage activity by PfSPP and PfSPP-GFP constructs.

Ring-stage parasites were transfected with the chimeric construct and selected in the presence of WR99210. Two rounds of drug cycling enriched the parasites that had integrated the chimeric PfSPP gene. The GFP signal in the live parasites was monitored by fluorescence microscopy. Both young and mature parasites showed GFP expression indicating successful integration of the gene in the transfected parasites carrying chimeric PfSPP with the GFP tag at the C-terminus (Figure 2.4A, bottom panel). However, upon transfection, the parasitemia fell dramatically and only a small number of resistant clones could be recovered after 15-20 days of parasite culture. The resistant parasites carrying the chimeric PfSPP gene showed aberrant morphology with essentially no healthy parasites detectable by microscopy. Interestingly, nearly all parasites carrying the chimeric PfSPP gene showed gametocyte-like morphology after 15-20 days of selection in culture (Figure 2.4B). To further investigate this unexpected finding, we measured and compared the cleavage of HSP101 by wild type PfSPP and PfSPP-GFP. The protease activity of PfSPP-GFP construct was markedly reduced to approximately 50% activity as compared to the wild type PfSPP construct (Figure 2.4C). Together, these results suggest that even partial inhibition of PfSPP activity by the insertion of GFP at the C-terminus is detrimental to the viability and normal differentiation of malaria parasites during intraerythrocytic development.

Contributions:

The work outlined in this chapter was published in *Biochemical and Biophysical Research Communications* (Baldwin et al. 2014). Xuerong Li and Crystal Russo are also

authors on this publication and performed a number of the biochemical and localization analyses outlined in Figures 2.1 and 2.2.

Chapter 3: Merozoite Surface Protein 1

Merozoite surface protein 1 binds to the band 3-glycophorin A complex during parasite invasion

Rationale

The erythrocyte invasion process consists of multiple molecular events during which RBC membrane proteins and merozoite coat proteins are engaged in specific receptor-ligand interactions to form unique invasion pathways (Cowman et al., 2012; Farrow et al., 2011). Continued interest in developing a multi-antigen malaria vaccine has drawn much attention on parasite proteins localized on the surface of the merozoite as potential vaccine candidates (Cowman et al., 2012). Merozoite surface protein 1 (MSP1) is a major ligand coating the surface of merozoites in all species of malaria (Holder et al., 1992). Due to its abundance and essentiality, it is considered one of the leading candidates for inclusion in a multi-subunit vaccine against malaria (Doolan and Hoffman, 1997). Thus, we have examined the function of two domains of MSP1 by multiple approaches. It is anticipated that continued study of ligand-receptor interactions occurring between the invading merozoite and host erythrocyte will unveil a detailed and comprehensive mechanism of parasite invasion.

Using a malaria phage display complementary DNA (cDNA) library, we uncovered multiple ligands functioning in the merozoite invasion process. It is expected that continued investigation into parasite invasion process will lead to a complete mechanism characterizing this important step. Ultimately, a multi-component vaccine targeting several stages and ligand-receptor interactions can be used to prevent the spread of malaria. The work outlined in this chapter unveils a previously unknown function of the N-terminal subunit of MSP1, and its role as an invasion ligand by recognizing the cognate receptor, glycophorin A. The C-terminal subunit of MSP1 had previously been characterized as a binding site for host band 3 (Goel et al., 2003). Moreover, additional

studies performed in this thesis focus on the use of antibodies against band 3 and their ability to inhibit parasite invasion. The results outlined in this chapter suggest a key role for MSP1 binding multiple erythrocyte receptors.

Materials and Methods

Phage library screen against intact erythrocytes and purified glycophorins

P. falciparum FCR3 strain was maintained in continuous culture according to standard conditions (Trager, 1978). The phage library screen against purified glycophorins was performed as described previously (Li et al., 2012). We used a bacteriophage display library constructed from *P. falciparum* cDNA and cloned into a T7Select10-3 Orient Express^{TM} vector. Purified glycophorins (Sigma) were coated in carbonate buffer (15 mM Na_2CO_3 and 35 mM $NaHCO_3$, pH = 9.6) on flat-bottom microtiter ELISA plates for 30 min at room temperature (100 ng/well). The plates were blocked with 1% milk in phosphate buffer saline (PBS) for one hour at 37°C. Plates were washed 3 times with PBS-T. A small volume (25 µl) of a combinatorial peptide phage library (~10^{14} pfu/ml, with a complexity of 10^9 transformants) was added in 125 µl PBS-T to each well. (To ensure successful isolation of a particular peptide, we used 2500 copies of each phage in the first round of panning.) Wells were sealed and incubated at room temperature for 2 h. After washing the wells three times with PBS-T, bound phage were eluted with 1% SDS in TBS at room temperature for 20 minutes. Eluted phage were added to a growing culture of BLT5403 and amplified until significant lysis occurred (≈2-3 hours). Bacterial cells were then pelleted at 8,000 x g for 20 minutes, and the supernatant containing amplified phage was used for subsequent rounds of biopanning. For binding to intact erythrocytes, erythrocytes were washed three times in PBS. Then the phage library was incubated with 50 µL of erythrocytes in 3% BSA in PBS for 2 hours at room temperature. Erythrocytes with specifically bound phage were passed through 500 µL of silicone oil, and washed three times in 1.0 mL PBS. Incubating with 150 µL of 3M NaCl for 20

minutes at room temperature eluted specifically bound phage. Eluted phage particles were amplified in *E. coli* BLT5403 strain, and the supernatant was used for biopanning. After multiple rounds of biopanning, diluted phage were titered using 4 mL of warmed top agar, 250 μL of BLT5403 overnight culture, and 100 μL of diluted phage. The mixture was poured onto LB-Ampicillin plates and spread evenly. Once the top agar had solidified, plates were inverted and incubated at 37°C until phage plaques appeared. Specific phage clones were identified via PCR amplification of individual plaques. Inverted pipet tips were used to scrape a portion of the top agar of a specific plaque and it was immersed into a tube containing 10 mM EDTA, pH = 8.0. This mixture was heated for 10 minutes at 65°C and subsequently used as a template for PCR-based identification.

Generation of MSP1 constructs and fusion proteins

The N-terminal fragment of MSP1 ($MSP1_{83A}$) (58-939 base pairs) was PCR amplified from *P. falciparum* (FCR3) genomic DNA using the primers 5′-GCCGGATCCGTAACACATGAAAGTTATC-3′ (sense, *Bam*HI) and 5′-GCCGTCGACAAGTAATTCCTTAATGTTT-3′ (antisense, *Sal*I). The C-terminal fragment of MSP1 ($MSP1_{83B}$) (940-2007 base pairs) was amplified using the primers 5′-GCCGGATCCGATAAGATAAATGAAATT-3′ (sense, *Bam*HI) and 5′-GCCGTCGACTTTTAATTTATCTACTTCT-3′ (antisense, *Sal*I). PCR products were digested with *Bam*HI and *Sal*I and ligated in the pET32a expression vector, respectively. The recombinant $MSP1_{83A}$ and $MSP1_{83B}$ were expressed in *E. coli* BL21 (DE3) as fusions to a Thioredoxin (Trx) and His tag. A 141-bp (631-771 bp encoding 47 amino

acids) region of $MSP1_{83A}$ (named here as $MSP1_{5kDa}$ or $MSP1_5$) was amplified from $MSP1_{83A}$ and cloned into pGEX-6P-2 using the primers 5′-GCCGGATCCCTTAAAAAA CTTGTGTTC-3′ (sense, *Bam*HI) and 5′-GCCGTCGACAATTGTTTTCTTACTTTC-3′ (antisense, *Sal*I). A 309-bp region (103 amino acids) of $MSP1_{83A}$ (named here as $MSP1_{12kDa}$ or $MSP1_{12}$) was amplified from $MSP1_{83A}$ and cloned into pET32a using primers 5′- GCGGATCCCTTAAAATTCGTGCAAATGAATTA-3′ (sense, *Bam*HI) and 5′- GCGTCGACTAAAGTGTCAATACGTTTTTCTAA-3′ (antisense, *Sal*I).

Expression of all MSP1 constructs was performed by inducing BL21 (DE3) expressing bacteria at 25°C and inducing with 0.5 mM IPTG for 4-5 hours. Bacterial pellets were purified in buffer containing 50 mM NaH_2PO4, 300 mM NaCl, 10 mM Imidazole, 5% glycerol, 0.2% CHAPS, and 1.0 mg/mL lysozyme. Bacterial lysate was incubated at 4°C for 30 minutes and then sonicated until clearing occurred. The soluble fraction was purified using an AKTA-FPLC instrument containing a high affinity Ni-NTA Superflow column to obtain very highly purified fusion proteins. Collected fractions were then used in subsequent binding and invasion assays. In smaller amounts, protein was also purified using ProBond Nickel-chelating resin and purified in batch mode (Life Technologies). Purification was also tested in S protein-agarose beads in order to recover a more pure eluted fraction. Recombinant proteins were dialyzed against 300 mM NaCl, 20 mM N-2-hydroxyethylpiperazine-N'-2-ethanesulfonic acid (HEPES) pH 7.4, 0.5 mM EDTA, 5 mM magnesium chloride ($MgCl_2$), 1.0 mM (Dithiothreitol) DTT, 5% Glycerol. Dialysis in RPMI 1640 was also required for proteins unstable in the aforementioned buffer.

Glycophorin binding assays

Trx-MSP1$_{83A}$, Trx-MSP1$_{83B,}$ and Trx proteins were mixed with 7.5 μg of solubilized glycophorins, predominantly glycophorin A (Sigma), in 600 μl of binding buffer (150 mM NaCl, 20 mM HEPES, 0.1% NP-40, 5 mM $MgCl_2$, 10% Glycerol, 1.0 mM DTT, 0.5 mM EDTA, pH 7.5) followed by incubation with 20 μl of packed S-protein agarose beads (Novagen) overnight at 4°C with gentle mixing. Bound proteins were detected by immunoblotting. Both monoclonal and polyclonal antibodies against GPA were used (Bigbee et al., 1983). A polyclonal antibody against the cytoplasmic domain of GPC was used as a control (Li et al., 2008a).

Erythrocyte binding assays

RBC binding assays were performed with 20 μL of fresh intact human erythrocytes in a buffer containing 50 mM Tris-HCl, pH 8.0, 200 mM NaCl, 1.0 mM EDTA, 2.5 mM $MgCl_2$, 2.0 mM DTT, and 1 % glycerol. Binding was performed at 37°C for 2 hours, erythrocytes were washed three times in 1.0 mL of buffer, and bound proteins were eluted using 2.0 M NaCl. Elutions were analyzed by immunoblotting against the Trx tag of MSP1 fusion proteins. The empty vector Trx fusion protein was used as a negative control. Chymotrypsin (C) and trypsin (T) treatment of intact RBCs was performed by incubating with 0.5 mg/mL protease in PBS or RPMI for 1.0 hr at 37°C. Cells were then washed three times in PBS before being treated with a Bowman-Birk inhibitor to eliminate any remaining protease activity. Neuraminidase treatment was performed using 1.0 unit of purchased neuraminidase from *Vibrio cholera* (Sigma). Sialic acid digestion was performed for 1.0 hr at 37°C.

The neuraminidase (Nm), Chymotrypsin (C), and Trypsin (T) treatment of intact RBCs to remove/deplete specific residues from the RBC surface, and the preparation of human RBC ghosts were performed as described previously (Goel et al., 2003).

Recombinant GPA binding assays

Plasmids containing full-length GPA were obtained from Dr. Reinhart Reithmeier at the University of Toronto. The putative extracellular domain of GPA (AA'S 1-72) was divided into two different glutathione S-transferase (GST) constructs termed GST-GPA* (amino acids 31-72) and GST-GPA^{o} (amino acids 1-30) into the pGEX-6P1 vector. The primers used to amplify the GPA* region were 5'-GCGGATCCCGGGACACATATGCAGCC-3' (Fwd. BamHI underlined) and 5'-GCGTCGACTCACTCTGGTTCAGAGAAATGATGGG-3' (Rev. SalI underlined). For the GST-GPA^{o} construct, the very short amino acid length insert gave rise to a number of complications. Therefore, an overlapping oligonucleotide annealing strategy was utilized analogous to that discussed with HSP101 (See Chapter 2: Materials and Methods). The following oligonucleotides were used in a 20 μL reaction containing 0.5 μL EconoTaq Polymerase, 1.0 mM dNTPs and 2.5 μM oligos of the following sequences 5'-CGGGGATCCTCAAGTACCACTGGTGTGGCAATGCACACTTCAACCTCTTCTTCAGTCACAAAGAGTT-3' (Fwd. BamHI underlined) and 5'-CGGGTCGACTCATTTGTGCGTATCATTTGTCTGTGATGAGATGTAACTCTTTGTGACTGAAGAAGAGGTTG-3' (Rev. SalI underlined). The resulting product of this PCR reaction was purified using a PCR purification kit (QIAGEN). The products were digested with their respective restriction enzymes and ligated into the pGEX-6P1 vector

for bacterial protein expression. All proteins were expressed in BL21 (DE3) *E. coli* cells via induction using 0.3 mM IPTG for 4 hours at 37°C. Bacterial pellets were lysed in 50 mM Tris-HCl, pH 8.0, 300 mM NaCl, 1% glycerol, 0.1% octylphenoxy poly(ethyleneoxy) ethanol (NP-40) and 100 μg/mL lysozyme. Lysate was incubated for 30 minutes at 4°C and then sonicated until clearing occurs. Following centrifugation for 20 minutes at 10,000 x g at 4°C, the soluble bacterial lysate was incubated with glutathione resin for 2 hours at 4°C. Binding assays were performed using GST proteins immobilized on glutathione resin. However, for elution 50 mM Tris-HCl, pH 8.0, 10 mM glutathione was used and proteins were subsequently dialyzed against 50 mM Tris-HCl, pH 8.0, 300 mM NaCl, 0.5 mM DTT, 1% Glycerol.

Binding assays using polypeptide regions of GPA were performed by immobilizing the GST, GST-GPA*, and GST-GPA^{o} on glutathione beads. MSP1$_{12}$ was incubated in 50 mM Tris-HCl, pH 8.0, 200 mM NaCl, 2.5 mM $MgCl_2$, 1.0 mM EDTA, 0.1% NP-40, 2.0 mM DTT and 1.0 mg/mL BSA for 2 hours at room temperature. Beads were washed three times and eluted in SDS sample buffer and analyzed by immunoblotting. Trx was used as a negative control.

RBC ghosts pull-down

Human ghosts were prepared as described previously (Goel et al., 2003). MSP1$_{12}$ (Trx as control) was incubated with 40 μl of human RBC ghosts in 1% BSA (RPMI 1640) for 1.0 hour at 4°C. Ghosts were centrifuged at 18,000 X g for 10 min at 4°C, and pellet was solubilized in modified RIPA buffer (150 mM NaCl, 50 mM Tris-HCl, pH 8.0, 1% NP-40, 5 mM 2-mercaptoethanol, 0.1 mM PMSF, and P8340 protease inhibitor cocktail from

Sigma). Lysate was added to 25 µl of Ni beads for 2 hours at 4°C, and proteins bound to beads were washed, eluted and analyzed by immunoblotting.

Infection of band 3 and protein 4.2 null mice by Plasmodium yoelii 17XL

The generation and characterization of band 3 null mice has been described previously (Hassoun et al., 1998; Southgate et al., 1996). Our band 3 null mouse model is unique because it selectively lacks erythroid band 3 but not its isoform in the kidney (Southgate et al., 1996). Band 3 null mice display a secondary loss of GPA and protein 4.2 in the RBC membrane (Hassoun et al., 1998). Band 4.2 null mice were generously provided by Dr. Luanne Peters at the Jackson Laboratory, Maine (Peters et al., 1999). Band 3 null and protein 4.2 null (2-3 months old) were challenged with the rodent *P. yoelii* 17XL infection (blood stage), essentially as described previously (Li et al., 2007). Wild type C57BL/6 mice and age matched heterozygous littermates were used as controls.

Anti-band 3 IgY and anti-RhopH3 antibodies

Peptides ASTPGAAAQIQEVKE and FKPPKYHPDVPYVK derived from the 5C and 6A regions of human erythrocyte band 3 were each conjugated to KLH by an N-terminal cysteine coupling. Using these peptides, antibodies were produced in chickens by Sigma-Genosys. Following six injections given every 14 days, eggs were collected and antibody titer was determined by ELISA throughout the course of injections using blood serum. Total IgY antibodies were purified from the egg yolk using Eggcellent Chicken IgY Purification Kit (Pierce). Anti-5C and anti-6A IgY antibodies were affinity purified from corresponding total IgY using columns prepared by conjugating the above antigen

peptides to the CNBr-activated resin (Pharmacia Biotech/GE Healthcare). The two mono-specific IgY antibodies were stored in PBS at 4°C. Eggs from two preimmune chickens were used to obtain total preimmune IgY antibodies as above. Peptide derived from the carboxyl region of *P. falciparum* RhopH3 (RDSSSDRILLEESKTFT) was conjugated to KLH by N-terminal cysteine coupling. Antibodies against this peptide were raised in rabbit, and antibody titer and purification was performed as mentioned above. A preimmune serum from rabbit was used as control.

Immunofluorescence Microscopy

Thin smears of normal and Nm-treated RBCs were fixed on glass slides with cold methanol for 30 min, blocked with 1% BSA in PBS (pH 7.4) for 30 min at RT, washed twice in PBS (5 min each), and incubated with affinity-purified anti-5C IgY or anti-6A IgY antibodies (100 µg/ml in 1% BSA in PBS). Preimmune IgY (100 µg/ml), the anti-B3/cd mAb, and the anti-GPA mAb reactive to extracellular residues of human GPA (Sigma) were also used as control. Slides were washed twice with PBS, incubated with appropriate secondary antibodies conjugated with Alexa 488 (green fluorescence) or Alexa 594 (red fluorescence) according to manufacturer's protocol (Invitrogen), and visualized at 100X magnification. Negative controls included incubation of slides with the Alexa 488-conjugated anti-chicken secondary antibody alone.

Detection of antibody binding to RBCs by flow cytometry

Normal and Nm-treated intact human RBCs were washed with PBS and resuspended in RPMI 1640 (50% hematocrit). A 100 µl sample of the RBC suspension was incubated

with anti-5C IgY (100 µg/ml), anti-6A IgY (100 µg/ml), preimmune IgY (100 µg/ml), anti-B3/cd mAb, or anti-GPA mAb for 30 min at 4°C. After three washes with PBS, the RBCs were resuspended in PBS containing FITC-conjugated anti-chicken or anti-mouse secondary antibody for 45 min at 4°C. Following three washes with PBS, the cells were resuspended in 300 µl of PBS and analyzed by recording 10,000 events using FACSCalibur (Becton Dickenson) equipped with a 15 mW Argon ion laser tuned at 488 nm. Fluorescent cell analysis was performed on the population gated on their forward scatter properties using the CellQuest (BD Bioscience) and WinMDI 2.8 software (http://facs.scripps.edu/software.html). Similarly, concentration-dependent binding of IgY antibodies to RBCs was carried out as described above. Briefly, normal and Nm-treated human RBCs were each incubated with a varying concentration (0, 25, 50, 100, 250 µg/ml) of anti-5C IgY, anti-6A IgY, or preimmune IgY in PBS. Mean fluorescence intensity (mean $\pm$ s.e.) from triplicate assays was plotted against the IgY concentration. Student's *t*-test was used to compare the mean. The dissociation constant (K_d) and maximum binding (B_{max}) for the IgY-RBC interaction was determined using the Ligand Binding macro in SigmaPlot 8.0.

Invasion inhibition assays

Parasites used in invasion assays were synchronized twice using 5% sorbitol treatment to isolate ring stage parasites. Synchronized *P. falciparum* FCR3 parasites at the schizont stage were seeded into a 96-well plate at 1.5-3.5% parasitemia (2% hematocrit). Recombinant, sterile filtered protein or antibodies were added to infected erythrocytes. For concentration-dependent inhibition assays, final IgY concentrations used for each

preimmune IgY (control), anti-5C IgY, and anti-6A IgY antibodies were 25, 50, 100, and 200 μg/ml. Samples containing a 1:1 mixture of two IgY antibodies were prepared by adding each IgY at 25, 50, 100, and 200 μg/ml final concentrations. A control sample having no IgY antibodies was included. For the invasion phenotype-specific inhibition study, anti-5C IgY, anti-6A IgY, or preimmune IgY were used at the 100 μg/ml final concentration. RBC invasion occurred under standard malaria culture conditions, and samples were analyzed after 20-24 hours post invasion.

RBC invasion was quantified using both microscopy and flow cytometry. For microscopy, at least 1,000 RBCs were counted for each measurement. For flow cytometry, parasitemia was quantified using SYTO-13 staining, propidium iodide staining (FACSCalibur) (Barkan et al., 2000) or Hoechst 33342 staining (BD LSR II flow cytometer) (Theron et al., 2010). For SYTO-13 staining, cells were fixed in 1% paraformaldehyde in PBS for 1 h at room temperature. An aliquot of these fixed infected erythrocytes were stained with 50 or 100 nM SYTO-13 in PBS for 15 minutes at room temperature. For staining with propidium iodide (PI), cells were washed in PBS twice, and fixed in 0.025% glutaraldehyde at 4°C for 1 hour. Following another round of two PBS washes, cells were permeabilized in 0.01% saponin (in PBS) at room temperature for 5-10 minutes. Cells were washed in PBS to remove excess saponin, and then stained in propidium iodide in 2% FBS in PBS at 37°C for 1-2 hours. For Hoechst 33342 staining, infected erythrocytes designated for analysis were washed twice in PBS, then treated in 2 μM Hoechst 33342 for 1 hour at 37°C. Cells were washed twice in PBS, and fixed in 0.2% glutaraldehyde, 2% paraformaldehyde for 1 hour at 4°C. Samples were analyzed in 2% FBS in PBS buffer.

Upon collecting 10,000-100,000 events using the FACSCalibur or BD LSR II, parasitemia for each sample was determined based on the newly formed ring-stage parasites.

MSP1, RhopH3, Band 3 binding assays

For *in vitro* binding assays, different combinations of 50 pmol each of Trx-RhopH3-C, Trx-$MSP1_{19}$, and GST-5ABC were added in a reaction volume (200 µl) of binding buffer (50 mM Tris-HCl, pH 7.6, 1.0 mM EDTA, 5.0 mM $MgCl_2$, 0.1% NP40, 5.0 mM DTT, 1.0 mg/ml BSA and 150 mM NaCl) for 1.0 h at room temperature or overnight at 4ºC. Bead-bound proteins were eluted and analyzed by Western blotting using respective antibodies (Goel et al., 2003). Parasite supernatant binding was performed by adding 1.0 mL of culture supernatant to GST-5ABC protein immobilized on glutathione beads. Following binding for 2 hours at RT, beads were washed twice in RPMI 1640, then eluted in SDS-sample buffer and analyzed by immunoblotting against RhopH3. Empty vector encoding GST was used as a negative control.

Quantitative ELISA

Quantification of recombinant RhopH3-C to band 3 (5ABC) and $MSP1_{19}$ was performed as described previously (Goel et al., 2003; Kariuki et al., 2005; Li et al., 2004). Briefly, ELISA plates were coated with GST and GST-5ABC in carbonate buffer, pH 9.6, at 4ºC overnight. After washing and blocking with PBS and PBS-T containing 5% milk, the Trx and Trx-RhopH3-C proteins were added (0-5 µM). Upon incubation, bound protein was measured using anti-His polyclonal antibody (GenScript), anti-rabbit–HRP conjugated

antibody, and TMB substrate (Pierce). Similarly, Trx and Trx-RhopH3-C were coated on the ELISA plate and MBP and MBP-$MSP1_{19}$ were added to the wells in varying concentrations (0-6 μM). Bound protein was measured using an anti-MBP antibody (NE BioLabs). Binding data were analyzed using SigmaPlot 11 (simple ligand binding using the equation for one site saturation).

Results

Identification of Plasmodium falciparum proteins binding to erythrocyte glycophorins

We used phage display technology to identify parasite invasion ligands interacting with glycophorins on the human RBC surface. Previously we used the same approach to successfully identify a specific segment of *P. falciparum* EBL-1 binding to RBC glycophorin B (Li et al., 2012). The previous study revealed a functional role of a specific segment of parasite EBL-1 in RBC invasion. Thus, an analogous approach was used in this study to identify additional parasite ligands binding to human glycophorins. Glycophorins, purified from human RBCs, were used as bait to capture phage display clones from a previously characterized cDNA library (Lauterbach et al., 2003). Along with several known malaria ligands such as EBA-175 that bind to glycophorins, we identified multiple overlapping phage clones of MSP1 that bind to immobilized glycophorins (Figure 3.1). DNA sequencing revealed a 141-bp region encoding amino acids 204-250 located within the N-terminal 83 kDa domain of MSP1 (Figure 3.1A). In parallel, we also performed several phage display screens using both native and Nm-treated RBCs. An overlapping phage clone of MSP1 containing amino acids 240-279, located within the N-terminal 83 kDa domain, was identified (Figure 3.1A). Since the entire 83 kDa domain of MSP1 was difficult to express as recombinant protein in bacteria, two smaller segments, termed $MSP1_{83A}$ and $MSP1_{83B}$, were expressed. Both overlapping MSP1 phage clones that bound to glycophorins were located within the $MSP1_{83A}$ segment (amino acids 20-313), whereas the $MSP1_{83B}$ (amino acids 314-669) segment served as a negative control. In addition, we made a GST fusion protein expressing the original MSP1 phage clone 1 (amino acids 204-250) that binds to

glycophorins. However, this GST fusion protein, termed $MSP1_5$, showed limited solubility and was susceptible to proteolysis (Figure 3.1B). To overcome this limitation, we scanned the flanking sequences of $MSP1_5$ using predictive algorithms of protein secondary structure, and designed a relatively stable $MSP1_{12}$ construct (amino acids 194-296) located within the $MSP1_{83A}$ domain of MSP1 (Figure 3.1B). In the initial binding assays, all recombinant fusion proteins of MSP1 were used, however the $MSP1_{12}$ construct was found to be most effective in subsequent assays.

Interaction of MSP1 with purified glycophorin A and erythrocytes

Using recombinant MSP1 segments and purified reconstituted glycophorins, liposome-binding assays were performed to test whether MSP1 interacts with human erythrocyte glycophorins. MSP1 fusion proteins ($MSP1_{83A}$, $MSP1_{83B}$, and $MSP1_{12}$), containing an internal S-tag, were immobilized to S-beads and the GST-tagged $MSP1_5$ segment was bound to glutathione beads. Beads containing the MSP1 fusion proteins were incubated with glycophorins reconstituted as liposomes, and specific binding was quantified along with appropriate negative controls (Figure 3.2). MSP1 binding to specific glycophorins was detected using antibodies against glycophorin A and glycophorin C. Multiple segments of MSP1 termed $MSP1_5$, $MSP1_{12}$, and $MSP1_{83A}$ specifically bound to GPA as compared to control Trx or GST proteins (Figure 3.2B, C, D). In contrast, $MSP1_{83B}$ showed minimal but detectable binding with GPA under these conditions (Figure 3.2D), which could originate from the partial overlap of the GPA-binding region of MSP1 extending into the $MSP1_{83B}$ segment. Interestingly, both $MSP1_5$ and $MSP1_{83A}$ preferentially pulled down monomeric form of GPA.

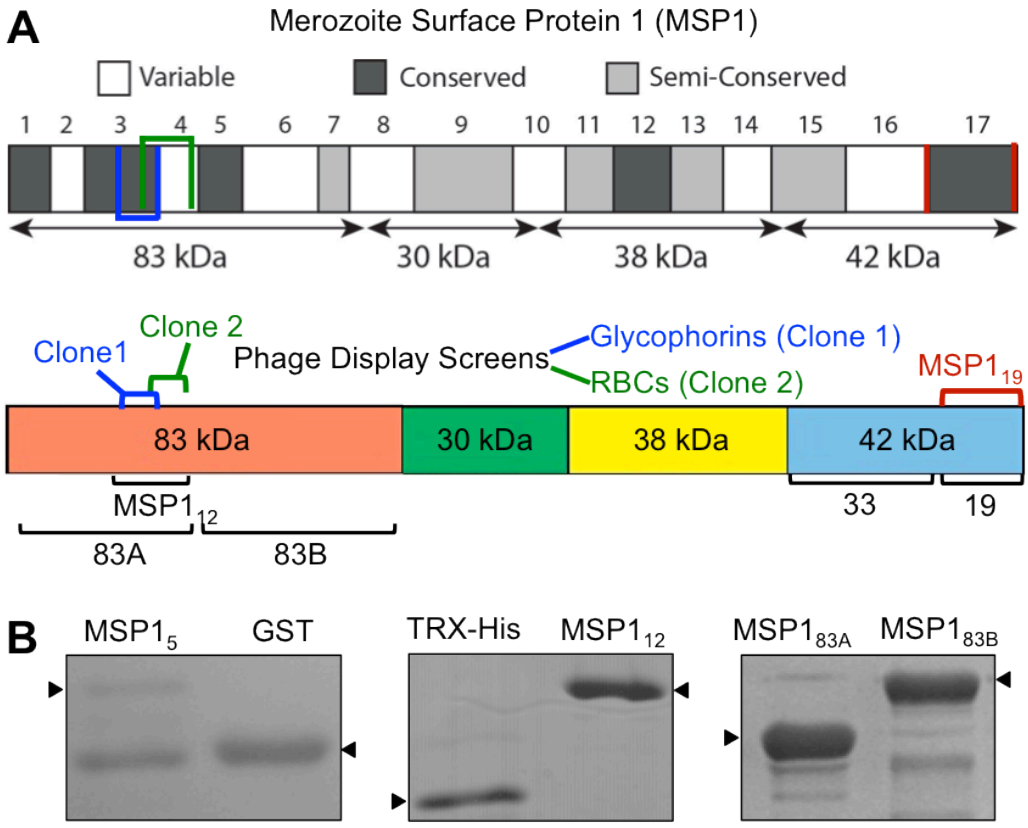

Figure 3.1. Domain organization of recombinant merozoite surface protein 1 (MSP1).
(A) MSP1 is grouped into 17 blocks classified as conserved, semi-conserved or variable. The diagram below shows 4 subunits of MSP1 following the action of subtilisin-1 (Harris et al., 2005). Two independent overlapping phage clones of MSP1 are indicated. Clone 1, identified in the screen using purified glycophorins, consists of amino acids 204-250 whereas clone 2, identified in the screen against neuraminidase-treated RBCs, encodes amino acids 240-279. The $MSP1_{12}$ construct incorporates both clones 1 and 2. The respective locations of $MSP1_{83A}$, $MSP1_{83B}$, and $MSP1_{19}$ are also annotated. (B) Coomassie-stained SDS-PAGE of MSP1 fusion proteins includes $MSP1_5$ containing amino acids 204-250 from phage clone 1. $MSP1_{12}$ (amino acids 194-296) expresses a stable protein encompassing both phage clones. The combination of $MSP1_{83A}$ and $MSP1_{83B}$ cover the entire 83 kDa amino-terminal subunit of MSP1.

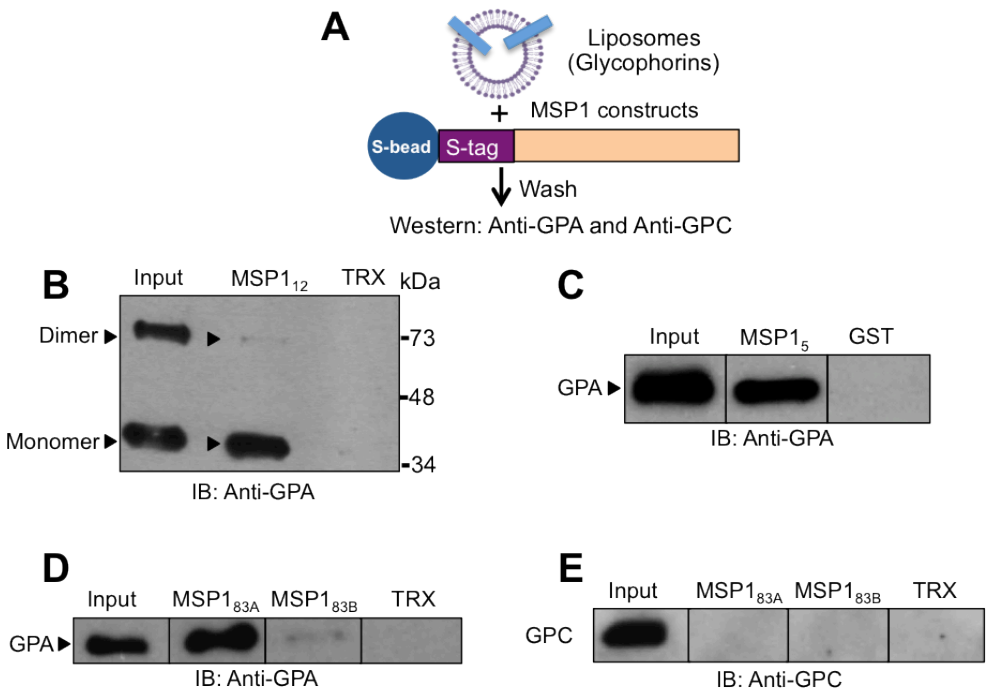

Figure 3.2. MSP1 binds to purified glycophorin A (GPA).
(A) MSP1 fusion proteins containing an S-tag (GST in $MSP1_5$) were immobilized to S-beads (or Glutathione beads) and incubated with glycophorin-containing liposomes. Bound proteins were detected by immunoblotting. The Trx fusion protein containing an S-tag and GST were used as negative controls. (B) $MSP1_{12}$ showed specific binding to GPA relative to control in both the monomer (lower band) and dimer species of GPA (upper band). Binding of GPA dimer was detected under mild conditions of beads washings whereas the GPA monomer binding was observed under both mild and stringent conditions. (C) GPA binding to $MSP1_5$ and (D) $MSP1_{83A}$, and a very faint signal to $MSP1_{83B}$ was also observed. (E) Immunoblotting against glycophorin C (GPC) did not detect any signal to either $MSP1_{83A}$ or $MSP1_{83B}$ fusion proteins.

The $MSP1_{12}$ segment bound to both monomeric and dimeric forms of GPA (Figure 3.2B). However, its binding to the dimer was significantly weaker as demonstrated by western blotting. The purified glycophorins used contain glycophorin A, glycophorin B, and glycophorin C, which served as an additional negative control for the liposome-binding assay. For example, binding of $MSP1_{83A}$ was specific to GPA, as immunoblotting against GPC did not detect any binding under these conditions (Figure 3.2E). Moreover, we tested the binding of $MSP1_{12}$ with freshly harvested intact RBCs. The RBC-bound $MSP1_{12}$ was eluted with high salt and detected by immunoblotting against the Trx tag showing specific interaction between $MSP1_{12}$ and human RBCs (Figure 3.3A). Pre-treatment of RBCs by neuraminidase did not affect their binding affinity for $MSP1_{12}$ (Figure 3.3A), consistent with the observation that MSP1 clones were originally identified in a phage display screen using Nm-treated RBCs as bait. Surprisingly, $MSP1_{12}$ binding to RBCs was not affected by pre-treatment with trypsin, which is known to cleave a large extracellular segment of GPA (Bigbee et al., 1983). Together, these data demonstrate that a short segment located within the $MSP1_{83A}$ region binds to a neuraminidase and trypsin insensitive site (or sites) on human RBCs.

MSP1 interaction with endogenous glycophorin A

To establish a biochemical interaction between $MSP1_{12}$ and endogenous GPA, a pull-down assay was performed using human RBC membranes (ghosts). Freshly isolated ghosts contain multiple species of GPA including the homodimer, heterodimer, and monomer (Figure 3.3B), consistent with published studies (Remaley et al., 1991). However, following detergent treatment of ghosts, which is required for the pull-down

assays, a previously unrecognized 18 kDa species of GPA was observed (Figure 3.3B) (Daniels, 1995; Remaley et al., 1991). It is known that solubilization of ghosts in non-ionic detergents releases and activates several proteases that may give rise to smaller species of GPA (Sheetz, 1979). The pull-down assays demonstrated that $MSP1_{12}$ associates with several species of GPA including the homodimer, heterodimer, monomer, as well as a ~18 kDa band (Figure 3.3B). Consistent with this finding, $MSP1_{83A}$ but not $MSP1_{83B}$ specifically pulled down the same species of GPA (Figure 3.3B). While the heterodimer, monomer, and 18 kDa species of GPA were pulled down with immobilized $MSP1_{12}$ in the neuraminidase and trypsin treated ghosts, the homodimer species of GPA was detected only in the untreated ghosts (Figure 3.3B). This finding is consistent with the observation that neuraminidase and trypsin treatment of ghosts eliminate the homodimer species of GPA as detected by immunoblotting. Previous studies demonstrated that neuraminidase treatment of RBCs removes the sialic acid content of GPA, and trypsin treatment removes a significant portion of the extracellular domain of GPA (Bigbee et al., 1983; Sim et al., 1994b). These two treatments, in addition to chymotrypsin, are frequently used to test for receptor enzyme sensitivity on the surface of erythrocytes. Glycophorin C is also known to be at least partially sensitive to trypsin treatment that eliminates EBA-140 binding to erythrocytes (Lobo et al., 2003). Interestingly, the neuraminidase treatment of intact RBCs appears to increase the relative amount of GPA heterodimer pulled down by $MSP1_{12}$. While it may increase the affinity of MSP1 for the heterodimeric form of GPA, it is also possible that Nm-treatment reduces the migration size of the GPA homodimer to that of the GPA/B heterodimer.

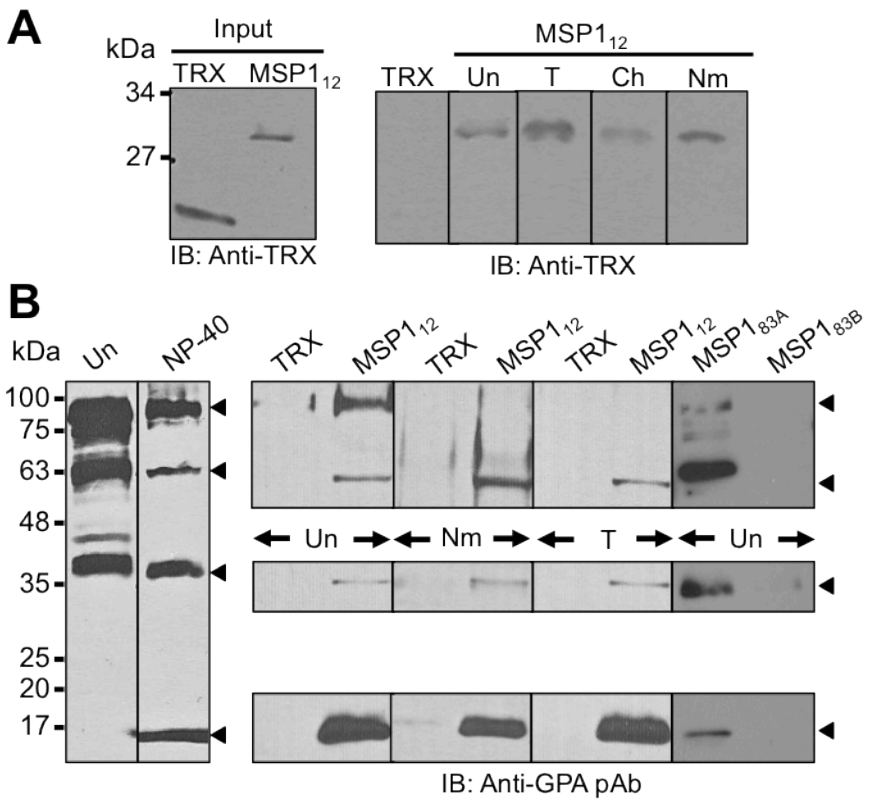

Figure 3.3. MSP1 binds to human erythrocytes and specifically binds to GPA in erythrocyte ghosts lysate.
(A) In erythrocyte binding assays, bound proteins were eluted by high salt and detected by immunoblotting. $MSP1_{12}$ showed specific binding to RBCs irrespective of their treatment with trypsin (T), chymotrypsin (Ch), and neuraminidase (Nm). Untreated RBCs (Un) were used as control. (B) Detection of GPA species in detergent-solubilized human RBC ghosts by immunoblotting. Four specific bands of GPA were detected corresponding to homodimer, heterodimer, monomer, and a previously unrecognized ~18 kDa band in the NP-40 solubilized ghosts. Immunoblotting using a polyclonal antibody against GPA showed specific binding of $MSP1_{12}$ and $MSP1_{83A}$ but not $MSP1_{83B}$ to multiple species of GPA.

This observation suggests that the $MSP1_{12}$ interaction with GPA is resistant to neuraminidase treatment, and occurs independent of the presence of sialic acids on host glycophorin A.

MSP1 binds to a unique region of human glycophorin A

While human erythrocyte GPA is considered trypsin-sensitive, this treatment is known to leave a short membrane-proximal extracellular segment of GPA on the RBC surface. Trypsin treatment of intact RBCs releases peptides of 31 and 39 amino acids from GPA (Bigbee et al., 1983). These two peptides correspond to Arg 31 and Arg 39 (Figure 3.4A), thus leaving ~40 amino acids exposed on the RBC surface after trypsin treatment. This short ectodomain peptide is contiguous to the single transmembrane domain of GPA consisting of amino acids 72-94. While the 10F7 mAb directed against the extracellular domain of GPA does not recognize the antigen in ghosts prepared from trypsin-treated RBCs, the polyclonal antibody raised against the cytoplasmic C-terminus of GPA recognizes several smaller species of GPA following trypsin treatment of intact RBCs (Figure 3.4B). We hypothesized that this trypsin-resistant segment of the extracellular domain of GPA is in fact responsible for mediating the binding of $MSP1_{12}$ with RBCs. Guided by the known trypsin cleavage sites of GPA, and combined with a topological model of GPA, we expressed the putative MSP1 binding region of GPA (amino acids 31-72) (Figure 3.4A), herein referred to as GPA* (Bigbee et al., 1983; Young and Tanner, 2003). This short segment was expressed as a GST-GPA* fusion protein and used for the binding assays (Figure 3.4C).

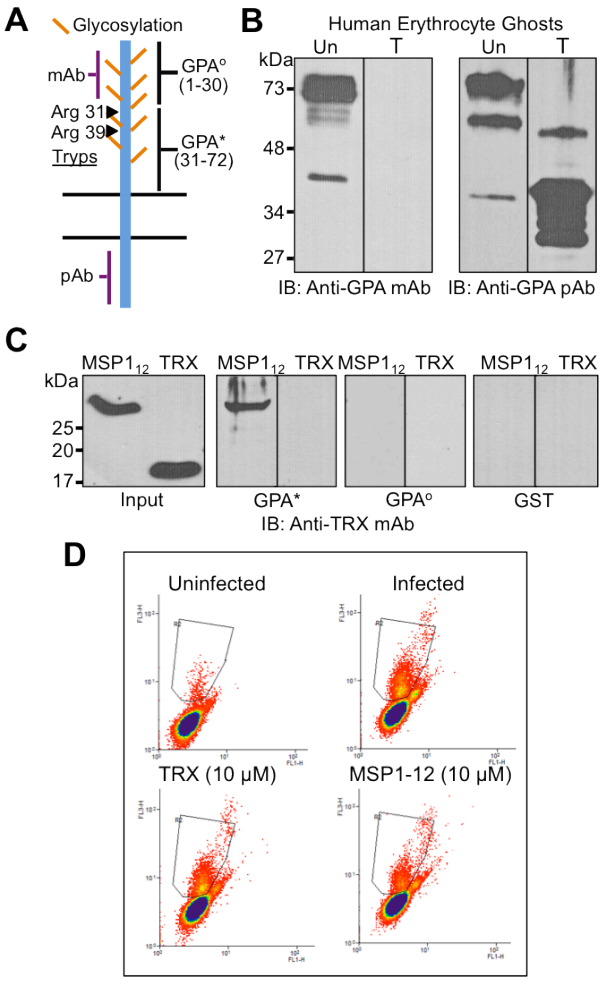

Figure 3.4. MSP1 binds to a specific region of the GPA extracellular domain. (A) Glycophorin A, a single transmembrane protein, shows significant glycosylation in the extracellular domain that can be removed by neuraminidase treatment. The approximate locations of the sites recognized by the monoclonal antibody (mAb) and polyclonal antibody (pAb) are indicated. Trypsin cleavage of GPA occurs at two distinct arginine residues (31 and 39) on the extracellular domain. The extracellular domain of GPA was expressed as two non-overlapping contiguous segments designated as GPA^{o} and GPA*. (B) Both untreated (Un) and trypsin-treated (T) erythrocyte ghosts were tested by immunoblotting using monoclonal and polyclonal antibodies against GPA. (C) Binding of MSP1$_{12}$ to the trypsin-resistant segment of GPA (GPA*, amino acids 31-72) was detected by immunoblotting against Trx. The trypsin-sensitive segment of GPA (GPA^{o}, amino acids 1-30) was also expressed and tested under identical conditions. Since both fusion proteins contained the GST tag, GST was also used as a negative control. (D) Sample FACS analysis of invasion inhibition assays using recombinant MSP1$_{12}$ at 10 µM concentration and propidium iodide staining. Freshly invaded ring-stage parasites were quantified by measuring the percentage of events within the gated region as outlined above. MSP1$_{12}$ shows partial reduction in parasitemia relative to TRX at 10 µM under defined experimental conditions.

The pull-down experiments demonstrated specific binding of $MSP1_{12}$ to the trypsin-resistant extracellular domain of GPA* (Figure 3.4C). Moreover, to demonstrate specificity, we expressed the N-terminal segment of GPA encoded by amino acids 1-30 designated as GST-GPA^o. Unlike GST-GPA*, the GST-GPA^o fusion protein did not bind to $MSP1_{12}$ (Figure 3.4C). This observation is consistent with our conclusion that the $MSP1_{12}$ interaction with human RBCs is sialic acid independent (SAID) since the recombinant proteins expressed in bacteria are devoid of sialic acid residues.

Functional role of MSP1-Glycophorin A interaction

We tested the activity of $MSP1_{12}$ to inhibit *P. falciparum* invasion of human RBCs. This N-terminal segments of MSP1 partially inhibited parasite invasion in human RBCs achieving up to ~40% inhibition of *P. falciparum* invasion in human RBCs under defined experimental conditions at very high protein concentrations (Figure 3.4D). This inhibitory activity required the presence of a reducing agent in protein storage and dialysis buffer, consistent with its requirement in binding assays. It is worth noting that high concentrations of reducing agents can cause alterations in parasite morphology, although this phenomenon was not observed in these studies (Chaubey et al., 2014). Following protein sterilization through a 0.2 μm filter, proteins are added directly to invading parasites. However, these results are highly consistent with previous studies providing strong evidence that $MSP1_{83}$ inhibits parasite invasion. For example, in one study a peptide synthesized within the $MSP1_{12}$ region inhibited RBC invasion by 60%, and even showed some activity against parasite development (Urquiza et al., 1996). In a separate study, antibodies against the $MSP1_{83}$ domain potently inhibited malaria invasion

and growth relative to other domains of MSP1 (Woehlbier et al., 2006). Similarly, another study tested the activity of purified erythrocyte glycophorins and demonstrated a significant inhibitory effect on parasite invasion (Breuer et al., 1983; Okoye and Bennett, 1985). Enzyme treatment of RBCs prior to glycophorin purification altered invasion inhibitory activity of purified glycophorins. Interestingly, glycophorins isolated from trypsinized RBCs maintained a significant inhibitory activity indicating that the trypsin-resistant regions of RBC glycophorins play a significant role in *P. falciparum* parasite invasion of RBCs (Breuer et al., 1983). It is unlikely that this is due to inhibition of the EBA-175-GPA interaction, as EBA-175 binding to RBCs is trypsin-sensitive (Wanaguru et al., 2013). Therefore, the trypsin-resistant region of GPA is playing a secondary role in invasion outside of EBA-175 binding. We have identified it as an interacting segment with $MSP1_{12}$ and it is likely to perform a functional role during malaria parasite invasion.

Glycophorin A deficient band 3 null erythrocytes are resistant to malaria infection

We generated band 3 null mice that were completely deficient in erythroid band 3 (Southgate et al., 1996). As a consequence of band 3 loss, the mature RBC membrane also showed a secondary loss of GPA and protein 4.2 (Hassoun et al., 1998; Southgate et al., 1996). Based on our previous findings showing a functional interaction between the C-terminus of MSP1 and band 3 (Goel et al., 2003), we examined the possibility that RBCs lacking both band 3 and GPA may be resistant to malaria infection. The band 3 null mice lacking erythrocyte band 3, GPA, and protein 4.2 are completely resistant to invasion by a virulent strain of murine malaria, *P. yoelii* 17XL (Figure 3.5A).

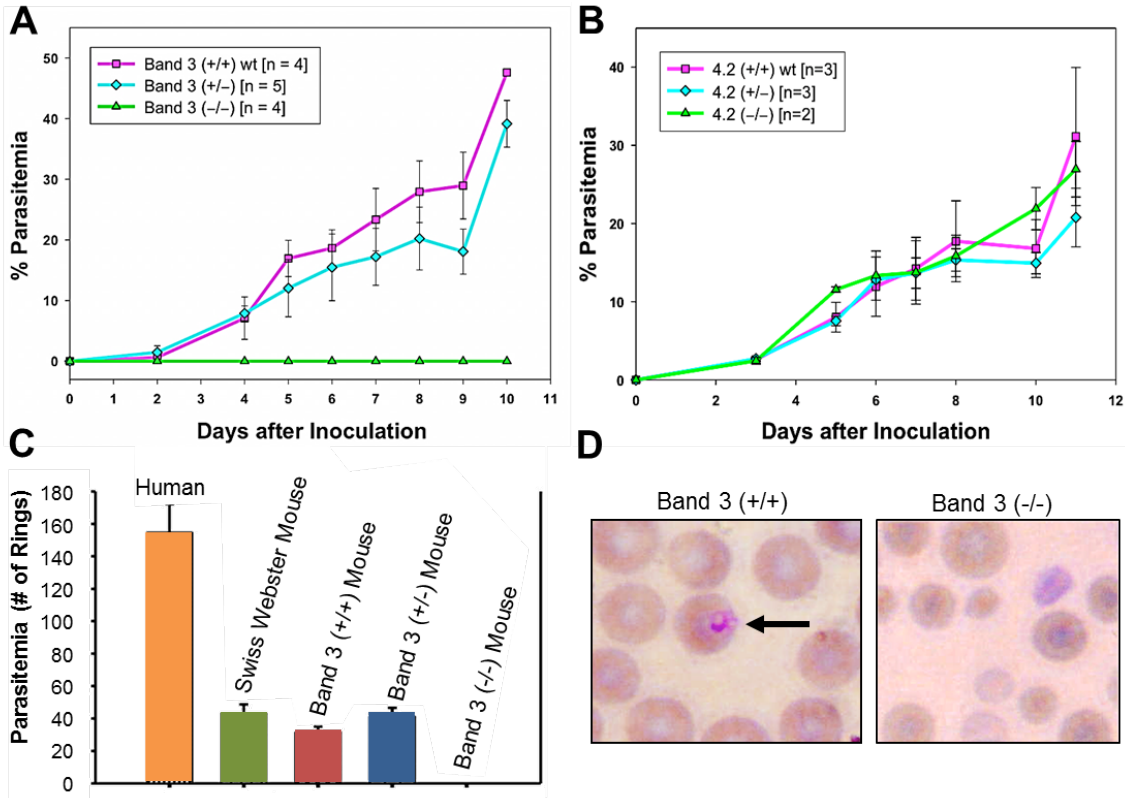

Figure 3.5. Resistance of band 3-GPA deficient mice to malaria infection.
(A) *P. yoelii* 17XL infection of wild type (band 3 +/+), heterozygous (+/-), and band 3-GPA deficient (-/-) mice *in vivo* as described in the Methods section. (B) *P. yoelii* challenge in mice deficient in protein 4.2. (C) Human and mouse RBCs were challenged with *P. falciparum in vitro* and parasitemia was quantified by counting the ring stage parasites. No invasion of *P. falciparum* was detected in band 3-GPA deficient (-/-) RBCs during the first cycle of invasion *in vitro*. (D) Representative images of RBCs from infected wild type and band 3-GPA deficient (-/-) mice (panel C) indicate the relative intact morphology of mutant RBCs under the *in vitro* invasion conditions. Wright-Giemsa stain was used for staining and images were observed at 100X magnification. It is noteworthy that the putative regions of *P. falciparum* MSP1 that bind to band 3 ($MSP1_{19}$) and GPA ($MSP1_{12}$), show 48.5% and 43.8% sequence identity, respectively, with their counterparts in *P. yoelii* MSP1.

Band 3 null mice, lacking GPA and protein 4.2 (n=4), did not display any patent parasitemia, whereas wild type mice succumbed to infection in 7-9 days. Mice heterozygous for band 3 displayed a similar invasion phenotype. However, ten days following parasite infection these heterozygotes showed a statistically significant decrease in overall parasitemia. Thus mutant mice heterozygous for band 3 showed a slightly protective phenotype when compared to wild type littermates (Figure 3.5A). To detect any subpatent infection in the band 3 null mice, blood collected from the band 3 null mice on day 14 following inoculation was transferred to wild type mice. None of the sub-inoculated mice developed malaria infection, indicating that there were no viable parasites in the band 3 null mice, which were absent in the peripheral blood smears or flow cytometry. Further, the serum prepared from the band 3 null mice had no inhibitory effect on the *in vitro* culture of *P. yoelli* 17XL in wild type murine RBCs at least for 24 hours, indicating that the cause of the protection from *P. yoelli* 17XL in band 3 null mice is unrelated to the composition of the blood serum. In contrast, protein 4.2 null mice (Peters et al., 1999) did not show inhibition of parasitemia when challenged with *P. yoelii* 17XL (Figure 3.5B). These results indicate that deficiency of the band 3-glycophorin A-protein 4.2 complex in the mouse RBC membrane is sufficient for complete resistance to *P. yoelii* 17XL invasion of RBCs. It is noteworthy that a previous study used GPA null mice, which retain erythrocyte band 3, to demonstrate that GPA is not required for lethal *P. yoelii* 17XL infection (Hamamoto et al., 2008). Therefore, it appears that GPA alone is not essential, but in combination with band 3, this complex is required for malaria infection *in vivo*. Other studies in human malaria have shown partial resistance conferred by GPA knockout (Hadley et al., 1987; Pasvol et al., 1982). Interestingly, the GPA null

mice showed reduced parasitemia and improved survival when challenged with *Babesia rodhaini*, a parasite homologous to malaria, thus indicating a functional role of GPA in Apicomplexan parasite invasion (Takabatake et al., 2007). The effect of GPA deficiency is highly strain specific in *P. falciparum*, and it is likely that alterations between *P. falciparum* and *p. yoelii* account for this difference in GPA dependence.

To further investigate the role of the host band 3-GPA complex in *P. falciparum* invasion, we tested the susceptibility of band 3 null mouse RBCs to *P. falciparum* (3D7 strain) invasion *in vitro*. When infected with synchronized *P. falciparum* trophozoites, RBCs from both wild type and band 3 heterozygous mice showed a typical invasion profile after 24 hours post-invasion (Figure 3.5C), consistent with previous studies (Klotz et al., 1987). However, the band 3 null RBCs lacking both GPA and protein 4.2 did not show any new infection (rings) by *P. falciparum* (Figure 3.5C). Band 3 null mouse RBCs remained essentially intact in the culture as judged by smear during the course of the experiment (Figure 3.5D). This observation suggests that the increased fragility of mutant RBCs is unlikely to be the reason for their resistance to malaria infection. To our knowledge, no experimental model system exists where the deficiency of band 3-GPA-protein 4.2 complex can be investigated in structurally normal red blood cells.

Band 3 antibody targeting

Given the importance of the aforementioned GPA-band 3 receptors for invasion, we investigated the possibility of targeting these with inhibitory antibodies that could reduce malaria invasion. We specifically focused on band 3, given that loss of GPA alone did not demonstrate an effect *in vivo*. Therefore, we selected to develop and test

antibodies against a specific region of band 3 that overlaps with receptor region of $MSP1_{19}$.

Interaction of anti-Band 3 IgY antibodies with RBCs

We generated antibodies against the 5C and 6A regions of human RBC band 3 (Figures 1.10 and 3.6). These two regions are thought to shape the core of the band 3 invasion receptor based on our earlier studies (Goel et al., 2003; Kariuki et al., 2005; Li et al., 2004), and have been predicted to adopt extracellular orientation in several topology models (Kanki et al., 2002; Popov et al., 1999; Zhu and Casey, 2004). Because human and mouse band 3 polypeptides share high sequence identity in these regions, we had little success in inducing an immune response against human 5C or 6A sequences in mice. However, we produced anti-5C and anti-6A antibodies in chicken egg yolk using short peptides derived from human 5C and 6A as immunogens. Antibody titers were low for both 5C and 6A based on ELISA even after several injections, presumably due to high sequence homology in these regions of band 3 between human and chicken.

Affinity-purified anti-5C and anti-6A IgY antibodies reacted specifically to recombinant proteins GST-5ABC and GST-6A, respectively, via Western blot (Figure 3.6B). Further, anti-6A specifically recognized band 3 in RBC ghosts prepared from normal human RBCs (Figure 3.6B). However, anti-5C IgY failed to react to band 3 in the normal RBC ghosts sample in Western blot (Figure 3.6B). Interestingly, when the RBC ghosts sample was prepared from human RBCs pretreated with neuraminidase to remove sialic acid residues from the cell surface, the anti-5C IgY reactivity to band 3 was restored under the same conditions (Figure 3.6B).

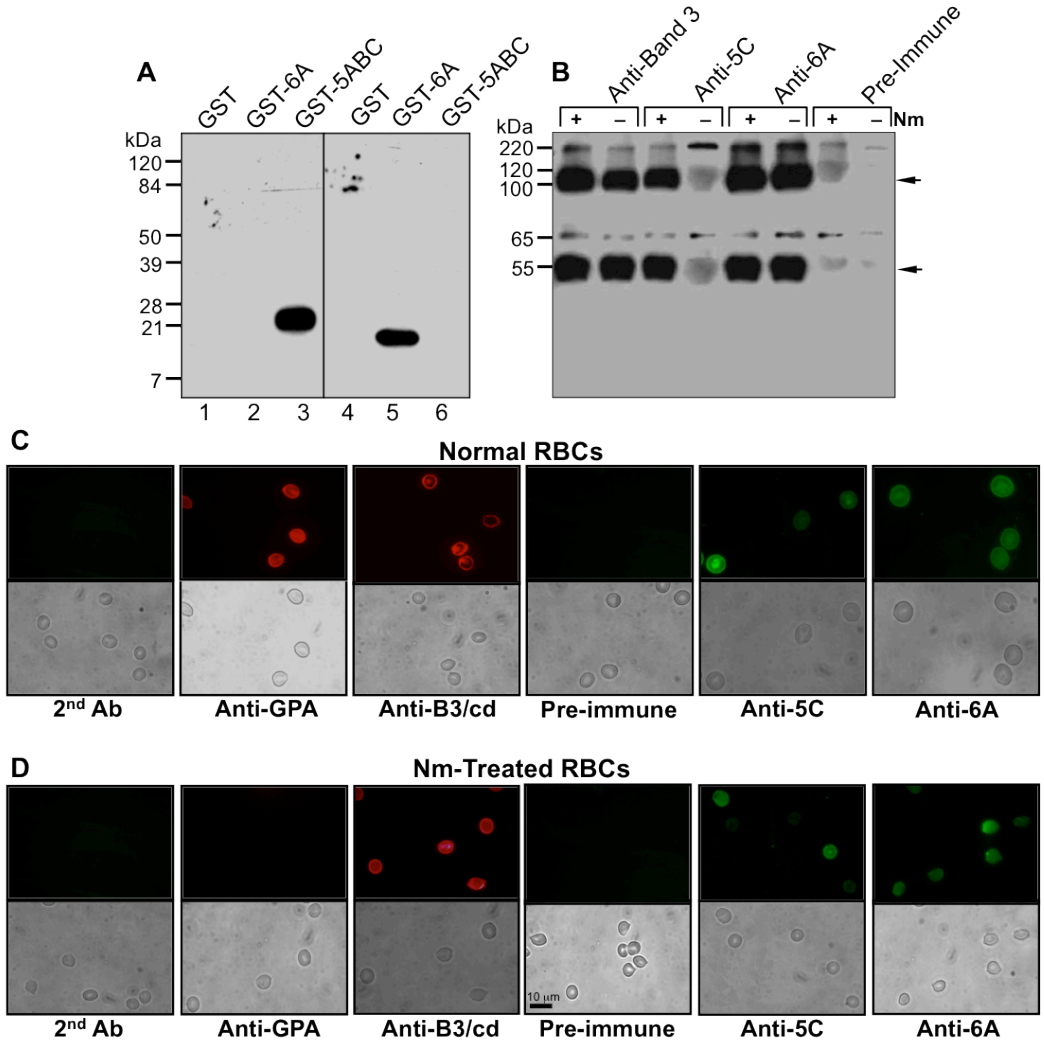

Figure 3.6. Band 3 antibodies show specific activity against their epitopes by immunoblotting and immunofluorescence.
(A) Mono-specific anti-5C (left panel) and anti-6A (right panel) IgY antibodies are reactive against the 5ABC and 6A domain of purified GST-fusion proteins, respectively, by western blotting. (B) Anti-5C and anti-6A IgY antibodies reacting to full-length band 3 in human RBC ghosts. A truncated band 3 product is also observed. Nm− (no Nm treatment), ghosts from normal human RBCs. Nm+ (Nm treatment), ghosts from neuraminidase-treated intact human RBCs. (C) Normal human RBCs reacting to anti-chicken secondary antibody (conjugated to Alexa 488), anti-GPA mAb against extracellular residues, anti-band 3 mAb against the cytoplasmic domain (anti-band 3/cd), preimmune IgY, mono-specific anti-5C IgY, and mono-specific anti-6A IgY are shown (100X magnification). Secondary antibodies were conjugated to either Alexa 488 or Alexa 594 to produce green or red fluorescence, respectively. Phase contrast is shown in the lower panel. (D) This panel shows reactivity to antibodies, as in panel C, in the neuraminidase-treated (Nm) RBCs.

Although the precise reason of this differential reactivity response is not yet known, one may speculate that the sialic acid residues on co-migrating sialoglycoproteins may suppress the accessibility of anti-5C IgY to its 5C epitope on band 3 under these Western blotting conditions. Sialic acid residues had no appreciable effect on the reactivity of anti-6A IgY antibodies to band 3 in Western blot (Figure 3.6B). As positive control, a monoclonal antibody (mAb) against the N-terminal cytoplasmic domain of human band 3 was used to detect band 3 in normal and Nm-treated RBC ghosts. Purified preimmune control IgY showed no reactivity to either the recombinant proteins (not shown) or the human RBC ghosts proteins (Figure 3.6B). These results indicate the generation of two affinity-purified mono-specific antibodies, anti-5C and anti-6A IgY, reactive against human RBC band 3.

Since anti-5C and anti-6A IgY antibodies showed characteristic band 3 recognition patterns on RBC ghosts in Western blot (Figure 3.6B), we investigated their band 3-binding properties on intact RBCs. In the first method, we examined the binding of anti-5C IgY and anti-6A IgY to methanol-fixed human RBCs by immunofluorescence microscopy. Normal RBCs (Figure 3.6C) as well as sialic acid-depleted RBCs prepared by treating the intact cells with Nm prior to fixing (Figure 3.6D) were used. Indirect immunofluorescence assay (IFA) showed that both anti-5C and anti-6A antibodies specifically bound to normal and Nm-treated RBCs. The control preimmune IgY as well as the anti-chicken secondary antibody alone did not show any interaction with fixed RBCs. As a positive control, the anti-band 3 mAb bound to both normal and Nm-treated RBCs as methanol fixation permeabilized the membrane enabling antibodies to react to proteins in the intracellular compartments (Figure 3.6A, B). As expected, the monoclonal

anti-GPA antibody/clone E4 (Sigma) raised against extracellular residues of human GPA, which are sensitive to sialic acid residues, interacted with normal RBCs bearing sialic acid residues, but not with Nm-treated RBCs where sialic acid residues on the RBC surface have been depleted (Figure 3.6C, D).

In the second method, we examined the binding of anti-5C IgY and anti-6A IgY to RBCs in suspension. Normal and Nm-treated intact human RBCs were reacted with the anti-5C and anti-6A antibodies (100 μg/ml) and analyzed by flow cytometry. As compared to the preimmune IgY control, histograms showed that each anti-5C IgY and anti-6A IgY bound to both normal and Nm-treated RBCs (Figure 3.7). The anti-5C IgY showed a stronger interaction with the sialic acid-depleted RBCs than normal RBCs in suspension as indicated by higher fluorescence intensity. This observation is consistent with the earlier Western blot result (Figure 3.6B) where the reactivity of anti-5C IgY to band 3 in RBC ghosts was apparent only in the Nm-treated RBCs. The anti-band 3 mAb reactive to the N-terminal cytoplasmic domain of band 3 did not bind to either normal or Nm-treated RBCs indicating that the cells were fully intact (Figure 3.7). The anti-GPA mAb reactive to surface residues of human GPA bound to normal RBCs but not with Nm-treated RBCs consistent with the IFA results (Figure 3.7). These results demonstrate that the anti-5C and anti-6A IgY antibodies react to the extracellular epitopes of band 3 on the surface of normal and Nm-treated intact RBCs. Subsequent biochemical quantification was performed to determine the affinity of these interactions (Table 3). The B_{max} for anti-5C IgY was significantly lower in untreated vs. Nm-treated erythrocytes. However, the dissociation constant (K_d) remained relatively unchanged.

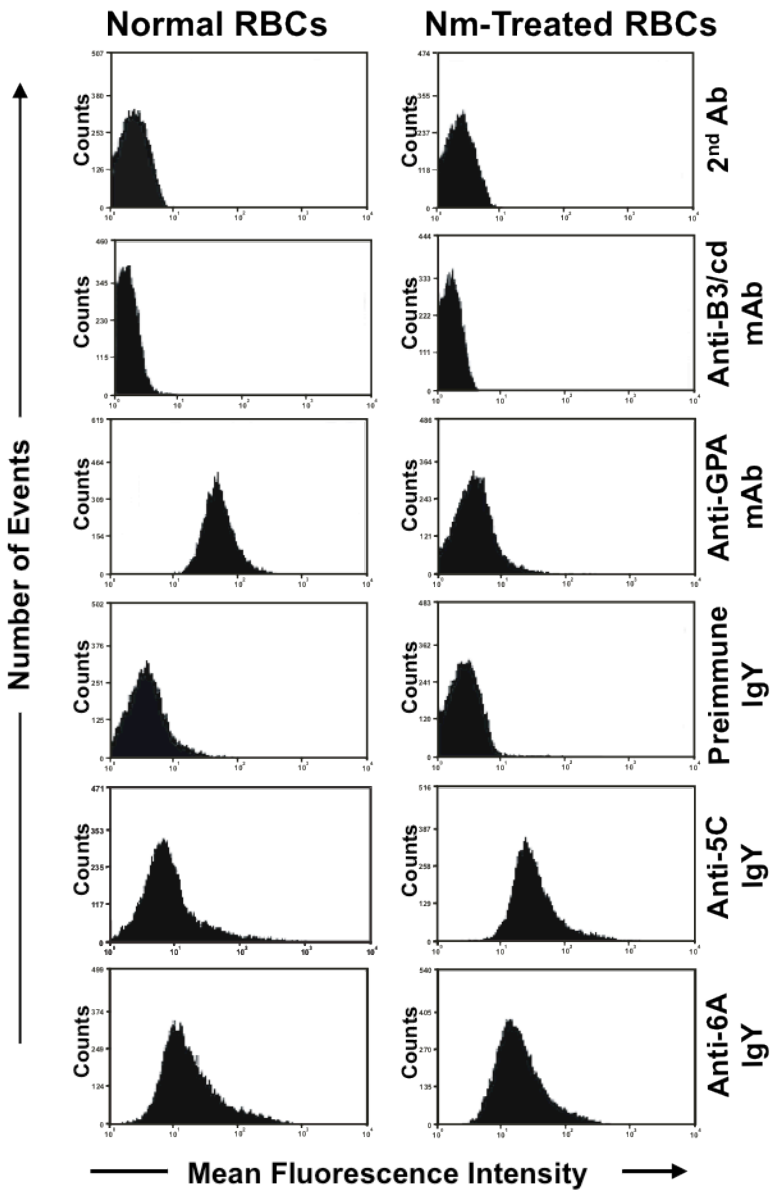

Figure 3.7. Binding of antibodies to intact RBCs by flow cytometry.
Binding data obtained by flow cytometry were analyzed using histograms (x-axis, fluorescence intensity in logarithmic scale; y-axis, number of events) and then plotted on an identical x-axis ($10^0 – 10^4$ scale) for a visual comparison of fluorescence intensity. In both normal and Nm-treated RBC samples, binding measurements were performed with the following antibodies: anti-chicken secondary antibodies as controls, anti-band 3 mAb against the cytoplasmic domain (anti-band 3/cd), anti-GPA mAb against extracellular regions, and preimmune IgY. Fluorescence intensity for the binding of mono-specific anti-5C and anti-6A IgY antibodies (100 μg/ml) to RBCs was compared with the preimmune IgY (100 μg/ml) control.

Table 3. Band 3 antibody equilibrium binding constants.

	Bmax (mean fluorescence intensity)		Kd (µg/ml)	
Antibodies	Normal RBCs	Neu-treated RBCs	Normal RBCs	Neu-treated RBCs
Anti-5C IgY	8.2 ± 0.7	25.8 ± 2.7	25.7 ± 7.9	36.6 ± 12.5
Anti-6A IgY	19.6 ± 1.7	20.7 ± 1.4	32.7 ± 9.6	43.7 ± 8.9

Some effect was seen on anti-6A IgY after Nm-treatment, however this effect was minimal.

Blocking P. falciparum invasion in human RBCs using anti-band 3 IgY

Since the binding of anti-5C and anti-6A IgY antibodies to the RBC surface was concentration-dependent, we investigated whether these antibodies would block *P. falciparum* invasion. The invasion blocking assay was carried out in the *P. falciparum* (3D7 strain) culture as described, using mono-specific anti-5C IgY and anti-6A IgY, either independently or together (Goel et al., 2003). The range of IgY concentrations used was similar to the above RBC binding assay. Assay mixtures were analyzed by flow cytometry to quantify newly formed ring-stage parasites and calculate percent parasitemia for each sample (Table 4). To visualize the invasion blocking effect of IgY antibodies, results are presented as the percent inhibition of invasion at a given IgY concentration, by taking the preimmune IgY sample at the equivalent concentration as 0% inhibition (or 100% invasion). In both normal and sialic acid-depleted RBC samples, anti-5C IgY was superior in blocking RBC invasion as compared to anti-6A IgY (Figure 3.8A and B). Consistent with its RBC binding property, the rate of invasion inhibition for anti-5C IgY was significantly higher (about 2-3 fold) in the sialic acid-depleted RBCs throughout the IgY concentrations. At 200 μg/ml IgY concentration, the anti-5C IgY blocked Nm-treated RBC invasion by 58% as compared to the preimmune IgY, which had no detectable effect on invasion at all concentrations. Although the B_{max} for anti-5C IgY binding to normal RBCs was about two-fold less than for anti-6A IgY (Table 3), the rate of RBC invasion inhibition for anti- 5C IgY was about two-fold higher than for

Table 4. IgY concentration-dependent inhibition of RBC invasion by the *P. falciparum* 3D7 strain.

		% Parasitemia (mean +/- s.e)				
		IgY concentration (μg/ml)				
RBCs	**IgY**	**0**	**25**	**50**	**100**	**200**
Normal	Pre-immune	3.19 +/- 0.03	2.99 +/- 0.14	3.01 +/- 0.11	3.00 +/- 0.02	2.98 +/- 0.11
	Anti-5C	---	2.31 +/- 0.04	1.97 +/- 0.02	1.89 +/- 0.03	1.78 +/- 0.02
	Anti-6A	---	2.61 +/- 0.03	2.21 +/- 0.04	2.16 +/- 0.13	2.11 +/- 0.01
	Both	---	1.37 +/- 0.04	1.16 +/- 0.01	1.00 +/- 0.12	1.04 +/- 0.02
Neu-treated	Pre-immune	1.39 +/- 0.01	1.35 +/- 0.07	1.29 +/- 0.06	1.30 +/- 0.03	1.41 +/- 0.01
	Anti-5C	---	0.97 +/- 0.11	0.67 +/- 0.03	0.58 +/- 0.01	0.53 +/- 0.01
	Anti-6A	---	1.11 +/- 0.01	0.98 +/- 0.01	0.87 +/- 0.02	0.81 +/- 0.07
	Both	---	0.44 +/- 0.03	0.21 +/- 0.01	0.16 +/- 0.05	0.17 +/- 0.02

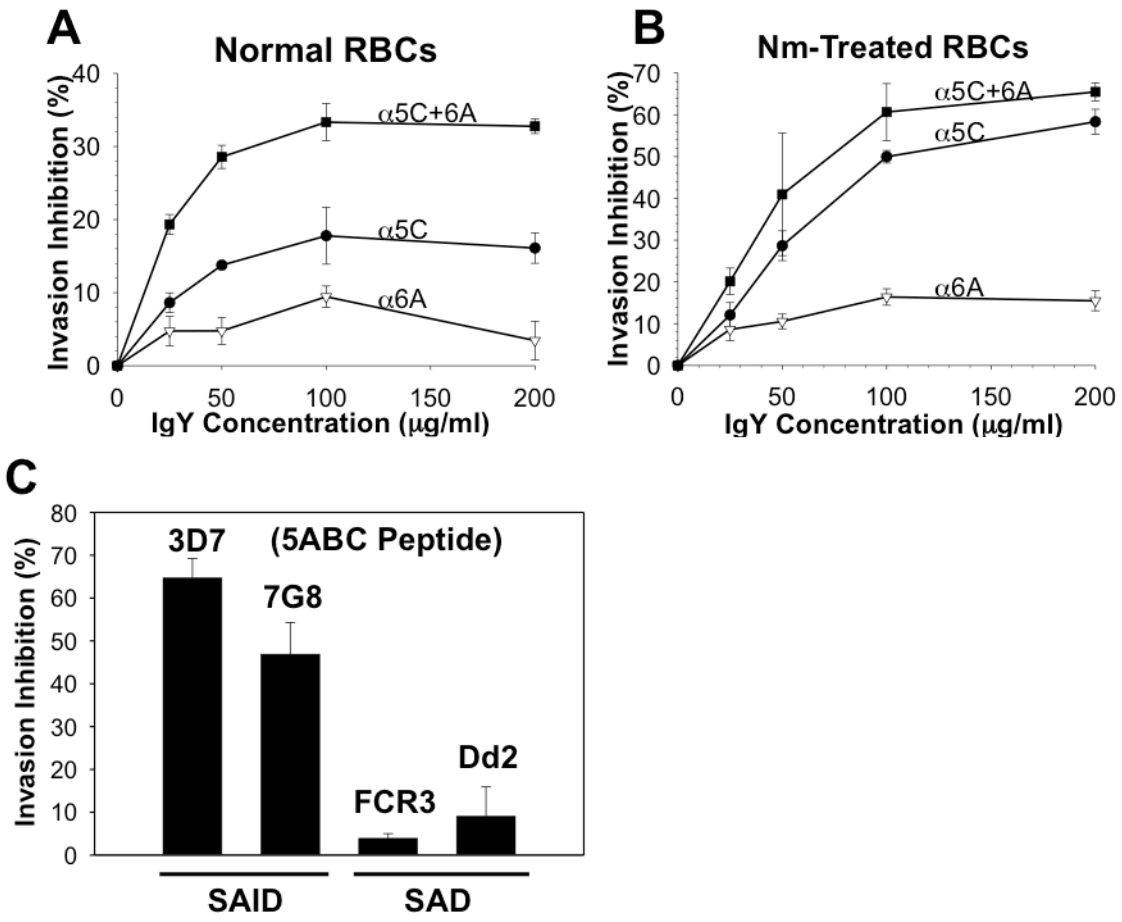

Figure 3.8. Band 3 antibodies inhibit *Plasmodium falciparum* invasion *in vitro*. (A) RBC invasion assay was carried out using freshly added normal or (B) Nm-treated human RBCs in trophozoite-enriched *P. falciparum* (3D7 strain) samples having increasing concentrations of anti-band 3 IgY antibodies. Each anti-5C and anti-6A IgY was used at 0, 25, 50, 100, and 200 µg/ml concentrations either as a single inhibitor or as a mixture of the two. Newly formed ring-stage parasites were counted by flow cytometry using SYTO-13, and mean parasitemia (new infection) was determined from triplicate assay samples. The data are presented as percent invasion inhibition (mean ± s.e.) based on the preimmune IgY control sample taken as 0% inhibition (or 100% invasion). (C) Invasion inhibition assays were carried out for both SAID and SAD invasion phenotypes of *P. falciparum*. The assays were performed in triplicate using 8.0 µM of soluble recombinant proteins, GST-5ABC and GST (control). Student's *t*-test was used to compare the mean. The data presented as percent invasion inhibition is based on the GST control sample taken as 0% inhibition.

anti-6A IgY (Figure 3.8A). No accumulation of trophozoites and schizonts was observed during the course of the assay, indicating that the addition of antibodies to the culture medium at the trophozoite stage did not affect intracellular maturation and release of the parasites.

When both anti-5C and anti-6A antibodies were added to the culture medium as a 1:1 mixture, an additive effect was observed (Figure 3.8A, Table 4). It was also evident that this additive effect was not simply due to the doubling of the total IgY concentration. For example, in normal RBC samples, 100 μg/ml anti-5C IgY produced 18% invasion inhibition, while a mixture of 50 μg/ml anti-5C IgY and 50 μg/ml anti-6A IgY gave 29% inhibition. Similarly, doubling the anti-5C IgY concentration from 25 to 50 μg/ml increased the inhibition rate from 12% to 29% inhibition in Nm-treated RBC samples, but adding 25 μg/ml of each IgY as a mixture resulted in only 20% invasion inhibition. These results suggest that each anti-5C and anti-6A IgY plays an important role in blocking RBC invasion by *P. falciparum*. Both the binding and invasion inhibition by each IgY increased dose dependently and reached a near maximum at 200 μg/ml. However, the binding and the inhibition slowed down significantly starting at about 100 μg/ml. Similar rate profiles suggest that the invasion blocking effects of these antibodies correlates with the binding to their respective epitopes (Table 3).

Since the anti-5C IgY antibody showed a significant inhibitory effect on the invasion of RBCs by the SAID invasion phenotype, we asked whether the human RBC band 3 peptide, 5ABC, would have a similar invasion blocking effect and invasion phenotype specificity. The invasion blocking mechanism for the 5ABC peptide is thought to be distinct from anti-5C IgY. The 5ABC peptide mimicking the band 3 receptor is

expected to interact directly with the parasite ligand(s) in competition with band 3, whereas anti-5C IgY would bind to band 3 epitopes and block the band 3 invasion receptor function. However, we anticipated a similar result because in principle both types of inhibition approaches would disrupt interaction between the host receptor band 3 and the parasite ligand(s) during RBC invasion. Considering the mechanism of invasion inhibition by the 5ABC peptide, it was not necessary to use sialic acid-depleted RBCs. Thus, RBC invasion assays were carried out using only normal RBCs in *P. falciparum* cultures containing 3D7, 7G8, FCR3, and Dd2 strains. Soluble GST-5ABC was used as the inhibitor and GST as control each at 8 μM concentration. The results are plotted as percent inhibition of RBC invasion taking the GST control as 0%. The 5ABC peptide inhibited invasion significantly in strains that primarily use the SAID invasion pathway of *P. falciparum* (48-65% inhibition), but not in those that utilize the SAD invasion pathway (<10% inhibition) (Figure 3.8C). No accumulation of trophozoites and schizonts was observed in any samples during the course of the assay (data not shown) indicating that recombinant proteins, GST-5ABC and GST did not affect intracellular maturation and release of the parasites. Together, these results indicate that 5C and 6A regions of human band 3 are exposed on the RBC surface and serve as a host invasion receptor predominantly in the SAID invasion pathway. It appears that the 5C region in particular is an exceptionally important part of the band 3 invasion receptor.

Invasion phenotype-specific inhibition of RBC invasion

In our previous studies, we showed that 5C and 6A regions of RBC band 3 function as an invasion receptor interacting with *P. falciparum* merozoite surface

proteins, $MSP1_{42}$/$MSP1_{19}$ and MSP9 by a SAID mechanism (Goel et al., 2003; Kariuki et al., 2005; Li et al., 2004). In this study, our data show that both anti-5C and anti-6A antibodies blocked RBC invasion by the *P. falciparum* 3D7 strain, which favors the SAID invasion pathway (Figure 3.8A, B). Hence, we asked whether the invasion-blocking function of anti-5C and anti-6A antibodies is limited to a specific invasion phenotype of *P. falciparum*. To investigate this possibility, we carried out the RBC invasion assays using 3D7 and 7G8 strains representing the SAID invasion phenotype, and FCR3 and Dd2 strains representing the SAD invasion phenotype (Figure 3.9). The concentration of IgY antibodies added as inhibitors in the assay was 100 µg/ml. Normal and sialic acid-depleted (Nm-treated) RBCs were used. Newly formed ring-stage parasites were quantified and parasitemia determined for each assay sample using the flow cytometry method. When the data are presented as percent inhibition of RBC invasion by taking the preimmune IgY control as 0% inhibition, it was evident that anti-5C IgY blocked RBC invasion by the SAID invasion phenotype of *P. falciparum* in both normal and sialic acid-depleted RBC samples (Table 5) (Figure 3.9A, B). However, the effect of anti-5C IgY on the SAD invasion phenotype was marginal in both RBC types. In comparison, the anti-6A IgY antibodies showed a relatively weak, nevertheless, significant inhibitory effect on RBC invasion by the SAID invasion phenotype particularly in Nm-treated samples (Table 5). In normal RBC samples, anti-6A IgY alone had little effect on blocking RBC invasion by the either invasion phenotype (Figure 3.9C, D) (Table 5).

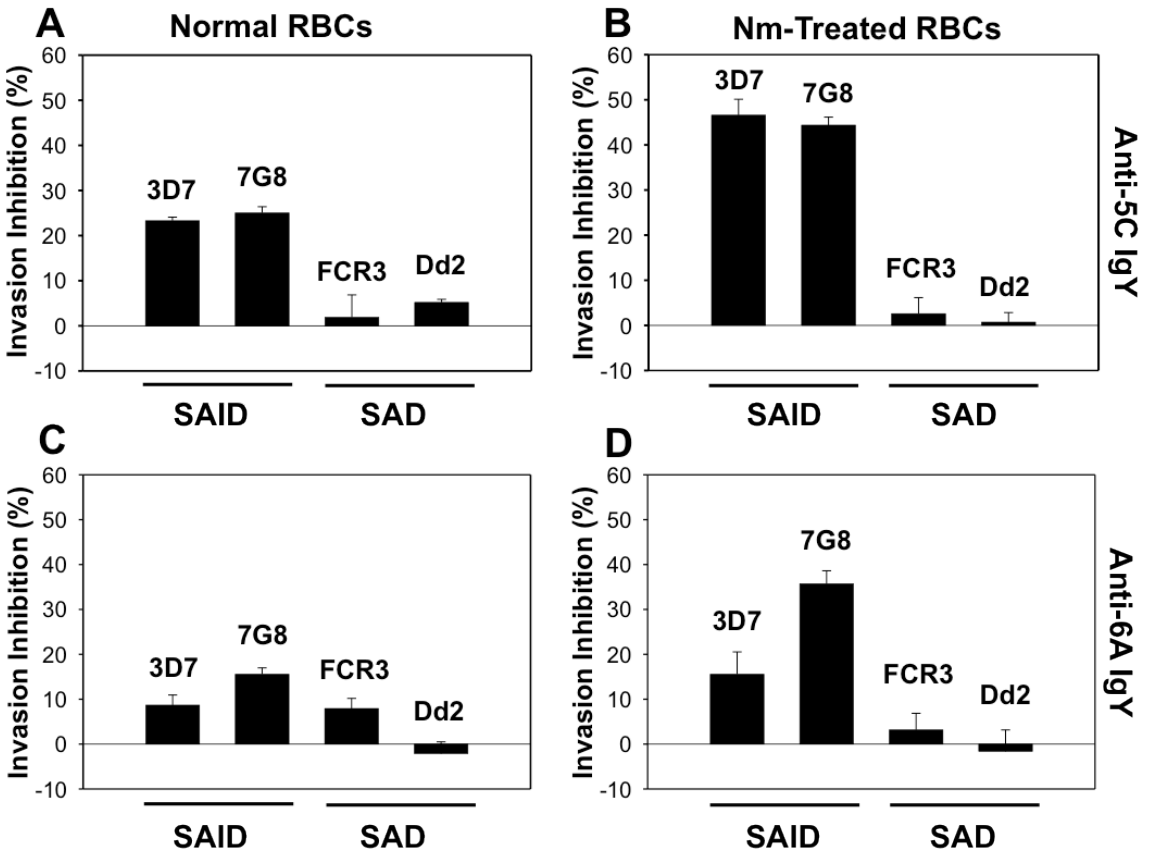

Figure 3.9. Antibodies against a specific region of band 3 specifically inhibit the SAID pathway of *P. falciparum* invasion *in vitro*.
(A-D) Using 100 μg/ml of anti-5C, anti-6A, and preimmune IgY as inhibitors, invasion inhibition assays were carried out for both SAID and SAD invasion phenotypes of *P. falciparum*. The assays were performed in triplicates using normal and Nm-treated RBCs. Flow cytometry using SYTO-13 staining allowed rapid analysis of multiple assay samples as described before. Results are presented as percent invasion inhibition (mean ± s.e.) where the preimmune IgY sample was taken as 0% inhibition. Student's *t*-test was used to compare the mean.

Table 5. Inhibition of RBC invasion using 3D7, 7G8, FCR3, and Dd2 strains of *Plasmodium falciparum*.

		% Parasitemia (mean +/- s.e)*		
		IgY Inhibitors		
Strains	**RBCs**	**Pre-immune**	**Anti-5C**	**Anti-6A**
3D7	Normal	3.63 +/- 0.03	1.73 +/- 0.07	2.63 +/- 0.03
	Nm-treated	0.97 +/- 0.18	0.57 +/- 0.01	0.86 +/- 0.05
7G8	Normal	2.69 +/- 0.07	1.56 +/- 0.03	2.18 +/- 0.04
	Nm-treated	1.02 +/- 0.06	0.39 +/- 0.01	0.75 +/- 0.02
FCR3	Normal	3.11 +/- 0.01	4.04 +/- 0.24	2.96 +/- 0.02
	Nm-treated	0.22 +/- 0.05	0.12 +/- 0.07	0.17+/- 0.03
Dd2	Normal	3.77 +/- 0.13	2.71 +/- 0.04	3.11 +/- 0.22
	Nm-treated	0.17 +/- 0.15	0.09 +/- 0.01	0.11+/- 0.01

* (Number of ring-infected RBCs after invasion / Total RBCs) x 100

Interaction of Plasmodium falciparum RhopH3 with human RBC Band 3

Identification of the 5ABC region of host RBC band 3 as an invasion receptor raised the possibility that the parasite might utilize multiple ligands to interact with this region, either directly or indirectly to facilitate pathogen entry into host cells. To test this possibility, we performed a yeast two-hybrid screen of a *P. falciparum* cDNA library (3D7, a SAID strain) using the 5ABC peptide (amino acids 720-761) of human RBC band 3 as bait. Sequencing of at least three clones revealed the C-terminal region of RhopH3 protein (amino acids 431-876) as the binding segment (Figure 3.10A). RhopH3 is a component of the high molecular weight complex (HMW) of rhoptry proteins (Kats et al., 2006). Although the precise membrane topology of RhopH3 is not yet known, multiple predictive models indicate several short transmembrane domains embedded within the primary structure of RhopH3 (Ranjan et al., 2011). The ConPred II (Arai et al., 2004) program predicted a transmembrane region (amino acids 593-613) within the yeast two-hybrid clone of RhopH3 **(**Figure 3.10A). Thus, we excluded the predicted transmembrane domain(s) to express a shorter segment of RhopH3 (amino acids 620-897), termed RhopH3-C, in order to validate its biochemical interaction with the 5ABC peptide of RBC band 3. The RhopH3-C segment was expressed as a fusion protein containing Trx and His tags with an apparent mass of 52 kDa (Trx-RhopH3-C) (Figure 3.10B). In addition, we developed an affinity-purified polyclonal anti-peptide (amino acids 876-892; Figure 3.10A and B) antibody against RhopH3 to confirm the identity and intactness of recombinant RhopH3-C protein (Figure 3.10C).

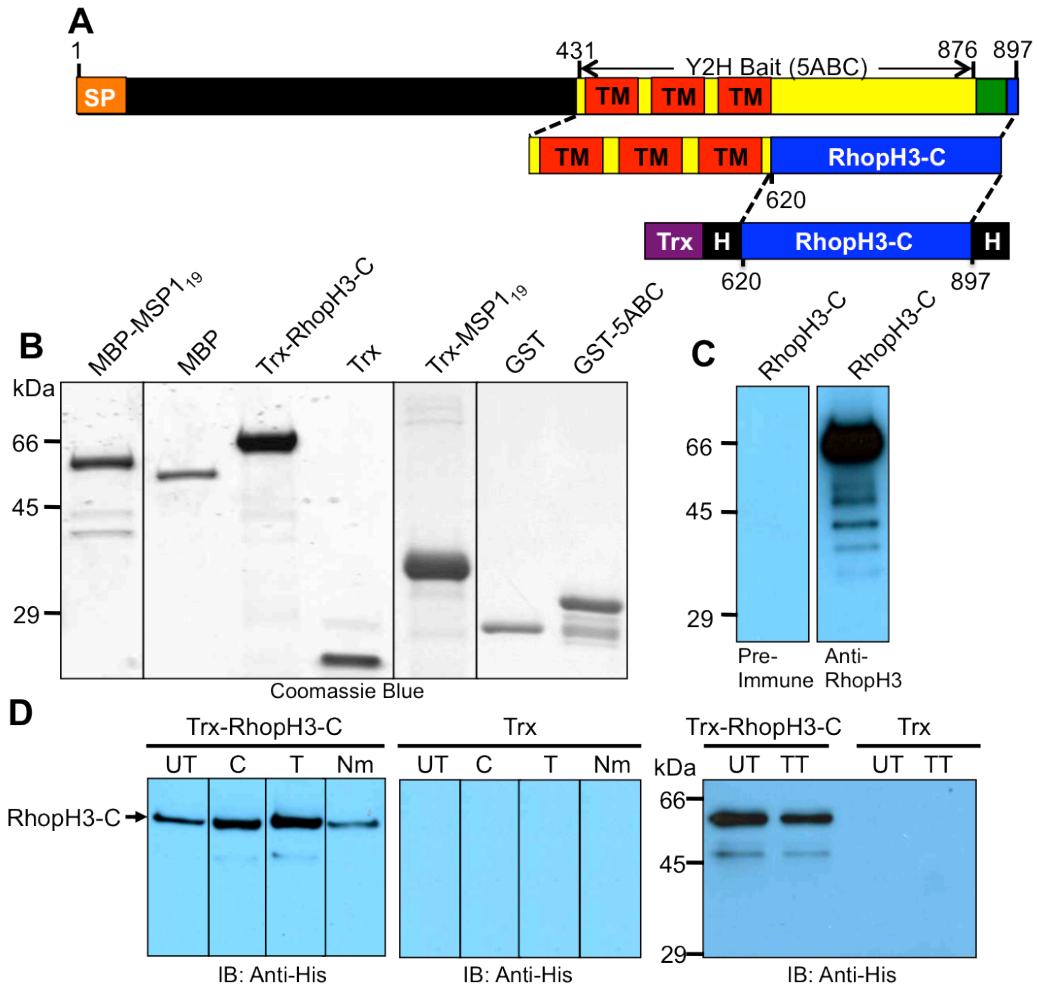

Figure 3.10. RhopH3 binds to the 5ABC domain of band 3 on human erythrocytes. (A) Diagram of full-length RhopH3 protein with its predicted transmembrane domains colored in red, the antibody epitope used in this study is shown in green, and the region identified as binding to the 5ABC domain of band 3 in a Y2H screen is colored in yellow. Recombinant RhopH3 was expressed by excluding the predicted transmembrane domains for optimum protein stability. This construct contains an N-terminal thioredoxin (Trx) tag, and both an N-terminal and C-terminal 6-His tag, and it was termed Trx-RhopH3-C. (B) Purified recombinant proteins include Trx-RhopH3-C, its band 3-binding site (GST-5ABC), Trx-MSP1$_{19}$, and respective fusion tags (MBP, Trx, GST). Gel was stained with Coomassie blue. (C) Polyclonal antibody was raised against the RhopH3 peptide (amino acids 876-892), and characterized by ELISA and Western blotting. This antibody was used to confirm the identity of recombinant Trx-RhopH3-C by Western blotting. (D) RhopH3 binds to untreated and enzyme-treated RBCs. RBCs were treated with chymotrypsin (C), trypsin (T), neuraminidase (Nm), or triply treated (TT) prior to Trx-RhopH3-C binding. Specifically bound proteins were eluted under high NaCl conditions.

RhopH3 binds to human erythrocytes

Trx-RhopH3-C binds specifically to human RBCs in a solution binding assay (Figure 3.10D). Its interaction with intact RBCs was unaffected upon treatment of RBCs with neuraminidase, trypsin or chymotrypsin (Figure 3.10D). In fact, binding of Trx-RhopH3-C to RBCs was slightly increased upon trypsin treatment of RBCs, presumably due to the removal of glycophorin A from the glycophorin A-band 3 complex. The chymotrypsin treatment of RBCs is known to cleave RBC band 3 into two lower MW bands that would retain the 5 ABC peptide sequence. Indeed, chymotrypsin treatment (C) of RBCs did not affect the Trx-RhopH3-C interaction under the same assay conditions (Figure 3.10D). Moreover, Trx-RhopH3-C binding to RBCs that were sequentially treated with trypsin, chymotrypsin, and neuraminidase (TT) essentially remained unchanged (Figure 3.10D). These results suggest that RhopH3 binds to RBCs in a protease-resistant and sialic acid-independent manner.

Biochemical interactions between RhopH3, MSP1, and Band 3

Solution binding assays confirmed a specific biochemical interaction between Trx-RhopH3-C and 5ABC peptide immobilized to glutathione beads (Figure 3.11A). The affinity of Trx-RhopH3-C interaction with 5ABC, as measured by a quantitative ELISA, yielded a K_d value of 183 nM ± 0.111 (Figure 3.11B). A truncated version of 5ABC peptide (Δ5ABC, AA'S 720-742), lacking the last 19 amino acids, showed similar binding to RhopH3, indicating that these residues do not consist of the RhopH3 binding site within this domain (Figure 3.11A).

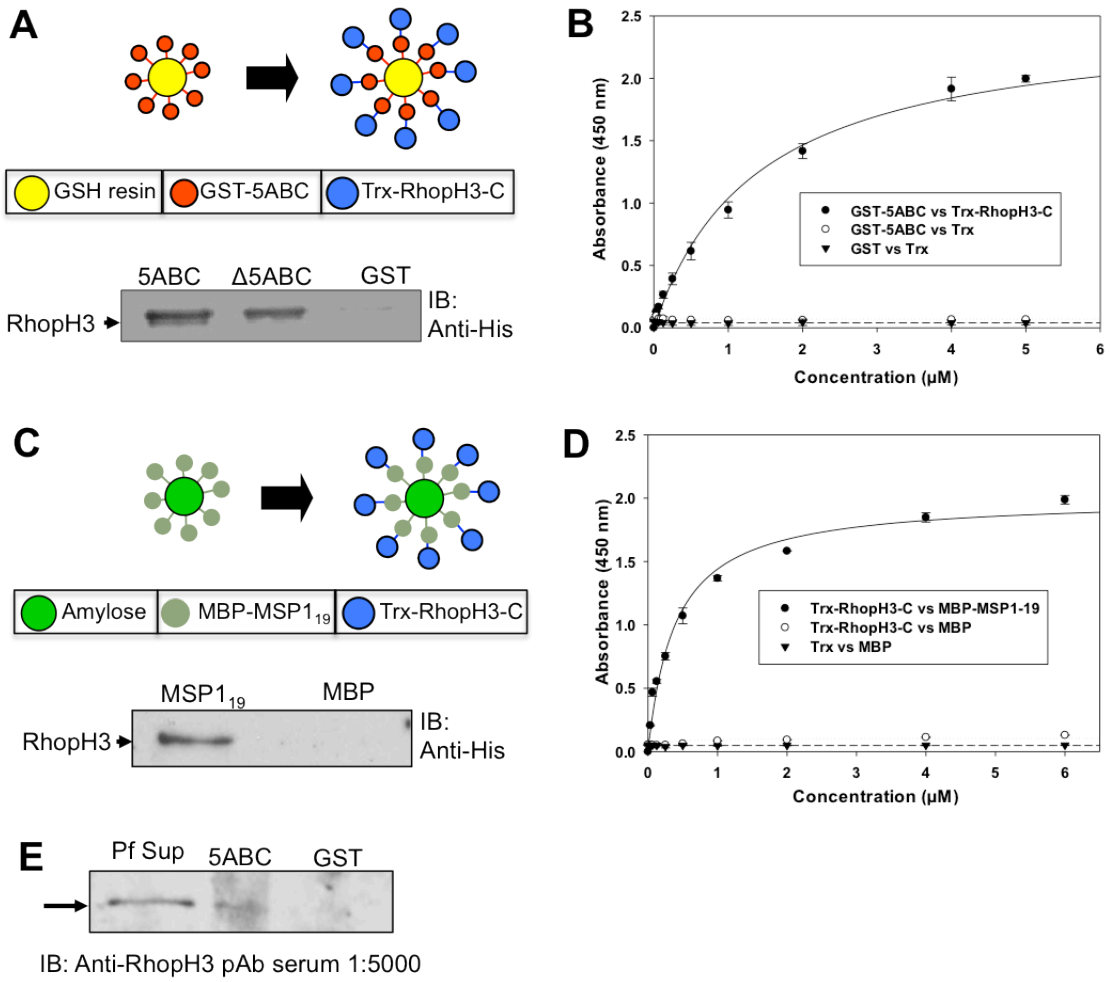

Figure 3.11. Biochemical interactions between RhopH3, band 3, and MSP1.
(A) The 5ABC region of band 3 was expressed as a GST fusion protein, which was then bound to GSH resin. Trx-RhopH3-C was added to the mixture and allowed to bind. After washing, bound protein was eluted and analyzed by immunoblotting against the His tag to detect RhopH3-C fusion protein. (B) Concentration-dependent binding of soluble Trx-RhopH3-C (0-5 μM) to GST-5ABC (0.1 μM) immobilized to an ELISA plate. The values are (means ± S.D.), and the dissociation constant was estimated from duplicate measurements. The ligand binding curves are shown in the range of 0-5 μM. Trx binding to GST-5ABC and GST was insignificant. (C) MSP1$_{19}$ expressed as an MBP fusion protein was immobilized to amylose beads. Trx-RhopH3-C was added to the mixture, allowed to bind, washed, and eluted. Immunoblotting against the His tag was used to detect the RhopH3-C fusion protein. (D) Concentration-dependent binding of soluble MBP-MSP1$_{19}$ (0-6 μM) to Trx-RhopH3-C (0.1 μM) immobilized on an ELISA plate. The ligand binding curves are shown in the range of 0-6 μM. Trx-RhopH3 binding to MBP and Trx binding to MBP were insignificant. (D) Parasite supernatant binding was performed using culture supernatant and immobilized GST-5ABC protein. Analysis was performed by immunoblotting against RhopH3.

Together, these results indicate that the C-terminal segment of RhopH3 directly interacts with the 5ABC region of human RBC band 3.

A global interaction network analysis of *P. falciparum* predicted a major role of MSP1 by virtue of its interactions with more than 80 proteins in the malaria genome (LaCount et al., 2005). Consistent with the interaction network, the C-terminal 19 kDa segment of MSP1 ($MSP1_{19}$) interacted with the C terminal segment (amino acids 734-865) of RhopH3 (LaCount et al., 2005; Ranjan et al., 2011). To assess the inter-dependence of biochemical interactions between RhopH3, MSP1, and band 3, we expressed $MSP1_{19}$ (amino acids 1665-1760) as a fusion with maltose binding protein (MBP) (Figure 3.11C). Amylose beads with immobilized MBP-$MSP1_{19}$ specifically bound soluble Trx-RhopH3-C indicating a direct biochemical interaction (Figure 3.11C). The affinity of Trx-RhopH3-C interaction with MBP-$MSP1_{19}$, as measured by an ELISA, yielded a K_d value of 390 nM ± 0.032 (Figure 3.11D).

Additionally, a parasite supernatant binding assay was performed to test for endogenous RhopH3 binding to 5ABC. Parasite supernatant demonstrated a very low abundance of endogenous RhopH3, detectable only by immunoblotting; however this endogenous protein specifically bound 5ABC protein immobilized on GST beads (Figure 3.11E). Thus, in addition to recombinant RhopH3-C, native RhopH3 demonstrates a specific interaction with 5ABC.

Since RhopH3 interacts directly with both MSP1 and 5ABC and $MSP1_{19}$ is known to bind to 5ABC, we developed a competitive binding assay to evaluate the inter-dependence of RhopH3 and $MSP1_{19}$ interactions with 5ABC.

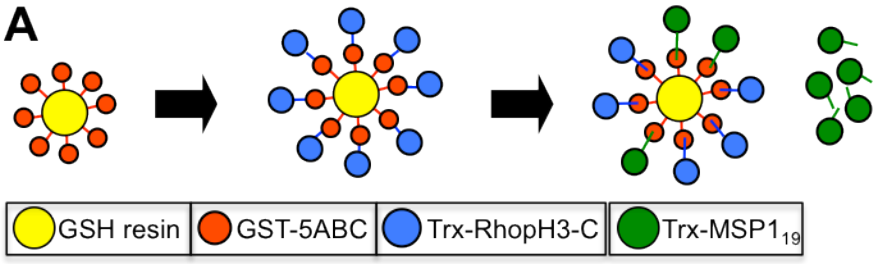

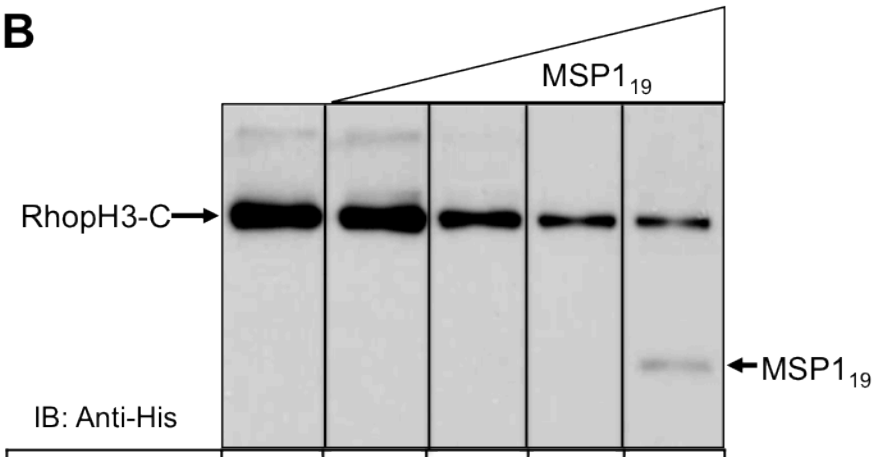

GST-5ABC	50	50	50	50	50
Trx-RhopH3-C	50	50	50	50	50
Trx	500				
Trx-MSP1$_{19}$		50	125	250	500

(Picomoles of proteins added)

Figure 3.12. MSP1 and RhopH3 compete for occupation of the 5ABC binding site of band 3.
(A) The 5ABC peptide of band 3 was expressed as GST fusion protein bound to GSH resin beads. Beads were allowed to interact with Trx-RhopH3-C, followed by the addition Trx-MSP1$_{19}$ at varying concentrations. (B) Bound proteins were eluted and analyzed by immunoblotting against the His tag to detect Trx-RhopH3-C and Trx-MSP1$_{19}$ fusion proteins. Trx-RhopH3-C was added to saturate the binding sites of GST-5ABC on beads. Increasing amounts of Trx-MSP1$_{19}$ were added to determine the displacement of RhopH3-C interaction with the GST-5ABC peptide immobilized onto beads.

For this assay, $MSP1_{19}$ was expressed as a Trx fusion protein, and ternary interactions between MSP_{19}, RhopH3, and 5ABC were examined (Figure 3.12A). Glutathione beads saturated with GST-5ABC were incubated with an equimolar concentration of Trx-RhopH3-C to allow saturation binding (Figure 3.12B). Trx-$MSP1_{19}$ was then added at increasing molar ratios (1, 2.5, 5, and 10) to compete off bound Trx-RhopH3-C from immobilized 5ABC (Figure 3.12B). $MSP1_{19}$ progressively displaced RhopH3 from 5ABC at increasing molar concentrations (Figure 3.12B). At 10 molar excess of $MSP1_{19}$, the $MSP1_{19}$ and RhopH3-C formed a ternary complex with 5ABC suggesting a concentration dependent occupancy of the binding sites under these conditions.

Contributions:

The work outlined in this chapter was published in *Blood* (Baldwin et al. 2015) and *Biochimica Biophysica Acta: Molecular Cell Research* (Baldwin et al. 2014). Figure 3.2 contains significant contributions from Xuerong Li, and the work in Figure 3.5 was performed in part by Athar Chishti and Steven Oh. Figures 3.6-3.9 include significant contributions by several other previous members of the lab including Innocent Yamodo, Ravi Ranjan, and Xuerong Li. Figures 3.9-3.12 were completed in part by Steven Oh, Marina Marinkovic, and Gregory Mines.

Chapter 4: Discussion and Future Directions

Plasmodium falciparum signal peptide peptidase

This study was initiated to investigate our earlier observations showing pharmacological inhibition of *Plasmodium falciparum* signal peptide peptidase (PfSPP) at the ring stage causes complete inhibition of malaria parasite growth in human erythrocytes (Li et al., 2009). Notwithstanding a role of PfSPP in parasite invasion (Li et al., 2008b), an essential requirement of PfSPP in parasite growth suggests that it is likely to play a functional role by cleaving critical substrates residing within an intracellular compartment during protein synthesis. This prediction is consistent with the ER localization of eukaryotic signal peptide peptidases (Friedmann et al., 2006; Krawitz et al., 2005). Using an affinity purified polyclonal antibody raised against the C-terminal 20 amino acids of PfSPP, we detected two major species of PfSPP in the parasite lysate by immunoblotting corresponding to 32 and 35 kDa bands (Figure 2.1B, C, D, E). It is well known that multi-span transmembrane proteins often aggregate or degrade at higher temperatures (Khan et al., 2008). Indeed, the 32 kDa band was rapidly lost when parasite lysate samples were subjected to higher temperatures prior to electrophoresis (Figure 2.1D). The 35 kDa band was the only species detected when PfSPP was expressed in heterologous cells further validating its identification as PfSPP (Figure 2.1C). In contrast to the 35 and 32 kDa bands of PfSPP observed by direct immunoblotting of the parasite lysate, two major bands of 35 kDa and 65 kDa were detected when PfSPP was immunoprecipitated and then immunoblotted using the same polyclonal antibody (Figure 2.1F). This finding suggests that PfSPP exists in both monomeric and dimeric forms, and is consistent with prior evidence that human SPP forms distinct oligomeric complexes *in vivo* (Lu et al., 2012; Nyborg et al., 2004a; Nyborg et al., 2006b; Schrul et al., 2010). It is

to be noted that the detection and ratio of multiple bands of PfSPP are markedly influenced by the experimental conditions of sample preparation including the composition of detergents and temperature (Figure 2.1D, E). Based on these observations, we suggest that the 35 kDa and 65 kDa forms reflect the monomer and dimer forms of PfSPP whereas the origin of other bands presumably arises from unknown post-translational modifications.

Mammalian SPPs cleave signal peptides following the action of a SP_{ase} in the ER membrane during protein processing (Lemberg and Martoglio, 2002; Narayanan et al., 2007; Sato et al., 2006). These observations suggest that PfSPP localizes to the parasite ER and cleaves ER-resident signal peptides. Our immunofluorescence and electron microscopy data further confirm the localization of PfSPP to the ER/perinuclear endomembrane system of the malaria parasite (Figure 2.2). Using a polyclonal antibody directed against the predicted ectoplasmic domain of PfSPP, previous studies detected PfSPP signal on the merozoite surface as well as in the interior compartments of unknown origin (Li et al., 2008b), consistent with the expression of PfSPP in merozoites as detected by mass spectrometry-based proteomics (Florens et al., 2002). The dynamic and short lifespan of free merozoites often precludes precise distinction between their apical organelles, which are in close proximity to the ER in motile merozoites. Therefore, a distinction between micronemes and ER compartments is sometimes difficult to discern in free merozoites. Nonetheless, subcellular localization of PfSPP in the ER of trophozoites and schizonts is consistent with the ER localization of signal peptide peptidases both in malaria and other species (Figure 2.2) (Marapana et al., 2012).

Several substrates of eukaryotic SPPs have been identified since the discovery of signal peptide peptidase activity (Lemberg and Martoglio, 2002; Sato et al., 2006; Schrul et al., 2010; Weihofen et al., 2002). Since no substrate of PfSPP has been identified to date, we performed a bioinformatics screen to identify potential type II transmembrane signal peptides that could serve as substrates of PfSPP. Using several stringent criteria, a short list of putative PfSPP substrates was assembled, including heat shock protein 101 (HSP101) (Table 2). HSP101, containing an N-terminal ER signal sequence overlapping with one type II transmembrane domain, emerged as the most likely candidate. Given that *P. falciparum* contains approximately 1,000 genes that code for a signal peptide, it is highly unlikely that Table 2 represents all endogenous PfSPP substrates. However, limiting this list to a specific amino acid motif identified in homologous SPP substrates enabled us to rapidly test more promising candidates for PfSPP cleavage. Using an established cell-based cleavage luminescence cleavage assay (Nyborg et al., 2004a), we identified parasite HSP101 as a substrate of PfSPP (Figure 2.3). SPP inhibitors, but not DAPT (a presenilin-specific inhibitor) reduced PfSPP cleavage of HSP101 (Figure 2.3). Upon release of the soluble domain of HSP101 by parasite SP_{ase}, PfSPP is expected to cleave the resident signal peptide within the ER. This accounts for a key trafficking step in parasite maturation and development (Figure 4.1). The soluble components of signal peptide-bound proteins play a variety of post-targeting functions, some of which are translocated into the erythrocyte cytosol. In this case, we are investigating the signal peptide of HSP101, whose soluble domain serves as a core component of the parasite translocation machinery where it is thought to perform a protein unfolding function prior to translocation through the PTEX pore (Figure 4.1) (de Koning-Ward et al., 2009).

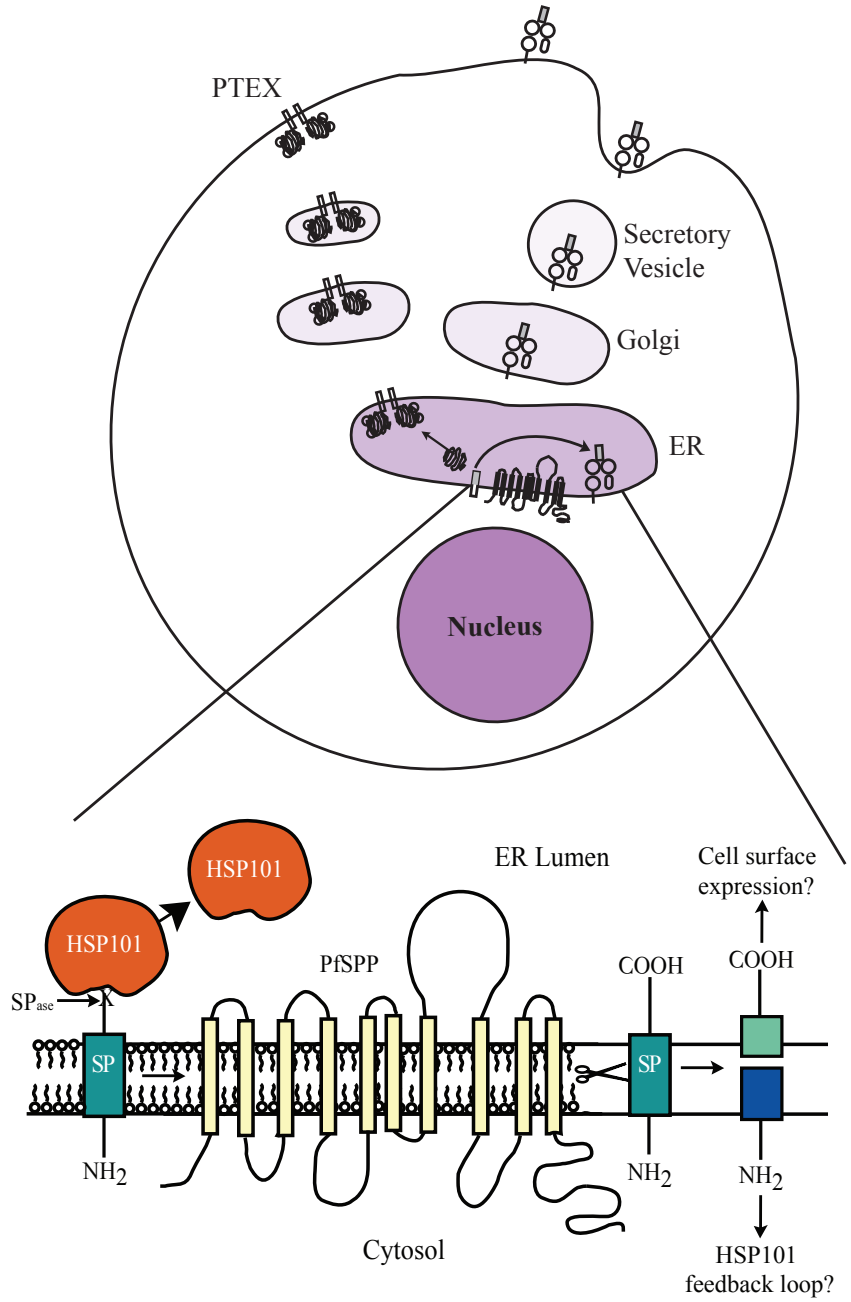

Figure 4.1. Schematic depiction of HSP101 protein processing in the parasite endoplasmic reticulum.
Parasite-derived signal peptidase (SP_{ase}) cleaves the full-length HSP101 releasing the soluble domain required for the parasite translocon machinery. PfSPP then cleaves the remaining signal peptide embedded in the membrane, thus releasing two stubs from the membrane where they may perform post-targeting signaling functions.

The inability to recover viable parasites upon genetic disruption of HSP101 underscores a critical role of HSP101 in malaria pathogenesis (Starnes and Waters, 2010). The role of the translocation machinery is to export the parasite proteins across the parasitophorous vacuole and into the host cytosol. A complex of proteins associated with HSP101, including PTEX 150, PTEX88, TRX2, and exported protein 2 (EXP2) makes up this translocon, and it is an essential portal for a variety of parasite processes. The complexity of this protein machinery, coupled to the advanced trafficking network within the parasite stresses the requirement for a finely tuned regulated system. Thus the essential requirement of HSP101 is consistent with the indispensable role PfSPP at the blood stage of the malaria parasite life cycle, given their roles in protein trafficking and processing (Li et al., 2009; Li et al., 2008b).

Our findings suggest that PfSPP plays an essential clearing function within the ER membrane, analogous to other species containing SPP (Martoglio and Golde, 2003). It is likely that PfSPP cleaves other substrates and inhibition of PfSPP activity would lead to toxic accumulation of signal peptides within the ER membrane resulting in significant ER stress, and impaired parasite development. Alternatively, the cleaved signal peptides of HSP101 by PfSPP may be released from the ER membrane in order to perform critical post-targeting functions. The *Plasmodium* translocon of exported proteins complex (PTEX) is essential for parasite viability and the soluble domain of HSP101 plays a critical role by regulating this complex located at the parasitophorous vacuole membrane (de Koning-Ward et al., 2009). Thus, a possibility exists that inhibition of HSP101 signal peptide cleavage by PfSPP may trigger a negative feedback loop or inhibition of alternative regulatory pathways by reducing the functionality of the PTEX complex.

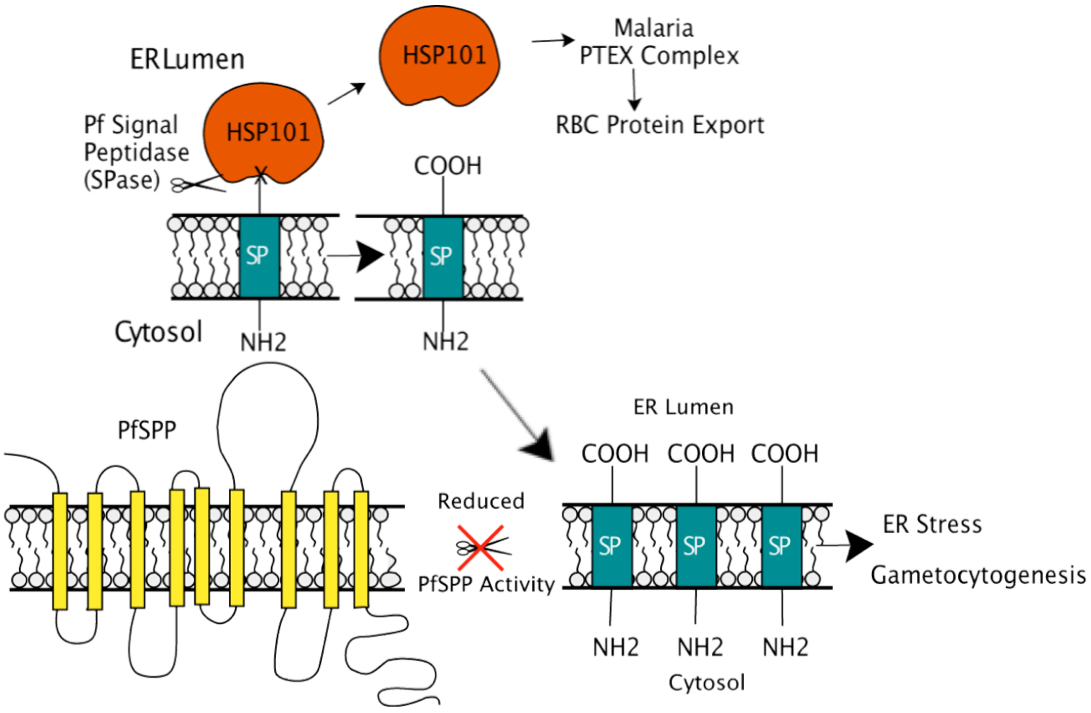

Figure 4.2. PfSPP functions as a key part of the ERAD machinery in *P. falciparum*. Following the activity of SP_{ase} the remaining membrane-bound signal peptide is cleaved by SPP. In the event of reduced SPP activity, dysfunction in the ERAD pathway is observed according to Harbut *et al.* (2012). Furthermore, we observed a decrease in SPP activity is linked to increased gametocytogenesis, putatively via an increase in ER stress, a known trigger of gametocytogenesis (Chaubey et al., 2014).

A schematic model of PfSPP mediated cleavage of the HSP101 signal peptide "stub" left behind in the ER membrane by parasite SP_{ase} highlights this view (Figure 4.2). It is likely that PfSPP will cleave multiple type II transmembrane signal peptides to ensure optimal ER membrane clearance at multiple stages of parasite development.

A previous study has shown that pharmacological inhibition of malaria signal peptide peptidase inhibits growth of sporozoites in hepatocytes (Parvanova et al., 2009). It is noteworthy that like other malaria drug targets, the development of therapeutics against PfSPP poses two familiar challenges. The emergence of drug resistance against PfSPP inhibitors has been shown recently, and potential toxicity arising from the off-target effects of these inhibitors against host signal peptide peptidases is a concern (Harbut et al., 2012). Indeed, our proteomics analysis of erythrocyte integral membrane proteins identified a homologue of SPP termed SPPL2A (Khan et al., 2008). Because of the presence of both parasite and host derived signal peptide peptidases, it would be important in future studies to determine whether PfSPP inhibition will modulate the activity of erythrocyte SPPL2A, which may alter host intra-membrane proteolysis.

A recent study reported that PfSPP is an ER-resident protease that is required for parasite growth but not invasion (Marapana et al., 2012). A major conclusion of this study that PfSPP is an ER-resident protease confirms the localization of PfSPP to endoplasmic reticulum originally made by John Dame's group (Bonilla A, Bonilla T, Yowell, C, and Dame, J. PfSPP as a novel target for malarial chemotherapy. *Molecular Parasitology Abstracts 2008*). Our findings are also consistent with the localization of PfSPP to endoplasmic reticulum (Figure 2.2). Similar to the previous study, we used an anti-PfSPP-CT polyclonal antibody and demonstrated the presence of a major 35 kDa

species of PfSPP in parasite lysate (Figure 2.1). However, we also provide evidence for the dimerization of PfSPP under mild conditions of immunoprecipitation (Figure 2.1E). The previous study utilized E64-treated merozoites to rule out a functional role of PfSPP in erythrocyte invasion (Marapana et al., 2012). While this method of merozoite isolation results in pure merozoites, its global cysteine protease inhibition may alter the function of PfSPP. Since PfSPP is expressed in merozoites, one cannot rule out a functional role of PfSPP in merozoite invasion particularly in conditions where invasion and re-invasion events are not distinguishable experimentally (Florens et al., 2002).

A serendipitous but potentially intriguing finding in our study is the observation that expression of a chimeric form of PfSPP carrying a green fluorescent protein (GFP) tag at the C-terminus caused a significant conversion of intraerythrocytic parasites to gametocyte lineage (Figure 2.4B). While the precise mechanism accounting for this phenomenon is unclear, we observed a significant increase in gametocytes upon expression of this chimeric PfSPP-GFP enzyme. Furthermore, in our cleavage assay, PfSPP-GFP demonstrates significantly reduced activity relative to the untagged protease (Figure 2.4C). Coincidentally, recent work has demonstrated that ER stress triggers gametocytogenesis (Chaubey et al., 2014). The mechanism of this phenomenon is via the increased expression of the Pf-AP2 transcription factors, which are known to play a key role in transitioning to the sexual stage of reproduction (Kafsack et al., 2014; Sinha et al., 2014). Coupling this to the fact that PfSPP is an ER-resident protease that cleaves type II signal peptides indicates that PfSPP may play a key role in ER homeostasis. Based on our initial observations, we hypothesize that impaired activity of PfSPP-GFP causes a significant level of stress at the ER, which triggers a stress response resulting in

substantial elevation of gametocytogenesis (Figure 4.2). The endoplasmic reticulum is sensitive to stress and causes a cascade of signals known as the unfolded protein response (UPR) (Harbut et al., 2012). Coincidentally, one of the most common hypotheses for inducing gametocytogenesis is stress (Baker, 2010; Dyer and Day, 2000; Talman et al., 2004). While we cannot rule out the possibility that PfSPP cleaves a signal peptide that subsequently plays a role in the gametocyte transition, no such link has been experimentally established. Future studies are likely to test a functional link between PfSPP, ER stress, and gametocytogenesis, thus underscoring the relevance of this novel pathway as a potential drug target against malaria.

MSP1 binds to glycophorin A as part of malaria invasion

Development of an effective subunit vaccine against malaria requires a precise description of the mechanism by which the merozoites invade host red blood cells. The invasion process consists of a sequence of events where the merozoite coat proteins are engaged with host RBC membrane proteins in specific ligand-receptor interactions to form unique invasion pathways. One of the most abundant ligands coating the entire surface of the merozoite is MSP1, a highly conserved protein across multiple parasite species (Holder et al., 1992). MSP1 is essential for parasite invasion of RBCs, and its genetic disruption is lethal (Cowman et al., 2012; O'Donnell et al., 2000). The detection of antibodies against the $MSP1_{19}$ segment in an infected host triggered an intense scrutiny of MSP1 as a potential malaria vaccine candidate (Riley et al., 1993). Despite these efforts, the $MSP1_{19}$ based vaccine efforts have only produced partial protection, suggesting the involvement of other MSP1 domains and/or associated proteins in the

invasion process. Therefore, a better understanding of MSP1 interactions is essential for the development of an effective vaccine against malaria.

Early studies on *P. falciparum* MSP1 have shown its interaction with both human and Saimiri monkey RBCs in a sialic acid-dependent manner (Perkins and Rocco, 1988). However, separate studies using peptides derived from *P. falciparum* $MSP1_{83}$, $MSP1_{42}$, and $MSP1_{38}$ domains demonstrated that these peptides can bind to sialic acid-depleted human RBCs with relatively high affinity (Urquiza et al., 1996). Furthermore, several of these regions demonstrated significant invasion inhibition including a peptide overlapping with the $MSP1_{19}$ domain that inhibited invasion by 30%. Consistent with these findings, our previous work showed that $MSP1_{19}$ interacts with host band 3, mediating parasite invasion of RBCs via the SAID pathway (Baldwin et al., 2014; Goel et al., 2003; Li et al., 2004). Band 3 is the most abundant membrane protein in RBCs, and forms a tight stoichiometric complex with glycophorin A. Like band 3, GPA is also highly abundant and serves as a SAD receptor binding the parasite ligand EBA-175 (Orlandi et al., 1992; Sim et al., 1994a). Based on these observations, we hypothesize that merozoites may display ligands that can potentially bind to both band 3 and GPA simultaneously, thus integrating distinct invasion pathways. In this study, we employed several phage display screening strategies that identified a unique sequence located within the N-terminal 83 kDa domain of MSP1 which directly binds to a peptide segment located within the extracellular domain of GPA (Figure 3.4A). $MSP1_{12}$, which includes the GPA-binding sequence, interacts with purified as well as endogenous GPA and recognizes multiple species of GPA (Figures 3.2 and 3.3). Together, our findings reinforce the possibility that a specific peptide sequence of MSP1 could function as a

potent inhibitor of malaria parasite invasion of human RBCs. Interestingly, antibodies targeting the trypsin-resistant region of GPA, a region that overlaps with the $MSP1_{12}$ binding site (Figure 3.4), caused a pronounced effect on RBC membrane rigidity (Chasis and Mohandas, 1992; Chasis et al., 1985). It was concluded that the increase in membrane rigidity requires a ligand-induced interaction with GPA that subsequently alters the RBC cytoskeletal interactions (Chasis et al., 1985). Thus, $MSP1_{12}$ binding to GPA may also alter the RBC membrane properties during parasite invasion. Similarly, a separate study found that reduced RBC membrane deformability upon GPA engagement correlated with reduced malaria parasite invasion (Pasvol et al., 1989). This finding raises the possibility that $MSP1_{12}$ binding to GPA may function by altering the RBC membrane properties during parasite invasion.

A recent study reported identification of two novel proteins, MSPDBL1 and MSPDBL2, associated with MSP1 (Lin et al., 2014). However, this study did not detect a direct interaction of MSP1 with human RBCs. In our view, this discrepancy could originate from the protein preparations used in that study. A full-length recombinant MSP1 assembled by tandem tethering of respective MSP1 fragments was used for the RBC binding assays (Lin et al., 2014). Due to poor solubility, recombinant full length MSP1 was subjected to denaturation and renaturation steps likely resulting in the loss of conformational folding and protein binding activity. The $MSP1_{19}$ domain contains two EGF-like motifs each of which contains three disulfide bonds, the re-folding of which is extremely difficult (Planson et al., 2013). Given that these disulfide bridges are key to its function and required for its immunogenicity, it is likely that denaturation and renaturation steps are not permissible for readily studying MSP1 function.

In our experience, recombinant MSP1 is best expressed as soluble sub-domains without subjecting them to denaturation-renaturation steps (Figure 3.1). Given the putative redundancy among parasite-ligand binding partners, it is likely that several interactions occur during the initial merozoite adhesion process presumably involving multiple host receptors. Previous studies have predicted a close proximity of band 3, involving its 12 transmembrane domains, with the transmembrane domain of GPA, and it was shown that Glu-658 of band 3 is required for its association to GPA (Williamson and Toye, 2008; Young and Tanner, 2003). Similarly, topology models predicting the association of band 3 with GPA place the region of band 3, which binds to $MSP1_{19}$, and MSP1-binding region of GPA (GPA*) adjacent to each other within the RBC membrane (Figure 4.3A) (Goel et al., 2003; Williamson and Toye, 2008). Based on these observations, our results support a model where MSP1 and its associated protein complex anchors the merozoite on the RBC surface by engaging with two distinct closely-apposed binding sites located within the surface exposed domains of band 3 and GPA (Figure 4.3). We hypothesize this receptor and co-receptor complex is likely to give rise to redundancy while also mediating the initial adhesion step of merozoite invasion.

In *P. falciparum* invasion of RBCs, glycophorin A was identified as the first RBC receptor binding the merozoite EBA-175 in a sialic acid-dependent manner (Orlandi et al., 1992; Sim et al., 1994a). Human En(a-) RBCs lacking GPA, and M^kM^k RBCs lacking both GPA and GPB, confer partial resistance to *P. falciparum* invasion (Hadley et al., 1987; Miller et al., 1977; Pasvol et al., 1982). A short hairpin RNA-based knockdown GPA in $CD34^+$ stem cells generated GPA-deficient erythrocytes showing partial reduction of *P. falciparum* invasion by sialic acid-dependent strains (Bei et al., 2010).

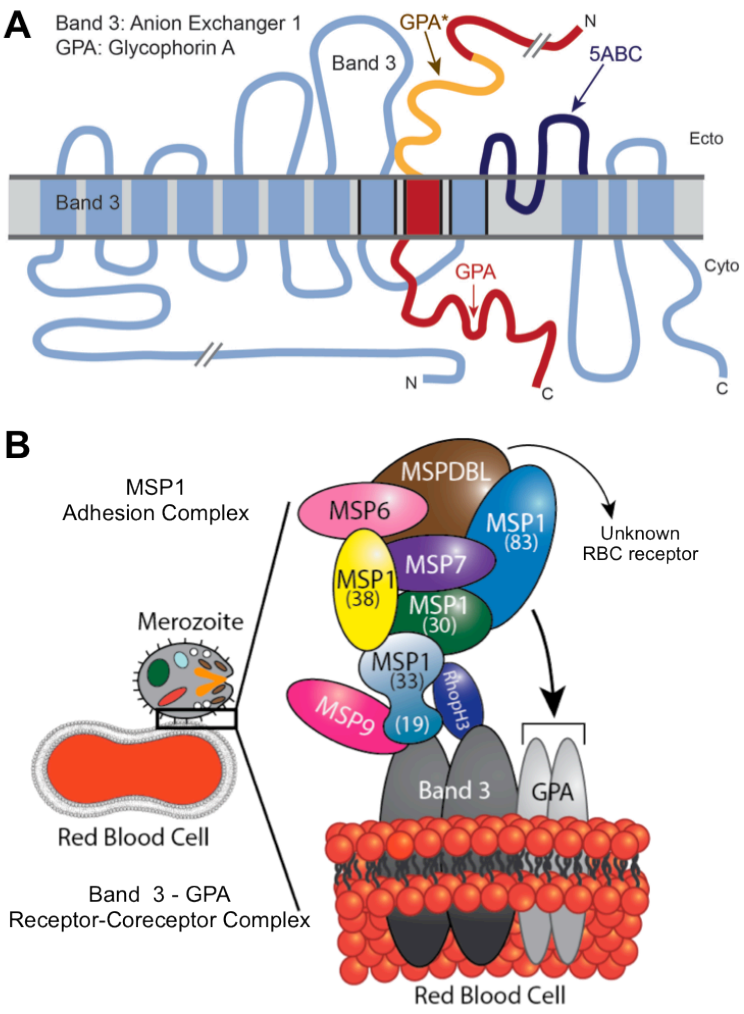

Figure 4.3. A putative model of the malaria MSP1-RBC receptor complex. (A) Band 3 and GPA are known to exhibit close physical association in the RBC membrane. The 5ABC region of band 3 that binds to malaria $MSP1_{19}$ (dark blue) is adjacent to GPA* (in orange), which binds to $MSP1_{12}$. (Adapted from Williamson et al., 2008) (B) Proposed model of malaria merozoite adhesion to the erythrocyte by engaging the MSP1 protein complex with a host band 3-GPA receptor-coreceptor complex. The recently identified MSPDBL proteins of the MSP1 complex are also shown.

In contrast, several previous studies have shown that the majority of the inhibitory effect of GPA on malaria invasion stems from its polypeptide backbone and not its sialic acid content (Breuer et al., 1983; Deas and Lee, 1981; Perkins, 1981; Weiss et al., 1981). Our studies also demonstrate that the trypsin-resistant peptide of GPA binds to MSP1 (Figure 3.4), and plays a functional role as a host receptor via the sialic acid-independent invasion pathway. Future studies will determine how the co-occupancy of GPA by two major malaria ligands MSP1 and EBA-175 is regulated during the RBC invasion process.

Host erythrocyte GPA serves as an important receptor for malaria invasion of human RBCs. Stable incorporation of GPA in the human RBC membrane requires the presence of band 3 protein, as both mouse and human RBCs genetically lacking band 3 also show a secondary loss of GPA (Hassoun et al., 1998; Perrotta et al., 2005; Ribeiro et al., 2000). The existence of a tightly bound band 3-GPA complex in the RBC membrane suggests that the merozoite may exploit this complex to provide some measure of redundancy, or a switching mechanism between the sialic acid-dependent and independent pathways during invasion. Our findings showing complete resistance of band 3 and GPA deficient mouse RBCs to malaria infection both *in vivo* and *in vitro* (Figure 3.5) lends further support to this model. Genetic abnormalities of human RBC band 3 are known to provide resistance to malaria infection (Jarolim et al., 1991; Perrotta et al., 2005; Ribeiro et al., 2000). For example, the band 3 mutation in South-East Asian Ovalocytosis (SAO) confers partial resistance malaria infection. Despite multiple explanations including RBC membrane rigidity, cytoskeletal stiffness, and metabolic imbalance, a precise molecular mechanism of malaria resistance in SAO erythrocytes

remains poorly understood. Our findings raise the possibility that some of the altered properties of SAO erythrocytes could originate from aberrant GPA-band 3 interactions. Band 3 and GPA constitute the most abundant membrane proteins on the RBC surface, whereas parasite MSP1 represents the most abundant protein on the merozoite surface. Their respective abundant expression patterns are consistent with the merozoite's ability to adhere to RBCs regardless of its orientation. Hence, we propose a model where multiple subunits of MSP1 bind to the band 3-GPA complex during the initial adhesion stage of the invasion process (Figure 4.3B). This initial adhesion step is then followed by the engagement of additional ligand-receptor interactions thus facilitating the parasite re-orientation and penetration in erythrocytes. Upon merozoite entry into RBCs, the bulk of the MSP1 complex is released from the merozoite surface. Our model also provides a rationale for the exquisite selectivity of the merozoite's preference for RBCs in circulation since the band 3-GPA complex is not expressed in other blood cells.

Host receptors are thought to mediate initial attachment, reorientation, and penetration of merozoites in RBCs by regulating signaling of specifically timed molecular steps of the invasion process. Over the last three decades or so, significant progress has been made towards the functional identification of *Plasmodium* proteins/ligands localized to the merozoite surface, rhoptries, and micronemes that are known to interact with host receptors during invasion (Cowman et al., 2012; Cowman and Crabb, 2006). In contrast, molecular understanding of the cognate receptors on host RBCs is relatively limited. Naturally occurring mutations in human genes encoding RBC membrane proteins have been informative (Oh and Chishti, 2005); however these abnormal RBCs are rare and their utility is limited to certain non-lethal hereditary genetic

mutations. Targeted mutations of genes encoding RBC membrane proteins in mice are technically challenging and time consuming. Moreover, this approach suffers from the criticism that the receptor-ligand interaction(s) governing murine malaria parasites might be different from *P. falciparum*. More recently, genetic manipulation of erythroid progenitors has been used to interrogate novel host-parasite interactions (Bei et al., 2010; Crosnier et al., 2011). This strategy identified CD55 as an essential host receptor for *P. falciparum* invasion (Egan et al., 2015). Erythrocytes from individuals with the Inab phenotype, characterized by a complete absence of CD55, demonstrate normal osmotic fragility. Furthermore, CD55 mutant erythrocytes were completely resistant to *P. falciparum* invasion *in vitro*. Evidence provided in this study suggests that CD55 does not serve as a host receptor for initial adhesion of parasite entry in erythrocytes, but likely plays a role in the irreversible attachment during tight junction formation (Egan et al., 2015). The parasite ligand for host CD55 is not currently known.

Band 3 as an antibody target for malaria invasion

Using molecular and biochemical approaches, we previously identified human RBC band 3 as an important host invasion receptor for *P. falciparum*, binding to a parasite co-ligand complex containing $MSP1_{19}$ (or $MSP1_{42}$) and MSP9 (Goel et al., 2003; Kariuki et al., 2005; Li et al., 2004). The core of the band 3 invasion receptor includes two putative exofacial regions designated as 5C and 6A. The 5C peptide is part of the 5ABC region of band 3 as described previously (Goel et al., 2003). In this study, using mono-specific anti-5C IgY and anti-6A IgY antibodies, we demonstrate that 5C and 6A (or considerable parts of these two regions) are exposed on the normal human RBC

membrane (Figure 4.4A). Since regions 5C and 6A share nearly identical amino acid sequences between humans and mice, our failed attempts to generate antibodies in mice against these two regions supports the notion that the 5C and 6A regions are exposed on the mouse RBC surface. Flow cytometry analysis of RBCs suggests that the epitope for anti-5C IgY is masked to some extent by sialic acids on the RBC surface, because the antibody showed increased reactivity towards its epitope(s) on sialic acid-depleted cells (Figure 3.7). It is unlikely that removing negatively charged sialic acid residues would affect the normal folding of RBC membrane proteins for the following two reasons: First, in the concentration-dependent invasion inhibition assay (Table 4), preimmune IgY control samples for normal and Nm-treated RBCs retained a similar level of parasitemia (5.6%-6.6%) in all IgY concentrations (0-200 μg/ml). Second, the binding of anti-6A IgY to its epitope(s) on the intact RBC surface was unaffected as judged by the B_{max} (Figure 3.7, Table 3). Native band 3 is folded in the RBC membrane mainly as homodimers and tetramers, which are part of a larger protein complex (Bruce et al., 2003).

It is well established that GPA, heavily glycosylated with sialic acid residues, interacts directly with band 3 (Auffray et al., 2001; Hassoun et al., 1998; Nigg et al., 1980). Therefore, we postulate a sub-population of band 3 dimers and/or tetramers on the human RBC membrane contains 5C that is fully exposed, whereas the remaining population has 5C masked by sialic acid residues branched out from the surrounding RBC membrane proteins (e.g., GPA). Furthermore, compensatory glycosylation of band 3 is observed in the absence of GPA in En(a-) and M^kM^k phenotypes, indicating that increased sialic acid content is dependent on membrane and cellular conditions (Gahmberg et al., 1976).

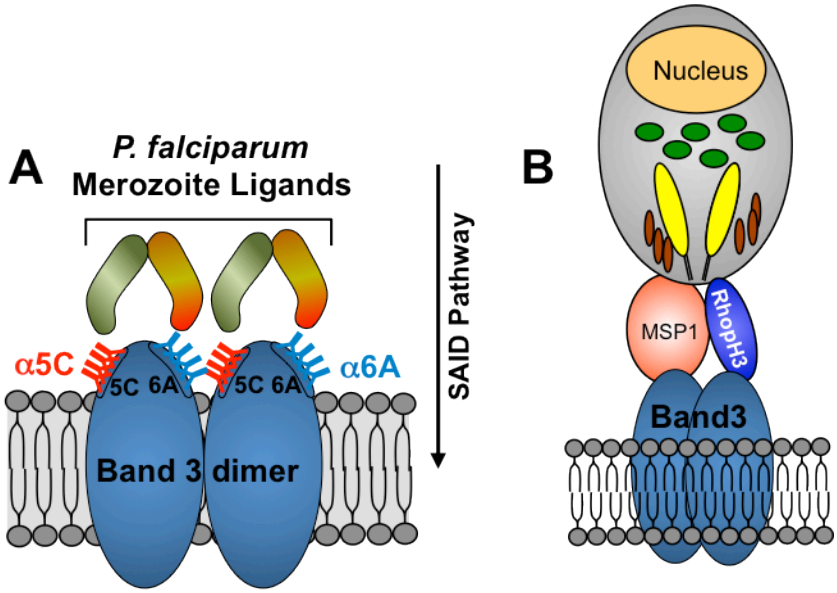

Figure 4.4. Merozoites are proposed to interact with band 3 via multiple ligands. (A) Illustration of the proposed model of the band 3-parasite interactions occurring at both 5C and 6A regions. Invasion is reduced when these interactions are inhibited through the use of recombinant peptides or antibodies against these regions. (B) Proposed model of merozoite attachment to RBCs via interactions involving band 3, MSP1, and RhopH3.

Interestingly, sialic acid content of band 3 decreases during erythrocyte aging (Mehdi et al., 2012). It has been additionally hypothesized that oxidative stress may influence this desialylation process. And while an altered glycosylation pattern of band 3 did not show a significant hematological affect *in vivo*, other work has shown that glycosylation of band 3 is inhibitory towards oxidative cross-linking (Pantaleo et al., 2009; Zdebska et al., 2003).

This view is supported by the equilibrium binding parameters estimated for anti-5C IgY in normal and Nm-treated RBC samples (Table 3), in which the K_d remained relatively unchanged despite a three-fold increase in the B_{max}. These observations further support our conclusion that the epitope(s) for mono-specific anti-5C IgY antibody is exposed on the surface of normal RBCs. Our findings provide direct evidence for the exofacial folding of 5C and 6A regions of band 3 in the normal human RBC membrane, thus lending support to multiple topology models for human RBC band 3 delineating the transmembrane 10-12 segments of the membrane domain (Hirai et al., 2011; Kanki et al., 2002; Popov et al., 1999; Yamaguchi et al., 2010b; Zhu and Casey, 2004).

Interestingly, the level of inhibition between the SAID and SAD invasion phenotypes was much more significant in the sialic acid-depleted RBCs (Figures 3.8 and 3.9). We believe this is mainly because the alternate SAD invasion pathway utilizing RBC sialic acid residues has been practically eliminated by the Nm-treatment of erythrocytes. Under such conditions, 3D7 and 7G8 strains would have no option to switch to the SAD invasion pathway even in the presence of a pressuring effect of anti-5C IgY, but continue to rely on the SAID invasion pathway (Figure 4.4A). Switching between SAD and SAID pathways is observed following specific treatments or pressures

in vitro (Stubbs et al., 2005). This appears to be the case in the 3D7 and 7G8 strains because the preimmune control samples showed no appreciable difference in the invasion rate between normal and Nm-treated RBCs (Table 4). Moreover, the depletion of sialic acid residues increases the anti-5C IgY binding capacity of RBCs (Figure 3.6B, D) and in turn provides better protection from invasion by the SAID invasion phenotype (Figure 3.8B). Taken together, sialic acid-depleted RBCs provide a better model for determining the effect of anti-band 3 antibodies on the SAID invasion phenotype and/or pathway.

The mechanism by which *P. falciparum* invades human RBCs is more complex than what is known for other *Plasmodium* species, as two alternate (SAD and SAID) invasion pathways have been implicated (Dolan et al., 1990; Mitchell et al., 1986). Moreover, these two broadly defined invasion pathways seem to tolerate additional complexity, because there are further disparities within each SAD and SAID invasion pathway characterized by the sensitivity of the host invasion receptor function to proteolytic activities (Duraisingh et al., 2003a; Lobo et al., 2004). In our invasion inhibition assays using the 3D7 strain, the mixture of anti-5C and anti-6A IgY antibodies at a near saturating concentration (200 μg/ml/each IgY) was able to block RBC invasion by 33% and 65% in normal and sialic acid-depleted RBC samples, respectively (Figure 3.8). These results, together with our invasion phenotype-specific inhibition study, suggest that band 3 is a major host invasion receptor in the SAID invasion pathway, but additional host receptors are also taking part in this pathway (Figure 3.9). Moreover, in sialic acid-depleted RBC samples, the invasion rates for FCR3 and Dd2 strain (SAD invasion phenotype) were reduced to 49% and 56%, respectively, as compared to normal RBC samples, when preimmune IgY antibodies (control) were present in the culture

medium (Table 5). As neither anti-5C nor anti-6A antibodies showed the invasion blocking effect at a significant level in SAD strains, our data suggest that this invasion phenotype does not rely on band 3 during RBC invasion. As pointed out above, other alternate host receptor(s) could be providing a dominant interaction in order for FCR3 and Dd2 strains to invade Nm-treated RBCs. It has been suggested that a molecular hierarchy of parasite ligands set by an unknown mechanism may determine the dominant interaction(s) between a particular *P. falciparum* clone and host RBCs during invasion (Baum et al., 2005).

The abundance of band 3 in the RBC membrane suggests that this multi-transmembrane protein could serve as an anchor for multiple malaria parasite proteins, facilitating a complex merozoite invasion cascade in host RBCs (Figure 4.4B). Band 3 exists in multiple subpopulations in the host membrane, including mobile and anchored dimers/tetramers as well as a tightly bound complex of band 3 with glycophorin A (Bruce et al., 2003). These unique features of band 3 could be exploited by the parasite to engage multiple ligands in a sequential manner to facilitate invasion in RBCs.

As part of our long term goal to map the network of parasite invasion ligands that interact with the host band 3-glycophorin A complex, we identified the C-terminus of *P. falciparum* RhopH3 as the ligand interacting with the 5ABC region of human band 3 (Figure 3.11A, B). A direct interaction between RhopH3-C with $MSP1_{19}$ was established (Figure 3.11C, D), consistent with our previous findings showing binding of the MSP1-MSP9 complex with Band 3 (Kariuki et al., 2005). We also show that RhopH3-C binds to intact RBCs (Figure 3.10D). Our results are consistent with previous findings that MSP1 participates in a macro-protein complex of *P. falciparum* schizont-merozoite ligands

MSP-3, MSP-6, MSP-7, MSP-9, RhopH3, RhopH1/Clag, RAP-1, RAP-2, and two putative RAP domain containing proteins (LaCount et al., 2005). Antibodies against RhopH3 inhibit merozoite invasion, and it is possible this protein may be playing a secondary role to MSP1 during invasion (Ranjan et al., 2011). Together, our findings provide the first evidence that the 5ABC region of band 3 serves as a host receptor for *P. falciparum* RhopH3.

Future Directions

Given that malaria remains one of the most deadly parasitic diseases in the world, continued interest in malaria research is essential for its eventual eradication. Extensive investigations into the development of novel therapeutics have been met with relatively little progress, as the best available therapies stem from serendipitous discoveries in holistic remedies. The observed reduction in the number of malaria deaths each year can mostly be attributed to the implementation of public health initiatives including the use of mosquito bed nets and insecticide spraying. The most effective therapies to treat malaria have been developed from discoveries in nature and not typical drug development strategies. Artemisinin is the best available malaria treatment, and it was discovered over forty years ago from extracts of a sweet wormwood tree in China. Chloroquine preceded artemisinin as the top-line malaria treatment, and was developed as a result of altering the chemical structure of quinine. Quinine, which is now chemically synthesized, was found as the active ingredient in the bark of a cinchona tree in South America. Coupled to the limited pipeline of malaria drugs is the fact that no vaccine has conferred significant enough protection in order to warrant widespread use and implementation. The troubling

emergence of multidrug resistant parasites underscores the need for research geared towards strategies for malaria eradication.

Thus, the focus of studies presented in this thesis has revolved largely around two therapeutic targets. One area of study is on a malaria protease that could serve as a potential drug target, and the second aspect deals with parasite surface proteins and their potential as vaccine candidates. Studies into PfSPP are geared towards a therapeutic target for future drug candidates, and MSP1 studies are directly linked to ongoing vaccine endeavors.

Signal Peptide Peptidase

Our investigation into PfSPP revealed a number of findings into its localization and mechanism. We successfully confirmed the location of this aspartic acid protease at the parasite endoplasmic reticulum and unveiled its first known substrate. Furthermore we propose an ER-clearing function of PfSPP as it relates to the transition between the sexual and asexual stages of parasite reproduction. Given the feasibility of our luminescence assay, it is likely that several other malaria substrates of this enzyme will be identified in the future. Thus, a specific substrate-cleavage motif by PfSPP could be identified. A mutagenic approach altering the cleavage site is thought to be a viable strategy towards identifying a core motif required for activity of PfSPP within the ER membrane. The human homologue of SPP (hSPP) shares distinct similarities with its parasite counterpart. Therefore, comparative studies must be performed to isolate substrates and their unique properties in order to avoid cross-contamination with the mammalian host. Our expectation is that the discovery of a substrate specific to the

parasite homologue of SPP will aid in the development of a dominant negative peptide specific to the parasite protease. Such leads may ultimately result in the development of chemical inhibitors of PfSPP function without affecting its mammalian counterparts.

Given the feasibility of peptidomimetic inhibitors against SPP, future studies will likely investigate the use of other aspartic acid protease inhibitors against SPP activity and malaria infection. Established assays are available to determine their selectivity for parasites relative to human cells. For example, an analogous approach has been used to suppress HIV infection where viral aspartic proteases proteases are used as drug targets. Thus, similar strategies offer promising avenues into the possibility of PfSPP being used as a target for the development of a novel antimalarial compounds.

Merozoite Surface Protein 1

The conclusions made in this thesis about MSP1 coincide with its previously known function as a malaria invasion ligand. Our previous studies have shown that MSP1 binds to band 3 during parasite invasion, and the work in this thesis demonstrates a similar function of MSP1 binding to the polypeptide backbone of glycophorin A. Additionally, erythrocytes lacking the band 3-GPA complex are resistant to parasite invasion both *in vivo* and *in vitro*. Thus, the band 3-GPA complex plays an essential role in the parasite invasion process on the host erythrocyte membrane.

The ability of two distinct domains of MSP1 coexisting as invasion ligands likely provides a measure of redundancy during the early stages of merozoite binding. We hypothesize that the stage of MSP1 binding to the host erythrocyte occurs during red blood cell adhesion. Unfortunately, exhaustive investigations into utilizing MSP1 as a

vaccine candidate have afforded limited success. One hurdle is the poor antigenicity of functionally conserved regions, coupled to the fact that "blocking" antibodies exist which prevent the inhibitory antibodies from exerting their therapeutic function. An additional issue is the possibility that due to the hypervariability of merozoite surface proteins, like MSP1, antibodies will select for resistant mutants of MSP1 thus leading to rapid obsolescence of the antibody-based therapeutics. Thus, it is unlikely that MSP1 alone will be sufficient for development of a universal protective malaria vaccine. However, its use in a multi-component vaccine containing parasite ligands from the reorientation and invagination stages of erythrocyte invasion offers a particularly intriguing avenue of malaria treatment. Specifically, AMA1 and Rh5 are indispensable antigens in the invasion process, and could be considered promising candidates for inclusion in a multi-component vaccine (Reddy et al., 2014; Treeck et al., 2009). While MSP1 and AMA1 possess significant genetic variation across strains of *P. falciparum*, Rh5 is highly conserved, and antibodies against this ligand neutralize a number of diverse *P. falciparum* strains (Douglas et al., 2014).

Highly encouraging results were recently published demonstrating the possibility of targeting the C-terminal domain of MSP1, $MSP1_{19}$, with a small molecule inhibitor (Chandramohanadas et al., 2014). In this study, the authors demonstrated that inhibitors against this subunit of MSP1 reduce parasitemia both *in vitro* and *in vivo* against several *Plasmodium* species. Generally, multi-targeted therapies are quite effective in preventing multidrug resistance. Therefore, it is possible that inhibitors designed against other domains, like the N-terminal 83 kDa domain, may provide an alternative target to be used in combination with the 19 kDa domain of MSP1.

However, surface proteins are generally considered strong targets for an antimalarial vaccine. Thus, future studies with MSP1 will require a set of experiments to determine the level of parasite reduction *in vivo* as a result of blocking MSP1 function at multiple domains. This approach will allow evaluation of the protection conferred by immunizing with specific domains of MSP1 across a number of *Plasmodium* species and strains. In summary, further elucidation of the specific function(s) of MSP1 may contribute directly to the development of an effective antimalarial vaccine.

Band 3

A functional role of band 3 as a malaria ligand receptor, specifically for MSP1, has been established before as described previously. However, this thesis provides the first evidence toward the development of antibodies against erythrocyte band 3 to reduce parasite invasion. Band 3 is essential for malaria invasion, as shown in Figure 3.5A, and the work outlined here developed a number of specific antibodies against the 5C and 6A regions on the extracellular domain of band 3. These antibodies could inhibit parasite invasion *in vitro*. Moreover, these antibodies showed significantly more functional inhibition using SAID strains (Figure 3.9). The ability of the merozoite to alternate between sialic acid-dependent and independent pathways is a key feature for its survival (Stubbs et al., 2005). Parasites rapidly alternate between ligands during invasion, and therefore further scrutiny of the dependence of specific receptors on sialic acids is likely to provide a better understanding of the molecular mechanism of the invasion process.

An issue of importance with developing vaccines against malaria is the genetic diversity of malaria proteins on the surface of the merozoite. Antibodies specific for one

isoform do not always demonstrate significant activity against alternative strains. Thus, a plausible approach could be envisaged by targeting specific elements within the highly conserved host receptor proteins. The work outlined in this thesis represents the first step towards the development of a similar approach. However, the analysis of other receptors and their relative importance must be established. Currently, a number of erythrocyte receptors are known to be involved in *P. falciparum* invasion including GPA, GPB, GPC, CR1, Basigin, CD55 and several other unidentified receptors. Future studies will reveal novel aspects of other ligand-receptor interactions thus contributing to the inhibition of parasite invasion and the development of a multi-subunit vaccine against this devastating disease.

References

Aikawa, M., Uni, Y., Andrutis, A.T., and Howard, R.J. (1986). Membrane-associated electron-dense material of the asexual stages of Plasmodium falciparum: evidence for movement from the intracellular parasite to the erythrocyte membrane. Am J Trop Med Hyg *35*, 30-36.

Alam, A. (2014). Serine Proteases of Malaria Parasite Plasmodium falciparum: Potential as Antimalarial Drug Targets. Interdisciplinary perspectives on infectious diseases *2014*, 453186.

Aly, A.S., Vaughan, A.M., and Kappe, S.H. (2009). Malaria parasite development in the mosquito and infection of the mammalian host. Annual review of microbiology *63*, 195-221.

Amino, R., Thiberge, S., Martin, B., Celli, S., Shorte, S., Frischknecht, F., and Menard, R. (2006a). Quantitative imaging of Plasmodium transmission from mosquito to mammal. Nat Med *12*, 220-224.

Amino, R., Thiberge, S., Shorte, S., Frischknecht, F., and Menard, R. (2006b). Quantitative imaging of Plasmodium sporozoites in the mammalian host. Comptes rendus biologies *329*, 858-862.

An, X.L., Takakuwa, Y., Nunomura, W., Manno, S., and Mohandas, N. (1996). Modulation of band 3-ankyrin interaction by protein 4.1. Functional implications in regulation of erythrocyte membrane mechanical properties. J Biol Chem *271*, 33187-33191.

Arai, M., Mitsuke, H., Ikeda, M., Xia, J.X., Kikuchi, T., Satake, M., and Shimizu, T. (2004). ConPred II: a consensus prediction method for obtaining transmembrane topology models with high reliability. Nucleic Acids Res *32*, W390-393.

Arevalo-Pinzon, G., Curtidor, H., Vanegas, M., Vizcaino, C., Patarroyo, M.A., and Patarroyo, M.E. (2010). Conserved high activity binding peptides from the Plasmodium falciparum Pf34 rhoptry protein inhibit merozoites in vitro invasion of red blood cells. Peptides *31*, 1987-1994.

Arimitsu, N., Akimitsu, N., Kotani, N., Takasaki, S., Kina, T., Hamamoto, H., Kamura, K., and Sekimizu, K. (2003). Glycophorin A requirement for expression of O-linked antigens on the erythrocyte membrane. Genes to cells : devoted to molecular & cellular mechanisms *8*, 769-777.

Auffray, I., Marfatia, S., de Jong, K., Lee, G., Huang, C.H., Paszty, C., Tanner, M.J., Mohandas, N., and Chasis, J.A. (2001). Glycophorin A dimerization and band 3 interaction during erythroid membrane biogenesis: in vivo studies in human glycophorin A transgenic mice. Blood *97*, 2872-2878.

Avci, D., Fuchs, S., Schrul, B., Fukumori, A., Breker, M., Frumkin, I., Chen, C.Y., Biniossek, M.L., Kremmer, E., Schilling, O.*, et al.* (2014). The Yeast ER-Intramembrane Protease Ypf1 Refines Nutrient Sensing by Regulating Transporter Abundance. Mol Cell.

Baker, D.A. (2010). Malaria gametocytogenesis. Mol Biochem Parasitol *172*, 57-65.

Baldacci, P., and Menard, R. (2004). The elusive malaria sporozoite in the mammalian host. Mol Microbiol *54*, 298-306.

Baldwin, M., Yamodo, I., Ranjan, R., Li, X., Mines, G., Marinkovic, M., Hanada, T., Oh, S.S., and Chishti, A.H. (2014). Human erythrocyte band 3 functions as a receptor for the sialic acid-independent invasion of Plasmodium falciparum. Role of the RhopH3-MSP1 complex. Biochim Biophys Acta *1843*, 2855-2870.

Bannister, L., and Mitchell, G. (2003). The ins, outs and roundabouts of malaria. Trends in parasitology *19*, 209-213.

Bannister, L.H., Hopkins, J.M., Fowler, R.E., Krishna, S., and Mitchell, G.H. (2000). A brief illustrated guide to the ultrastructure of Plasmodium falciparum asexual blood stages. Parasitol Today *16*, 427-433.

Barkan, D., Ginsburg, H., and Golenser, J. (2000). Optimisation of flow cytometric measurement of parasitaemia in plasmodium-infected mice. International journal for parasitology *30*, 649-653.

Baum, J., Maier, A.G., Good, R.T., Simpson, K.M., and Cowman, A.F. (2005). Invasion by P. falciparum merozoites suggests a hierarchy of molecular interactions. PLoS pathogens *1*, e37.

Bei, A.K., Brugnara, C., and Duraisingh, M.T. (2010). In vitro genetic analysis of an erythrocyte determinant of malaria infection. J Infect Dis *202*, 1722-1727.

Bennett, V., and Stenbuck, P.J. (1980). Association between ankyrin and the cytoplasmic domain of band 3 isolated from the human erythrocyte membrane. J Biol Chem *255*, 6424-6432.

Besteiro, S., Dubremetz, J.F., and Lebrun, M. (2011). The moving junction of apicomplexan parasites: a key structure for invasion. Cellular microbiology *13*, 797-805.

Betz, T., Lenz, M., Joanny, J.F., and Sykes, C. (2009). ATP-dependent mechanics of red blood cells. Proc Natl Acad Sci U S A *106*, 15320-15325.

Bharara, R., Singh, S., Pattnaik, P., Chitnis, C.E., and Sharma, A. (2004). Structural analogs of sialic acid interfere with the binding of erythrocyte binding antigen-175 to glycophorin A, an interaction crucial for erythrocyte invasion by Plasmodium falciparum. Mol Biochem Parasitol *138*, 123-129.

Bigbee, W.L., Vanderlaan, M., Fong, S.S., and Jensen, R.H. (1983). Monoclonal antibodies specific for the M- and N-forms of human glycophorin A. Mol Immunol *20*, 1353-1362.

Blackman, M.J., Scott-Finnigan, T.J., Shai, S., and Holder, A.A. (1994). Antibodies inhibit the protease-mediated processing of a malaria merozoite surface protein. J Exp Med *180*, 389-393.

Boddey, J.A., and Cowman, A.F. (2013). Plasmodium nesting: remaking the erythrocyte from the inside out. Annual review of microbiology *67*, 243-269.

Boyle, M.J., Richards, J.S., Gilson, P.R., Chai, W., and Beeson, J.G. (2010). Interactions with heparin-like molecules during erythrocyte invasion by Plasmodium falciparum merozoites. Blood *115*, 4559-4568.

Bradley, P.J., Ward, C., Cheng, S.J., Alexander, D.L., Coller, S., Coombs, G.H., Dunn, J.D., Ferguson, D.J., Sanderson, S.J., Wastling, J.M*., et al.* (2005). Proteomic analysis of rhoptry organelles reveals many novel constituents for host-parasite interactions in Toxoplasma gondii. J Biol Chem *280*, 34245-34258.

Breuer, W.V., Kahane, I., Baruch, D., Ginsburg, H., and Cabantchik, Z.I. (1983). Role of internal domains of glycophorin in Plasmodium falciparum invasion of human erythrocytes. Infect Immun *42*, 133-140.

Bronckers, A.L., Gueneli, N., Lullmann-Rauch, R., Schneppenheim, J., Moraru, A.P., Himmerkus, N., Bervoets, T.J., Fluhrer, R., Everts, V., Saftig, P*., et al.* (2013). The intramembrane protease SPPL2A is critical for tooth enamel formation. J Bone Miner Res *28*, 1622-1630.

Bruce, L.J., Beckmann, R., Ribeiro, M.L., Peters, L.L., Chasis, J.A., Delaunay, J., Mohandas, N., Anstee, D.J., and Tanner, M.J. (2003). A band 3-based macrocomplex of integral and peripheral proteins in the RBC membrane. Blood *101*, 4180-4188.

Bruce, L.J., Ring, S.M., Anstee, D.J., Reid, M.E., Wilkinson, S., and Tanner, M.J. (1995). Changes in the blood group Wright antigens are associated with a mutation at amino acid 658 in human erythrocyte band 3: a site of interaction between band 3 and glycophorin A under certain conditions. Blood *85*, 541-547.

Brunati, A.M., Bordin, L., Clari, G., James, P., Quadroni, M., Baritono, E., Pinna, L.A., and Donella-Deana, A. (2000). Sequential phosphorylation of protein band 3 by Syk and Lyn tyrosine kinases in intact human erythrocytes: identification of primary and secondary phosphorylation sites. Blood *96*, 1550-1557.

Brunati, A.M., Bordin, L., Clari, G., and Moret, V. (1996). The Lyn-catalyzed Tyr phosphorylation of the transmembrane band-3 protein of human erythrocytes. Eur J Biochem *240*, 394-399.

Burghaus, P.A., and Holder, A.A. (1994). Expression of the 19-kilodalton carboxy-terminal fragment of the Plasmodium falciparum merozoite surface protein-1 in Escherichia coli as a correctly folded protein. Mol Biochem Parasitol *64*, 165-169.

Campanella, M.E., Chu, H., and Low, P.S. (2005). Assembly and regulation of a glycolytic enzyme complex on the human erythrocyte membrane. Proc Natl Acad Sci U S A *102*, 2402-2407.

Cao, J., Kaneko, O., Thongkukiatkul, A., Tachibana, M., Otsuki, H., Gao, Q., Tsuboi, T., and Torii, M. (2009). Rhoptry neck protein RON2 forms a complex with microneme protein AMA1 in Plasmodium falciparum merozoites. Parasitol Int *58*, 29-35.

Carrolo, M., Giordano, S., Cabrita-Santos, L., Corso, S., Vigario, A.M., Silva, S., Leiriao, P., Carapau, D., Armas-Portela, R., Comoglio, P.M.*, et al.* (2003). Hepatocyte growth factor and its receptor are required for malaria infection. Nat Med *9*, 1363-1369.

Carter, R., and Miller, L.H. (1979). Evidence for environmental modulation of gametocytogenesis in Plasmodium falciparum in continuous culture. Bulletin of the World Health Organization *57 Suppl 1*, 37-52.

Casso, D.J., Tanda, S., Biehs, B., Martoglio, B., and Kornberg, T.B. (2005). Drosophila signal peptide peptidase is an essential protease for larval development. Genetics *170*, 139-148.

Cavanagh, D.R., Dobano, C., Elhassan, I.M., Marsh, K., Elhassan, A., Hviid, L., Khalil, E.A., Theander, T.G., Arnot, D.E., and McBride, J.S. (2001). Differential patterns of human immunoglobulin G subclass responses to distinct regions of a single protein, the merozoite surface protein 1 of Plasmodium falciparum. Infect Immun *69*, 1207-1211.

Cavanagh, D.R., Dodoo, D., Hviid, L., Kurtzhals, J.A., Theander, T.G., Akanmori, B.D., Polley, S., Conway, D.J., Koram, K., and McBride, J.S. (2004). Antibodies to the N-terminal block 2 of Plasmodium falciparum merozoite surface protein 1 are associated with protection against clinical malaria. Infect Immun *72*, 6492-6502.

Cavanagh, D.R., and McBride, J.S. (1997). Antigenicity of recombinant proteins derived from Plasmodium falciparum merozoite surface protein 1. Mol Biochem Parasitol *85*, 197-211.

Chandramohanadas, R., Basappa, Russell, B., Liew, K., Yau, Y.H., Chong, A., Liu, M., Gunalan, K., Raman, R., Renia, L.*, et al.* (2014). Small Molecule Targeting Malaria Merozoite Surface Protein-1 (MSP-1) Prevents Host Invasion of Divergent Plasmodial Species. J Infect Dis *210*, 1616-1626.

Chasis, J.A., and Mohandas, N. (1992). Red blood cell glycophorins. Blood *80*, 1869-1879.

Chasis, J.A., Mohandas, N., and Shohet, S.B. (1985). Erythrocyte membrane rigidity induced by glycophorin A-ligand interaction. Evidence for a ligand-induced association between glycophorin A and skeletal proteins. J Clin Invest *75*, 1919-1926.

Chasis, J.A., Reid, M.E., Jensen, R.H., and Mohandas, N. (1988). Signal transduction by glycophorin A: role of extracellular and cytoplasmic domains in a modulatable process. J Cell Biol *107*, 1351-1357.

Chaubey, S., Grover, M., and Tatu, U. (2014). Endoplasmic reticulum stress triggers gametocytogenesis in the malaria parasite. J Biol Chem.

Chen, C.Y., Malchus, N.S., Hehn, B., Stelzer, W., Avci, D., Langosch, D., and Lemberg, M.K. (2014). Signal peptide peptidase functions in ERAD to cleave the unfolded protein response regulator XBP1u. EMBO J *33*, 2492-2506.

Chen, L., Lopaticki, S., Riglar, D.T., Dekiwadia, C., Uboldi, A.D., Tham, W.H., O'Neill, M.T., Richard, D., Baum, J., Ralph, S.A.*, et al.* (2011). An EGF-like protein forms a complex with PfRh5 and is required for invasion of human erythrocytes by Plasmodium falciparum. PLoS pathogens *7*, e1002199.

Cheng, X.J., Hayasaka, H., Watanabe, K., Tao, Y.L., Liu, J.Y., Tsukamoto, H., Horii, T., Tanabe, K., and Tachibana, H. (2007). Production of high-affinity human monoclonal antibody fab fragments to the 19-kilodalton C-terminal merozoite surface protein 1 of Plasmodium falciparum. Infect Immun *75*, 3614-3620.

Child, M.A., Epp, C., Bujard, H., and Blackman, M.J. (2010). Regulated maturation of malaria merozoite surface protein-1 is essential for parasite growth. Mol Microbiol *78*, 187-202.

Chiu, C.Y., Hodder, A.N., Lin, C.S., Hill, D.L., Li Wai Suen, C.S., Schofield, L., Siba, P.M., Mueller, I., Cowman, A.F., and Hansen, D.S. (2015). Antibodies to the Plasmodium falciparum proteins MSPDBL1 and MSPDBL2 opsonise merozoites, inhibit parasite growth and predict protection from clinical malaria. J Infect Dis.

Citron, M., Westaway, D., Xia, W., Carlson, G., Diehl, T., Levesque, G., Johnson-Wood, K., Lee, M., Seubert, P., Davis, A.*, et al.* (1997). Mutant presenilins of Alzheimer's disease increase production of 42-residue amyloid beta-protein in both transfected cells and transgenic mice. Nat Med *3*, 67-72.

Cohen, C.M., Dotimas, E., and Korsgren, C. (1993). Human erythrocyte membrane protein band 4.2 (pallidin). Seminars in hematology *30*, 119-137.

Collins, C.R., Withers-Martinez, C., Bentley, G.A., Batchelor, A.H., Thomas, A.W., and Blackman, M.J. (2007). Fine mapping of an epitope recognized by an invasion-inhibitory monoclonal antibody on the malaria vaccine candidate apical membrane antigen 1. J Biol Chem *282*, 7431-7441.

Cowman, A.F., Berry, D., and Baum, J. (2012). The cellular and molecular basis for malaria parasite invasion of the human red blood cell. J Cell Biol *198*, 961-971.

Cowman, A.F., and Crabb, B.S. (2006). Invasion of red blood cells by malaria parasites. Cell *124*, 755-766.

Crabb, B.S., Cooke, B.M., Reeder, J.C., Waller, R.F., Caruana, S.R., Davern, K.M., Wickham, M.E., Brown, G.V., Coppel, R.L., and Cowman, A.F. (1997). Targeted gene disruption shows that knobs enable malaria-infected red cells to cytoadhere under physiological shear stress. Cell *89*, 287-296.

Crawshaw, S.G., Martoglio, B., Meacock, S.L., and High, S. (2004). A misassembled transmembrane domain of a polytopic protein associates with signal peptide peptidase. Biochem J *384*, 9-17.

Crosnier, C., Bustamante, L.Y., Bartholdson, S.J., Bei, A.K., Theron, M., Uchikawa, M., Mboup, S., Ndir, O., Kwiatkowski, D.P., Duraisingh, M.T.*, et al.* (2011). Basigin is a receptor essential for erythrocyte invasion by Plasmodium falciparum. Nature *480*, 534-537.

Daniels, G. (1995). Human blood groups (Oxford ; Cambridge, Mass., USA: Blackwell Science).

Das, S., Radtke, A., Choi, Y.J., Mendes, A.M., Valenzuela, J.G., and Dimopoulos, G. (2010). Transcriptomic and functional analysis of the Anopheles gambiae salivary gland in relation to blood feeding. Bmc Genomics *11*, 566.

Dasgupta, S., Auth, T., Gov, N.S., Satchwell, T.J., Hanssen, E., Zuccala, E.S., Riglar, D.T., Toye, A.M., Betz, T., Baum, J.*, et al.* (2014). Membrane-wrapping contributions to malaria parasite invasion of the human erythrocyte. Biophys J *107*, 43-54.

de Koning-Ward, T.F., Gilson, P.R., Boddey, J.A., Rug, M., Smith, B.J., Papenfuss, A.T., Sanders, P.R., Lundie, R.J., Maier, A.G., Cowman, A.F.*, et al.* (2009). A newly discovered protein export machine in malaria parasites. Nature *459*, 945-949.

De Rosa, M.C., Carelli Alinovi, C., Galtieri, A., Russo, A., and Giardina, B. (2008). Allosteric properties of hemoglobin and the plasma membrane of the erythrocyte: new insights in gas transport and metabolic modulation. IUBMB Life *60*, 87-93.

de Villiers, K.A., Marques, H.M., and Egan, T.J. (2008). The crystal structure of halofantrine-ferriprotoporphyrin IX and the mechanism of action of arylmethanol antimalarials. Journal of inorganic biochemistry *102*, 1660-1667.

Deas, J.E., and Lee, L.T. (1981). Competitive inhibition by soluble erythrocyte glycoproteins of penetration by Plasmodium falciparum. Am J Trop Med Hyg *30*, 1164-1167.

Deitsch, K., Driskill, C., and Wellems, T. (2001). Transformation of malaria parasites by the spontaneous uptake and expression of DNA from human erythrocytes. Nucleic Acids Res *29*, 850-853.

Deponte, M., Hoppe, H.C., Lee, M.C., Maier, A.G., Richard, D., Rug, M., Spielmann, T., and Przyborski, J.M. (2012). Wherever I may roam: Protein and membrane trafficking in P. falciparum-infected red blood cells. Mol Biochem Parasitol *186*, 95-116.

Desai, S.A. (2014). Why do malaria parasites increase host erythrocyte permeability? Trends in parasitology *30*, 151-159.

Dev, K.K., Chatterjee, S., Osinde, M., Stauffer, D., Morgan, H., Kobialko, M., Dengler, U., Rueeger, H., Martoglio, B., and Rovelli, G. (2006). Signal peptide peptidase dependent cleavage of type II transmembrane substrates releases intracellular and extracellular signals. Eur J Pharmacol *540*, 10-17.

Dluzewski, A.R., Ling, I.T., Hopkins, J.M., Grainger, M., Margos, G., Mitchell, G.H., Holder, A.A., and Bannister, L.H. (2008). Formation of the food vacuole in Plasmodium falciparum: a potential role for the 19 kDa fragment of merozoite surface protein 1 (MSP1(19)). PLoS One *3*, e3085.

Dolan, S.A., Miller, L.H., and Wellems, T.E. (1990). Evidence for a switching mechanism in the invasion of erythrocytes by Plasmodium falciparum. J Clin Invest *86*, 618-624.

Doolan, D.L., and Hoffman, S.L. (1997). Multi-gene vaccination against malaria: A multistage, multi-immune response approach. Parasitol Today *13*, 171-178.

Douglas, A.D., Williams, A.R., Knuepfer, E., Illingworth, J.J., Furze, J.M., Crosnier, C., Choudhary, P., Bustamante, L.Y., Zakutansky, S.E., Awuah, D.K.*, et al.* (2014). Neutralization of Plasmodium falciparum merozoites by antibodies against PfRH5. J Immunol *192*, 245-258.

Dultz, E., Hildenbeutel, M., Martoglio, B., Hochman, J., Dobberstein, B., and Kapp, K. (2008). The signal peptide of the mouse mammary tumor virus Rem protein is released from the endoplasmic reticulum membrane and accumulates in nucleoli. J Biol Chem *283*, 9966-9976.

Duraisingh, M.T., Maier, A.G., Triglia, T., and Cowman, A.F. (2003a). Erythrocyte-binding antigen 175 mediates invasion in Plasmodium falciparum utilizing sialic acid-dependent and -independent pathways. Proc Natl Acad Sci U S A *100*, 4796-4801.

Duraisingh, M.T., Triglia, T., Ralph, S.A., Rayner, J.C., Barnwell, J.W., McFadden, G.I., and Cowman, A.F. (2003b). Phenotypic variation of Plasmodium falciparum merozoite proteins directs receptor targeting for invasion of human erythrocytes. EMBO J *22*, 1047-1057.

Dutta, S., Haynes, J.D., Barbosa, A., Ware, L.A., Snavely, J.D., Moch, J.K., Thomas, A.W., and Lanar, D.E. (2005). Mode of action of invasion-inhibitory antibodies directed against apical membrane antigen 1 of Plasmodium falciparum. Infect Immun *73*, 2116-2122.

Dyer, M., and Day, K.P. (2000). Commitment to gametocytogenesis in Plasmodium falciparum. Parasitol Today *16*, 102-107.

Egan, A., Waterfall, M., Pinder, M., Holder, A., and Riley, E. (1997). Characterization of human T- and B-cell epitopes in the C terminus of Plasmodium falciparum merozoite surface protein 1: evidence for poor T-cell recognition of polypeptides with numerous disulfide bonds. Infect Immun *65*, 3024-3031.

Egan, A.F., Blackman, M.J., and Kaslow, D.C. (2000). Vaccine efficacy of recombinant Plasmodium falciparum merozoite surface protein 1 in malaria-naive, -exposed, and/or -rechallenged Aotus vociferans monkeys. Infect Immun *68*, 1418-1427.

Egan, E.S., Jiang, R.H., Moechtar, M.A., Barteneva, N.S., Weekes, M.P., Nobre, L.V., Gygi, S.P., Paulo, J.A., Frantzreb, C., Tani, Y.*, et al.* (2015). Malaria. A forward genetic screen identifies erythrocyte CD55 as essential for Plasmodium falciparum invasion. Science *348*, 711-714.

Ekala, M.T., Jouin, H., Lekoulou, F., Issifou, S., Mercereau-Puijalon, O., and Ntoumi, F. (2002). Plasmodium falciparum merozoite surface protein 1 (MSP1): genotyping and humoral responses to allele-specific variants. Acta Trop *81*, 33-46.

Elliott, D.A., McIntosh, M.T., Hosgood, H.D., 3rd, Chen, S., Zhang, G., Baevova, P., and Joiner, K.A. (2008). Four distinct pathways of hemoglobin uptake in the malaria parasite Plasmodium falciparum. Proc Natl Acad Sci U S A *105*, 2463-2468.

Farrow, R.E., Green, J., Katsimitsoulia, Z., Taylor, W.R., Holder, A.A., and Molloy, J.E. (2011). The mechanism of erythrocyte invasion by the malarial parasite, Plasmodium falciparum. Semin Cell Dev Biol *22*, 953-960.

Ferru, E., Giger, K., Pantaleo, A., Campanella, E., Grey, J., Ritchie, K., Vono, R., Turrini, F., and Low, P.S. (2011). Regulation of membrane-cytoskeletal interactions by tyrosine phosphorylation of erythrocyte band 3. Blood *117*, 5998-6006.

Filosa, S., Fico, A., Paglialunga, F., Balestrieri, M., Crooke, A., Verde, P., Abrescia, P., Bautista, J.M., and Martini, G. (2003). Failure to increase glucose consumption through the pentose-phosphate pathway results in the death of glucose-6-phosphate dehydrogenase gene-deleted mouse embryonic stem cells subjected to oxidative stress. Biochem J *370*, 935-943.

Fleck, S.L., Birdsall, B., Babon, J., Dluzewski, A.R., Martin, S.R., Morgan, W.D., Angov, E., Kettleborough, C.A., Feeney, J., Blackman, M.J.*, et al.* (2003). Suramin and suramin analogues inhibit merozoite surface protein-1 secondary processing and erythrocyte invasion by the malaria parasite Plasmodium falciparum. J Biol Chem *278*, 47670-47677.

Fleig, L., Bergbold, N., Sahasrabudhe, P., Geiger, B., Kaltak, L., and Lemberg, M.K. (2012). Ubiquitin-dependent intramembrane rhomboid protease promotes ERAD of membrane proteins. Mol Cell *47*, 558-569.

Florens, L., Washburn, M.P., Raine, J.D., Anthony, R.M., Grainger, M., Haynes, J.D., Moch, J.K., Muster, N., Sacci, J.B., Tabb, D.L.*, et al.* (2002). A proteomic view of the Plasmodium falciparum life cycle. Nature *419*, 520-526.

Fluhrer, R., Grammer, G., Israel, L., Condron, M.M., Haffner, C., Friedmann, E., Bohland, C., Imhof, A., Martoglio, B., Teplow, D.B.*, et al.* (2006). A gamma-secretase-like intramembrane cleavage of TNFalpha by the GxGD aspartyl protease SPPL2b. Nat Cell Biol *8*, 894-896.

Fluhrer, R., Multhaup, G., Schlicksupp, A., Okochi, M., Takeda, M., Lammich, S., Willem, M., Westmeyer, G., Bode, W., Walter, J.*, et al.* (2003). Identification of a beta-secretase activity, which truncates amyloid beta-peptide after its presenilin-dependent generation. J Biol Chem *278*, 5531-5538.

Freeman, R.R., and Holder, A.A. (1983). Surface antigens of malaria merozoites. A high molecular weight precursor is processed to an 83,000 mol wt form expressed on the surface of Plasmodium falciparum merozoites. J Exp Med *158*, 1647-1653.

Frevert, U., Engelmann, S., Zougbede, S., Stange, J., Ng, B., Matuschewski, K., Liebes, L., and Yee, H. (2005). Intravital observation of Plasmodium berghei sporozoite infection of the liver. PLoS biology *3*, e192.

Friedmann, E., Hauben, E., Maylandt, K., Schleeger, S., Vreugde, S., Lichtenthaler, S.F., Kuhn, P.H., Stauffer, D., Rovelli, G., and Martoglio, B. (2006). SPPL2a and SPPL2b promote intramembrane proteolysis of TNFalpha in activated dendritic cells to trigger IL-12 production. Nat Cell Biol *8*, 843-848.

Friedmann, E., Lemberg, M.K., Weihofen, A., Dev, K.K., Dengler, U., Rovelli, G., and Martoglio, B. (2004). Consensus analysis of signal peptide peptidase and homologous human aspartic proteases reveals opposite topology of catalytic domains compared with presenilins. J Biol Chem *279*, 50790-50798.

Furthmayr, H., Galardy, R.E., Tomita, M., and Marchesi, V.T. (1978). The intramembranous segment of human erythrocyte glycophorin A. Arch Biochem Biophys *185*, 21-29.

Gahmberg, C.G., Myllyla, G., Leikola, J., Pirkola, A., and Nordling, S. (1976). Absence of the major sialoglycoprotein in the membrane of human En(a--) erythrocytes and increased glycosylation of band 3. J Biol Chem *251*, 6108-6116.

Gao, X., Gunalan, K., Yap, S.S., and Preiser, P.R. (2013). Triggers of key calcium signals during erythrocyte invasion by Plasmodium falciparum. Nat Commun *4*, 2862.

Gao, X., Yeo, K.P., Aw, S.S., Kuss, C., Iyer, J.K., Genesan, S., Rajamanonmani, R., Lescar, J., Bozdech, Z., and Preiser, P.R. (2008). Antibodies targeting the PfRH1 binding domain inhibit invasion of Plasmodium falciparum merozoites. PLoS pathogens *4*, e1000104.

Gaur, D., and Chitnis, C.E. (2011). Molecular interactions and signaling mechanisms during erythrocyte invasion by malaria parasites. Curr Opin Microbiol *14*, 422-428.

Gaur, D., Furuya, T., Mu, J., Jiang, L.B., Su, X.Z., and Miller, L.H. (2006). Upregulation of expression of the reticulocyte homology gene 4 in the Plasmodium falciparum clone Dd2 is associated with a switch in the erythrocyte invasion pathway. Mol Biochem Parasitol *145*, 205-215.

Gaur, D., Singh, S., Singh, S., Jiang, L., Diouf, A., and Miller, L.H. (2007). Recombinant Plasmodium falciparum reticulocyte homology protein 4 binds to erythrocytes and blocks invasion. Proc Natl Acad Sci U S A *104*, 17789-17794.

Gilberger, T.W., Thompson, J.K., Triglia, T., Good, R.T., Duraisingh, M.T., and Cowman, A.F. (2003). A novel erythrocyte binding antigen-175 paralogue from Plasmodium falciparum defines a new trypsin-resistant receptor on human erythrocytes. J Biol Chem *278*, 14480-14486.

Gilson, P.R., and Crabb, B.S. (2009). Morphology and kinetics of the three distinct phases of red blood cell invasion by Plasmodium falciparum merozoites. International journal for parasitology *39*, 91-96.

Gilson, P.R., Nebl, T., Vukcevic, D., Moritz, R.L., Sargeant, T., Speed, T.P., Schofield, L., and Crabb, B.S. (2006). Identification and stoichiometry of glycosylphosphatidylinositol-anchored membrane proteins of the human malaria parasite Plasmodium falciparum. Mol Cell Proteomics *5*, 1286-1299.

Glushakova, S., Yin, D., Li, T., and Zimmerberg, J. (2005). Membrane transformation during malaria parasite release from human red blood cells. Curr Biol *15*, 1645-1650.

Goel, V.K., Li, X., Chen, H., Liu, S.C., Chishti, A.H., and Oh, S.S. (2003). Band 3 is a host receptor binding merozoite surface protein 1 during the Plasmodium falciparum invasion of erythrocytes. Proc Natl Acad Sci U S A *100*, 5164-5169.

Golde, T.E., Wolfe, M.S., and Greenbaum, D.C. (2009). Signal peptide peptidases: a family of intramembrane-cleaving proteases that cleave type 2 transmembrane proteins. Semin Cell Dev Biol *20*, 225-230.

Gov, N.S., and Safran, S.A. (2005). Red blood cell membrane fluctuations and shape controlled by ATP-induced cytoskeletal defects. Biophys J *88*, 1859-1874.

Grey, J.L., Kodippili, G.C., Simon, K., and Low, P.S. (2012). Identification of contact sites between ankyrin and band 3 in the human erythrocyte membrane. Biochemistry *51*, 6838-6846.

Grigorenko, A.P., Moliaka, Y.K., Soto, M.C., Mello, C.C., and Rogaev, E.I. (2004). The Caenorhabditis elegans IMPAS gene, imp-2, is essential for development and is functionally distinct from related presenilins. Proc Natl Acad Sci U S A *101*, 14955-14960.

Groves, J.D., and Tanner, M.J. (1994). The effects of glycophorin A on the expression of the human red cell anion transporter (band 3) in Xenopus oocytes. The Journal of membrane biology *140*, 81-88.

Gruring, C., Heiber, A., Kruse, F., Ungefehr, J., Gilberger, T.W., and Spielmann, T. (2011). Development and host cell modifications of Plasmodium falciparum blood stages in four dimensions. Nat Commun *2*, 165.

Gupta, A., Thiruvengadam, G., and Desai, S.A. (2015). The conserved clag multigene family of malaria parasites: essential roles in host-pathogen interaction. Drug resistance updates : reviews and commentaries in antimicrobial and anticancer chemotherapy *18*, 47-54.

Hadley, T., Saul, A., Lamont, G., Hudson, D.E., Miller, L.H., and Kidson, C. (1983). Resistance of Melanesian elliptocytes (ovalocytes) to invasion by Plasmodium knowlesi and Plasmodium falciparum malaria parasites in vitro. J Clin Invest *71*, 780-782.

Hadley, T.J., Klotz, F.W., Pasvol, G., Haynes, J.D., McGinniss, M.H., Okubo, Y., and Miller, L.H. (1987). Falciparum malaria parasites invade erythrocytes that lack glycophorin A and B (MkMk). Strain differences indicate receptor heterogeneity and two pathways for invasion. J Clin Invest *80*, 1190-1193.

Hamamoto, H., Akimitsu, N., Arimitsu, N., and Sekimizu, K. (2008). Roles of the Duffy antigen and glycophorin A in malaria infectionand erythrocyte. Drug discoveries & therapeutics *2*, 58-63.

Hamasaki, N. (1999). The role of band 3 protein in oxygen delivery by red blood cells. Indian journal of clinical biochemistry : IJCB *14*, 49-58.

Harbut, M.B., Patel, B.A., Yeung, B.K., McNamara, C.W., Bright, A.T., Ballard, J., Supek, F., Golde, T.E., Winzeler, E.A., Diagana, T.T.*, et al.* (2012). Targeting the ERAD pathway via inhibition of signal peptide peptidase for antiparasitic therapeutic design. Proc Natl Acad Sci U S A *109*, 21486-21491.

Harris, P.K., Yeoh, S., Dluzewski, A.R., O'Donnell, R.A., Withers-Martinez, C., Hackett, F., Bannister, L.H., Mitchell, G.H., and Blackman, M.J. (2005). Molecular identification of a malaria merozoite surface sheddase. PLoS pathogens *1*, 241-251.

Harrison, M.L., Isaacson, C.C., Burg, D.L., Geahlen, R.L., and Low, P.S. (1994). Phosphorylation of human erythrocyte band 3 by endogenous p72syk. J Biol Chem *269*, 955-959.

Harrison, M.L., Rathinavelu, P., Arese, P., Geahlen, R.L., and Low, P.S. (1991). Role of band 3 tyrosine phosphorylation in the regulation of erythrocyte glycolysis. J Biol Chem *266*, 4106-4111.

Hassoun, H., Hanada, T., Lutchman, M., Sahr, K.E., Palek, J., Hanspal, M., and Chishti, A.H. (1998). Complete deficiency of glycophorin A in red blood cells from mice with targeted inactivation of the band 3 (AE1) gene. Blood *91*, 2146-2151.

Hayton, K., Gaur, D., Liu, A., Takahashi, J., Henschen, B., Singh, S., Lambert, L., Furuya, T., Bouttenot, R., Doll, M.*, et al.* (2008). Erythrocyte binding protein PfRH5 polymorphisms determine species-specific pathways of Plasmodium falciparum invasion. Cell host & microbe *4*, 40-51.

Hempelmann, E. (2007). Hemozoin biocrystallization in Plasmodium falciparum and the antimalarial activity of crystallization inhibitors. Parasitol Res *100*, 671-676.

Hirai, T., Hamasaki, N., Yamaguchi, T., and Ikeda, Y. (2011). Topology models of anion exchanger 1 that incorporate the anti-parallel V-shaped motifs found in the EM structure. Biochemistry and cell biology = Biochimie et biologie cellulaire *89*, 148-156.

Holder, A.A. (1988). The precursor to major merozoite surface antigens: structure and role in immunity. Progress in allergy *41*, 72-97.

Holder, A.A. (2009). The carboxy-terminus of merozoite surface protein 1: structure, specific antibodies and immunity to malaria. Parasitology *136*, 1445-1456.

Holder, A.A., Blackman, M.J., Burghaus, P.A., Chappel, J.A., Ling, I.T., McCallum-Deighton, N., and Shai, S. (1992). A malaria merozoite surface protein (MSP1)-structure, processing and function. Memorias do Instituto Oswaldo Cruz *87 Suppl 3*, 37-42.

Holder, A.A., and Freeman, R.R. (1982). Biosynthesis and processing of a Plasmodium falciparum schizont antigen recognized by immune serum and a monoclonal antibody. J Exp Med *156*, 1528-1538.

Holder, A.A., Lockyer, M.J., Odink, K.G., Sandhu, J.S., Riveros-Moreno, V., Nicholls, S.C., Hillman, Y., Davey, L.S., Tizard, M.L., Schwarz, R.T.*, et al.* (1985). Primary structure of the precursor to the three major surface antigens of Plasmodium falciparum merozoites. Nature *317*, 270-273.

Howell, S.A., Well, I., Fleck, S.L., Kettleborough, C., Collins, C.R., and Blackman, M.J. (2003). A single malaria merozoite serine protease mediates shedding of multiple surface proteins by juxtamembrane cleavage. J Biol Chem *278*, 23890-23898.

Huaman, M.C., Martin, L.B., Malkin, E., Narum, D.L., Miller, L.H., Mahanty, S., and Long, C.A. (2008). Ex vivo cytokine and memory T cell responses to the 42-kDa fragment of Plasmodium falciparum merozoite surface protein-1 in vaccinated volunteers. J Immunol *180*, 1451-1461.

Janse, C.J., and Waters, A.P. (2007). The exoneme helps malaria parasites to break out of blood cells. Cell *131*, 1036-1038.

Jarolim, P., Palek, J., Amato, D., Hassan, K., Sapak, P., Nurse, G.T., Rubin, H.L., Zhai, S., Sahr, K.E., and Liu, S.C. (1991). Deletion in erythrocyte band 3 gene in malaria-resistant Southeast Asian ovalocytosis. Proc Natl Acad Sci U S A *88*, 11022-11026.

Jiang, L., Gaur, D., Mu, J., Zhou, H., Long, C.A., and Miller, L.H. (2011). Evidence for erythrocyte-binding antigen 175 as a component of a ligand-blocking blood-stage malaria vaccine. Proc Natl Acad Sci U S A *108*, 7553-7558.

Kadekoppala, M., and Holder, A.A. (2010). Merozoite surface proteins of the malaria parasite: the MSP1 complex and the MSP7 family. International journal for parasitology *40*, 1155-1161.

Kafsack, B.F., Rovira-Graells, N., Clark, T.G., Bancells, C., Crowley, V.M., Campino, S.G., Williams, A.E., Drought, L.G., Kwiatkowski, D.P., Baker, D.A*., et al.* (2014). A transcriptional switch underlies commitment to sexual development in malaria parasites. Nature *507*, 248-252.

Kaneko, O., Fidock, D.A., Schwartz, O.M., and Miller, L.H. (2000). Disruption of the C-terminal region of EBA-175 in the Dd2/Nm clone of Plasmodium falciparum does not affect erythrocyte invasion. Mol Biochem Parasitol *110*, 135-146.

Kanki, T., Sakaguchi, M., Kitamura, A., Sato, T., Mihara, K., and Hamasaki, N. (2002). The tenth membrane region of band 3 is initially exposed to the luminal side of the endoplasmic reticulum and then integrated into a partially folded band 3 intermediate. Biochemistry *41*, 13973-13981.

Kariuki, M.M., Li, X., Yamodo, I., Chishti, A.H., and Oh, S.S. (2005). Two Plasmodium falciparum merozoite proteins binding to erythrocyte band 3 form a direct complex. Biochem Biophys Res Commun *338*, 1690-1695.

Kats, L.M., Black, C.G., Proellocks, N.I., and Coppel, R.L. (2006). Plasmodium rhoptries: how things went pear-shaped. Trends in parasitology *22*, 269-276.

Kauth, C.W., Epp, C., Bujard, H., and Lutz, R. (2003). The merozoite surface protein 1 complex of human malaria parasite Plasmodium falciparum: interactions and arrangements of subunits. J Biol Chem *278*, 22257-22264.

Kauth, C.W., Woehlbier, U., Kern, M., Mekonnen, Z., Lutz, R., Mucke, N., Langowski, J., and Bujard, H. (2006). Interactions between merozoite surface proteins 1, 6, and 7 of the malaria parasite Plasmodium falciparum. J Biol Chem *281*, 31517-31527.

Keitel, W.A., Kester, K.E., Atmar, R.L., White, A.C., Bond, N.H., Holland, C.A., Krzych, U., Palmer, D.R., Egan, A., Diggs, C*., et al.* (1999). Phase I trial of two recombinant vaccines containing the 19kd carboxy terminal fragment of Plasmodium falciparum merozoite surface protein 1 (msp-1(19)) and T helper epitopes of tetanus toxoid. Vaccine *18*, 531-539.

Khan, A.A., Hanada, T., Mohseni, M., Jeong, J.J., Zeng, L., Gaetani, M., Li, D., Reed, B.C., Speicher, D.W., and Chishti, A.H. (2008). Dematin and adducin provide a novel link between the spectrin cytoskeleton and human erythrocyte membrane by directly interacting with glucose transporter-1. J Biol Chem *283*, 14600-14609.

Khater, E.I., Sinden, R.E., and Dessens, J.T. (2004). A malaria membrane skeletal protein is essential for normal morphogenesis, motility, and infectivity of sporozoites. J Cell Biol *167*, 425-432.

Kirkin, V., Cahuzac, N., Guardiola-Serrano, F., Huault, S., Luckerath, K., Friedmann, E., Novac, N., Wels, W.S., Martoglio, B., Hueber, A.O*., et al.* (2007). The Fas ligand intracellular domain is released by ADAM10 and SPPL2a cleavage in T-cells. Cell death and differentiation *14*, 1678-1687.

Klemba, M., Beatty, W., Gluzman, I., and Goldberg, D.E. (2004). Trafficking of plasmepsin II to the food vacuole of the malaria parasite Plasmodium falciparum. J Cell Biol *164*, 47-56.

Kliman, H.J., and Steck, T.L. (1980). Association of glyceraldehyde-3-phosphate dehydrogenase with the human red cell membrane. A kinetic analysis. J Biol Chem *255*, 6314-6321.

Klotz, F.W., Chulay, J.D., Daniel, W., and Miller, L.H. (1987). Invasion of mouse erythrocytes by the human malaria parasite, Plasmodium falciparum. J Exp Med *165*, 1713-1718.

Koussis, K., Withers-Martinez, C., Yeoh, S., Child, M., Hackett, F., Knuepfer, E., Juliano, L., Woehlbier, U., Bujard, H., and Blackman, M.J. (2009). A multifunctional serine protease primes the malaria parasite for red blood cell invasion. EMBO J *28*, 725-735.

Krawitz, P., Haffner, C., Fluhrer, R., Steiner, H., Schmid, B., and Haass, C. (2005). Differential localization and identification of a critical aspartate suggest non-redundant proteolytic functions of the presenilin homologues SPPL2b and SPPL3. J Biol Chem *280*, 39515-39523.

Krettli, A.U., and Dantas, L.A. (2000). Which routes do Plasmodium sporozoites use for successful infections of vertebrates? Infect Immun *68*, 3064-3065.

Kudo, S., and Fukuda, M. (1989). Structural organization of glycophorin A and B genes: glycophorin B gene evolved by homologous recombination at Alu repeat sequences. Proc Natl Acad Sci U S A *86*, 4619-4623.

Kuhn, P.H., Voss, M., Haug-Kroper, M., Schroder, B., Schepers, U., Brase, S., Haass, C., Lichtenthaler, S.F., and Fluhrer, R. (2015). Secretome analysis identifies novel signal peptide peptidase-like 3 (SPPL3) substrates and reveals a role of SPPL3 in multiple Golgi glycosylation pathways. Mol Cell Proteomics.

Kushwaha, A., Perween, A., Mukund, S., Majumdar, S., Bhardwaj, D., Chowdhury, N.R., and Chauhan, V.S. (2002). Amino terminus of Plasmodium falciparum acidic basic repeat antigen interacts with the erythrocyte membrane through band 3 protein. Mol Biochem Parasitol *122*, 45-54.

LaCount, D.J., Vignali, M., Chettier, R., Phansalkar, A., Bell, R., Hesselberth, J.R., Schoenfeld, L.W., Ota, I., Sahasrabudhe, S., Kurschner, C*., et al.* (2005). A protein interaction network of the malaria parasite Plasmodium falciparum. Nature *438*, 103-107.

Lamarque, M., Besteiro, S., Papoin, J., Roques, M., Vulliez-Le Normand, B., Morlon-Guyot, J., Dubremetz, J.F., Fauquenoy, S., Tomavo, S., Faber, B.W*., et al.* (2011). The RON2-AMA1 interaction is a critical step in moving junction-dependent invasion by apicomplexan parasites. PLoS pathogens *7*, e1001276.

Lanzillotti, R., and Coetzer, T.L. (2006). The 10 kDa domain of human erythrocyte protein 4.1 binds the Plasmodium falciparum EBA-181 protein. Malar J *5*, 100.

Lauterbach, S.B., Lanzillotti, R., and Coetzer, T.L. (2003). Construction and use of Plasmodium falciparum phage display libraries to identify host parasite interactions. Malar J *2*, 47.

Lazarov, V.K., Fraering, P.C., Ye, W., Wolfe, M.S., Selkoe, D.J., and Li, H. (2006). Electron microscopic structure of purified, active gamma-secretase reveals an aqueous intramembrane chamber and two pores. Proc Natl Acad Sci U S A *103*, 6889-6894.

Lee, M.C., Moura, P.A., Miller, E.A., and Fidock, D.A. (2008). Plasmodium falciparum Sec24 marks transitional ER that exports a model cargo via a diacidic motif. Mol Microbiol *68*, 1535-1546.

Lee, S.O., Cho, K., Cho, S., Kim, I., Oh, C., and Ahn, K. (2010). Protein disulphide isomerase is required for signal peptide peptidase-mediated protein degradation. EMBO J *29*, 363-375.

Lemberg, M.K., Bland, F.A., Weihofen, A., Braud, V.M., and Martoglio, B. (2001). Intramembrane proteolysis of signal peptides: an essential step in the generation of HLA-E epitopes. J Immunol *167*, 6441-6446.

Lemberg, M.K., and Martoglio, B. (2002). Requirements for signal peptide peptidase-catalyzed intramembrane proteolysis. Mol Cell *10*, 735-744.

Lemmon, M.A., Flanagan, J.M., Hunt, J.F., Adair, B.D., Bormann, B.J., Dempsey, C.E., and Engelman, D.M. (1992). Glycophorin A dimerization is driven by specific interactions between transmembrane alpha-helices. J Biol Chem *267*, 7683-7689.

Li, X., Chen, H., Bahamontes-Rosa, N., Kun, J.F., Traore, B., Crompton, P.D., and Chishti, A.H. (2009). Plasmodium falciparum signal peptide peptidase is a promising drug target against blood stage malaria. Biochem Biophys Res Commun *380*, 454-459.

Li, X., Chen, H., Jeong, J.J., and Chishti, A.H. (2007). BDA-410: a novel synthetic calpain inhibitor active against blood stage malaria. Mol Biochem Parasitol *155*, 26-32.

Li, X., Chen, H., Khan, A.A., Lauterbach, S.B., Lanzillotti, R., Rai, P.R., Kane, R.S., Coetzer, T.L., and Chishti, A.H. (2008a). Receptor-based identification of an inhibitory peptide against blood stage malaria. Biochem Biophys Res Commun *376*, 489-493.

Li, X., Chen, H., Oh, S.S., and Chishti, A.H. (2008b). A Presenilin-like protease associated with Plasmodium falciparum micronemes is involved in erythrocyte invasion. Mol Biochem Parasitol *158*, 22-31.

Li, X., Chen, H., Oo, T.H., Daly, T.M., Bergman, L.W., Liu, S.C., Chishti, A.H., and Oh, S.S. (2004). A co-ligand complex anchors Plasmodium falciparum merozoites to the erythrocyte invasion receptor band 3. J Biol Chem *279*, 5765-5771.

Li, X., Marinkovic, M., Russo, C., McKnight, C.J., Coetzer, T.L., and Chishti, A.H. (2012). Identification of a specific region of Plasmodium falciparum EBL-1 that binds to host receptor glycophorin B and inhibits merozoite invasion in human red blood cells. Mol Biochem Parasitol *183*, 23-31.

Lin, C.S., Uboldi, A.D., Marapana, D., Czabotar, P.E., Epp, C., Bujard, H., Taylor, N.L., Perugini, M.A., Hodder, A.N., and Cowman, A.F. (2014). The merozoite surface protein 1 complex is a platform for binding to human erythrocytes by Plasmodium falciparum. J Biol Chem *289*, 25655-25669.

Lingnau, A., Margos, G., Maier, W.A., and Seitz, H.M. (1993). The effects of hormones on the gametocytogenesis of Plasmodium falciparum in vitro. Applied parasitology *34*, 153-160.

Liu, S.C., Palek, J., Yi, S.J., Nichols, P.E., Derick, L.H., Chiou, S.S., Amato, D., Corbett, J.D., Cho, M.R., and Golan, D.E. (1995). Molecular basis of altered red blood cell membrane properties in Southeast Asian ovalocytosis: role of the mutant band 3 protein in band 3 oligomerization and retention by the membrane skeleton. Blood *86*, 349-358.

Lobo, C.A., de Frazao, K., Rodriguez, M., Reid, M., Zalis, M., and Lustigman, S. (2004). Invasion profiles of Brazilian field isolates of Plasmodium falciparum: phenotypic and genotypic analyses. Infect Immun *72*, 5886-5891.

Lobo, C.A., Rodriguez, M., Reid, M., and Lustigman, S. (2003). Glycophorin C is the receptor for the Plasmodium falciparum erythrocyte binding ligand PfEBP-2 (baebl). Blood *101*, 4628-4631.

Lopaticki, S., Maier, A.G., Thompson, J., Wilson, D.W., Tham, W.H., Triglia, T., Gout, A., Speed, T.P., Beeson, J.G., Healer, J.*, et al.* (2011). Reticulocyte and erythrocyte binding-like proteins function cooperatively in invasion of human erythrocytes by malaria parasites. Infect Immun *79*, 1107-1117.

Lopez, M.C., Silva, Y., Thomas, M.C., Garcia, A., Faus, M.J., Alonso, P., Martinez, F., Del Real, G., and Alonso, C. (1994). Characterization of SPf(66)n: a chimeric molecule used as a malaria vaccine. Vaccine *12*, 585-591.

Loureiro, J., Lilley, B.N., Spooner, E., Noriega, V., Tortorella, D., and Ploegh, H.L. (2006). Signal peptide peptidase is required for dislocation from the endoplasmic reticulum. Nature *441*, 894-897.

Low, P.S., Allen, D.P., Zioncheck, T.F., Chari, P., Willardson, B.M., Geahlen, R.L., and Harrison, M.L. (1987). Tyrosine phosphorylation of band 3 inhibits peripheral protein binding. J Biol Chem *262*, 4592-4596.

Low, P.S., Rathinavelu, P., and Harrison, M.L. (1993). Regulation of glycolysis via reversible enzyme binding to the membrane protein, band 3. J Biol Chem *268*, 14627-14631.

Lu, S.H., Jeon, A.H., Schmitt-Ulms, G., Qamar, S., Dodd, R., McDonald, B., Li, Y., Meadows, W., Cox, K., Bohm, C.*, et al.* (2012). Vigilin interacts with Signal Peptide Peptidase. Proteome Sci *10*, 33.

Lyon, M., Deakin, J.A., and Gallagher, J.T. (1994). Liver heparan sulfate structure. A novel molecular design. J Biol Chem *269*, 11208-11215.

Maier, A.G., Baum, J., Smith, B., Conway, D.J., and Cowman, A.F. (2009a). Polymorphisms in erythrocyte binding antigens 140 and 181 affect function and binding but not receptor specificity in Plasmodium falciparum. Infect Immun *77*, 1689-1699.

Maier, A.G., Cooke, B.M., Cowman, A.F., and Tilley, L. (2009b). Malaria parasite proteins that remodel the host erythrocyte. Nat Rev Microbiol *7*, 341-354.

Malkin, E., Long, C.A., Stowers, A.W., Zou, L., Singh, S., MacDonald, N.J., Narum, D.L., Miles, A.P., Orcutt, A.C., Muratova, O.*, et al.* (2007). Phase 1 study of two merozoite surface protein 1 (MSP1(42)) vaccines for Plasmodium falciparum malaria. PLoS Clin Trials *2*, e12.

Malpede, B.M., Lin, D.H., and Tolia, N.H. (2013). Molecular basis for sialic acid-dependent receptor recognition by the Plasmodium falciparum invasion protein erythrocyte-binding antigen-140/BAEBL. J Biol Chem *288*, 12406-12415.

Marapana, D.S., Wilson, D.W., Zuccala, E.S., Dekiwadia, C.D., Beeson, J.G., Ralph, S.A., and Baum, J. (2012). Malaria parasite signal peptide peptidase is an ER-resident protease required for growth but not for invasion. Traffic *13*, 1457-1465.

Marchesi, V.T., and Andrews, E.P. (1971). Glycoproteins: isolation from cellmembranes with lithium diiodosalicylate. Science *174*, 1247-1248.

Martin, L., Fluhrer, R., and Haass, C. (2009). Substrate requirements for SPPL2b-dependent regulated intramembrane proteolysis. J Biol Chem *284*, 5662-5670.

Martin, L., Fluhrer, R., Reiss, K., Kremmer, E., Saftig, P., and Haass, C. (2008). Regulated intramembrane proteolysis of Bri2 (Itm2b) by ADAM10 and SPPL2a/SPPL2b. J Biol Chem *283*, 1644-1652.

Martoglio, B., and Golde, T.E. (2003). Intramembrane-cleaving aspartic proteases and disease: presenilins, signal peptide peptidase and their homologs. Hum Mol Genet *12 Spec No 2*, R201-206.

Martoglio, B., Graf, R., and Dobberstein, B. (1997). Signal peptide fragments of preprolactin and HIV-1 p-gp160 interact with calmodulin. EMBO J *16*, 6636-6645.

Masinde, G.L., Krogstad, D.J., Gordon, D.M., and Duffy, P.E. (1998). Immunization with SPf66 and subsequent infection with homologous and heterologous Plasmodium falciparum parasites. Am J Trop Med Hyg *59*, 600-605.

Maswoswe, S.M., Peters, W., and Warhurst, D.C. (1985). Corticosteroid stimulation of the growth of Plasmodium falciparum gametocytes in vitro. Ann Trop Med Parasitol *79*, 607-616.

Matsumi, R., Atomi, H., and Imanaka, T. (2006). Identification of the amino acid residues essential for proteolytic activity in an archaeal signal peptide peptidase. J Biol Chem *281*, 10533-10539.

Mayer, D.C., Cofie, J., Jiang, L., Hartl, D.L., Tracy, E., Kabat, J., Mendoza, L.H., and Miller, L.H. (2009). Glycophorin B is the erythrocyte receptor of Plasmodium falciparum erythrocyte-binding ligand, EBL-1. Proc Natl Acad Sci U S A *106*, 5348-5352.

Mayer, D.C., Mu, J.B., Kaneko, O., Duan, J., Su, X.Z., and Miller, L.H. (2004). Polymorphism in the Plasmodium falciparum erythrocyte-binding ligand JESEBL/EBA-181 alters its receptor specificity. Proc Natl Acad Sci U S A *101*, 2518-2523.

McLauchlan, J., Lemberg, M.K., Hope, G., and Martoglio, B. (2002). Intramembrane proteolysis promotes trafficking of hepatitis C virus core protein to lipid droplets. EMBO J *21*, 3980-3988.

Mehdi, M.M., Singh, P., and Rizvi, S.I. (2012). Erythrocyte sialic acid content during aging in humans: correlation with markers of oxidative stress. Disease markers *32*, 179-186.

Miller, L.H., Ackerman, H.C., Su, X.Z., and Wellems, T.E. (2013). Malaria biology and disease pathogenesis: insights for new treatments. Nat Med *19*, 156-167.

Miller, L.H., Haynes, J.D., McAuliffe, F.M., Shiroishi, T., Durocher, J.R., and McGinniss, M.H. (1977). Evidence for differences in erythrocyte surface receptors for the malarial parasites, Plasmodium falciparum and Plasmodium knowlesi. J Exp Med *146*, 277-281.

Mitchell, G.H., Hadley, T.J., McGinniss, M.H., Klotz, F.W., and Miller, L.H. (1986). Invasion of erythrocytes by Plasmodium falciparum malaria parasites: evidence for receptor heterogeneity and two receptors. Blood *67*, 1519-1521.

Mitchell, G.H., Thomas, A.W., Margos, G., Dluzewski, A.R., and Bannister, L.H. (2004). Apical membrane antigen 1, a major malaria vaccine candidate, mediates the close attachment of invasive merozoites to host red blood cells. Infect Immun *72*, 154-158.

Miyashita, H., Maruyama, Y., Isshiki, H., Osawa, S., Ogura, T., Mio, K., Sato, C., Tomita, T., and Iwatsubo, T. (2011). Three-dimensional structure of the signal peptide peptidase. J Biol Chem *286*, 26188-26197.

Mohandas, N., and An, X. (2012). Malaria and human red blood cells. Medical microbiology and immunology *201*, 593-598.

Morgan, W.D., Birdsall, B., Frenkiel, T.A., Gradwell, M.G., Burghaus, P.A., Syed, S.E., Uthaipibull, C., Holder, A.A., and Feeney, J. (1999). Solution structure of an EGF module pair from the Plasmodium falciparum merozoite surface protein 1. J Mol Biol *289*, 113-122.

Mota, M.M., and Rodriguez, A. (2002). Invasion of mammalian host cells by Plasmodium sporozoites. Bioessays *24*, 149-156.

Mundwiler-Pachlatko, E., and Beck, H.P. (2013). Maurer's clefts, the enigma of Plasmodium falciparum. Proc Natl Acad Sci U S A *110*, 19987-19994.

Narayanan, S., Sato, T., and Wolfe, M.S. (2007). A C-terminal region of signal peptide peptidase defines a functional domain for intramembrane aspartic protease catalysis. J Biol Chem *282*, 20172-20179.

Narum, D.L., Haynes, J.D., Fuhrmann, S., Moch, K., Liang, H., Hoffman, S.L., and Sim, B.K. (2000). Antibodies against the Plasmodium falciparum receptor binding domain of EBA-175 block invasion pathways that do not involve sialic acids. Infect Immun *68*, 1964-1966.

Nigg, E., and Cherry, R.J. (1979). Dimeric association of band 3 in the erythrocyte membrane demonstrated by protein diffusion measurements. Nature *277*, 493-494.

Nigg, E.A., Bron, C., Girardet, M., and Cherry, R.J. (1980). Band 3-glycophorin A association in erythrocyte membrane demonstrated by combining protein diffusion measurements with antibody-induced cross-linking. Biochemistry *19*, 1887-1893.

Nikodem, D., and Davidson, E. (2000). Identification of a novel antigenic domain of Plasmodium falciparum merozoite surface protein-1 that specifically binds to human erythrocytes and inhibits parasite invasion, in vitro. Mol Biochem Parasitol *108*, 79-91.

Nunes, J.K., Cardenas, V., Loucq, C., Maire, N., Smith, T., Shaffer, C., Maseide, K., and Brooks, A. (2013). Modeling the public health impact of malaria vaccines for developers and policymakers. BMC infectious diseases *13*, 295.

Nwuba, R.I., Sodeinde, O., Anumudu, C.I., Omosun, Y.O., Odaibo, A.B., Holder, A.A., and Nwagwu, M. (2002). The human immune response to Plasmodium falciparum includes both antibodies that inhibit merozoite surface protein 1 secondary processing and blocking antibodies. Infect Immun *70*, 5328-5331.

Nyborg, A.C., Herl, L., Berezovska, O., Thomas, A.V., Ladd, T.B., Jansen, K., Hyman, B.T., and Golde, T.E. (2006a). Signal peptide peptidase (SPP) dimer formation as assessed by fluorescence lifetime imaging microscopy (FLIM) in intact cells. Mol Neurodegener *1*, 16.

Nyborg, A.C., Jansen, K., Ladd, T.B., Fauq, A., and Golde, T.E. (2004a). A signal peptide peptidase (SPP) reporter activity assay based on the cleavage of type II membrane protein substrates provides further evidence for an inverted orientation of the SPP active site relative to presenilin. J Biol Chem *279*, 43148-43156.

Nyborg, A.C., Kornilova, A.Y., Jansen, K., Ladd, T.B., Wolfe, M.S., and Golde, T.E. (2004b). Signal peptide peptidase forms a homodimer that is labeled by an active site-directed gamma-secretase inhibitor. J Biol Chem *279*, 15153-15160.

Nyborg, A.C., Ladd, T.B., Jansen, K., Kukar, T., and Golde, T.E. (2006b). Intramembrane proteolytic cleavage by human signal peptide peptidase like 3 and malaria signal peptide peptidase. FASEB J *20*, 1671-1679.

O'Donnell, R.A., Saul, A., Cowman, A.F., and Crabb, B.S. (2000). Functional conservation of the malaria vaccine antigen MSP-119across distantly related Plasmodium species. Nat Med *6*, 91-95.

Ockenhouse, C.F., Barbosa, A., Blackall, D.P., Murphy, C.I., Kashala, O., Dutta, S., Lanar, D.E., and Daugherty, J.R. (2001). Sialic acid-dependent binding of baculovirus-expressed recombinant antigens from Plasmodium falciparum EBA-175 to Glycophorin A. Mol Biochem Parasitol *113*, 9-21.

Oh, S.S., and Chishti, A.H. (2005). Host receptors in malaria merozoite invasion. Curr Top Microbiol Immunol *295*, 203-232.

Okamoto, K., Mori, Y., Komoda, Y., Okamoto, T., Okochi, M., Takeda, M., Suzuki, T., Moriishi, K., and Matsuura, Y. (2008). Intramembrane processing by signal peptide peptidase regulates the membrane localization of hepatitis C virus core protein and viral propagation. J Virol *82*, 8349-8361.

Okoye, V.C., and Bennett, V. (1985). Plasmodium falciparum malaria: band 3 as a possible receptor during invasion of human erythrocytes. Science *227*, 169-171.

Orlandi, P.A., Klotz, F.W., and Haynes, J.D. (1992). A malaria invasion receptor, the 175-kilodalton erythrocyte binding antigen of Plasmodium falciparum recognizes the terminal Neu5Ac(alpha 2-3)Gal- sequences of glycophorin A. J Cell Biol *116*, 901-909.

Pachebat, J.A., Kadekoppala, M., Grainger, M., Dluzewski, A.R., Gunaratne, R.S., Scott-Finnigan, T.J., Ogun, S.A., Ling, I.T., Bannister, L.H., Taylor, H.M.*, et al.* (2007). Extensive proteolytic processing of the malaria parasite merozoite surface protein 7 during biosynthesis and parasite release from erythrocytes. Mol Biochem Parasitol *151*, 59-69.

Pachebat, J.A., Ling, I.T., Grainger, M., Trucco, C., Howell, S., Fernandez-Reyes, D., Gunaratne, R., and Holder, A.A. (2001). The 22 kDa component of the protein complex on the surface of Plasmodium falciparum merozoites is derived from a larger precursor, merozoite surface protein 7. Mol Biochem Parasitol *117*, 83-89.

Pantaleo, A., Ferru, E., Giribaldi, G., Mannu, F., Carta, F., Matte, A., de Franceschi, L., and Turrini, F. (2009). Oxidized and poorly glycosylated band 3 is selectively phosphorylated by Syk kinase to form large membrane clusters in normal and G6PD-deficient red blood cells. Biochem J *418*, 359-367.

Parvanova, I., Epiphanio, S., Fauq, A., Golde, T.E., Prudencio, M., and Mota, M.M. (2009). A small molecule inhibitor of signal peptide peptidase inhibits Plasmodium development in the liver and decreases malaria severity. PLoS One *4*, e5078.

Passow, H. (1986). Molecular aspects of band 3 protein-mediated anion transport across the red blood cell membrane. Reviews of physiology, biochemistry and pharmacology *103*, 61-203.

Pasvol, G., Chasis, J.A., Mohandas, N., Anstee, D.J., Tanner, M.J., and Merry, A.H. (1989). Inhibition of malarial parasite invasion by monoclonal antibodies against glycophorin A correlates with reduction in red cell membrane deformability. Blood *74*, 1836-1843.

Pasvol, G., Wainscoat, J.S., and Weatherall, D.J. (1982). Erythrocytes deficiency in glycophorin resist invasion by the malarial parasite Plasmodium falciparum. Nature *297*, 64-66.

Pearce, J.A., Triglia, T., Hodder, A.N., Jackson, D.C., Cowman, A.F., and Anders, R.F. (2004). Plasmodium falciparum merozoite surface protein 6 is a dimorphic antigen. Infect Immun *72*, 2321-2328.

Perkins, M. (1981). Inhibitory effects of erythrocyte membrane proteins on the in vitro invasion of the human malarial parasite (Plasmodium falciparum) into its host cell. J Cell Biol *90*, 563-567.

Perkins, M.E., and Rocco, L.J. (1988). Sialic acid-dependent binding of Plasmodium falciparum merozoite surface antigen, Pf200, to human erythrocytes. J Immunol *141*, 3190-3196.

Perrin, L.H., Ramirez, E., Er-Hsiang, L., and Lambert, P.H. (1980). Plasmodium falciparum: characterization of defined antigens by monoclonal antibodies. Clinical and experimental immunology *41*, 91-96.

Perrotta, S., Borriello, A., Scaloni, A., De Franceschi, L., Brunati, A.M., Turrini, F., Nigro, V., del Giudice, E.M., Nobili, B., Conte, M.L.*, et al.* (2005). The N-terminal 11 amino acids of human erythrocyte band 3 are critical for aldolase binding and protein phosphorylation: implications for band 3 function. Blood *106*, 4359-4366.

Peters, L.L., Jindel, H.K., Gwynn, B., Korsgren, C., John, K.M., Lux, S.E., Mohandas, N., Cohen, C.M., Cho, M.R., Golan, D.E.*, et al.* (1999). Mild spherocytosis and altered red cell ion transport in protein 4. 2-null mice. J Clin Invest *103*, 1527-1537.

Peterson, D.S., and Wellems, T.E. (2000). EBL-1, a putative erythrocyte binding protein of Plasmodium falciparum, maps within a favored linkage group in two genetic crosses. Mol Biochem Parasitol *105*, 105-113.

Pimenta, P.F., Touray, M., and Miller, L. (1994). The journey of malaria sporozoites in the mosquito salivary gland. The Journal of eukaryotic microbiology *41*, 608-624.

Pinzon-Ortiz, C., Friedman, J., Esko, J., and Sinnis, P. (2001). The binding of the circumsporozoite protein to cell surface heparan sulfate proteoglycans is required for plasmodium sporozoite attachment to target cells. J Biol Chem *276*, 26784-26791.

Planson, A.G., Guijarro, J.I., and Chaffotte, A.F. (2013). New insights for native production of MSP1(19), the disulfide-rich C-terminal fragment from Plasmodium falciparum merozoite surface protein 1. PLoS One *8*, e57086.

Ponting, C.P., Hutton, M., Nyborg, A., Baker, M., Jansen, K., and Golde, T.E. (2002). Identification of a novel family of presenilin homologues. Hum Mol Genet *11*, 1037-1044.

Poole, J. (2000). Red cell antigens on band 3 and glycophorin A. Blood reviews *14*, 31-43.

Popov, M., Li, J., and Reithmeier, R.A. (1999). Transmembrane folding of the human erythrocyte anion exchanger (AE1, Band 3) determined by scanning and insertional N-glycosylation mutagenesis. Biochem J *339 (Pt 2)*, 269-279.

Pouvelle, B., Buffet, P.A., Lepolard, C., Scherf, A., and Gysin, J. (2000). Cytoadhesion of Plasmodium falciparum ring-stage-infected erythrocytes. Nat Med *6*, 1264-1268.

Pradel, G., and Frevert, U. (2001). Malaria sporozoites actively enter and pass through rat Kupffer cells prior to hepatocyte invasion. Hepatology *33*, 1154-1165.

Proellocks, N.I., Coppel, R.L., and Waller, K.L. (2010). Dissecting the apicomplexan rhoptry neck proteins. Trends in parasitology *26*, 297-304.

Prudencio, M., Rodriguez, A., and Mota, M.M. (2006). The silent path to thousands of merozoites: the Plasmodium liver stage. Nat Rev Microbiol *4*, 849-856.

Ranjan, R., Chugh, M., Kumar, S., Singh, S., Kanodia, S., Hossain, M.J., Korde, R., Grover, A., Dhawan, S., Chauhan, V.S.*, et al.* (2011). Proteome analysis reveals a large merozoite surface protein-1 associated complex on the Plasmodium falciparum merozoite surface. J Proteome Res *10*, 680-691.

Rath, A., Glibowicka, M., Nadeau, V.G., Chen, G., and Deber, C.M. (2009). Detergent binding explains anomalous SDS-PAGE migration of membrane proteins. Proc Natl Acad Sci U S A *106*, 1760-1765.

Reddy, K.S., Amlabu, E., Pandey, A.K., Mitra, P., Chauhan, V.S., and Gaur, D. (2015). Multiprotein complex between the GPI-anchored CyRPA with PfRH5 and PfRipr is crucial for Plasmodium falciparum erythrocyte invasion. Proc Natl Acad Sci U S A *112*, 1179-1184.

Reddy, K.S., Pandey, A.K., Singh, H., Sahar, T., Emmanuel, A., Chitnis, C.E., Chauhan, V.S., and Gaur, D. (2014). Bacterially expressed full-length recombinant Plasmodium falciparum RH5 protein binds erythrocytes and elicits potent strain-transcending parasite-neutralizing antibodies. Infect Immun *82*, 152-164.

Reid, M.E., Chasis, J.A., and Mohandas, N. (1987). Identification of a functional role for human erythrocyte sialoglycoproteins beta and gamma. Blood *69*, 1068-1072.

Reithmeier, R.A. (2001). A membrane metabolon linking carbonic anhydrase with chloride/bicarbonate anion exchangers. Blood cells, molecules & diseases *27*, 85-89.

Remaley, A.T., Ugorski, M., Wu, N., Litzky, L., Burger, S.R., Moore, J.S., Fukuda, M., and Spitalnik, S.L. (1991). Expression of human glycophorin A in wild type and glycosylation-deficient Chinese hamster ovary cells. Role of N- and O-linked glycosylation in cell surface expression. J Biol Chem *266*, 24176-24183.

Ribeiro, M.L., Alloisio, N., Almeida, H., Gomes, C., Texier, P., Lemos, C., Mimoso, G., Morle, L., Bey-Cabet, F., Rudigoz, R.C.*, et al.* (2000). Severe hereditary spherocytosis and distal renal tubular acidosis associated with the total absence of band 3. Blood *96*, 1602-1604.

Richard, D., MacRaild, C.A., Riglar, D.T., Chan, J.A., Foley, M., Baum, J., Ralph, S.A., Norton, R.S., and Cowman, A.F. (2010). Interaction between Plasmodium falciparum apical membrane antigen 1 and the rhoptry neck protein complex defines a key step in the erythrocyte invasion process of malaria parasites. J Biol Chem *285*, 14815-14822.

Riglar, D.T., Richard, D., Wilson, D.W., Boyle, M.J., Dekiwadia, C., Turnbull, L., Angrisano, F., Marapana, D.S., Rogers, K.L., Whitchurch, C.B.*, et al.* (2011). Super-resolution dissection of coordinated events during malaria parasite invasion of the human erythrocyte. Cell host & microbe *9*, 9-20.

Riley, E.M., Morris-Jones, S., Blackman, M.J., Greenwood, B.M., and Holder, A.A. (1993). A longitudinal study of naturally acquired cellular and humoral immune responses to a merozoite surface protein (MSP1) of Plasmodium falciparum in an area of seasonal malaria transmission. Parasite Immunol *15*, 513-524.

Rodriguez, M., Lustigman, S., Montero, E., Oksov, Y., and Lobo, C.A. (2008). PfRH5: a novel reticulocyte-binding family homolog of plasmodium falciparum that binds to the erythrocyte, and an investigation of its receptor. PLoS One *3*, e3300.

Rogalski, A.A., Steck, T.L., and Waseem, A. (1989). Association of glyceraldehyde-3-phosphate dehydrogenase with the plasma membrane of the intact human red blood cell. J Biol Chem *264*, 6438-6446.

Ruffing, W., Gartner, E.M., Lepke, S., Legrum, B., and Passow, H. (1996). Transport-related conformational states of the band 3 protein: probing with 1-fluoro-2,4-dinitrobenzene. Cell Mol Biol (Noisy-le-grand) *42*, 1097-1118.

Sakihama, N., Kaneko, A., Hattori, T., and Tanabe, K. (2001). Limited recombination events in merozoite surface protein-1 alleles of Plasmodium falciparum on islands. Gene *279*, 41-48.

Salmon, B.L., Oksman, A., and Goldberg, D.E. (2001). Malaria parasite exit from the host erythrocyte: a two-step process requiring extraerythrocytic proteolysis. Proc Natl Acad Sci U S A *98*, 271-276.

Sato, T., Nyborg, A.C., Iwata, N., Diehl, T.S., Saido, T.C., Golde, T.E., and Wolfe, M.S. (2006). Signal peptide peptidase: biochemical properties and modulation by nonsteroidal antiinflammatory drugs. Biochemistry *45*, 8649-8656.

Scheuner, D., Eckman, C., Jensen, M., Song, X., Citron, M., Suzuki, N., Bird, T.D., Hardy, J., Hutton, M., Kukull, W*., et al.* (1996). Secreted amyloid beta-protein similar to that in the senile plaques of Alzheimer's disease is increased in vivo by the presenilin 1 and 2 and APP mutations linked to familial Alzheimer's disease. Nat Med *2*, 864-870.

Schneppenheim, J., Huttl, S., Kruchen, A., Fluhrer, R., Muller, I., Saftig, P., Schneppenheim, R., Martin, C.L., and Schroder, B. (2014a). Signal-peptide-peptidase-like 2a is required for CD74 intramembrane proteolysis in human B cells. Biochem Biophys Res Commun.

Schneppenheim, J., Huttl, S., Mentrup, T., Lullmann-Rauch, R., Rothaug, M., Engelke, M., Dittmann, K., Dressel, R., Araki, M., Araki, K*., et al.* (2014b). The intramembrane proteases signal Peptide peptidase-like 2a and 2b have distinct functions in vivo. Mol Cell Biol *34*, 1398-1411.

Schrul, B., Kapp, K., Sinning, I., and Dobberstein, B. (2010). Signal peptide peptidase (SPP) assembles with substrates and misfolded membrane proteins into distinct oligomeric complexes. Biochem J *427*, 523-534.

Scopel, K.K., Fontes, C.J., Ferreira, M.U., and Braga, E.M. (2005). Plasmodium falciparum: IgG subclass antibody response to merozoite surface protein-1 among Amazonian gold miners, in relation to infection status and disease expression. Exp Parasitol *109*, 124-134.

Sega, M.F., Chu, H., Christian, J., and Low, P.S. (2012). Interaction of deoxyhemoglobin with the cytoplasmic domain of murine erythrocyte band 3. Biochemistry *51*, 3264-3272.

Sheetz, M.P. (1979). DNase-I-dependent dissociation of erythrocyte cytoskeletons. J Cell Biol *81*, 266-270.

Siddiqui, W.A., Tam, L.Q., Kramer, K.J., Hui, G.S., Case, S.E., Yamaga, K.M., Chang, S.P., Chan, E.B., and Kan, S.C. (1987). Merozoite surface coat precursor protein completely protects Aotus monkeys against Plasmodium falciparum malaria. Proc Natl Acad Sci U S A *84*, 3014-3018.

Siems, W.G., Sommerburg, O., and Grune, T. (2000). Erythrocyte free radical and energy metabolism. Clinical nephrology *53*, S9-17.

Sim, B.K., Carter, J.M., Deal, C.D., Holland, C., Haynes, J.D., and Gross, M. (1994a). Plasmodium falciparum: further characterization of a functionally active region of the merozoite invasion ligand EBA-175. Exp Parasitol *78*, 259-268.

Sim, B.K., Chitnis, C.E., Wasniowska, K., Hadley, T.J., and Miller, L.H. (1994b). Receptor and ligand domains for invasion of erythrocytes by Plasmodium falciparum. Science *264*, 1941-1944.

Sim, B.K., Orlandi, P.A., Haynes, J.D., Klotz, F.W., Carter, J.M., Camus, D., Zegans, M.E., and Chulay, J.D. (1990). Primary structure of the 175K Plasmodium falciparum erythrocyte binding antigen and identification of a peptide which elicits antibodies that inhibit malaria merozoite invasion. J Cell Biol *111*, 1877-1884.

Singh, S., Alam, M.M., Pal-Bhowmick, I., Brzostowski, J.A., and Chitnis, C.E. (2010). Distinct external signals trigger sequential release of apical organelles during erythrocyte invasion by malaria parasites. PLoS pathogens *6*, e1000746.

Singh, S., and Chitnis, C.E. (2012). Signalling mechanisms involved in apical organelle discharge during host cell invasion by apicomplexan parasites. Microbes Infect *14*, 820-824.

Sinha, A., Hughes, K.R., Modrzynska, K.K., Otto, T.D., Pfander, C., Dickens, N.J., Religa, A.A., Bushell, E., Graham, A.L., Cameron, R.*, et al.* (2014). A cascade of DNA-binding proteins for sexual commitment and development in Plasmodium. Nature *507*, 253-257.

Sinnis, P., Willnow, T.E., Briones, M.R., Herz, J., and Nussenzweig, V. (1996). Remnant lipoproteins inhibit malaria sporozoite invasion of hepatocytes. J Exp Med *184*, 945-954.

Smalley, M.E., and Brown, J. (1981). Plasmodium falciparum gametocytogenesis stimulated by lymphocytes and serum from infected Gambian children. Trans R Soc Trop Med Hyg *75*, 316-317.

Soni, S., Dhawan, S., Rosen, K.M., Chafel, M., Chishti, A.H., and Hanspal, M. (2005). Characterization of events preceding the release of malaria parasite from the host red blood cell. Blood cells, molecules & diseases *35*, 201-211.

Southgate, C.D., Chishti, A.H., Mitchell, B., Yi, S.J., and Palek, J. (1996). Targeted disruption of the murine erythroid band 3 gene results in spherocytosis and severe haemolytic anaemia despite a normal membrane skeleton. Nat Genet *14*, 227-230.

Sowa, K.M., Cavanagh, D.R., Creasey, A.M., Raats, J., McBride, J., Sauerwein, R., Roeffen, W.F., and Arnot, D.E. (2001). Isolation of a monoclonal antibody from a malaria patient-derived phage display library recognising the Block 2 region of Plasmodium falciparum merozoite surface protein-1. Mol Biochem Parasitol *112*, 143-147.

Spadafora, C., Awandare, G.A., Kopydlowski, K.M., Czege, J., Moch, J.K., Finberg, R.W., Tsokos, G.C., and Stoute, J.A. (2010). Complement receptor 1 is a sialic acid-independent erythrocyte receptor of Plasmodium falciparum. PLoS pathogens *6*, e1000968.

Spielmann, T., and Gilberger, T.W. (2010). Protein export in malaria parasites: do multiple export motifs add up to multiple export pathways? Trends in parasitology *26*, 6-10.

Srinivasan, P., Yasgar, A., Luci, D.K., Beatty, W.L., Hu, X., Andersen, J., Narum, D.L., Moch, J.K., Sun, H., Haynes, J.D*., et al.* (2013). Disrupting malaria parasite AMA1-RON2 interaction with a small molecule prevents erythrocyte invasion. Nat Commun *4*, 2261.

Stagg, H.R., Thomas, M., van den Boomen, D., Wiertz, E.J., Drabkin, H.A., Gemmill, R.M., and Lehner, P.J. (2009). The TRC8 E3 ligase ubiquitinates MHC class I molecules before dislocation from the ER. J Cell Biol *186*, 685-692.

Starnes, G.L., and Waters, A.P. (2010). Home improvements: how the malaria parasite makes the red blood cell home sweet home. Journal of molecular cell biology *2*, 11-13.

Steck, T.L. (1978). The band 3 protein of the human red cell membrane: a review. Journal of supramolecular structure *8*, 311-324.

Sterling, D., Reithmeier, R.A., and Casey, J.R. (2001a). Carbonic anhydrase: in the driver's seat for bicarbonate transport. JOP : Journal of the pancreas *2*, 165-170.

Sterling, D., Reithmeier, R.A., and Casey, J.R. (2001b). A transport metabolon. Functional interaction of carbonic anhydrase II and chloride/bicarbonate exchangers. J Biol Chem *276*, 47886-47894.

Stubbs, J., Simpson, K.M., Triglia, T., Plouffe, D., Tonkin, C.J., Duraisingh, M.T., Maier, A.G., Winzeler, E.A., and Cowman, A.F. (2005). Molecular mechanism for switching of P. falciparum invasion pathways into human erythrocytes. Science *309*, 1384-1387.

Sturm, A., Amino, R., van de Sand, C., Regen, T., Retzlaff, S., Rennenberg, A., Krueger, A., Pollok, J.M., Menard, R., and Heussler, V.T. (2006). Manipulation of host hepatocytes by the malaria parasite for delivery into liver sinusoids. Science *313*, 1287-1290.

Suarez, C., Volkmann, K., Gomes, A.R., Billker, O., and Blackman, M.J. (2013). The Malarial Serine Protease SUB1 Plays an Essential Role in Parasite Liver Stage Development. PLoS pathogens *9*, e1003811.

Sullivan, D.J., Jr., Gluzman, I.Y., Russell, D.G., and Goldberg, D.E. (1996). On the molecular mechanism of chloroquine's antimalarial action. Proc Natl Acad Sci U S A *93*, 11865-11870.

Takabatake, N., Okamura, M., Yokoyama, N., Ikehara, Y., Akimitsu, N., Arimitsu, N., Hamamoto, H., Sekimizu, K., Suzuki, H., and Igarashi, I. (2007). Glycophorin A-knockout mice, which lost sialoglycoproteins from the red blood cell membrane, are resistant to lethal infection of Babesia rodhaini. Veterinary parasitology *148*, 93-101.

Takala, S., Branch, O., Escalante, A.A., Kariuki, S., Wootton, J., and Lal, A.A. (2002). Evidence for intragenic recombination in Plasmodium falciparum: identification of a novel allele family in block 2 of merozoite surface protein-1: Asembo Bay Area Cohort Project XIV. Mol Biochem Parasitol *125*, 163-171.

Takala, S.L., Escalante, A.A., Branch, O.H., Kariuki, S., Biswas, S., Chaiyaroj, S.C., and Lal, A.A. (2006). Genetic diversity in the Block 2 region of the merozoite surface protein 1 (MSP-1) of Plasmodium falciparum: additional complexity and selection and convergence in fragment size polymorphism. Infect Genet Evol *6*, 417-424.

Talman, A.M., Domarle, O., McKenzie, F.E., Ariey, F., and Robert, V. (2004). Gametocytogenesis: the puberty of Plasmodium falciparum. Malar J *3*, 24.

Tamura, T., Asakura, T., Uemura, T., Ueda, T., Terauchi, K., Misaka, T., and Abe, K. (2008). Signal peptide peptidase and its homologs in Arabidopsis thaliana--plant tissue-specific expression and distinct subcellular localization. FEBS J *275*, 34-43.

Tanabe, K., Mackay, M., Goman, M., and Scaife, J.G. (1987). Allelic dimorphism in a surface antigen gene of the malaria parasite Plasmodium falciparum. J Mol Biol *195*, 273-287.

Tanner, M.J., Jenkins, R.E., Anstee, D.J., and Clamp, J.R. (1976). Abnormal carbohydrate composition of the major penetrating membrane protein of En(a-) human erythrocytes. Biochem J *155*, 701-703.

Targett-Adams, P., Hope, G., Boulant, S., and McLauchlan, J. (2008). Maturation of hepatitis C virus core protein by signal peptide peptidase is required for virus production. J Biol Chem *283*, 16850-16859.

Targett-Adams, P., Schaller, T., Hope, G., Lanford, R.E., Lemon, S.M., Martin, A., and McLauchlan, J. (2006). Signal peptide peptidase cleavage of GB virus B core protein is required for productive infection in vivo. J Biol Chem *281*, 29221-29227.

Tetteh, K.K., and Conway, D.J. (2011). A polyvalent hybrid protein elicits antibodies against the diverse allelic types of block 2 in Plasmodium falciparum merozoite surface protein 1. Vaccine *29*, 7811-7817.

Tham, W.H., Healer, J., and Cowman, A.F. (2012). Erythrocyte and reticulocyte binding-like proteins of Plasmodium falciparum. Trends in parasitology *28*, 23-30.

Tham, W.H., Wilson, D.W., Lopaticki, S., Schmidt, C.Q., Tetteh-Quarcoo, P.B., Barlow, P.N., Richard, D., Corbin, J.E., Beeson, J.G., and Cowman, A.F. (2010). Complement receptor 1 is the host erythrocyte receptor for Plasmodium falciparum PfRh4 invasion ligand. Proc Natl Acad Sci U S A *107*, 17327-17332.

Thathy, V., Fujioka, H., Gantt, S., Nussenzweig, R., Nussenzweig, V., and Menard, R. (2002). Levels of circumsporozoite protein in the Plasmodium oocyst determine sporozoite morphology. EMBO J *21*, 1586-1596.

Theron, M., Hesketh, R.L., Subramanian, S., and Rayner, J.C. (2010). An adaptable two-color flow cytometric assay to quantitate the invasion of erythrocytes by Plasmodium falciparum parasites. Cytometry Part A : the journal of the International Society for Analytical Cytology *77*, 1067-1074.

Tomita, M., Furthmayr, H., and Marchesi, V.T. (1978). Primary structure of human erythrocyte glycophorin A. Isolation and characterization of peptides and complete amino acid sequence. Biochemistry *17*, 4756-4770.

Tomita, M., and Marchesi, V.T. (1975). Amino-acid sequence and oligosaccharide attachment sites of human erythrocyte glycophorin. Proc Natl Acad Sci U S A *72*, 2964-2968.

Topolska, A.E., Lidgett, A., Truman, D., Fujioka, H., and Coppel, R.L. (2004). Characterization of a membrane-associated rhoptry protein of Plasmodium falciparum. J Biol Chem *279*, 4648-4656.

Trager, W. (1978). Cultivation of parasites in vitro. Am J Trop Med Hyg *27*, 216-222.

Trager, W., and Gill, G.S. (1992). Enhanced gametocyte formation in young erythrocytes by Plasmodium falciparum in vitro. J Protozool *39*, 429-432.

Trager, W., and Jenson, J.B. (1978). Cultivation of malarial parasites. Nature *273*, 621-622.

Treeck, M., Zacherl, S., Herrmann, S., Cabrera, A., Kono, M., Struck, N.S., Engelberg, K., Haase, S., Frischknecht, F., Miura, K.*, et al.* (2009). Functional analysis of the leading malaria vaccine candidate AMA-1 reveals an essential role for the cytoplasmic domain in the invasion process. PLoS pathogens *5*, e1000322.

Triglia, T., Chen, L., Lopaticki, S., Dekiwadia, C., Riglar, D.T., Hodder, A.N., Ralph, S.A., Baum, J., and Cowman, A.F. (2011). Plasmodium falciparum merozoite invasion is inhibited by antibodies that target the PfRh2a and b binding domains. PLoS pathogens *7*, e1002075.

Triglia, T., Duraisingh, M.T., Good, R.T., and Cowman, A.F. (2005). Reticulocyte-binding protein homologue 1 is required for sialic acid-dependent invasion into human erythrocytes by Plasmodium falciparum. Mol Microbiol *55*, 162-174.

Trucco, C., Fernandez-Reyes, D., Howell, S., Stafford, W.H., Scott-Finnigan, T.J., Grainger, M., Ogun, S.A., Taylor, W.R., and Holder, A.A. (2001). The merozoite surface protein 6 gene codes for a 36 kDa protein associated with the Plasmodium falciparum merozoite surface protein-1 complex. Mol Biochem Parasitol *112*, 91-101.

Urny, J., Hermans-Borgmeyer, I., Gercken, G., and Schaller, H.C. (2003). Expression of the presenilin-like signal peptide peptidase (SPP) in mouse adult brain and during development. Gene Expr Patterns *3*, 685-691.

Urquiza, M., Rodriguez, L.E., Suarez, J.E., Guzman, F., Ocampo, M., Curtidor, H., Segura, C., Trujillo, E., and Patarroyo, M.E. (1996). Identification of Plasmodium falciparum MSP-1 peptides able to bind to human red blood cells. Parasite Immunol *18*, 515-526.

van Dooren, G.G., Marti, M., Tonkin, C.J., Stimmler, L.M., Cowman, A.F., and McFadden, G.I. (2005). Development of the endoplasmic reticulum, mitochondrion and apicoplast during the asexual life cycle of Plasmodium falciparum. Mol Microbiol *57*, 405-419.

Van Kim, C.L., Colin, Y., and Cartron, J.P. (2006). Rh proteins: key structural and functional components of the red cell membrane. Blood reviews *20*, 93-110.

van Wijk, R., and van Solinge, W.W. (2005). The energy-less red blood cell is lost: erythrocyte enzyme abnormalities of glycolysis. Blood *106*, 4034-4042.

Vaughan, A.M., Mikolajczak, S.A., Wilson, E.M., Grompe, M., Kaushansky, A., Camargo, N., Bial, J., Ploss, A., and Kappe, S.H. (2012). Complete Plasmodium falciparum liver-stage development in liver-chimeric mice. J Clin Invest *122*, 3618-3628.

Voigt, S., Hanspal, M., LeRoy, P.J., Zhao, P.S., Oh, S.S., Chishti, A.H., and Liu, S.C. (2000). The cytoadherence ligand Plasmodium falciparum erythrocyte membrane protein 1 (PfEMP1) binds to the P. falciparum knob-associated histidine-rich protein (KAHRP) by electrostatic interactions. Mol Biochem Parasitol *110*, 423-428.

von Ruckmann, B., and Schubert, D. (2002). The complex of band 3 protein of the human erythrocyte membrane and glyceraldehyde-3-phosphate dehydrogenase: stoichiometry and competition by aldolase. Biochim Biophys Acta *1559*, 43-55.

Voss, M., Fukumori, A., Kuhn, P.H., Kunzel, U., Klier, B., Grammer, G., Haug-Kroper, M., Kremmer, E., Lichtenthaler, S.F., Steiner, H.*, et al.* (2012). Foamy virus envelope protein is a substrate for signal peptide peptidase-like 3 (SPPL3). J Biol Chem *287*, 43401-43409.

Voss, M., Kunzel, U., Higel, F., Kuhn, P.H., Colombo, A., Fukumori, A., Haug-Kroper, M., Klier, B., Grammer, G., Seidl, A.*, et al.* (2014). Shedding of glycan-modifying enzymes by signal peptide peptidase-like 3 (SPPL3) regulates cellular N-glycosylation. EMBO J *33*, 2890-2905.

Wanaguru, M., Crosnier, C., Johnson, S., Rayner, J.C., and Wright, G.J. (2013). Biochemical analysis of the Plasmodium falciparum erythrocyte-binding antigen-175 (EBA175)-glycophorin-A interaction: implications for vaccine design. J Biol Chem *288*, 32106-32117.

Wang, B., and Brand-Miller, J. (2003). The role and potential of sialic acid in human nutrition. European journal of clinical nutrition *57*, 1351-1369.

Weihofen, A., Binns, K., Lemberg, M.K., Ashman, K., and Martoglio, B. (2002). Identification of signal peptide peptidase, a presenilin-type aspartic protease. Science *296*, 2215-2218.

Weihofen, A., Lemberg, M.K., Ploegh, H.L., Bogyo, M., and Martoglio, B. (2000). Release of signal peptide fragments into the cytosol requires cleavage in the transmembrane region by a protease activity that is specifically blocked by a novel cysteine protease inhibitor. J Biol Chem *275*, 30951-30956.

Weiss, G.E., Gilson, P.R., Taechalertpaisarn, T., Tham, W.H., de Jong, N.W., Harvey, K.L., Fowkes, F.J., Barlow, P.N., Rayner, J.C., Wright, G.J.*, et al.* (2015). Revealing the Sequence and Resulting Cellular Morphology of Receptor-Ligand Interactions during Plasmodium falciparum Invasion of Erythrocytes. PLoS pathogens *11*, e1004670.

Weiss, M.M., Oppenheim, J.D., and Vanderberg, J.P. (1981). Plasmodium falciparum: assay in vitro for inhibitors of merozoite penetration of erythrocytes. Exp Parasitol *51*, 400-407.

White, N.J., Nosten, F., Looareesuwan, S., Watkins, W.M., Marsh, K., Snow, R.W., Kokwaro, G., Ouma, J., Hien, T.T., Molyneux, M.E.*, et al.* (1999). Averting a malaria disaster. Lancet *353*, 1965-1967.

White, N.J., Pukrittayakamee, S., Hien, T.T., Faiz, M.A., Mokuolu, O.A., and Dondorp, A.M. (2014). Malaria. Lancet *383*, 723-735.

Wickham, M.E., Culvenor, J.G., and Cowman, A.F. (2003). Selective inhibition of a two-step egress of malaria parasites from the host erythrocyte. J Biol Chem *278*, 37658-37663.

Wickramarachchi, T., Cabrera, A.L., Sinha, D., Dhawan, S., Chandran, T., Devi, Y.S., Kono, M., Spielmann, T., Gilberger, T.W., Chauhan, V.S.*, et al.* (2009). A novel Plasmodium falciparum erythrocyte binding protein associated with the merozoite surface, PfDBLMSP. International journal for parasitology *39*, 763-773.

Williams, T.N. (2006). Human red blood cell polymorphisms and malaria. Curr Opin Microbiol *9*, 388-394.

Williamson, R.C., and Toye, A.M. (2008). Glycophorin A: Band 3 aid. Blood cells, molecules & diseases *41*, 35-43.

Winzeler, E.A. (2008). Malaria research in the post-genomic era. Nature *455*, 751-756.

Woehlbier, U., Epp, C., Hackett, F., Blackman, M.J., and Bujard, H. (2010). Antibodies against multiple merozoite surface antigens of the human malaria parasite Plasmodium falciparum inhibit parasite maturation and red blood cell invasion. Malar J *9*, 77.

Woehlbier, U., Epp, C., Kauth, C.W., Lutz, R., Long, C.A., Coulibaly, B., Kouyate, B., Arevalo-Herrera, M., Herrera, S., and Bujard, H. (2006). Analysis of antibodies directed against merozoite surface protein 1 of the human malaria parasite Plasmodium falciparum. Infect Immun *74*, 1313-1322.

Wolfe, M.S. (2010). Structure, mechanism and inhibition of gamma-secretase and presenilin-like proteases. Biol Chem *391*, 839-847.

Wolfe, M.S., and Kopan, R. (2004). Intramembrane proteolysis: theme and variations. Science *305*, 1119-1123.

Wu, Y., Sifri, C.D., Lei, H.H., Su, X.Z., and Wellems, T.E. (1995). Transfection of Plasmodium falciparum within human red blood cells. Proc Natl Acad Sci U S A *92*, 973-977.

Xia, W., and Wolfe, M.S. (2003). Intramembrane proteolysis by presenilin and presenilin-like proteases. J Cell Sci *116*, 2839-2844.

Yamaguchi, T., Fujii, T., Abe, Y., Hirai, T., Kang, D., Namba, K., Hamasaki, N., and Mitsuoka, K. (2010a). Helical image reconstruction of the outward-open human erythrocyte band 3 membrane domain in tubular crystals. Journal of structural biology *169*, 406-412.

Yamaguchi, T., Ikeda, Y., Abe, Y., Kuma, H., Kang, D., Hamasaki, N., and Hirai, T. (2010b). Structure of the membrane domain of human erythrocyte anion exchanger 1 revealed by electron crystallography. J Mol Biol *397*, 179-189.

Yeoh, S., O'Donnell, R.A., Koussis, K., Dluzewski, A.R., Ansell, K.H., Osborne, S.A., Hackett, F., Withers-Martinez, C., Mitchell, G.H., Bannister, L.H.*, et al.* (2007). Subcellular discharge of a serine protease mediates release of invasive malaria parasites from host erythrocytes. Cell *131*, 1072-1083.

Ying, P., Shakibaei, M., Patankar, M.S., Clavijo, P., Beavis, R.C., Clark, G.F., and Frevert, U. (1997). The malaria circumsporozoite protein: interaction of the conserved regions I and II-plus with heparin-like oligosaccharides in heparan sulfate. Exp Parasitol *85*, 168-182.

Young, M.T., Beckmann, R., Toye, A.M., and Tanner, M.J. (2000). Red-cell glycophorin A-band 3 interactions associated with the movement of band 3 to the cell surface. Biochem J *350 Pt 1*, 53-60.

Young, M.T., and Tanner, M.J. (2003). Distinct regions of human glycophorin A enhance human red cell anion exchanger (band 3; AE1) transport function and surface trafficking. J Biol Chem *278*, 32954-32961.

Zdebska, E., Bader-Meunier, B., Schischmanoff, P.O., Dupre, T., Seta, N., Tchernia, G., Koscielak, J., and Delaunay, J. (2003). Abnormal glycosylation of red cell membrane band 3 in the congenital disorder of glycosylation Ig. Pediatric research *54*, 224-229.

Zhang, Y., Manning, L.R., Falcone, J., Platt, O., and Manning, J.M. (2003). Human erythrocyte membrane band 3 protein influences hemoglobin cooperativity. Possible effect on oxygen transport. J Biol Chem *278*, 39565-39571.

Zhao, X., Chang, Z., Tu, Z., Yu, S., Wei, X., Zhou, J., Lu, H., Jiang, N., and Chen, Q. (2014). PfRON3 is an erythrocyte-binding protein and a potential blood-stage vaccine candidate antigen. Malar J *13*, 490.

Zhu, Q., and Casey, J.R. (2004). The substrate anion selectivity filter in the human erythrocyte Cl-/HCO3- exchange protein, AE1. J Biol Chem *279*, 23565-23573.